# SEDIMENT PROPERTIES AND PROCESSES INFLUENCING KEY GEOENVIRONMENTAL ASPECTS OF A LARGE ALLUVIAL RIVER, THE BRAHMAPUTRA IN ASSAM

A thesis submitted to IIT Guwahati
in partial fulfillment of the requirements
for the award of the degree of

**DOCTOR OF PHILOSOPHY**

By

**Lalit Saikia**

Roll no: 07610410

*Under the guidance of*

*Prof. Chandan Mahanta*


Department of Civil Engineering

**Indian Institute of Technology Guwahati**

Guwahati - 781039, Assam, INDIA

October, 2017

*Dedicated to*

*My Grandfather*

*Late Dimbeswar Saikia*

# DECLARATION

I hereby declare that the thesis entitled **Sediment properties and processes influencing key geoenvironmental aspects of a large alluvial river, the Brahmaputra in Assam** is a presentation of my original research work done under the guidance of my thesis supervisor Prof. Chandan Mahanta in the Department of Civil Engineering, Indian Institute of Technology Guwahati. I hereby confirm that the thesis is free from any plagiarized material and does not infringe any rights of others. In keeping with the general practice and reporting of scientific observations, due acknowledgements have been made wherever the work described is based on the findings of other investigators, with due reference to the literature.

(Lalit Saikia)
Roll No: 07610410
Research Scholar
Department of Civil Engineering
Indian Institute of Technology Guwahati
E-mail: lalitsaikia@yahoo.com
lalitsaikia2008@gmail.com

October, 2017
IIT Guwahati

भारतीय प्रौद्योगिकी संस्थान गुवाहाटी
INDIAN INSTITUTE OF TECHONOLOGY GUWAHATI
Guwahati 781 039, India
Phone: +91-361-2582407
Fax: +91-361-2582440
E-mail: chandan@iitg.ernet.in
mahantaiit@gmail.com

**Prof. Chandan Mahanta**
Professor, Department of Civil Engineering
Dean, Students' Affairs

October 23, 2017

# CERTIFICATE

This is to certify that the thesis entitled **Sediment properties and processes influencing key geoenvironmental aspects of a large alluvial river, the Brahmaputra in Assam** submitted by **Lalit Saikia** (Roll no: 07610410) to the Indian Institute of Technology Guwahati, for the award of the degree of Doctor of Philosophy, is a record of research work carried out by him under my supervision and guidance. The thesis, in my opinion, is worthy of consideration for the degree of Doctor of Philosophy in accordance with the regulations of this Institute. The results contained in the thesis have not been submitted elsewhere in part or full for the award of any degree or diploma to the best of my knowledge and belief.

(C. Mahanta)

# ABSTRACT

The research attempted to evaluate key sediment properties and processes of a large alluvial river, the Brahmaputra in Assam, India and examine how different sediment properties and processes influence major geoenvironmental behavior of the river. Based on primary as well as secondary data, the thesis focusses physico-chemical properties of sediments including contamination status, sediment budget, bank line shifting, river bank erosion, role of geochemical properties of bank materials in erosion, braiding and land use & land cover of the river in post-monsoon months. One objective of the research was to understand geoenvironmental changes of Brahmaputra in Assam and seeking solution to the bank erosion problem.

Suspended sediment and bed sediment samples were collected from six different locations of Brahmaputra River in Assam. For suspended sediment samples, four water samples were collected from each sampling location during pre-monsoon (January-March, 2011), monsoon (June, 2011) and post-monsoon (November, 2011) months. Suspended sediments were obtained from water samples by filtration using micro-pore filters. Bed sediments were collected by scooping of freshly deposited sediments from river bed in the months of December' 2010 and January' 2011. Considering severity of bank erosion problem in the last few years, six locations namely *Rohmoria (A), Dibrugarh (B), Nematighat (C), Majuli (D), Gamerighat (E)* and *Palasbari* (F) were selected for collection of bank material samples. Soil samples were collected at 10 cm depth and then at 30 cm intervals from vertical profiles of exposed steep banks of erosion sites and nearby non-erosion sites.

pH, organic content (OC), carbonate content (CC), sodium absorption ratio (SAR), exchangeable sodium percentage (ESP), cation exchange capacity (CEC), mineralogy and particle size of collected sediments and bank materials were analyzed by standard methods and instruments, e.g., pH by pH meter; OC and CC by loss on ignition method; SAR, ESP, CEC using flame photometer, mineral composition and texture using XRD and SEM; particle size using laser particle size analyzer. Heavy metals in sediment samples were analyzed using the USEPA 3050B method and an atomic absorption spectrophotometer.

Modified BCR sequential extraction method was applied to understand the geochemical association and to predict the probable mobile fraction of heavy metals in sediments. Angle of internal friction and cohesion of bank materials were estimated by direct shear tests. Role of individual bank material properties in bank erosion were studied with binary logistic regression using SPSS.

Besides scientific references, secondary data needed for the study was collected from reports of North Eastern Council, Brahmaputra Board, Water Resources Department (Govt. of Assam) and Ministry of Water Resources (Govt. of India).

Braiding, erosion-deposition and land use and land cover of Brahmaputra River was studied extracting information from Landsat images using Remote sensing and GIS techniques. Brahmaputra River in Assam at three different years, i.e., 1973, 1994 and 2014 was divided into 16 reaches with equal length of 40 km (Reach 1 in the upstream and reach 16 in the downstream). Erosion and deposition during 1973 – 2014 was studied using overlay analysis in ArcGIS 10.1. Braiding indices for different reaches of Brahmaputra in 1973 and 2014 were calculated by seven different methods suggested by Brice (1964), Howard et al. (1970), Rust (1978), Mosely (1981), Ashmore (1982), Friend & Sinha (1993) and Sharma (2004). A new braiding index for an alluvial and large braided river like the Brahmaputra has been introduced in the present study using number of mid channel bars as an input parameter. LULC analysis for 1994 – 2014 was carried out by categorizing the satellite images into different classes, i.e., river/ water, sandbar, vegetation (including natural grass land) and agriculture (including human settlement), using unsupervised classification in an image processing software, i.e., ERDAS Imagine 2014.

Young lithology, seismicity, unconsolidated sedimentary rocks of the Himalayas, steep slope of Brahmaputra and its tributaries in the Himalayas, heavy rainfall in monsoon, deforestation and sediment generating cultivation were the causes of sediment generation in the river, whereas decrease of slope in Assam plains was the main cause of sediment deposition. Steepness of Brahmaputra River is high compared to most of the large rivers of the world like Amazon, Congo, Yangtze, Volga, Mississippi, Ganges and Indus. Slope of Brahmaputra River created for the present study by using data from 175 points along the

channel demonstrated a clearer picture with marked departure from the earlier figures based on fewer points proposed by other researcher. Average gradient of Brahmaputra River was found to be 1.52 m $km^{-1}$. Steep slopes of river (slope of Brahmaputra in the reach between PE and entry to India was 8.27 m/km) and tributaries in the mountainous reaches led to high amount of sediment generation and transportation whereas a sudden decrease in slope (slope in the reach between India border and *Pasighat* is 1.52 m/km) results in a large amount of sediment deposition, developing a prominent braided pattern.

Slope of Brahmaputra has further decreased during the course of the river in Assam plains (from 0.81 m $km^{-1}$ between *Pasighat* and *Dibrugarh* at upstream to 0.09 m $km^{-1}$ between *Guwahati* and India-Bangladesh border at downstream), causing more prominent braided pattern and river instability in terms lateral shifting and bank erosion. Average scour of 1.92 cm per year was noticed in the entire reaches with maximum scouring of 4.96 cm per year in the middle reaches (C/S 31 – 41). Decrease in average bed slope at the second reach (C/S 42 – 52) and then increase in the third and the fourth reaches (C/S 32 – 42, 22 – 32) favored more erosion in the cross-sections 42 – 52 and deposition in other reaches.

The river was widened to both the banks at upstream in earlier years, i.e., 1911–28 and 1971–71. There was severe erosion in the south (left) bank of the river during 1973 – 2014 with downward shifting of the main channel. Total area of erosion and deposition during 1973 – 2014 were 1557 $km^2$ and 204 $km^2$ respectively. There was more erosion in the south bank (829 $km^2$) and more deposition in the north bank (122 $km^2$) during the period.

An attempt was made to construct a sediment budget for Brahmaputra River in Assam using a mass balance approach. The tributaries were found collectively to contribute $698\times10^6$ t suspended sediment annually to Brahmaputra. Since a large portion of river-derived sediments of Tibetan rivers are trapped in low reaches, considering 40% of riverine sediments trapped in the river bed and flood-plains, $419\times10^6$ t sediments (60% of $698\times10^6$ t) were estimated to be in suspension at downstream, i.e., at India-Bangladesh Border, whereas $279\times10^6$ t (40% of $698\times10^6$ t) was estimated to be deposited in river bed and floodplains. From scouring and deposition data, mass of deposited sediment on river bed was estimated to be $69\times10^6$ t in a year. Average annual land area lost due to bank

erosion was found to be $38\times10^6$ $m^2$ during 1973 – 2014. Considering depth of bank erosion as 4.7 m (average difference of yearly observed highest and the lowest water level of Brahmaputra for the period 1914 – 1990) and sediment density 1.36 $g/cm^3$, mass of eroded soil was found to be $243\times10^6$ t. Considering 3 m as average uniform height of sand bars, mass of deposited sediments on $4.97\times10^6$ $m^2$ area was found to be $20\times10^6$ t. Total sediment load in the river at downstream (India-Bangladesh border) was estimated to be $814\times10^6$ t/year. Considering 10% of sediment load of Brahmaputra as bed load, suspended sediment load at downstream estimated to be $733\times10^6$ t/year. Tributaries, bank erosion and scouring of river bed were found to contribute 52%, 27% and 21% respectively to sediment load of Brahmaputra at downstream.

Particle size distribution of suspended sediments revealed dominance of silt (3.9 – 62.5µm), very fine sand (62.5 – 125µm) and fine sand (125 – 250µm) fractions. XRD analysis revealed dominance of silt sized Quartz, Kaolinite, Illite and Albite. Dominance of Quartz, Kaolinite, Montmorrillonite in suspended sediments suggest less adsorbing capacity of metals. Prolate, oblate and bladed shape of suspended sediments suggested immature sediments from bank erosion or scouring with short transportation history.

Concentrations of Fe, Mn, Cu, Zn and Ni content in suspended sediment during pre-monsoon season were higher compared to monsoon and post-monsoon seasons. All metal concentrations except Mn were in higher concentrations in Brahmaputra River (Fe: 6.5%, Cu: 41.3 µg/gm, Pb: 23.3 µg/gm, Zn: 94 µg/gm, Mn: 503.2 µg/gm, Ni: 40.3 µg/gm) compared to that of Indian average river (Fe: 2.9%, Cu: 28 µg/gm, Pb: 15 µg/gm, Zn: 16 µg/gm, Mn: 605 µg/gm, Ni: 37 µg/gm) and that of Bay of Bengal (Fe: 3.9%, Cu: 26 µg/gm, Mn: 529 µg/gm, Ni: 64 µg/gm).

Geo-accumulation indices show uncontaminated sediment quality with respect to all the metals except moderate Fe enrichment in three locations. Dominance of residual fraction and less amount of bioavailable portion of heavy metals may be attributed to low organic matter, dominant coarser fraction in sediments coupled with low pollution in the river from less industrial activities in the region.

Among the analyzed parameters, pH, organic content (OC), carbonate content (CC), cation exchange capacity (CEC), exchangeable sodium percentage (ESP), $d_{10}$, $d_{50}$ and $d_{90}$ were found to be more heterogeneous in erosion sites than those of non-erosion sites. Low (<2%) organic content, dominance of silt and sand sized particles, particularly in lower layers of sediment profile were found to be the major geochemical properties of bank materials contributing to bank erosion in sites *A, B, E* and *F*. Decrease of SAR, ESP and CEC towards deeper depth showed consistency to results over erodible areas at different locations.

Erosion site *A* had comparatively high sand content and the lowest value of minimum clay content (0.3%) among the study areas. Erosion sites of *B, D, E* and *F* also had high sand content (52%, 44%, 36% and 31% respectively) with very low amount of clay sized particles (3–8%). These two factors including low organic content are likely to be considered as significant geochemical factors for low cohesion in the studied locations as revealed from direct shear test results. High angle of internal friction of samples in spite of low cohesion could be explained by aggregation of soil particles as suggested by different researchers. Average velocities of Brahmaputra corresponding to a pre-monsoon discharge and peak monsoon discharge were two to hundred folds higher than that required for threshold movement of sediment.

Correlation matrices showed that pH, OC, Carbonate content, SAR had negative correlation with erosion, whereas particle size ($d_{50}$ and $d_{90}$) had positive correlation with erosion. To evaluate contribution of selected geochemical properties to erosion event, binary logistic regression in SPSS was used with 'Erosion' ('Yes' or 'No') as dependent variable and OC, SAR and particle size ($d_{50}$ and $d_{90}$) as predictor variables. Moderate relationship of 59% between prediction and grouping was observed with predictor variables OC, SAR and $d_{90}$. Particle size and OC were found the most important geochemical factors of bank erosion in Brahmaputra, holding other parameters constant. Role of particle size and OC in erosion was already documented by different researchers. Experimental and statistical analysis revealed that value of OC, SAR and $d_{90}$ of bank materials could be used for rapid assessment of probability of erosion in a particular location in Brahmaputra.

Braiding of Brahmaputra has increased from 1973 to 2014. In spite of variations of braiding values in different approaches, almost similar trend of braiding values has been observed for all the reaches. The newly suggested braiding index has showed comparable result with other approaches. Moreover, the new index has very good correlation (0.97) with number of sandbars. The new index also showed relatively better correlation with sinuosity than braiding values obtained from other methods. With reference to braiding values for different reaches from different approaches, threshold values are suggested for a broad range of classification of braiding phenomenon: highly braided: $B > 30$, moderately braided: $5 < B < 30$, and low braided: $B < 5$. Thirteen reaches were moderately braided and three were low braided in 1973. But in 2014, six reaches were highly braided and nine reaches were moderately braided. The reaches which were only low or moderately braided in 1973, became moderately braided or highly braided during 1973 – 2014. Braiding value was increased by more than 50% in reach no 2, 5, 6, 8, 10, 11, 12, 13, 14 & 15 during 1973 – 2014. In some cases, more than 100% increase of braiding was observed (in reach no 5, 12 and 14). Increase of braiding was due to development of more sandbars and distributaries resulting in increased mid-channel lengths and sandbar lengths. Minimum braiding in a few reaches was due to comparatively narrow channel width with less number of distributaries and mid-channel bars. Area covered by Brahmaputra River in Assam has increased from 4906 $km^2$ in 1973 to 6258 $km^2$ in 2014. Widening of the river has resulted in loss of major land area by bank erosion process in many locations. However, increased area of Brahmaputra in Assam is not necessarily linked to river bank erosion in every case. 28% increase in area of Brahmaputra during 1973 – 2014 is also due to bifurcation of streams without any significant loss of land.

LULC study of Brahmaputra in post-monsoon months has revealed that in 1994, 37% area of the river was occupied by water, i.e., live channels, and 63% area was bars out of which 30% was sand and 33% was under agricultural practices and vegetation. Thus, more than 60% area of Brahmaputra was covered by temporary sandbars and permanent islands in the post-monsoon months. However, reaches had varied amount (34% – 79%) of sandbars and islands. In 2014, 29% area was occupied by channels and 71% area was occupied by sandbar, vegetated bars and agriculture. Thus, amount of submerged part in post monsoon

months has decreased (from 37% to 29%) during 1994 – 2014. A reduction in natural grassland and forest has been observed with corresponding increase in agricultural practices in different bars and islands of Brahmaputra in Assam during the period. Agricultural activity has increased in lower reaches, i.e., reach no 15 (25%) and 16 (18%). Socio-political factor is responsible for LULC change in Brahmaputra River floodplain particularly in lower reaches. Loss of agricultural land and homestead land from river bank erosion and growing population in the lower reaches has compelled the riverine people to explore agricultural activities in inter fluvial landmasses in post-monsoon months. Identification of sandbars/ islands and evaluation of nutrient status is necessary for better agricultural utilization or other activities in post-monsoon months.

The research describes prominent dynamic nature of Brahmaputra in terms of increased braiding, channel migration, bifurcation of the distributaries with development of temporary mid-channel bars, bank line shifting causing sever bank erosion. Causes and mechanisms of bank erosion differ at different parts of the river due to variations in flow direction of the main channel, topography and bank material properties. It is essential to study the whole river to identify effected and erosion prone areas based on severity of the problem and probability of occurrence.

Different reaches of the river can be categorized into two major groups based on braiding, shifting of the main channel and bank material properties to select appropriate river training works. For places eroded by direct attack of the main channel, e.g., *Rohmoria* at upstream, revetments along with flow deflectors at immediate upstream areas can be suitable option. Articulated Concrete Block Mattress has an appropriate flexibility that can be installed on different conditions of slope revetments. Bank revetment, spurs etc. have proved to be highly capital intensive and hence can't be applied to long reaches seeking erosion protection. In erosion sites of highly braided area where secondary channels attack the banks, pro-siltation devices can be applied to induce siltation in banks and channelization of the main channel. RCC Jack Jetty and bamboo submerged vanes can be considered as a semi-permanent cost effective approach of river management for sedimentation along with erosion protection. Low slope banks with loose structure having relatively more organic content can be managed with geo bags/ tubes coupled with

bioengineering tools, e.g., vetiver plantation for its effectiveness with cost effective nature, low maintenance, longevity and little environmental impacts. A braided reach of Brahmaputra can be narrowed by using submerged vanes which are effective in managing braided rivers to close off selected secondary branches and reduce the lateral extent. Existing embankments under direct attack of the river need erosion protection and it may be revetment/ mattressing, spurs, grade control measures or improvement of shear strength (by growing shallow rooted vegetation). Recently the state government of Assam has decided to start dredging of the Brahmaputra with objectives of erosion control, sediment management and flood control. Dredged material can be used to fill geo-tubes and to strengthen existing embankments to super levee as developed in Japan. Super levee concept will overcome the drawbacks of existing embankment system.

The present study is based on sediment properties and processes including erosion behavior and protection measures of a few selected locations of a unique and complex river, the Brahmaputra. The present study has the potential scope of studying fate and transport of sediments of a large alluvial river with more data from tributaries as well as the main stem. Considering the environmental impacts from different erosion protection measures, all approaches for erosion management should be carried out in line with the hydrological character of Brahmaputra. Integration of all findings and a strong R&D backup can be a base for a detailed survey of entire Brahmaputra for effectiveness of erosion management measures.

# ACKNOWLEDGEMENT

I take this opportunity to express my indebtedness and deep sense of gratitude to my supervisor, *Prof. Chandan Mahanta* for his inspiring guidance, untiring supervision and valuable suggestions which enabled me to bring my work into present shape. His stimulating ideas and versatile personality will keep on influencing me forever.

I should thank IIT Guwahati for giving me the opportunity of carrying out my PhD in the Department of Civil Engineering. I am thankful to hon'ble Director sir as well as Head of the Department of Civil Engineering of the institute for their approval. I am grateful to *Prof. Gautam Barua* (Chairman, Doctoral Committee) for his kind cooperation and suggestions. My sincere thanks go to other members of Doctoral Committee namely *Prof. Utpal Bora* and *Dr. Sreeja P.* for their useful comments and suggestions during my presentations on PhD work. I am grateful to *Prof. A. Dutta, Prof. A. K. Sarma, Prof. S. Dutta, Dr. P. K. Ghosh, Prof. S. Gokhale, Dr. T. V. Bharat* and other faculty members of the department for their encouragements.

I would like to extend my thankfulness to all persons who helped me in assessing secondary data from different organizations/ departments, e.g., NEC, Brahmaputra Board, WRD Assam. I am grateful to all who accompanied me in collecting sediment and bank material samples and relevant information from different locations of the Brahmaputra River in Assam.

I have to acknowledge the role of the laboratories of Environmental Engineering, Geotechnical Engineering, Centre for Nanotechnology and Chemical Engineering of IITG for providing me opportunities and support in analyzing my samples. Special thanks go to Central Instruments Facility, Laxminath Bezbaroa Central library and Computer Centre of the institute for the facilities offered to me.

I record my gratitude to *Mrs. Anjana Mahanta, Dr. Deva Borah, Prof. K. P. Sarma, Dr. R. R. Hoque, Dr. Amit Choudhury, Dr. Gopal Phukan, Dr. Anuj Barua (MD), Dr. Narayan Chetry, Dr. B. C. Kalita, Dr. Poulose,* Dean of Academic Affairs (IITG) and *Mr. P. N. Das (ACS)* for their support. My thanks will acknowledge *Jonali Saikia, Kaustoov Acharya* and *Payodhar Pathak* for their help in the laboratory. I am thankful to staff of Civil Engineering Department (particularly *Juri Jyoti Hazarika, Rajib Gogoi, Kumud Deka, Dipak Deka and Tapan Das*), Academic section (particularly *Pradip Sinha*) and Hostel Siang (particularly *Farid Ali*) for their assistance in need.

Let me say "Thank you" to *Rajib Lochan Deka, Jitu Tamuli, Runti Choudhury, Suranjana Bhaswati Borah, Pronob Jyoti Borah, Pranab Saikia, Ranjit Kalita, Wazir Alam, Debajit Borah, Naba Hazarika, Nayanmoni Gogoi, Venkatesh, Biju Prava Sahariah, Juri Borborah, Ajit Konwer, Juna Probha Devi, Nayan Moni Baishya* and *Barbie Hazarika* for their help in need. I acknowledge my current employer University of Science & Technology, Meghalaya for providing support in writing two thesis chapters. I am thankful to 'Bani Mandir' for printing and binding of thesis copies.

At this juncture, I remember with great fondness and respect my grandfather (*Late Dimbeswar Saikia*) who must have showered his blessings on me. I must express my sincere gratefulness to my parents (*Arun Saikia* and *Sewali Saikia*) for believing in me and for the unconditional support in fulfilling my academic ambitions. I sincerely acknowledge and appreciate the sacrifice, understanding and unfailing support received from my wife *Binita* in my PhD work. My sister *Jahnabi* deserves special thanks for her encouragement and concern. I extend my thankfulness to *Abala Barman, Ratul Borah, Bhabesh Hujuri, Rita Hujuri, Tapan Deka, Babita Deka* and other family members/ relatives and well-wishers for their wishes and support. I would like to mention the name of my cute niece (*Jurmalaya*) and nephew (*Gaurab Ujjwal*) for adding sweetness to our family while my thesis was on.

Last but not the least, thanks to God for HIS blessings.

*Lalit Saikia*

# CONTENTS


Page no

- Declaration ii
- Certificate iii
- Abstract iv
- Acknowledgement xii
- Contents xiv
- List of tables xvii
- List of figures xix
- Abbreviations xxiv

**Chapter 1 Introduction 1-10**

1.1 Introduction to sediments 1
1.2 Sediments: physical and chemical characteristics 4
1.3 Role of sediments in river morphology 6
1.4 Objectives of the study 8
1.5 Organization of the thesis 9

**Chapter 2 Review of literature 11-29**

2.1 Sediment properties of Brahmaputra and other large rivers 11
2.1.1 Physical properties 11
2.1.2 Chemical properties: metal concentration in river sediments 13
2.2 Sediment dynamics of the major fluvial basins 17
2.3 River bank erosion in large rivers 22
2.4 Geochemical properties of bank materials as a facilitator of erosion 25
2.5 Land use and land cover change of large rivers 28

**Chapter 3 Materials and methods 30-53**

3.1 Study area: The Brahmaputra River in Assam 30
3.1.1 River bank erosion in Brahmaputra 35
3.1.1.1 Extent of the erosion problem in Brahmaputra 35

3.1.1.2 Factors responsible for erosion in Brahmaputra 36
3.2 Sources of secondary data 38
3.3 Collection of sediments 38
3.4 Collection of bank materials 40
3.5 Evaluation of physico-chemical properties of sediments/ bank materials 45
3.5.1 Determination of pH 45
3.5.2 Organic matter 46
3.5.3 Heavy metal 46
3.5.3.1 Geochemical fractionation of metals 47
3.5.3.2 Quality control and quality assurance 48
3.5.4 SAR, ESP and CEC 48
3.5.5 Elemental and mineral composition 48
3.5.6 Particle size distribution 49
3.6 Analysis of data 50
3.7 Braiding indices and land use & land cover analysis 51

**Chapter 4 Genesis and deposition of sediments in Brahmaputra 54-84**
4.1 Causes of high sediment load in Brahmaputra 54
4.2 Sources of sediments in Brahmaputra 63
4.2.1 Tributaries of Brahmaputra 63
4.2.2 Scour and deposition of sediments in Brahmaputra 64
4.2.3 Shifting of Brahmaputra and river bank erosion 68
4.3 Slope variation 77
4.4 A sediment budget of Brahmaputra River in Assam 78

**Chapter 5 Physico-chemical properties of sediments of Brahmaputra 85-98**
5.1 Size distribution of bed sediments 85
5.2 Heavy metal concentrations in suspended sediments 88
5.2.1 Geochemical fractionation of metals 92
5.2.2 Geo-accumulation indices 96

**Chapter 6 Geochemical evaluation of bank materials 99-122**

6.1 Analysis of geochemical properties of bank materials 99

6.1.1 Analysis of bank materials of erosion site *A* 99

6.1.2 Analysis of bank materials of erosion site *B* 102

6.1.3 Analysis of bank materials of erosion site *C* 104

6.1.4 Analysis of bank materials of location *D* 106

6.1.5 Analysis of bank materials of erosion site *E* 111

6.1.6 Analysis of bank materials of erosion site *F* 112

6.2 Synthesis of observations and interpretation from different experiments and test results 114

6.2.1 Role of geochemical properties of bank materials in erosion 118

6.2.2 Results of analysis of data using logistic regression in SPSS 119

**Chapter 7 Braiding and land use and land cover of Brahmaputra River 123-145**

7.1 Braiding indices of Brahmaputra River 123

7.2 Land use and land cover of Brahmaputra River 134

**Chapter 8 Bank erosion management 146-151**

8.1 Existing flood and erosion management practices in Brahmaputra 146

8.2 Promising erosion management options for Brahmaputra 148

**Chapter 9 Summary and conclusions 152-165**

9.1 Genesis and deposition of sediments in Brahmaputra 153

9.2 Physico-chemical properties of sediments of Brahmaputra 156

9.3 Geochemical evaluation of bank materials 157

9.4 Braiding and LULC of the Brahmaputra river 160

9.5 Understanding of geoenvironmental changes in Brahmaputra and solution to the bank erosion problem 162

9.6 Future scope of research 165

**References** 166-198

**Appendices** 199-210

## LIST OF TABLES


| Table no | | Page |
|---|---|---|
| Table 2.1 | Geological settings of different sub-basins of Brahmaputra Basin | 12 |
| Table 2.2 | Heavy metal pollution in different rivers of the world | 15 |
| Table 2.3 | Sediment budget and human & climatic impacts in a few large rivers | 20 |
| Table 2.4 | Classification of erosion mechanism | 23 |
| Table 2.5 | River bank erosion in a few large rivers | 24 |
| Table 3.1 | Particulars of a few large rivers of the world | 31 |
| Table 3.2 | Flood damage in the Brahmaputra valley during 2006 – 2011 | 34 |
| Table 3.3 | Affected areas of Assam and India during high flood years | 35 |
| Table 3.4 | Overall damages due to bank erosion in Assam | 35 |
| Table 3.5 | Reaches under active erosion in Brahmaputra River | 36 |
| Table 3.6 | Extent of erosion in *Rohmoria* | 41 |
| Table 3.7 | Extent of erosion in *Dibrugarh* town | 42 |
| Table 3.8 | Extent of erosion in *Palasbari* area | 45 |
| Table 3.9 | Association of different metal phases extracted | 47 |
| Table 3.10 | Extractants used and extraction condition of modified BCR protocol | 47 |
| Table 3.11 | Minerals and their 2θ values | 49 |
| Table 3.12 | Satellite dataset used in the present study | 51 |
| Table 4.1 | Age of a few large rivers | 55 |
| Table 4.2 | Magnitude-wise distribution of earthquakes for the period of 1920 – 1988 | 56 |
| Table 4.3 | Gradients of a few large rivers of the world | 59 |
| Table 4.4 | Slope of the Brahmaputra River | 59 |
| Table 4.5 | Annual soil loss estimates from water erosion in Northeast India | 62 |
| Table 4.6 | Average width, length and area of reaches | 65 |
| Table 4.7 | Average bed levels of Brahmaputra | 77 |
| Table 4.8 | Sediment load of Brahmaputra from different studies | 83 |
| Table 5.1 | Characteristics of bed materials at different cross sections of | |

| | | |
|---|---|---|
| | Brahmaputra River | 86 |
| Table 5.2 | Metal concentration (average) in suspended sediments | 92 |
| Table 5.3 | $I_{geo}$ values and assessment of sediment quality | 97 |
| Table 6.1 | Descriptive statistics of different parameters of soil samples from erosion sites | 115 |
| Table 6.2 | Descriptive statistics of different parameters of soil samples from non-erosion sites | 115 |
| Table 6.3 | Particle size and corresponding velocities for threshold movement of sediments | 118 |
| Table 6.4 | Correlations matrices of different parameters of all samples | 119 |
| Table 6.5a | Variables in the equation (for the first set of variables) | 120 |
| Table 6.5b | Model Summary (for the first set of variables) | 120 |
| Table 6.6a | Variables in the equation (for the second set of variables) | 120 |
| Table 6.6b | Model Summary (for the second set of variables) | 120 |
| Table 7.1 | Different approaches for calculation of braiding indices | 124 |
| Table 7.2 | Length of the center line, the widest channel, mid-channels and sandbars | 127 |
| Table 7.3 | Fraction of area covered by bars, number of mid-channel bars and maximum width and length of reaches in 1973 | 128 |
| Table 7.4 | Fraction of area covered by bars, number of mid-channel bars and maximum width and length of reaches in 2014 | 128 |
| Table 7.5 | Braiding parameters of Brahmaputra river from different approaches | 130 |
| Table 7.6 | Correlation matrix of different braiding parameters | 132 |
| Table 7.7 | Braiding pattern of different reaches of Brahmaputra in Assam | 133 |
| Table 7.8 | LULC of Brahmaputra River in post monsoon months of 1994 and 2014 1994 | 142 |
| Table 7.9 | LULC change of Brahmaputra River during 1994 – 2014 | 142 |

## LIST OF FIGURES


| Figure no | | Page |
|---|---|---|
| Figure 1.1 | Hjulström diagram | 3 |
| Figure 1.2 | Main channel patterns in selected larger river reaches | 7 |
| Figure 2.1 | Conceptual model of dynamically linked sediment properties and processes that affect sediment erodibility | 25 |
| Figure 3.1 | Location of the Angsi glacier | 31 |
| Figure 3.2 | The Brahmaputra River system within India | 32 |
| Figure 3.3 | Flood damage in Assam during 1953 – 2006 | 34 |
| Figure 3.4 | Linked hydrological, hydraulic, geochemical and geotechnical factors responsible for bank erosion | 36 |
| Figure 3.5 | Sampling locations for suspended and bed sediments | 39 |
| Figure 3.6 | Major erosion sites of Brahmaputra River main stem in Assam and sampling locations | 40 |
| Figure 3.7 | Erosion sites of *Rohmoria* | 41 |
| Figure 3.8 | Erosion sites of *Dibrugarh* | 42 |
| Figure 3.9 | Erosion site of *Nematighat* | 43 |
| Figure 3.10 | Erosion sites and non-erosion sites of *Majuli* | 43 |
| Figure 3.11 | Erosion sites of *Gamerighat* | 44 |
| Figure 3.12 | Erosion sites of *Palasbari* | 44 |
| Figure 3.13 | Collection of samples from *Palasbari* erosion site | 45 |
| Figure 3.14 | Sixteen reaches of Brahmaputra River in Assam | 53 |
| Figure 4.1 | Water levels of Brahmaputra at *Dibrugarh* during 1913 – 1990 | 56 |
| Figure 4.2 | Slope of Brahmaputra River | 60 |
| Figure 4.3 | Braided pattern of Brahmaputra | 61 |
| Figure 4.4 | Sediment concentration of Brahmaputra at *Pandu* site during 1955 – 1983 | 62 |
| Figure 4.5 | Contribution of suspended sediment load by tributaries to Brahmaputra | 63 |
| Figure 4.6 | Average sediment load of the major tributaries of | |

| | | |
|---|---|---|
| | Brahmaputra | 64 |
| Figure 4.7 | Twenty cross-sections of Brahmaputra River identified for present study | 65 |
| Figure 4.8 | Scour and deposition in the Brahmaputra | 66 |
| Figure 4.9 | Deposition/ scour in different reaches in different periods | 67 |
| Figure 4.10 | Net deposition/ scour in all the reaches in different periods | 67 |
| Figure 4.11 | Net deposition/ scour in different reaches during 1957– 89 | 67 |
| Figure 4.12 | Shifting of bank line of Brahmaputra from 1911– 28 | 69 |
| Figure 4.13 | Erosion/ deposition in Brahmaputra during 1973 – 2014 at reach no 1 & 2 | 70 |
| Figure 4.14 | Erosion/ deposition in Brahmaputra during 1973 – 2014 at reach no 3 & 4 | 71 |
| Figure 4.15 | Erosion/ deposition in Brahmaputra during 1973 – 2014 at reach no 5 & 6 | 71 |
| Figure 4.16 | Erosion/ deposition in Brahmaputra during 1973 – 2014 at reach no 7 & 8 | 72 |
| Figure 4.17 | Erosion/ deposition in Brahmaputra during 1973 – 2014 at reach no 9 & 10 | 72 |
| Figure 4.18 | Erosion/ deposition in Brahmaputra during 1973 – 2014 at reach no 11 & 12 | 72 |
| Figure 4.19 | Erosion/ deposition in Brahmaputra during 1973 – 2014 at reach no 13 & 14 | 73 |
| Figure 4.20 | Erosion/ deposition in Brahmaputra during 1973 – 2014 at reach no 15 & 16 | 73 |
| Figure 4.21 | Erosion and deposition in different reaches (1 at the upstream, 16 at the downstream) of Brahmaputra during 1973 – 2014 | 75 |
| Figure 4.22 | Main channel of Brahmaputra in 1973, 1994 and 2014 | 76 |
| Figure 4.23 | Bed slope variation in Brahmaputra in 1971, 1977, 1981 & 1971 – 1981 | 77 |
| Figure 4.24 | Rivers/ tributaries within Assam with high sediment load | 80 |
| Figure 4.25 | A sediment budget for Brahmaputra River in Assam | 82 |

| | | |
|---|---|---|
| Figure 5.1 | Variation of $(d_{50})_x/(d_{50})_o$ with x | 87 |
| Figure 5.2 | Variation of $(d_{50})_x/(d_{50})_o$ with $x/(d_{50})_o$ | 87 |
| Figure 5.3 | Variation of $\sigma_g$ with $d_{50}$ | 87 |
| Figure 5.4 | Concentrations of Fe, Mn, Cu, Pb, Zn & Ni in suspended sediments during pre-monsoon, monsoon and post-monsoon months | 88 |
| Figure 5.5 | Particle size distribution of suspended sediments at location 1 | 89 |
| Figure 5.6 | X-Ray diffractogram of suspended sediment at location 1 | 89 |
| Figure 5.7 | X-Ray diffractogram of suspended sediment at location 6 | 90 |
| Figure 5.8 | EDX of suspended sediments during monsoon | 90 |
| Figure 5.9 | EDX of suspended sediments during non-monsoon | 90 |
| Figure 5.10 | SEM image of suspended sediment of location 3 | 91 |
| Figure 5.11 | SEM image of suspended sediment of location 5 | 91 |
| Figure 5.12 | Percentage of different fractions of metals | 92 |
| Figure 5.13 | Organic content and carbonate content in bed sediments | 95 |
| Figure 5.14 | Particle size distribution of bed sediments | 96 |
| Figure 5.15 | X-Ray diffractogram of bed sediment at location 1 | 96 |
| Figure 5.16 | X-Ray diffractogram of bed sediment at location 6 | 96 |
| Figure 5.17 | Geo-accumulation indices of metals at different locations | 97 |
| Figure 6.1 (a-b) | pH, OC and CC of bank materials of erosion site *A* | 99 |
| Figure 6.1 (c-e) | SAR, ESP and CEC of bank materials of erosion site *A* | 100 |
| Figure 6.1f | Particle size distribution of bank materials of erosion site *A* | 100 |
| Figure 6.1g | SEM images of bank materials of erosion site *A* | 100 |
| Figure 6.1h | EDX of bank materials of erosion site *A* | 101 |
| Figure 6.1i | XRD of bank materials of erosion site *A* | 101 |
| Figure 6.2 (a-b) | pH, OC and CC of bank materials of erosion site *B* | 102 |
| Figure 6.2 (c-e) | SAR, ESP and CEC of bank materials of erosion site *B* | 103 |
| Figure 6.2 (f) | Particle size distribution of bank materials of erosion site *B* | 103 |
| Figure 6.2 (g) | XRD of bank materials of erosion site *B* | 103 |
| Figure 6.3 | Composite structure of river bank in erosion site *B* | 104 |
| Figure 6.4 | Loose structure of river bank in erosion site *C* | 105 |

| | | |
|---|---|---|
| Figure 6.5 (a-e) | pH, OC, CC, SAR, ESP and CEC of bank materials of erosion site *C* | 105 |
| Figure 6.5f | Particle size distribution of bank materials of erosion site C | 106 |
| Figure 6.6 (a-b) | pH, OC & CC of bank materials of non-eroded sites of *D1* | 106 |
| Figure 6.6 (c-e) | SAR, ESP and CEC of bank materials of non-eroded sites of *D1* | 107 |
| Figure 6.6f | Particle size distribution of bank materials of non-eroded site *D1* | 107 |
| Figure 6.6(g-h) | pH, OC & CC of bank materials of non-eroded sites of *D5* | 107 |
| Figure 6.6 (i-k) | SAR, ESP and CEC of bank materials of non-eroded sites of *D5* | 108 |
| Figure 6.6l | Particle size distribution of bank materials of non-eroded sites of *D5* | 108 |
| Figure 6.7 (a-c) | pH of bank materials of erosion sites of *D3, D6* and *D8* | 109 |
| Figure 6.7 (d-k) | OC, CC, SAR, ESP and CEC of bank materials of erosion sites *D* | 109 |
| Figure 6.7l | Particle size distribution of bank materials of erosion sites of *D* | 110 |
| Figure 6.8 | Bank failure of a composite bank in erosion site *D* | 110 |
| Figure 6.9 (a-f) | pH, OC, CC, SAR, ESP, CEC and particle size distribution of bank materials of erosion site *E* | 111 |
| Figure 6.10 (a-e) | pH, OC, CC, SAR, ESP and CEC of bank materials of erosion site *E* | 112 |
| Figure 6.10f | Particle size distribution of bank materials of erosion site *F* | 112 |
| Figure 6.10g | SEM images of bank materials of erosion site *F* | 113 |
| Figure 6.10h | EDX of bank materials of erosion site *F* | 113 |
| Figure 6.10i | XRD of bank materials of erosion site *F* | 113 |
| Figure 6.11 | Direct shear test results of bank materials | 117 |
| Figure 7.1 | Main channel, center line, mid-channels and sandbar length in different reaches in 1973 | 125 |
| Figure 7.2 | Main channel, center line, mid-channels and sandbar | |

| | | |
|---|---|---|
| | length in different reaches in 2014 | 126 |
| Figure 7.3 | Braiding index of Brahmaputra River at different reaches calculated by different approaches | 131 |
| Figure 7.4 | % change of braiding parameters of Brahmaputra River during 1973 – 2014 at different reaches | 131 |
| Figure 7.5a | LULC of Brahmaputra in reach no 1 and 2 during post-monsoon months of 1994 and 2014 | 134 |
| Figure 7.5b | LULC of Brahmaputra in reach no 3 and 4 during post-monsoon months of 1994 and 2014 | 135 |
| Figure 7.5c | LULC of Brahmaputra in reach no 5 and 6 during post-monsoon months of 1994 and 2014 | 136 |
| Figure 7.5d | LULC of Brahmaputra in reach no 7 and 8 during post-monsoon months of 1994 and 2014 | 137 |
| Figure 7.5e | LULC of Brahmaputra in reach no 9 and 10 during post-monsoon months of 1994 and 2014 | 138 |
| Figure 7.5f | LULC of Brahmaputra in reach no 11 and 12 during post-monsoon months of 1994 and 2014 | 139 |
| Figure 7.5g | LULC of Brahmaputra in reach no 13 and 14 during post-monsoon months of 1994 and 2014 | 139 |
| Figure 7.5h | LULC of Brahmaputra in reach no 15 and 16 during post-monsoon months of 1994 and 2014 | 140 |
| Figure 7.6 | LULC of Brahmaputra in post-monsoon months in 1994 and 2014 | 145 |
| Figure 7.7 | LULC of Brahmaputra in Post monsoon months during 1994 – 2014 | 145 |

## ABBREVIATIONS

| | |
|---|---|
| Ag | : silver |
| Al | : aluminum |
| As | : arsenic |
| Au | : gold |
| B | : braiding |
| BCR | : Bureau Commune de Reference of the European |
| C | : chlorite |
| C/S | : cross-section |
| Ca | : calcium |
| CC | : carbonate content |
| Cd | : cadmium |
| CEC | : cation exchange capacity |
| cm | : centimetre |
| CPS | : counts per second |
| Cr | : chromium |
| Cu | : copper |
| EDX | : energy-dispersive X-ray spectroscopy |
| EPA | : Environmental Protection Agency |
| ERDAS | : Earth Resources Data Analysis System |
| Fe | : iron |
| g | : gram |
| GBM | : Ganges-Brahmaputra-Meghna |
| GIS | : geographic information system |
| Gt | : gigaton |
| ha | : hectare |
| Hg | : mercury |
| HKH | : Hindu Kush Himalaya |
| I | : illite |
| IRS | : Indian Remote Sensing |
| JCPDS | : Joint Committee on Powder Diffraction Standards |

| | |
|---|---|
| K | : kaolinite |
| kg | : kilogram |
| km | : kilometre |
| LOI | : loss on ignition |
| LULC | : land use and land cover |
| LUCC | : land use/ cover change |
| M | : montmorillonite |
| m | : metre |
| Mg | : magnesium |
| Mn | : manganese |
| msl | : mean sea level |
| MSS | : multi-spectral scanner |
| Mt | : megaton |
| Mu | : muscovite |
| Na | : sodium |
| NASA | : National Aeronautics and Space Administration |
| NEC | : North Eastern Council |
| Ni | : nickel |
| OC | : organic content |
| OLI | : operational land imager |
| P | : potassium |
| Pb | : lead |
| PFI | : Plan Form Index |
| pH | : power of hydrogen or potential of hydrogen |
| PTFE | : polytetrafluoroethylene |
| PWD | : Public Works Department |
| Q | : quartz |
| R&D | : research and development |
| RCC | : reinforced cement concrete |
| SAR | : sodium adsorption ratio |
| SEM | : scanning electron microscope |
| SPSS | : Statistical Package of Social Sciences |

| | |
|---|---|
| t | : ton |
| TGR | : Three Gorges Reservoir |
| TM | : thematic mapper |
| USEPA | : United States Environmental Protection Agency |
| USGS | : United States Geological Survey |
| UTM | : Universal Transverse Mercator |
| WGS84 | : World Geodetic System 1984 |
| WRD | : Water Resources Department |
| XRD | : X-ray diffractrogram |
| y | : year |
| Zn | : zinc |

Chapter 1

# Introduction

## 1.1 Introduction to sediments

Sediment is naturally occurring substance, originally derived from underlying bedrocks, which is broken down by weathering and erosion and is subsequently transported by the action of fluids such as wind, water or ice and/ or by the force of gravity acting on the particle itself. Although the term is often used to indicate soil-based mineral matter, decomposing organic substances and inorganic biogenic materials are also considered sediment (Wetzel, 2001). Most mineral sediments come from erosion and weathering, while organic sediment is typically detritus and decomposing material such as algae (EPA, 2014).

Weathering, breakdown of rocks at the Earth's surface to form discrete particles (Ollier, 1969), can be classified into three types: physical, chemical and biological (Selley, 2000). Climate, parent material, topography and organic activity are the variables which determine rates and types of weathering. Different processes of physical weathering are: breakdown due to stress exerted by the growth of crystals of ice or salt in rock crevices; pressure release caused by the denudation and removal of layers of overlying rocks; expansion and contraction caused by heating and cooling due to wild fire or solar radiation; and freeze-thaw action in mountainous regions with fluctuating temperature. The

main processes in chemical weathering are hydrolysis, carbonation, solution and oxidation. Formation of new minerals, principally the clays is an important result of chemical weathering (Wilson, 1999). Biological weathering is due to organic processes, which include both biochemical solution, brought about largely by the action of bacteria, and humic acids derived from rotting organic matter, as well as physical fracturing of rock, which may be caused by agents such as tree roots (Selley, 2000).

Newly formed sediment from bedrock is removed by the process of erosion. The word 'erosion' comes from 'erodere', a Latin verb meaning 'gnaw'. Erosion is what usually happens to the material loosened by weathering. Driving force for the process of particle entrainment is provided by the combined effect of two fluid forces, i.e., a drag force and a lift force, exerted on the particle by the flow. Coarse materials are transported as bed load along the bed of a river through rolling, sliding or saltation. Finer materials are carried aloft, suspended above the channel bed by turbulent eddies, and is transported downstream as suspended load and wash load by the process of advection and turbulent diffusion. Supply of fine material to a river is controlled by water discharge, rainfall intensity, antecedent temperature, moisture and discharge conditions, hydrograph shape and temporal variations in surface condition and vegetative cover (Walling, 1995). It is assumed that bed load represents some 10% of suspended or total load (Hay, 1998). Sediment is deposited in different circumstances and deposition is controlled by the bed shear stress, turbulence processes in the zone near the bed, settling velocity, type of sediment, depth of flow, suspension concentration and ionic constitution of the suspending fluid (Mehta and Partheniades, 1973). Bed load is deposited when the local bed shear stress falls below the critical shear stress for a given particle. Deposition of suspended load occurs when the fall velocity dominates over turbulent diffusion.

Hjulström diagram (Figure 1.1) proposed by F. Hjulström (1935) shows whether, for a given velocity, particles will be transported, deposited or eroded. The lower curve is the minimum velocity for given particle sizes at which sediments may continue to be transported (if previously eroded). The upper curve is the minimum velocity required to initially erode various particle sizes from the stream bed. For particles of a given size, at

flow velocities above the critical erosion velocity, which is in the erosion zone of the graph, stationary particles on the river bed will be scoured and transported by the river. Below the velocity needed to set particles in motion, particles that are already being carried by the river will continue to be transported, so long as the velocity remains in the transport zone of the graph. Only when the velocity drops below the mean settling velocity, and enters the deposition zone, the particles will be deposited.

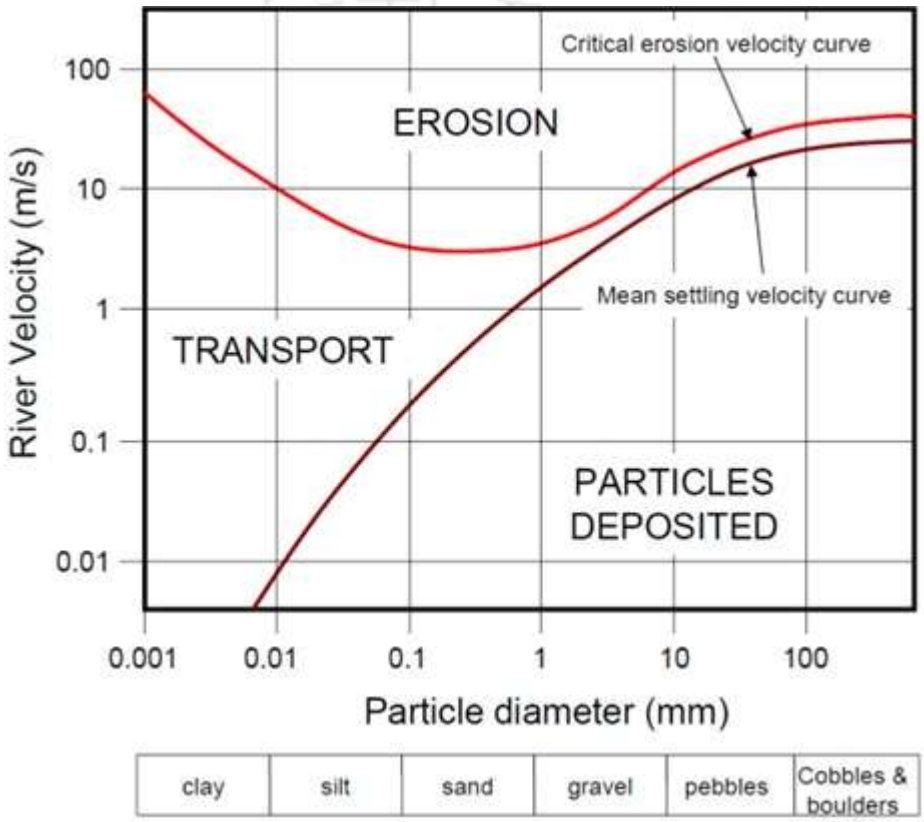


**Figure 1.1** Hjulström diagram

Erosion, transportation and deposition are the three major processes in a fluvial system (Schumm, 1977) and these are influenced by supply of sediment at the upstream end and sediment that is locally eroded from bed and banks (Charlton, 2008). Bank erosion is a major contributor of sediment load to many streams and rivers (Simon and Darby, 1999; Sekely et al., 2002; Evans et al., 2006; Wilson et al., 2008). Detachment and entrainment are the two distinct events of bank erosion (Thorne, 1991). Non-cohesive bank material is usually detached and entrained grain by grain, whereas cohesive bank material is eroded by aggregates of soil. Physico-chemical properties of the soil and the chemistry of the pore

and eroding fluids determine the erosion resistance of cohesive banks (Arulanandan et al., 1980). Alluvial banks often consist of layers of non-cohesive and cohesive materials and presence of a weak non-cohesive layer in a stratified bank can greatly reduce its resistance to bank retreat through fluvial erosion (Thorne, 1978; Pizzuto, 1984). Stability of a bank and its characteristic mode of failure depend on the geotechnical and geological properties of the bank materials (Thorne, 1991). Soil erosion is a physical process with considerable variation globally in its severity and frequency; but location and timing of erosion are also influenced by social, economic, political and institutional factors (Suif et al., 2013).

## 1.2 Sediments: physical and chemical characteristics

The physico-chemical properties of sediments commonly have been explained as reflecting the composition of the source rocks, mechanical and chemical weathering, winnowing & sorting, climate, and several other factors (Piper et al., 2006; Gilbert, 1917; Russell, 1937; Gibbs, 1967 and Knox, 2001). Investigation of sediment quality has been seen as a logical extension to studies of sediment dynamics and yields, and has the potential to further understanding of sediment behavior in rivers (Web et al., 1995). Sediment characteristics depend on climate, rock types, land use, the presence of dams, and events like floods, erosion, volcanic eruptions, and earthquakes that bring loose materials into a river (Eisma, 1993). The nature and amount of particles transported by rivers depend on weathering regime in a catchment area. Mechanical weathering regime generates a high proportion of immature particles that are transported in the river. In a transport limited regime, chemical weathering is faster than physical weathering (Carson and Kirby, 1972; Stallard and Edmond, 1983).

Particle size, shape, fall velocity are physical properties of particles, whereas size distribution, specific weight, angle of repose are properties of mixtures. The Sub-committee on Sediment Terminology of the American Geophysical Union proposed grade scale for size of sediment particles (Lane, 1947), which contains six consecutive size classes namely boulders, cobbles, gravel, sand, silt, and clay. Nominal diameter, sieve diameter, sedimentation diameter and fall diameter are generally used to express size of natural sediment particles. Particle size analysis throws light on provenance (Weltje and

Prins, 2007), transportation dynamics (deposition/ resuspension) (Singh et al., 2007), and pollutant adsorption potential (Fontaine et al., 2000) of sediments in a river. During transportation process, sediment size is reduced on its way by wear and sorting and the size distribution narrows (Raudkivi, 1999). Coarse-grained sediments generally have a limited transportation history and are often sourced from a limited continental area. By contrast, fine-grained river sediments consist of large amounts of particles with history of long distance transportation. The fine-grained particles are usually derived from a large continental region (Chaudhuri et al., 1992). Examination of mineralogical, mineral-magnetic, chemical, organic, radiometric, isotopic and physical characteristics of sediments allows tracing of original source of sediments by the technique of sediment fingerprinting (Collins et al., 1997).

Understanding of physico-chemical characteristics of river sediment is important as sediment strata serve as a significant habitat for the benthic macro invertebrates whose metabolic activities contribute to aquatic productivity (Abowei and Sikoki, 2005). Excessive levels of suspended load tend to have negative impacts on aquatic life (Kemker, 2014) whereas too little sediment transport can lead to nutrient depletion in floodplains and marshes, diminishing the habitat and vegetative growth (Czuba et al., 2011). Sediment properties are necessary in investigating the movement and transport of nutrients, contaminants, and pollutants through sediment particles. Due to smaller particles' high ratio of surface area to volume, clay particles can account for a large amount of adsorbed and/or partitioned mass of the pollutant in solution (Dunnivant et al., 2006). Sediments act both as source and sink of pollutants by desorption from and sorption into it (Förstner, 1987; González et al., 2000). Sediments have provided more significant tools for the better clarification of the origin identification and partitioning dynamics of heavy metals than the analysis of the overlying water column (Alonso Castillo et al., 2013). Sediments are the main abiotic reservoirs, where persistent organic pollutants (POPs) from different emission sources are accumulated (Eljarrat and Bercelo, 2009). During flood and bank erosion, soil and sediments wash into rivers, the particles aggregate and form larger particles that will settle in calm (quiescent) waters. When these particles have accumulated pollutants, the settling of these particles to the sediments can act as a removal mechanism for pollutants.

Over time, and when clean water and sediment return to the water body, the pollution will be buried by clean material and removed from interaction with the ecosystem. These sediments may be released to the overlying water under suitable conditions of turbulence, change in pH etc. and hence, deposited contaminated sediment was termed as 'Chemical time bomb' by Stigliani (1991). Again, the pollutants accumulated in the river bed sediment may affect the bio-community through food chain for a long period of time (Yi et al., 2008).

### 1.3 Role of sediments in river morphology

The evolution of alluvial rivers in nature, such as riverbed deformation, sandbar deposition, river broadening accompanied with bank collapse are triggered by the interaction of flow and riverbed or bank in the form of sediment transport (Zhang, 1989). Thus, morphology of an alluvial river channel is the consequence of sediment transport and sedimentation in the river (Church, 2006). Sediment discharge is a dependent river variable for short term period and independent variable for long-term equilibrium (Schumm, 1971, Chang, 1988). Sediment supply along with flow regime controls channel form. Main channel patterns in a few selected larger river reaches are shown in Figure 1.2.

Overloading of sediments and steep slopes are the primary causes of braided channels (Lane, 1957). Various conditions associated with braided channels are abundant bed load, erodible banks, high stream power, and highly variable discharge. However, braided channels can also form under conditions of constant discharge (Leopold and Wolman, 1957; Ashmore, 1991).

There is a balance, described as a qualitative equation by Lane in 1955, between the supply of bed load at the upstream end of a channel reach and the stream power available to transport it. If both the variables are balanced, neither erosion nor deposition will predominate. Increase of volume or caliber of the sediment load in relation to the available stream power leads to aggradation with net deposition along the reach. When the stream power exceeds, degradation predominates. Sediments accumulate on flood-plain surfaces

by various processes of accretion, i.e., vertical, lateral and braid bar accretion (Nanson and Croke, 1992).

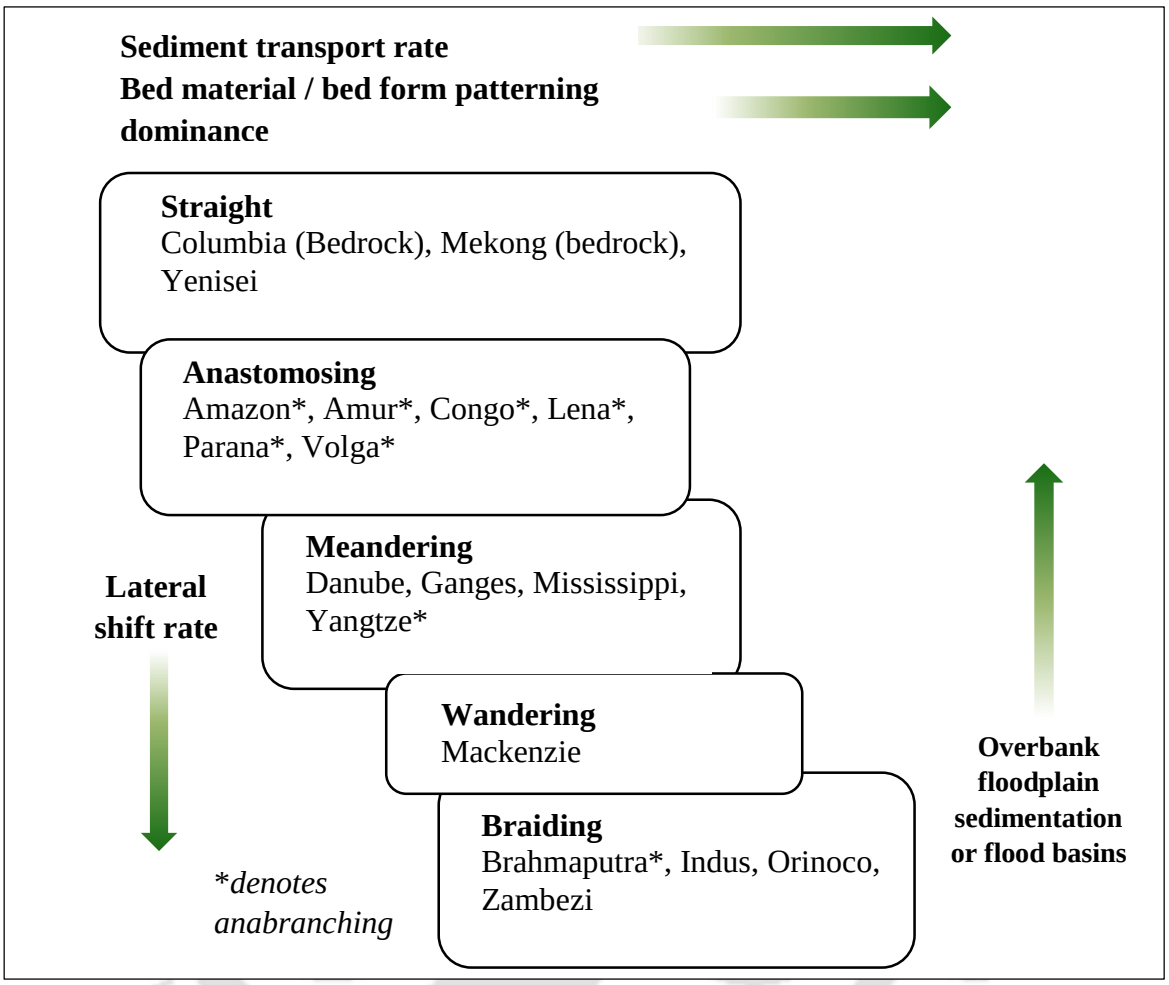


**Figure 1.2** Main channel patterns in selected larger river reaches (from Ashworth and Lewin, 2012; Lewin and Ashworth, 2014)

Both floods and erosion have direct links to sediment dynamics of a river. The amount of water on the floodplains and the amount exchanged with river channels are essential information for understanding the sediment delivery and nutrient exchanges that occur between the rivers and floodplains. The rivers of the world annually discharge about 35,000 $km^3$ of freshwater and 20-22×$10^9$ ton of solid and dissolved sediment to the ocean (Milliman and Meade, 1983; Milliman and Syvitski, 1992). Asian rivers contribute about 50% of sediment flux to world oceans (Milliman and Meade, 1983). Sediment load of the Himalayan rivers is disproportionally (~4 times) high compared to the fraction of areal

coverage of the rivers to the global drainage area, underscoring the important role of physical erosion in these river basins on the global sedimentary budget (Tripathy et al., 2014). However, most of the large rivers of Hindu Kush Himalayan region have been subject to a dramatic decline in sediment loads in recent years, due to both climate change and human impacts. The total sediment load transported from HKH and neighbouring regions to the oceans has decreased from about 4.3 Gt $y^{-1}$ prior to the 1980s, to ~2.1 Gt $y^{-1}$ currently (Liu et al., 2009). The ranking of the large Asian rivers in terms of the annual sediment fluxes to the oceans has changed from the Brahmaputra, Huanghe, Ganges, Changjiang, and Irrawaddy in the pre-1980s to the Brahmaputra, Irrawaddy, Ganges, Changjiang, and Mekong in the post-1990s (Liu et al., 2009). 30-50% river-derived sediments of the Tibetan rivers are trapped in the river's low reaches and contribute to extensive floodplain and delta plain development in eastern and southern Asia while the rest is discharged to the sea (Liu et al., 2009).

## 1.4 Objectives of the study

Tibetan plateau, the 'Water Tower' of Asia, is the source of almost all of Asia's major rivers: Yellow, Yangtze, Mekong, Salween, Ganges, Indus, Irrawaddy and Yarlung Tsangpo (which becomes Brahmaputra downstream). Compared to other large rivers like Amazon, Congo and Mississippi, where the channel patterns are developed in basins with gentle slopes with fairly homogenous and stable underlying geological structure with little or no control on river morphology (Twidale, 2004); Tibetan drainage systems are complex and distinct with different sub-basins. Tibetan drainage systems have been developed in a setting where the underlying geological structure is heterogeneous and active, and is the major factor controlling the course of rivers and the landscapes they carve out (Tandon and Sinha, 2007). Among the Tibetan rivers, the Brahmaputra is unique due to its peculiar drainage pattern, diverse geological setting, high sediment load and critical erosion problem. Brahmaputra is one among the large alluvial rivers (Coleman, 1969; Bristow, 1987) with plain widths of up to 20 km, individual channel widths of several kilometers and maximum scour depths of up to 50 km (Hassan and Galapatti, 2014). Brahmaputra supplies an estimated 1000 million ton of suspended material to the Bay of Bengal (Milliman and Meade, 1983; Milliman and Syvitski, 1992; Hay, 1998). There is additional

strong indication that erosion is a major factor of river instability in Brahmaputra due to the very large amount of sediment intrusion from bank erosion itself. This sediment causes further instability downstream, triggers more bank erosion, and apart from loss of land and flood protection, hampers navigation (ADB, 2007).

Role of sediments including bank material properties in overall process of erosion in a large alluvial river like Brahmaputra has not yet been explored adequately. In this research work, an attempt has been made to explore influence of sediment properties and processes on geoenvironmental aspects of Brahmaputra River in its valley part. The main objectives have been

i) To study the genesis and deposition of sediments in Brahmaputra River to understand the source and sink of sediments.

ii) To study the physico-chemical properties of sediments of Brahmaputra to evaluate their environmental behavior.

iii) To examine geochemical properties of river bank materials to evaluate their role in bank erosion.

iv) To study the braiding and land use & land cover change of Brahmaputra River.

v) To develop an understanding of the geoenvironmental changes brought about by sediment properties and processes towards seeking a solution to the critical bank erosion problem of Brahmaputra.

## 1.5 Organization of the thesis

The outcome of the study on **Sediment properties and processes influencing key geoenvironmental aspects of a large alluvial river, the Brahmaputra in Assam** is subdivided into nine chapters. Following this introduction chapter (Chapter 1), **Chapter 2** reviews literature in three aspects:

i) Sediment properties of Brahmaputra and other large rivers

ii) Geochemical properties of bank materials as a facilitator of erosion, and

iii) Bank erosion in other large rivers of the world.

**Chapter 3** outlines the study area, methodology used for collection and analysis of the samples, instruments used and tools and procedures followed to arrive at the results and findings.

**Results and discussions** are described in five chapters, from chapter 4 to chapter 8.

**Chapter 4** synthesizes findings on various aspects of sediments of Brahmaputra obtained from secondary sources. Causes and sources of high sediment, aggradation and degradation of the river, shifting of bank-line, bank erosion and a sediment budget using mass-balance equation are discussed in the chapter.

**Chapter 5** covers physico-chemical properties of sediments of Brahmaputra based on analysis of suspended sediment and bed sediment samples collected from different locations of Brahmaputra River within Assam.

**Chapter 6** covers geochemical evaluation of bank materials of both the erosion sites and non-erosion sites of Brahmaputra River. Role of geochemical properties of bank materials in the bank erosion is discussed.

**Chapter 7** discusses braiding and land use and land cover of Brahmaputra River in post-monsoon months using remote sensing and GIS tools.

**Chapter 8** discusses existing flood and erosion management measures. Based on understanding of sediment properties and processes of Brahmaputra, a few strategies are suggested for sustainable solution of bank erosion problem.

**Chapter 9** provides a summary and conclusions of the research work with future scope.

A reference section is included at the end, followed by appendices.

Chapter 2

# Review of literature

## 2.1 Sediment properties of Brahmaputra and other large rivers

### 2.1.1 Physical properties

A strong heterogeneity in terms of concentration and chemical composition has been observed in sediment vertical depth profiles of large rivers (Lupker et al., 2013). The mineralogy of sediments from the Himalayan system is dominated by quartz, micas and feldspar, with occurrences of other phyllosilicates, clay assemblages and hydroxides in the finer fraction (Garzanti et al., 2010, 2011). These minerals are segregated during sediment transport: coarse-grained quartz is enriched in the bed load and at the bottom of the water column while phyllosilicates such as micas and clays are comparatively enriched in the shallow surface waters of the river.

The Ganges-Brahmaputra-Meghna (GBM) river system is the primary conduit of Himalayan sediments to the Bay of Bengal, and the river system carries annually an estimated 1060 million ton of suspended solids, more than 1330 $km^3$ of water, and more than 173 million ton of total dissolved load to the Bay of Bengal (Milliman et al., 1995). GBM is the largest sediment dispersal system in the world (Kuehl et al., 1989) and shows the highest rate of chemical denudation in the Bengal Basin on a global scale (Datta and Subramanian 1997a). Brahmaputra exhibits significantly higher rate of physical and

chemical weathering than other large Himalayan catchments (Sarin et al., 1989; Harris et al., 1998; Galy and France-Lanord, 1999; Galy and France-Lanord, 2001; Dalai et al., 2002; Singh and France-Lanord, 2002; Singh et al., 2005). Spatially averaged chemical denudation rate in the Brahmaputra basin (105 t $km^{-2}$ $y^{-1}$; Sarin et al., 1989) are 2–3 times greater than the next largest Himalayan river, the Ganges (Galy and France-Lanord, 1999), and 5 times greater than the world average (Sarin et al., 1989). The Brahmaputra basin is underlain, for most part, by very young and un-weathered sedimentary formations and therefore, the river carries mainly fine sand and silt with little amount of clay (Goswami, 1998). Geological settings of different sub-basins of the Brahmaputra basin are mentioned in Table 2.1.

**Table 2.1** Geological settings of different sub-basins of the Brahmaputra basin

| Region | Geological settings |
|---|---|
| Tibet | Sedimentary rocks and gabbros, dolerite of the Trans-Himalayan plutonic batholiths and granites |
| Eastern syntaxis | Gneisses and calc-alkaline pluton of the Trans-Himalayan plutonic belt |
| Eastern drainage/ Mishmi hills | Calc-alkaline diorite-grano-diorite-tonalite rocks of Trans Himalayan plutonic belt |
| Himalaya | In the Lesser Himalaya, crystallines and sedimentaries, quartzite, dolomite and limestone |
| Southern drainage | Ophiolites of Naga Patkai ranges |

Brahmaputra sands (2.1±0.4 ϕ) tend to be coarser than Ganga (2.3±0.3 ϕ) and Padma–Meghna sands (2.5±1.5 ϕ). Mahanta and Subramanian (2004) had explained that in Brahmaputra the detrital contribution in the form of quartz, feldspar and mica make up more than 80% of the suspended sediment upstream. Then, it is gradually decreases downstream. The chemistry of bed sediments of Brahmaputra River differs from the world average river sediments due to the dominance of high silica minerals (quartz) in the bed load. It was mentioned that clay minerals showed an increasing trend as the river flow downstream. Chlorite, illite and kaolinite form more than 95% of the total clay minerals. Illites, being much more dominant in the upstream, suggest its primary origin to be from the granitic and metamorphic source rocks as a result of pre-dominant physical weathering in the cold and dry climate of the Tibetan Plateau.

Textural properties of the bed sediments of the Ganges river tributaries are characterized by predominance of fine to very fine sand, medium to fine sand, and very fine sand to clay respectively (Singh et al., 2007). Downstream textural variation in bed load and suspended load of the river are complex and are strongly influenced by lateral sediment inputs by the tributaries and channel slope. Mica dominates among the clay minerals, followed by chlorite, vermiculite, kaolinite, and smectite.

Viers et al. (2009) presented a new database on the chemical composition of suspended matter in the World Rivers, together with the associated elemental fluxes. With the exception of Ca, Mg, K and Na, most of the elements are mainly transported by the solid phase. High metal concentrations in the suspended sediment do not necessarily reflect inputs from human activities. High concentrations may result from a specific lithology.

### 2.1.2 Chemical properties: metal concentration in river sediments

Sediment acts both as source and sink of pollutants and many researchers have worked on the chemical characteristics of sediments, especially heavy metal concentrations. Heavy metal refers to any metallic element that has a relatively high density and is toxic or poisonous even at low concentration (Lenntech, 2004). "Heavy metals" is a general collective term, which applies to the group of metals and metalloids with atomic density greater than 4 g/cm$^3$, or 5 times or more, greater than water (Hutton and Symon, 1986; Battarbee et al., 1988; Nriagu and Pacyna 1988; Nriagu, 1989; Garbarino et al., 1995, Hawkes, 1997). However, being a heavy metal has little to do with density but concerns chemical properties. Heavy metals include lead (Pb), cadmium (Cd), zinc (Zn), mercury (Hg), arsenic (As), silver (Ag) chromium (Cr), copper (Cu) iron (Fe), and the platinum group elements.

Sources of metals in the environment may be natural (erosion, weathering and volcanic activity), anthropogenic (agricultural runoff, industrial discharge, rapid urbanization, mining etc.) or a hybrid of both (Pandey et al., 2014). Heavy metals are incorporated as trace elements into the crystal lattice of the primary minerals formed during cooling of magma by the process of isomorphic substitution (Bradl, 2005). Agricultural activities and

industrial activities are the major anthropogenic sources of heavy metal pollution. 90–99% of the total metal load in rivers is transported in the particulate phase, depending on the geochemical behavior of the metal and the nature of the physical and chemical environment (Miller, 1997).

Information on total metal concentrations is not sufficient for the assessment of environmental impact of sediment contamination, which lead to the particular interest of chemical fractionation of sediment (Jain, 2004; Nwuche and Ugoji, 2010). Förstner and Muller (1973) were the first who attempted to quantify the extent of heavy metal pollution in sediments by comparing heavy metals enrichment with the natural concentration of the respective elements in unpolluted sediments. A similar approach was used by Nikiforova and Smirnova (1975) by calculating the 'Technophility Index', that is the ratio of the annual input of a metal to its 'Clarke' concentration (means concentration in the earth's crust). Metal contamination in river sediments and associated eco-toxicity are serious issues in different rivers mainly due to mining, industrial and agricultural activities (Table 2.2). One of the major problems associated with the threat of heavy metals to the ecosystem is the potential for bioaccumulation and biomagnification (Gao and Chen, 2012).

**Table 2.2** Heavy metal pollution in different rivers of the world

| River | Major heavy metals in sediment | Sources of heavy metals | Extent/ impact of heavy metal pollution | References |
|---|---|---|---|---|
| Amazon | Hg | Amalgamation process in gold mining | Contamination of aquatic food chain, risk to fish eating human population | Maurice-Bourgoin et al. (2000), Rabitto et al. (2011) |
| Nile | Fe, Cu, Zn, Pb and Cd | Agricultural, domestic and industrial effluents | Serious pollution in bottom sediments | Ahmed and Fawzi (2009), El Bouraie et al. (2010) |
| Mississippi | Cd and Pb | Mining, agricultural and industrial activities | Sediment Pb and Cd concentrations in delta have been increased by 70% and 200% respectively over the past decades | Trefry and Shokes (1981), Garbarino et al. (1995) |
| Yangtze | Cr, Cd, Hg, Cu, Fe, Zn, Pb, As | Strong chemical weathering, industrial pollution | Bioaccumulation of heavy metals in benthic invertebrates; widespread enrichment of Cd, Cr and Ni in sediment | Qiao et al. (2007), Yi et al. (2008) |
| Yellow | Mn, Cu, Pb, Zn, Cr, Cd | Industrial and agricultural activities | Contamination in river delta, risk to water quality | Rui et al. (2008), Fan et al. (2008) |
| Mekong | Zn, Pb, As, Cr | Mining, industries and urban areas | Less ecological risk of heavy metal due to reservoir trapping and dilution | Fu et al. (2012) |
| Indus | Ag, As, Cd, Cr, Cu, Ni, Pb, Zn and Hg | Agricultural and industrial processes | High metal content in fish species, no reported case of metal toxicity. | Tariq et al. (1996), Gachal et al. (2006) |
| Narmada | Cd, Cu, Ni, Cr, Pb | Municipal waste, agricultural runoff, soil erosion | River sediment is highly polluted with Cd. Low amount of bioavailable heavy metals in water. | Jain et al. (2008) |
| Ganges | Cd, Ni, Pb, Zn, Cu | Atmospheric deposition, industrial effluents | Contamination of agro ecosystems. Accumulation of trace elements in edible shellfish species | Pandey et al. (2014), Mitra et al. (2012) |
| Brahmaputra | Fe, Al, Mn, Zn, Cu, Cr, Pb, Cd | Weathering and soil erosion | Unpolluted sediment quality and unperturbed alluvial basin | Subramanian et al. (1987), Datta and Subramanian (1997b), Mahanta and Subramanian (2004) |

Alagarsamy and Zhang (2005) studied the trace metal geochemistry in Indian and Chinese rivers to understand its variation on a global scale in terms of climate, geological condition and anthropogenic impacts. The suspended sediment chemistry of Indian rivers is less studied than bed sediment (Stummeyer et al., 2002). The suspended sediments are enriched in Fe, Mn and other transition elements relative to bed sediments (Stummeyer et al., 2002).

Nishina et al. (2010) studied pesticide residues in soils, sediments, and vegetables in Red River delta. Samples were collected from agricultural areas within and outside of embankments built to prevent flooding. Due to selective deposition during river flooding, the soils outside of the embankment were more clayey with higher organic matter contents. Clay samples were found to contain more pesticides than the sandy soils.

Mercury contamination was a major environmental issue in the Amazon basin. Maia et al. (2009) highlighted the importance of the hydrology and sediment dynamics of Amazon River and its major tributaries in the exchanges of filtered and particulate Hg between Amazon River and connected floodplain lakes. During the sediment and water exchanges between Amazon River and the connected lakes, Hg was mainly transported in its particulate phase. The maximum total filtered Hg (T-FHg) concentrations in the floodplain lakes coincided with the maximum T-FHg concentrations of Amazon River and are measured during the flooding period. The lowest T-FHg values were observed during the flood peak of the mainstream, during the rainy season, when waters were diluted by the local rainfall. The highest total particulate Hg (T-PHg) concentrations in the lakes were observed during the dry season. In the flooded system, the lakes showed different geochemical characteristics that control the Hg distribution and partition. The mercury mass budget estimated in the study confirmed that the floodplain system acted as a particulate mercury trap, with a net storage of particulate Hg of 150 kg PHg $year^{-1}$.

Compared to other large river of the world, heavy metals in sediments of the Himalayan rivers are still poorly known. Biogeochemistry of Ganges and that of Brahmaputra were found markedly different with respect to heavy metals such as Cu, Fe and Zn (Mahanta and Subramanian, 2004). Although heavy metal pollution is not a serious issue in Brahmaputra

valley, global estimate of river sediments is incomplete without taking into account of high sediment yielding rivers like Brahmaputra.

## 2.2 Sediment dynamics of the major fluvial basins

Geochemical investigation of large rivers gives important information about the biogeochemical cycles of the elements, weathering rates, physical erosion rates and $CO_2$ consumption by the acid degradation of continental rocks (Gaillardet et al., 1997). River waters carry the products of erosion processes over the continents in the form of dissolved salts and suspended particles. Deciphering the message coded in their components helps to describe erosion processes in their entirety (Negrel et al., 1993).

The concept of 'Sediment budget' was coined in Norway (Rapp, 1960) and in the USA in the 1970-80's to account the sources, sinks and redistribution pathways of sediments, solutes and nutrients in a unit region over unit time (Slaymaker, 2003). Construction of detailed sediment budgets (Walling and Collins, 2008) and basin sediment management policies (Owens, 2005) rely on the mean values of the sediment load calculated at the catchment outlet.

The fluvial transport and storage of sediments within channel–floodplain systems can act as important sinks of sediments. For example, in Amazon River, the floodplains act as a temporary storage system of dissolved and particulate elements as well as an exporting system of these elements into the main stream during floods (Maurice-Bourgoin et al., 2007). Dunne et al. (1998) estimated the magnitude of sediment exchange between the channel and the flood plain through the Brazilian sector of Amazon River valley based on sediment sampling and flow records. Deposition on the sand bars and floodplain exceeded bank erosion by 500 Mt $y^{-1}$ over a 10–16 year period. Another 300–400 Mt $y^{-1}$ were deposited in a downstream delta plain. Maurice-Bourgoin et al. (2007) documented the role of an Amazon floodplain for sediment storage from studies on network of gauging, meteorological and sediment monitoring stations and satellite data. The study area, located on the right bank of Amazon River, 900 km upstream of the mouth, contains more than 30 interconnected lakes linked to the mainstream by permanent and temporary channels. With

an open-water area varying between 600 $km^2$ and 2500 $km^2$, it represents ~13% of the total flooded area of Amazon River. Sediment accumulation occurred during the five months of the flood rise, from December to April. The mean average sediment storage calculated varies between 41% and 53% of the annual flux of sediments entering the floodplain through the main channels.

Martinez et al. (2009) attempted to quantify Amazon River sediment budget by looking at data from suspended sediment discharge monitoring network and remote sensing data. Suspended sediment discharge was found to increase by about 20% during 12 years since 1995. An increase in sediment discharge may be attributed to stronger erosion processes caused either by a global change (rainfall), or regional changes (land cover change resulting from deforestation for example) or both.

Knox (2006) used $^{14}C$ and $^{137}Cs$ isotopic dating methods to determine rates of sedimentation and morphologic change for a reach of the upper Mississippi River. The shift from pre-agriculture, natural land cover to landscape dominance by agricultural land use of the last 175–200 years typically increased rates and magnitudes of floodplain sedimentation in the Upper Mississippi Valley. Large floods have frequently provided major increments of sedimentation on floodplains of tributaries and the main valley upper Mississippi River.

Generally the river mouth is the main depocenter of the riverine sediment (Wang et al., 2007). However, in high flood years the picture is different. For example, in the Yangtze River, the amount of sediment discharged to the sea accounts for 68% of the total sediment supplied into the trunk river in the middle and lower reaches. The remaining 32% is deposited in the river channel and linked lakes. Dai and Lu (2010) examined the sediment process in two large flood years, i.e., 1954 and 1998 based on the re-evaluated sediment supply from the tributaries and the data from selected gauge stations on the main channel. 58% and 52% of the total supplied sediment were deposited in the river channel and floodplain in 1954 and 1998 respectively. The floodplains and channels in the middle and lower reaches of Yangtze River played an important role in regulating sediment discharge during extreme flood events.

***Modified sediment load due to human intervention***

Human activities are the most important factors that affect the variation in the pattern of river sediment load (Syvitski et al., 2005; Walling, 2006). Sediment budget and human & climatic impacts in a few large rivers are mentioned in Table 2.3. Liu et al (2008) showed that the average annual sediment yield per area has been decreased significantly in Yellow River over the past 10 years mainly due to impacts of human activities, including the operation of hydropower stations/ reservoirs, construction of dams, as well as soil conservation programs. Liu et al. (2008) showed marked decrease in annual sediment yield at the Lijin Station on the Yellow River in 1961, 1980 and 2000. Before 1960, Yellow River was under essentially natural conditions. From 1960 to 1964, the Sanmenxia reservoir was in operation for impounding water and trapping sediment. Thus, annual sediment transport downstream decreased dramatically. From 1965 to 1973, the operating mode of the Sanmenxia reservoir was changed to provide flood detention and sediment flushing. Thus, both annual sediment transport and runoff increased during this period. From 1974 to 1985, the operating mode of the Sanmenxia reservoir was further modified to provide for "storing clear water during low flow seasons and releasing turbid water during flood periods". Since 1980, due to increased water consumption by agriculture and industry and soil and water conservation projects, both annual sediment transport and runoff on the Lower Reach of the Yellow River decreased significantly (Liu et al., 2008).

During the past 50 years, the sediment loads are in increasing trend in most of the upstream stations of the Yangtze River basin, but in decreasing trend at other stations (Zhang et al., 2006). Studies by Xu and Milliman (2009) revealed that after the impoundment of the Three Gorges Reservoir (TGR), 60% of the sediment entering the TGR was trapped in flood seasons. Downstream of the TGR, substantial channel erosion is significant. However, downstream channel erosion (70 Mt/y) has not yet counteracted TGR trapping (118 Mt/y) and sediment delivered to the Yangtze estuary will probably continue to decrease.

Nile River, Mississippi River and Red River are other examples where reservoirs and dam construction has changed sediment dynamics of the floodplains. Before the High Aswan

Dam, Nile carried an average of 124 million ton of sediment to the sea each year, and deposited another 9.5 million ton on the flood plain. But due to construction of that dam, 98% of the sediment goes to the bottom of the Nasser reservoir (Billi, 2010). In Mississippi River, prior to 1930s, the floodplain was the major sediment source. But due to human modifications in terms of dams & reservoirs, artificial levees, dikes, concrete revetments and a series of channel cutoffs, floodplain provides only a minor amount of sediments today. Major degradation to the channel including the growth of channel bars has occurred as a result of these engineered modifications (Kesel, 2003). Similarly, the impoundment of two large reservoirs in the Da and the Lo watersheds in the 1980s has resulted in a considerable reduction (70%) of the total suspended load carried to the sea by the Red River (Le et al., 2007).

**Table 2.3** Sediment budget and human & climatic impacts in a few large rivers

| **River** | **Sediment budget and human & climatic impacts** |
|---|---|
| **Amazon** (the largest drainage basin) | • Sediment accumulation occurred during the five months of the flood rise, from December to April. Mean average sediment storage varies between 41% and 53% of the annual flux of sediments entering the floodplain through the main channels (Maurice-Bourgoin et al., 2007).<br>• Increased suspended sediment discharge by about 20% during 12 years since 1995, which may be attributed to stronger erosion processes caused either by a global change (rainfall), or regional land cover changes or both (Martinez et al., 2009). |
| **Nile** (the longest river) | • Prior to the construction of the Aswan Dam, the river annually delivered 60-180 million tones sediment and water to the Mediterranean Sea. Due to construction of the Aswan dam, 98% of the sediment goes to the bottom of the Nasser reservoir. Decreased sediment supply has created major erosion and shifting of sediment along the coast (Billi, 2010). |
| **Mississippi** | • Increased rate and magnitudes of floodplain sedimentation in the Upper Mississippi Valley due to land use change (Knox, 2006). |
| **Yangtze** | • Since 1950, Sediment load in the Yangtze River has been decreased |

| | |
|---|---|
| ($5^{th}$ in terms of discharge and $4^{th}$ in sediment load) | sharply due to dam construction (Dai and Lu, 2014), causing serious river management problems including channel erosion and delta retreat (Yang et al., 2011; Li et al., 2014)<br>• Since 2003, the Three Gorges Dam has trapped around 75% of the sediment coming from the upper reaches (Hu et al., 2009). Cumulative sedimentation rate in the Yangtze River basin is approximately 691 (±93.7) Mt $y^{-1}$. The TGR and other reservoirs are the major contributors to the sedimentation rate of ~ 494 Mt $y^{-1}$ in the upper Yangtze reaches (Yang and Lu, 2014).<br>• Climate change was considered responsible for a slight increase in sediment influx, approximately 3% (Dai and Lu, 2010). |
| **Yellow** (once the world's largest in terms of sediment discharge) | • Sediment budget produced for the period from 1855 to 1968 was characterized by a sediment input of $1.837 \times 10^{11}$ ton and a distribution between the lower Yellow River, the delta, and the deep sea of 64%, 33%, and 3%, respectively (Shi and Zhang, 2005).<br>• During 1970 – 2008, climate change and human activities were believed to respectively contribute 14% to 86% to the reduction in sediment yield in the upper reaches (Miao, 2010).<br>• Sediment reduction of Yellow River was 41 Gt during 1959 – 2007 due to dams and reservoirs (51%), soil and water conservation (25%), increased water consumption (19%), and channel sedimentation (13%) (Chu, 2014). |
| **Mekong** (Asia's third largest river in terms of sediment load) | • Approximately 80% of sediment has been trapped within the delta area (Xue, 2011).<br>• As of 2002, the construction of major dams on the headwaters in China appears to have had little impact on the sediment load, although as further larger dams are commissioned, the sediment load of the Mekong can be expected to decrease (Walling, 2008) |

| | |
|---|---|
| **Red** (the 2nd largest river in Vietnam) | • 70% decrease of the total suspended load since the impoundment of the Hoa Binh and Thac Ba reservoirs in the 1980s. Following the planned construction of two additional reservoirs, a further reduction by 20% of the suspended load of Red River was predicted, which might be compensated by an expected increase in suspended loading due to enhanced rainfall induced by climate change (Le et al., 2007) |
| **Indus** | • 87% of the annual erosion took place in the three summer months with greatest erosion potential. Major sources of eroded sediment were located in the Karakoram. Substantial sediment storage occurs on the flat Tibetan Plateau and Indus River valley reach (Ali, 2009) |
| **Ganges** | • Of the 794 $\times 10^6$ t/y transported in the rivers of the Ganga catchment, 80 ±10% sediment came from the High Himalaya, 20 ±10% from the Lesser Himalaya and the proportions from the Tethyan Himalaya, Siwaliks, Plain, and Peninsular while unknown are likely to be < 10%.<br>• About 8% of the river sediment was deposited on floodplains and delta plains in Bangladesh. The remaining ~ 45% was deposited in the subaqueous delta and the Bengal Fan (Wasson, 2003) |

## 2.3 River bank erosion in large rivers

Bank erosion includes two main groups of processes: hydraulic and gravitational mass failure. Hydraulic processes at or below the water surface entrain sediment and directly contribute to erosion, particularly of non-cohesive banks, by processes of bank undercutting, bed degradation and basal cleanout. Gravitational mass failure processes (including shallow and rotational slides, slab and cantilever failures, earthflows and dry granular flows) detach sediment primarily from cohesive banks and make it available for fluvial transport. Table 2.4 shows the classification of erosion mechanisms. Sarkar et al. (2012) studied erosion and deposition in the north bank and the south bank of Brahmaputra for the period 1990 – 2008. Erosion during 1990 – 2008 in north bank and south bank of Brahmaputra (within Assam) were 544 $km^2$ and 920 $km^2$ respectively, whereas corresponding amount of deposition were 145 $km^2$ and 68 $km^2$. Extent and causes of bank erosion in a few other large rivers are summarized in Table 2.5.

**Table 2.4** Classification of erosion mechanism

| Mechanisms | Classification | Typical flow conditions | Sediment characteristics | Bank moisture | Description |
|---|---|---|---|---|---|
| Shallow slides | Gravitational | Low | Fine grained, low cohesion | Saturated | Layer of bank material displaced along a plane parallel to bank surface |
| Rotational slip | Gravitational | Low | Fine grained, cohesive | Saturated | Deep seated movement along curved slip surface |
| Slab failure | Gravitational | Low | Fine grained, cohesive | Varies | Block of bank falls forward into channel |
| Cantilever failure | Gravitational | Low | Composite fine/coarse | Varies | Collapse of overhanging sediment block |
| Wet earth flow | Gravitational | Low | Fine grained, cohesive | Saturated | Saturated flow, often on low angled banks |
| Popout failure | Hydraulic/ Gravitational | Low | Fine grained, cohesive | Saturated | Small blocks forced out of bank due to excessive pore pressure |
| Dry granular flow | Gravitational | Low | Non-cohesive | Dry | Movement of individual grains in banks |
| Soil/ rock fall | Gravitational | Low | Weakly cohesive | Dry | Individual grains/ blocks fall into channel from very steep banks |
| Piping failure | Hydraulic/ Gravitational | Low | Inter-bedded fine/coarse | Saturated | Loss of strength due to flow in areas of high pore-water pressure |
| Bank undercutting | Hydraulic | High | Generally non-cohesive | N/A | Removal of cohesive material from toe of bank, causing bank to overhang |
| Bed degradation | Hydraulic | High | Relatively erodible bed | N/A | Removal of material from bed of stream |
| Basal cleanout | Hydraulic | Varies | All types | N/A | Removal of (often) non-cohesive material at base of bank |

**Table 2.5** River bank erosion in a few large rivers

| River | Extent & impacts of erosion | Causes of bank erosion | | | Protection measures | Reference |
|---|---|---|---|---|---|---|
| | | Hydrological | Geochemical | Other | | |
| Nile | Huge loss to cultivated lands | Meandering river, increased hydraulic erosional power of sediment deficient water | Easily erodible banks composed of clay, silt and fine sands | Arid climate, construction of dams & irrigation structures | Bank revetments, flow deflectors | Ahmed and Fawzi (2009) |
| Mississippi | Land loss, increased sediment load, river bed aggradation | High flow, meandering nature, seepage | Composite layer in river bank | Land use change, dam construction | Bank revetments, dredging of river bed | Wilson et al. (2011) |
| Amazon | Supply of sediment to river erosion: 1570 Mt | Increased sediment load in the river | Poor tropical soils | Deforestation and mining, slash and burn agriculture | Bank protection, afforestation | Dunne et al. (1998) |
| Yellow | Severe erosion prior to 1949 | Over-flooding | Loose bases, joints, poor structure of dykes | Unequal sediment accumulation across the river, tectonic activity | Channel stabilization, strengthening of dikes | Changxing and Qingchao (1997) |
| Yangtze | Average rate of erosion: 1559 t/km$^2$ /year | Increase in water discharge | Poor structural integrity of the soil | Constraint of levees along the riverbanks | Construction of levees, bank revetment | Li et al. (2007), Dingzhong & Ying (1996) |
| Mekong | Erosion rate: 10 to 30 m/year | Water-flow velocity, pore pressure | Layered structure of banks | Clearing of vegetation, sand /gravel extraction, deforestation, dam | Bank revetment | Miyazawa et al. (2008) |
| Ganges | Land eroded: 18582 hectares (during 1931–2004) | Fluctuation of discharge | Bank stratigraphy | Effluent flow of ground water into the river | Bank revetment with boulder, spur | Maitra (2004) |

Bank failure block is a major source of sediment (Nasermoaddeli and Pasche, 2008), making sediment concentration increase in a short time and influencing river bed morphology at downstream. For example, the appearance of the peak sediment concentration in Yellow River has link to bank failure of the river canyon in Shanxi-Shaanxi province (Liu et al., 2013).

## 2.4 Geochemical properties of bank materials as a facilitator of erosion

Physical properties of bed sediments and bank materials have been intensively studied, however, not as factors that influence the erodibility of cohesive sediment. Sediment properties can affect erodibility through changes in the size or quantity of sediment constituents, and include mean particle size, particle size distribution, bulk density, and water content. Geochemical properties of sediments influence the electrochemical attraction of particles, and include particle mineralogy and organic content. Dynamically linked sediment physical, geo-chemical and biological properties and processes that affect erodibility of sediments are shown in Figure 2.1 (Grabowski et al., 2011).

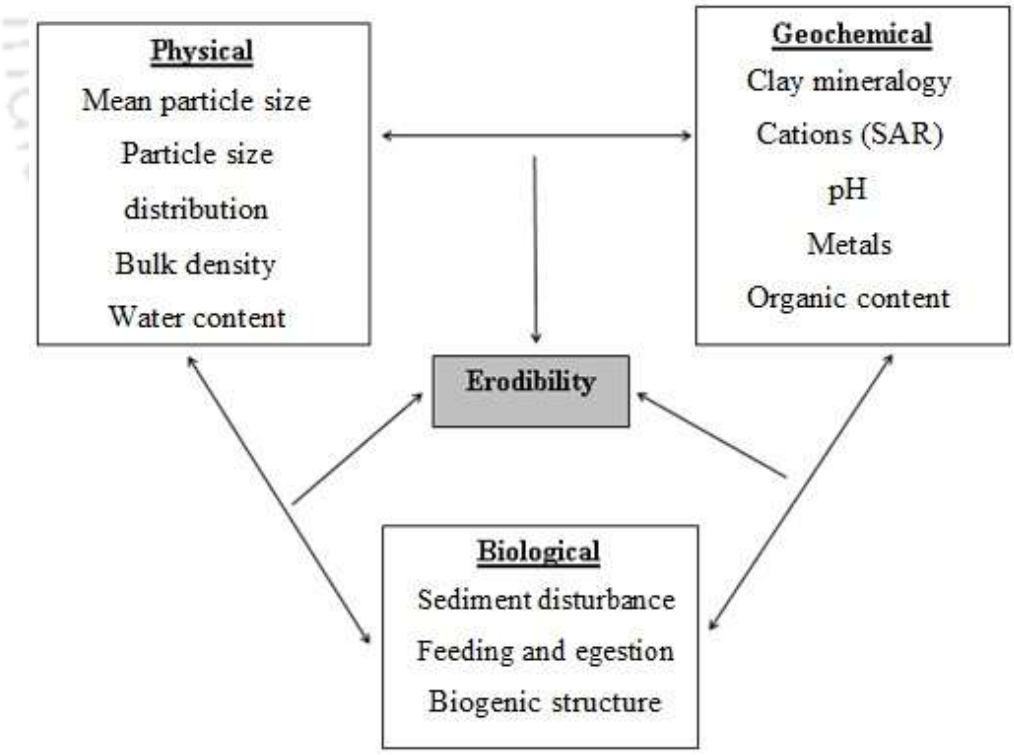


**Figure 2.1** Conceptual model of dynamically linked sediment properties and processes that can affect sediment erodibility (Grabowski et al., 2011)

Studies on river bank stability analysis have accounted the effect of multiple horizontal layers of soil with different physical properties (Takaldany, 2003; EPA, 2003). Soil pH is the single most important chemical property of the soil. Soil pH influences most chemical and biological processes occurring in soil and some physical processes. These include supply and availability of essential elements, growth of soil organisms of all kinds, nitrification of ammonia, and rock weathering. For a high-silt soil, increased pH increases erodibility if the structure is very fine or fine granular. This is probably due to an effect on surface crusting. If the structure is medium or coarse granular, subangular, or angular, erodibility decreases with increased pH (Wischmeier and Mannering, 1969).

Sodium adsorption ratio (SAR) is the relative proportion of monovalent (Na+) to divalent ($Ca^{2+}$ and $Mg^{2+}$) cation concentrations in soil or sediment. Soils with high SAR are labeled sodic. Sodic soils present a serious management problem for agriculture, particularly when they contain high percentages of expansive smectite clays. Clay minerals absorb more water at high SAR, and expansion and dispersion of the minerals results in a soil with high porosity, low permeability and high erodibility (Rowell, 1994; Brady and Weil, 2002).

Organic content has long been recognized as a critical factor determining the erodibility of soils (Morgan, 2005). Wischmeier and Mannering (1969) postulated that organic matter content ranked next to particle size distribution as an indicator of erodibility. Robinson and Phillips (2001) showed that a high concentration of organic matter can facilitate aggregate stabilization in the topmost horizons. Soil with less than 2% organic content is considered erodible, and erodibility is negatively correlated with organic content from 0 to 10% (Brady and Weil, 2002; Morgan, 2005).

Soil particle size and, particularly, the silt–clay content of the soil have long been recognized to influence fluvial erosion and mass failures (e.g. Wolman, 1959; Schumm, 1960; Walker et al., 1987). Dade et al. (1992) demonstrated that erosion threshold is positively correlated to particle size. While it is convenient to describe sediment by a mean particle size, most natural cohesive sediment is composed of a range of particle sizes, and the relative proportions of these different sized particles can substantially affect sediment

erodibility. Adding clay to a sand bed makes it more resistant to erosion, up to a maximum erosion threshold at 30–50% clay (Grabowski et al., 2011).

Clay minerals can be divided into three main groups based on their size and electro-chemical activity: (i) kaolinites; (ii) micas, e.g. illite; and (iii) smectites, e.g., montmorillonite and bentonite (Partheniades, 2007). Kaolinites have the largest particles and the lowest cation exchange capacity so are the least electro-chemically active mineral. The clay sub units are strongly bound by van der Waals forces, so water and cations can only interact with the outer faces and edges of the particles. Smectite clays are considered to have the highest erodibility for soils, followed in decreasing order by micas and kaolinite (Morgan, 2005). The reason for high erodibility is their high CEC and expansive nature. When water infiltrates in between the clay units, they are pushed apart. The further they are pushed apart, the more inter-particle attraction is reduced, and the more erodible the clay becomes. Laboratory flume experiments by Torfs (1995) support this hypothesis for sediment; artificial sediment mixtures with montmorillonite erode at lower critical shear stresses than kaolinite at the same clay content. The small, thin, plate-like units of clays have high surface area to volume ratios, and their surfaces carry strong electro-chemical charges. The flat surfaces, or faces, of a clay particle generally carry permanent negative charges caused by the preferential adsorption of stabilizing anions and isomorphous substitutions in the clay mineral structure. Clay particles experience net repulsive forces due to their similarly charged surfaces. However, inter-particle attraction can occur if the electric double layer is reduced. Positively charged cations dissolved in the water neutralize surface charges on the clay minerals, reducing the thickness of the electric double layer, allowing the particles to get close enough to attract by van der Waals forces. High valence cations, e.g., $Ca^{2+}$, are more effective at reducing the thickness of the electric double layer, so are more effective at coagulating clay minerals than lower valence ones, e.g. $Na^{+}$ (Partheniades, 2007).

The electro-chemical activity of a clay mineral, i.e., surface charge density, is linked to the cation exchange capacity and the particle size. CEC is a measure of the capacity of clay to adsorb cations in solution to the surface of the particles. A high CEC coupled with a small

particle size produces an electro-chemically active clay with a high charge density. In clay soils, the higher the Ca:Mg ratio, and the lower the Na%, the higher the likelihood of the soil being self-mulching. Self-mulching clays usually have Ca:Mg ratios of 2 to 4, and a Na% of 3% or less. Non-self-mulching clays generally have Ca:Mg ratios of about one, with the Na% usually exceeding 5%. Therefore, the Ca:Mg ratio and the exchangeable sodium percentage are important indicators of the structural stability of clay soils.

Metals can potentially alter the erodibility of cohesive sediment through several mechanisms as mentioned below; however, there is little empirical evidence.

(i) Soluble metals, particularly Fe, Al, and Mn can reduce the double layer thickness of clay particles, theoretically increasing cohesion and reducing sediment erodibility (Winterwerp and Kesteren, 2004). Soluble aluminum has been shown to increase the elastic strength of biofilms, and iron has been shown to increase their cohesive strength and resistance.

(ii) Divalent metal ions adsorbed to clays and organic matter can bind to metal ions on other particles, creating strong cation bridges (Dade et al., 1992).

(iii) Metals form insoluble complexes with oxides and carbonates, which act as cementing agents in soils (Brady and Weil, 2002). The compounds carry a net positive charge that strongly attracts two negatively charged clay particles (Partheniades, 2007).

## 2.5 Land use and land cover change of large rivers

Land use and land cover (LULC) change, which results from the complex interaction of social, ecological and geophysical processes (Munroe and Muller, 2007), is a major issue and the main cause of global environmental change (Fan et al., 2007; Peng et al., 2006). Land use/ cover change (LUCC) issues have attracted interest among a wide variety of researchers, for different purposes including modeling spatial and temporal patterns of land conversion and understanding the causes and influences of LUCC (Hietel et al, 2007; Long et al., 2008; Seto and Kaufmann, 2003; Veldkamp and Verburg, 2004; Xiao and Weng, 2007; Zhang et al., 2008). Although climate change, urbanization and population growth have been considered the most common factors contributing to LUCC on a global scale, there is no consensus concerning the relationships between LUCC and its driving forces,

largely because of the complex interactions among physical, biological, economic, political and social factors. LULC inventories are increasingly utilized in land-use planning, forest management and floodplain management (Bocco et al., 2001; Kotoky et al., 2012; Mahajan and Panwar, 2005; Schulz et al., 2010; Sun et al., 2009; Sylla et al., 2012; Boori et al., 2015). Studies on LULC change are also important from the perspective of studying global environmental change and sustainable development highlighting the intensity and pattern of relationship between the human and earth (Jiyuan et al., 2010).

Human land use activities have fundamentally changed the hydrogeomorphology of rivers. Since the late Holocene, anthropogenic changes to alluvial stratigraphy and channel morphology have often been greater than those left by climate change (James and Lecce, 2013). Amazonian landscape has experienced a dramatic land cover and land use changes since the early 1970s with the establishment of the Trans-Amazon Highway and large government projects. Agricultural settlement and cattle ranching were expanded by clearing significant tropical forest cover in the areas of new and accelerated human development (Souza-Filho et al., 2016). Land use and land cover change has contributed to increasing discharge in the Upper Mississippi River Basin (Schilling, 2010).

Although braided channels have the most complicated forms compared to other channel forms, quantitative studies and dynamics of braided rivers have been fewer than other channels (Best and Bristow, 1993; Richardson, 1997). Most studies of braided rivers have dealt with channels and bars over relatively small areas (Ferguson, 1993; Bryant and Gilvear, 1999; Brasington et al., 2000; Richardson and Thorne, 2001; Lane et al., 2003). There are limited studies on large braided rivers (Richardson, 1997) like Brahmaputra which have made it difficult to establish general theories of the form of braided channels (Takagi et al., 2007).

Chapter 3

# Materials and methods

This chapter describes study area, sources of secondary data, details of materials and methodologies of sampling and analysis.

## 3.1 Study area: The Brahmaputra River in Assam

Originated as the Yarlung Tsangpo ('Tsangpo' means purifier) from a glacier mass near Manasarovar lake in the Kailash range in southern Tibet, the Brahmaputra [in Bengali : *Jamuna*, Tibetan: *Tsangpo*, Chinese (Pinyin): *Yarlung Zangbo Jiang* or (Wade-Giles romanization) *Ya-lu-tsang-pu Chiang*] is a transboundary river flowing to the Bay of Bengal through China (Tibet), India and Bangladesh. The source of Brahmaputra was previously believed to be either on the Chema-yungdung glacier, as proposed by Indian geographer Swami Pranavananda in the 1930s, or on the Kobei glacier, as determined by Swedish explorer Sven Hedin in 1907. Analysis and field investigations by Chinese Academy of Sciences showed that Brahmaputra originates on the Angsi glacier (Figure 3.1), located on the northern side of the Himalayas in Burang County of China's Tibet Autonomous Region (Xinhua, 2011). According to the new findings, Brahmaputra is 3,848 kilometers long with drainage area of 7,12,035 sq. km. Previous documents showed the drainage area of Brahmaputra is 5,80,000 sq. km, 50.5% of which lie in China, 33.6 % in India, 8.1 % in Bangladesh and 7.8 % in Bhutan. Its basin in India is shared by Arunachal Pradesh (41.9%), Assam (36.3%), Nagaland (5.5%), Meghalaya (6.1%), Sikkim (3.7%)

and West Bengal (6.5%) (Ojha and Singh, 2004). Particulars of a few large rivers including the Brahmaputra are mentioned in Table 3.1.

The Brahmaputra basin is enclosed by the Himalayas on the north, the Patkai range of hills on the east running along the Indo-Burma border, the Mikir hills and Shillong plateau on south and the ridge separating it from the Ganga basin on the west. During the course of Brahmaputra in Assam, about 26 important tributaries on its north bank and about 13 on south bank join the river (Figure 3.2).


**Figure 3.1** Location of the Angsi glacier

**Table 3.1** Particulars of a few large rivers of the world

| River | Length (km) | Catchment area ($km^2$) | Average discharge ($\times 10^3 m^3 s^{-1}$) | Sediment yield (ton $km^2 y^{-1}$) |
|---|---|---|---|---|
| Brahmaputra | 3,848 | 712,035 | 19.83 ($4^{th}$) | 1128 |
| Ganges | 2,525 | 1,080,000 | 11.67 | -- |
| Indus | 3,200 | 1,165,000 | 6.6 | 103 |
| Yangtze | 6,380 | 1.940,000 | 21.80 ($3^{rd}$) | 246 |
| Yellow | 5,464 | 752,000 | 19.83 ($4^{th}$) | 1408 |
| Mekong | 4,023 | 811,000 | 14.8 | 214 |
| Congo | 4,371 | 3,822,000 | 39.66 ($2^{nd}$) | -- |
| Mississippi | 6,270 | 2,980,000 | 16.2 | 64 |
| Amazon | 6,992 | 6,915,000 | 99.15 ($1^{st}$) | 46 |
| Nile | 6,650 | 3,400,000 | 2.83 | 37 |
| Godabari | 1,465 | 312,812 | 3.06 | -- |
| Yamuna | 1,376 | 366,223 | 2.95 | -- |

(Islam et al., 1999; RSP, 1996; Goswami, 1985**)**

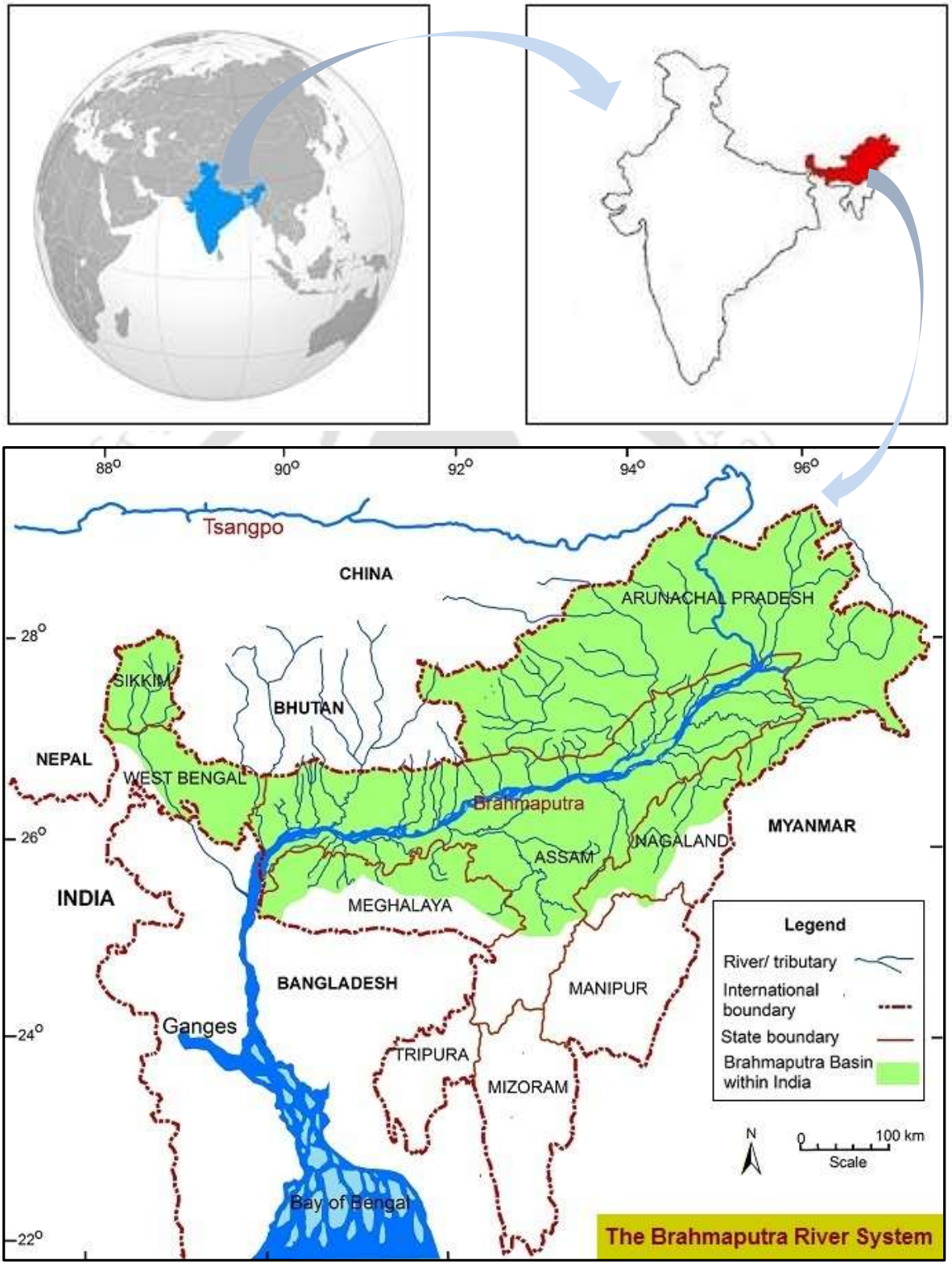


**Figure 3.2** The Brahmaputra River system within India

Average width of the Brahmaputra valley is 80 km, out of which, the river itself occupies about 1.5 km to 25 km. The Brahmaputra valley in upper Assam is strongly influenced by the Himalayan and Naga Patkai belt orogeny. The spatial variability in morphodynamics of Brahmaputra River is strongly linked to the three units of the central uplift, the slopes, and the depressions (Lahiri and Sinha, 2012).

The Brahmaputra is an extremely dynamic, predominantly braided river with scours even 40–45 m deep (Coleman, 1969). Uniqueness of Brahmaputra can be viewed from different aspects:

i) It provides the only example in the world where the drainage pattern runs in a diametrically opposite direction. In Tibet, it flows from west to east. But then it takes a U-turn in south of Tibet and flows from east to west in Assam (Hussain, 1994). However the other large river systems like Amazon, Congo, and Mississippi have relatively simple dendritic tributary networks that resemble a branching tree (Clark et al, 2004).

ii) The river drains diverse environments as the cold dry Tibetan plateau, the steep rain-drenched Himalayan slopes, alluvial Assam valley and fluvio-deltaic Bangladesh plain (Sarma, 2005).

iii) The Himalayas, where the origin of Brahmaputra lies, are considered to be younger in age than Brahmaputra River (Ojha and Singh, 2004).

iv) Besides flood hazards, in no other river of the world, the bank erosion hazard is so critical as in the Brahmaputra valley (Mahanta and Saikia, 2015).

The Brahmaputra and its tributaries and sub-tributaries cause major problems during the monsoon period every year in the shape of flood, bank erosion and drainage congestion. Being an agrarian state, the economy of Assam basically emerges from agriculture. More than 50 percent of the rural people of Assam are employed in the agriculture sector. The net cultivated area of the state is 28.11 lakh hectares (2009 – 2010), which is about 88 percent of the total land available for agricultural cultivation in the state. The successive wave of devastating floods almost every year has virtually destroyed the economy, more particularly the agro-economy of the state. Flood damage during 1953 – 2006 and 2006 –

2011 (WRD, 2013) shown in Figure 3.3 and Table 3. 2 respectively depicts the plight of the people of Assam under this hazard year after year. Brahmaputra River has destroyed nearly 4000 $km^2$ since last five decades at a rate of 80 $km^2$ per year and erosion also wiped out more than 2500 villages affecting nearly 5,00,000 people (Paul et al., 2013).

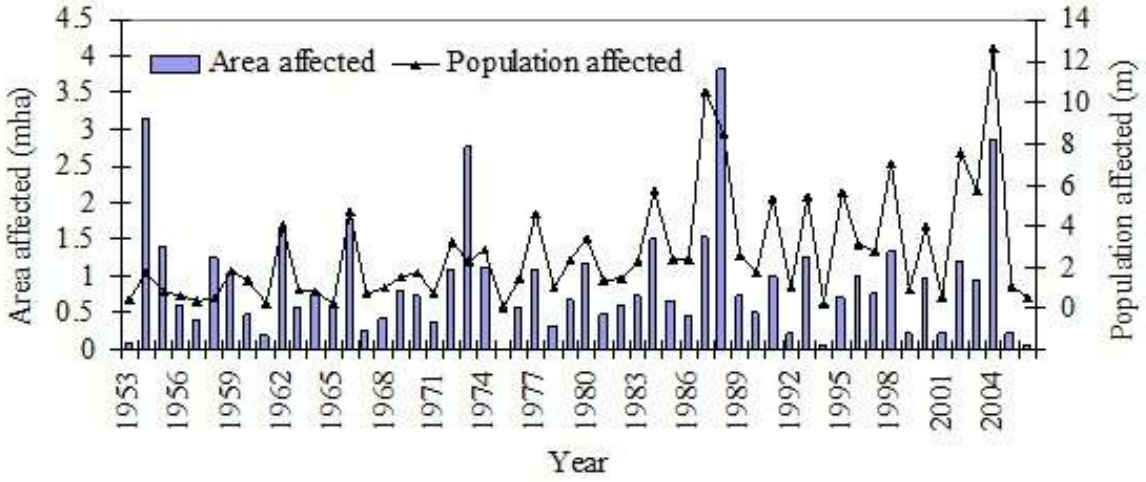


**Figure 3.3** Flood damage in Assam during 1953--2006

**Table 3.2** Flood damage in the Brahmaputra valley during 2006 –2011 (Bhuyan, 2013)

| Average annual area flooded | | Population affected in a year | Affected population per ha of flooded area | Average annual damage (Rs in Lakh) | Value of crop lost as % of total damage |
|---|---|---|---|---|---|
| Total | Cropped | | | | |
| 0.26 | 0.17 | 10,28,000 | 4.0 | 3,880 | 22% |

Assam accounts for 9.4% total flood prone areas in India. But in very high flood years, the picture is quite different, e.g. damage in Assam during high flood years, 1954, 1959, 1962, 1966, 1972, 1987, 1988 and 1993 were much higher in comparison to that of the total areas affected in the country. (Table 3.3).

The flood in Brahmaputra valley is a recurring phenomenon and has been causing large scale damages every year. Adverse physiography of the region, inadequate capacity of the river channel due to braided nature, heavy rainfall, excessive sedimentation, landslides, release of water from river dams, reduction of forest areas, and encroachment of riverine areas are some of the major factors causing floods in the region.

**Table 3.3** Affected areas of Assam and India during high flood years

| Sl No. | Years of high flood in Assam | Total area affected in the country in Mha | Area affected in Assam in Mha | % of total area affected in Assam |
|---|---|---|---|---|
| 1 | 1954 | 7.49 | 3.15 | 42 |
| 2 | 1959 | 5.77 | 1.04 | 18 |
| 3 | 1962 | 6.12 | 1.62 | 26 |
| 4 | 1966 | 4.74 | 1.78 | 38 |
| 5 | 1972 | 4.10 | 1.10 | 26.8 |
| 6 | 1987 | 8.89 | 1.53 | 17.2 |
| 7 | 1988 | 16.29 | 3.82 | 23.5 |
| 8 | 1993 | 4.63 | 1.25 | 36.9 |

(NEC, 1993)

### 3.1.1 River bank erosion in Brahmaputra

#### *3.1.1.1 Extent of the erosion problem in Brahmaputra*

The Brahmaputra valley has been facing a heavy instability of landmass due to river bank erosion, believed to be accelerated after the 1950 earthquake. The stretch falling within Assam, India, has already lost about 7.4% of its total land due to bank erosion and channel migration (Baruah and Goswami, 2013). The recurrent erosion has caused irreparable damage to many important places along the river bank in addition to other cultivable and homestead lands. The *Sadiya* town, on the confluence of the *Dibang* and *Lohit* was completely eroded away in 1953. There was severe erosion in *Dibrugarh* and *Palasbari* in 1953 –54. Table 3.4 shows overall damage due to bank erosion in Assam.

**Table 3.4** Overall damages due to bank erosion in Assam

| Year | Area eroded in ha | No of village affected | No of family affected | Value of property with land loss, Rs in Lakh |
|---|---|---|---|---|
| 2001 | 5348 | 227 | 7395 | 377.72 |
| 2002 | 6803 | 625 | 17985 | 2748.34 |
| 2003 | 12589.6 | 424 | 18202 | 9885.83 |
| 2004 | 20724 | 1245 | 62258 | 8337.97 |
| 2005 | 1984.27 | 274 | 10531 | 1534 |
| 2006 | 821.83 | 44 | 2832 | 106.93 |

(Bhuyan, 2013)

Reaches under active erosion identified by Govt. of Assam are mentioned in Table 3.5.

**Table 3.5** Reaches under active erosion in Brahmaputra River

| Sl no | Reach | Location of reach | |
|---|---|---|---|
| | | South bank | North bank |
| 1 | *Kobo* to *Dihingmukh* | *Nagaghuli, Maijan* | *Mothola-Oakland, Sonarighat, Matmora* |
| 2 | *Dihingmukh* to *Dhansirimukh* | *Hatisal, Mariahola, Kaziranga* | *Gamerighat, Majuli* |
| 3 | *Dhansirimukh* to *Pandu* | *Koliabhomora, Lahorighat-Dihing* | *Bhairabpad* and *Bihaguri* |
| 4 | *Pandu* to *Dhubri* | *Palasbari, Gumi, Kalatoli, Sukchar bazar, South Salmora* | *Howlighat-Mukalmua Baghbar-Bahari* |

(NEC, 1993)

### *3.1.1.2 Factors responsible for erosion in Brahmaputra*

Highly erosive characteristics of Brahmaputra have been extensively studied (Coleman, 1969; Goswami, 1985; Sarma, 2005; Pahuja and Goswami, 2006; Sarkar and Thorne, 2006; Wiebe, 2006). Dynamically linked hydrological, hydraulic, geochemical and geotechnical factors for bank erosion in Brahmaputra are outlined in the Figure 3.4.

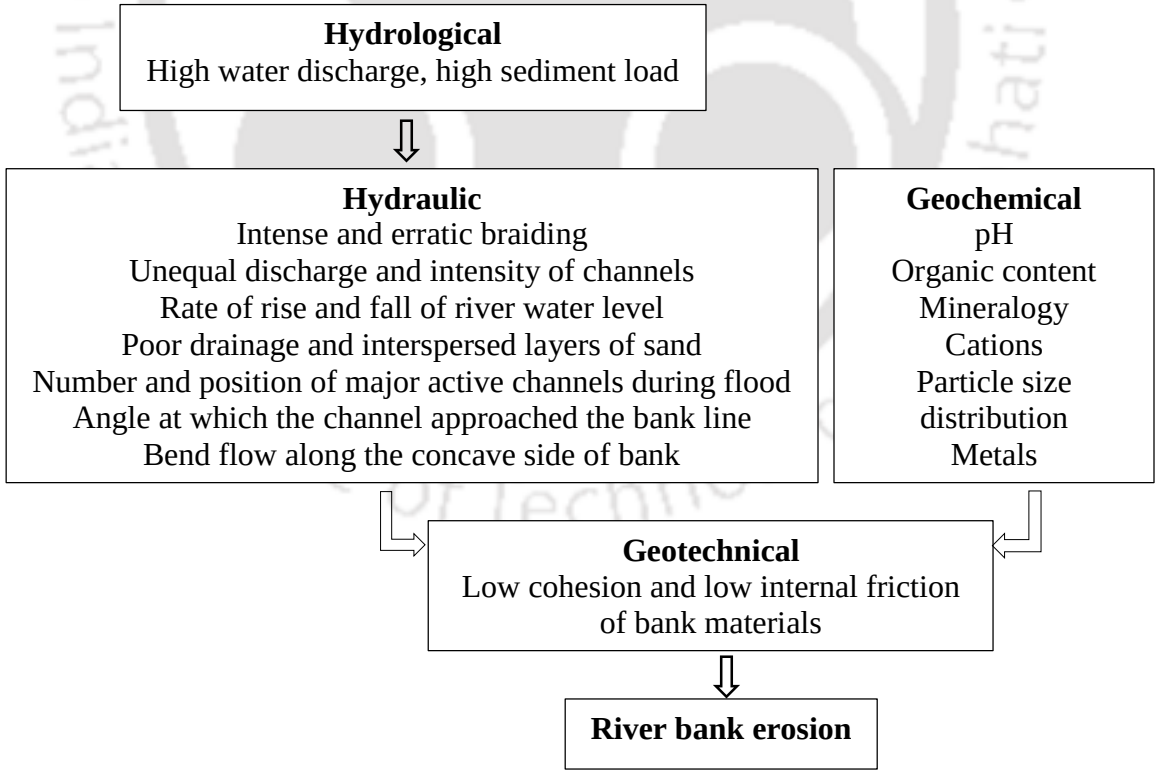


**Figure 3.4** Linked hydrological, hydraulic, geochemical and geotechnical factors responsible for bank erosion

High sediment load in tributaries and deposition of sediment at the outfall causes the tributary mouth to shift. When the flow in the river bifurcates and one of the deep channels comes very close to the banks, continuous erosion along the length takes place. When the flow is oblique, the bank is attacked locally and the flow gets deflected. Deep local embayment goes far in land till it joins a tributary and a part of the main river avulses in to the tributary. The sand bars between the main river and the tributary from the embayment upto the tributary confluence with the main river gets engulfed in the river bed, leading to widening to the main river (NEC, 1993).

Another factor responsible for bank erosion is bend flow along the concave side of bank. During the flood, the banks get saturated and during the falling stage of the river, seepage from the banks towards the river increases with the drawdown and the banks composed of sand with low cohesion collapse. Poor drainage and interspersed layers of sand are additional factor which accentuate bank failure.

Although hydrologic, hydraulic and geotechnical factors are studied for erosion in Brahmaputra River, there has been little study on impact of geochemical properties on erodibility of bank materials. Erosion generally occurs when erosive forces exceed the resistive forces within the sediment, which include gravity, friction, cohesion and adhesion. Erodibility is a measure of these resistive forces, which can be determined by evaluating the biogeochemical properties of the sediment (Winterwerp and Kesteren, 2004; Sanford, 2008). Precise evaluation of physical and geo-chemical characteristics can lead to long term solution options for mitigating the erosion of Brahmaputra River. Halting erosion by using only structural measures has a negative impact on habitats; it disrupts the natural balance of the river and, may exacerbate the problem as the river's erosive energy may be in excess. Also, some of the efforts are ineffective because activities often treat the symptoms of erosion, without addressing the underlying cause.

As of now, efforts to control bank erosion have remained centered around only physical structures, e.g., porcupine network to facilitate sedimentation. Anti-erosion works for locations, which are under attack have effect on only the local areas but not of much

significance to the general behavior of the river.

## 3.2 Sources of secondary data

There are a few limitations in collecting secondary data related to Brahmaputra River:

i) Non-availability of enough hydrological data for Brahmaputra and its tributaries, particularly in Assam plains.

ii) Most of the available data is discrete, i.e., confined to particular site or location and not continuous. Several organisations/ departments such as Brahmaputra Board, Water Resources Department, Assam PWD, Central Water and Power Commission, Joint River Commission, etc. are dealing with different hydrological aspects of Brahmaputra; with the result that data remained dispersed in different offices and is difficult to locate and access.

Besides published articles and reports, following volumes/ publications were considered in the present study:

i) Morphological studies of the Brahmaputra; North Eastern Council, Water and Power Consultancy Services (India) Limited, 1993

ii) Morphological studies of River Brahmaputra at Nagaghuli-Maijan-Oakland area upstream of Dibrugarh town, Assam; Central Water and Power Research Station, Technical Report no: 3590; March 1999

iii) Additional volume for master plan of Brahmaputra basin; Brahmaputra Board; 1995

iv) Hydrometeorology of the Brahmaputra basin; Brahmaputra Board; 1986

v) Task force for flood management/ erosion control Report; Ministry of Water Resources (Govt. of India); 2004

vi) Master plan of Brahmaputra basin, Part I, Main stem; Brahmaputra Board; 1986.

## 3.3 Collection of sediments

Suspended sediment and bed sediment samples of Brahmaputra River were collected from six locations of Assam in India as shown in Figure 3.5. For suspended sediment samples, four water samples were collected from each sampling location during pre-monsoon (January-March, 2011), monsoon (June, 2011) and post-monsoon (November, 2011)

seasons. Wide mouthed high grade plastic bottles of 1 liter volume were used, which were dipped into the river water and after being filled, they were capped inside the river water itself. Suspended sediments were obtained from those water samples by filtration using micro-pore filters. Bed sediments were collected by scooping of freshly deposited materials in the months of December 2010 and January 2011. All samples were brought to laboratory and preserved till analysis.

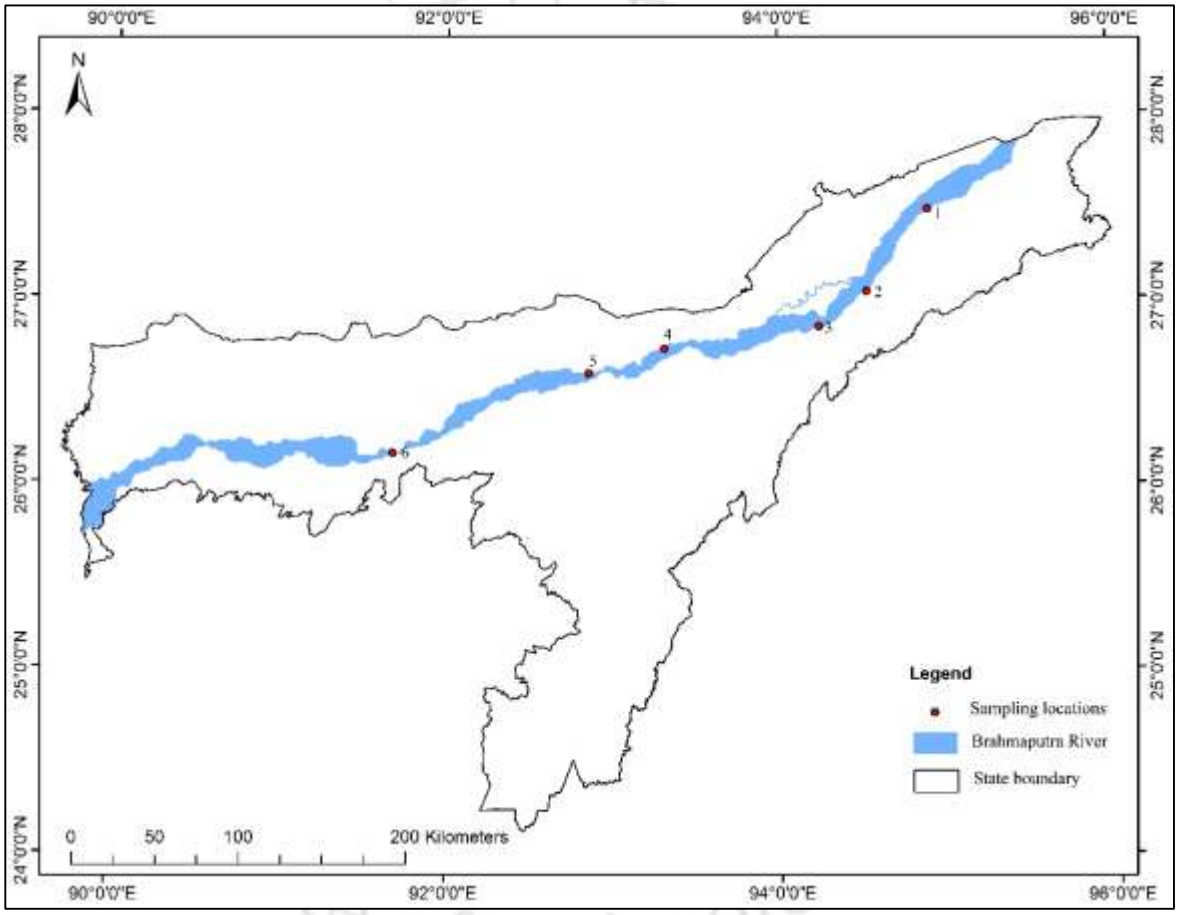


**Figure 3.5** Sampling locations of suspended sediments and bed sediments
[1) *Dibrugarh, 2) Disangmukh 3) Nematighat 4) Biswanathghat 5) Tezpur 6) Pandu*]

## 3.4 Collection of bank materials

Considering severity of river bank erosion problem in the last few years, six locations were selected for present study of geochemical evaluation of bank materials. The locations are: A) *Rohmoria, B) Dibrugarh, C) Nematighat, D) Majuli, E) Gamerighat,* and F) *Palasbari* (Figure 3.6).

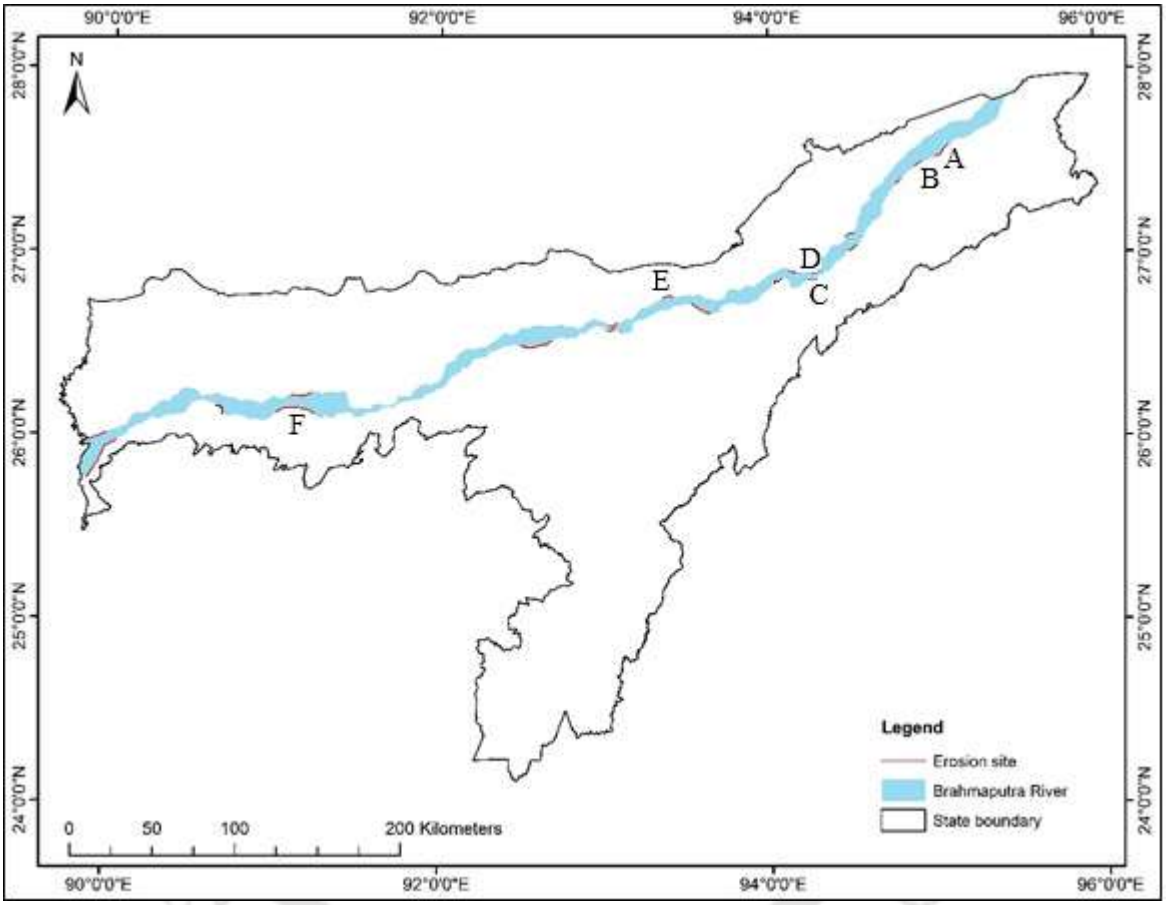


**Figure 3.6** Major erosion sites of Brahmaputra River main stem in Assam *(from records of Water Resources Department, Assam)* and sampling locations

A brief description of the erosion problem in these areas is mentioned below.

***Rohmoria (A):*** The village complex of *Rohmoria* is situated at a distance of 23 km to the east of *Dibrugarh* town. Earlier, there were several small villages, forests, bamboo groves, swamps, and cattle farms, which provided all commodities necessary for an affluent rural livelihood. Now, Brahmaputra has not only eroded away all those rich natural resources but also has been eroding the very villages of *Rohmoria* (Table 3.6).

**Table 3.6** Extent of erosion in *Rohmoria*

| | |
|---|---|
| Area of land eroded | 8,435 Ha |
| Bank line length | 9 km |
| Average depth of erosion | 800 m |
| No of villages affected | 16 |
| No of house hold effected | 1580 |
| Population affected | 23,000 |

Total bank area being eroded away by Brahmaputra from 1916 to 2009 along the 16 km segment around *Rohmoria* was about 108.48 sq. km. If this amount is divided by the time span of (2009 – 1916=) 93 years then the rate of erosion in this reach will be 1.17 sq. km per year. The rate of bank erosion in the south bank of Brahmaputra is the highest at *Rohmoria*. The main cause of erosion of *Rohmoria* is the development of a very large primary channel of Brahmaputra, which hits the bank at about $45^{0}$ near *Balijan* and flows along the bank for 12 km up to *Nagaghuli* area. This channel is now being reinforced by the flow of the *Lohit* that joins the same at *Balijan.*

**Figure 3.7** Erosion sites of *Rohmoria*

***Dibrugarh (B):*** Situated at upstream of Brahmaputra, *Dibrugarh* town is severely affected and vulnerable area of bank erosion (Table 3.7, Figure 3.8). Old records indicate that erosion was caused by the shifting of channel of river *Dibru* in 1880-1881, which was then meeting Brahmaputra downstream of *Dibrugarh* town. After the devastating earthquake in 1950, the erosive trend took a worst turn threatening the *Dibrugarh* town. Erosion was

alarmingly high during 1954--1955, when the entire south bank from *Nagakhelia*, west of *Dibrugarh*, up to *Saikowa* had been subjected to severe erosion and Brahmaputra was encroached upon by 2 km to the south till 1963. The names of the villages eroded away during this period were *Mohmara, Mohmara Chise, Mohmara South, Sagali Pathar, Sagali Block, Mohmara Nepaligaon, Kalangaon, Kalani Mirigaon, Upper Barala, Barala Block, Baralagaon* and *Bahanagaon*. Heavy erosion started in the year 1970-1971 in between *Mathola* and *Maijan* upstream of *Dibrugarh* town. The erosion was observed shifting upstream to *Nagaghuli-Maijan* area in the year 1991--1993 and then to the tea estates at Oakland during 1995 – 1997. Important erosive activity was located downstream of *Dibrugarh* during the year 1920 to year 1940, shifted upstream to *Dibrugarh* during 1950 to 1960 and then further upstream from the year 1970.

**Table 3.7** Extent of erosion in *Dibrugarh* town

| | |
|---|---|
| Annual flood effected area | 835 Ha |
| Bank line eroded | 25 km |
| Land area eroded (1967-2008) | 491 Ha |
| Rate of erosion | 4.72 m/year |
| Number of household lost (1988—2008) | 768 |
| Number of household affected | 4,036 |

(WRD, 2008)

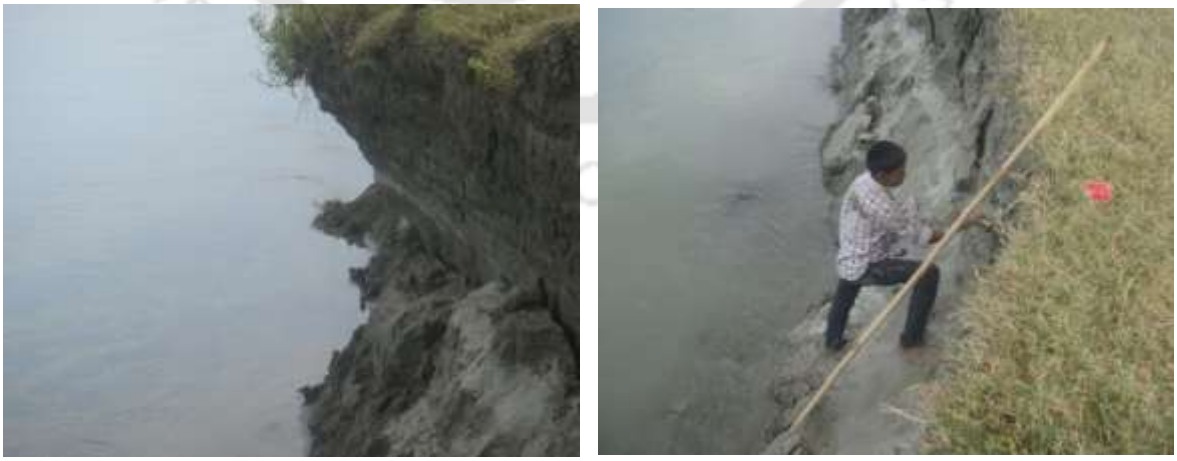

**Figure 3.8** Erosion sites of *Dibrugarh*

***Nematighat (C):*** *Nematighat* is facing severe problem from bank erosion (Figure 3.9) in recent years.

**Figure 3.9** Erosion sites of *Nematighat*

***Majuli (D):*** *Majuli* is one of the largest riverine islands in the world and the largest in Asia with a population of 0.16 million people and the site of Vaishnavite spiritual centers (Lahiri and Sinha, 2014). Constant and extensive land erosion particularly at southern and downstream edge by mighty Brahmaputra is the single most problem that threatens the very existence of the island and life and properties of its inhabitants (Figure 3.10).


**Figure 3.10** Erosion sites and non-erosion sites of *Majuli*

Areal extent of *Majuli* has been decreased from 787.9 $km^2$ to 508.2 $km^2$ during 1915–2005 with 35.5% reduction and average erosion of 3.1 $km^2$/y (Lahiri and Sinha, 2014).

***Gamerighat (E):*** *Gamerighat* near *Gohpur* in north bank of Brahmaputra was a busy center during the British rule. Migration of Brahmaputra towards north has already covered large area. Severe bank erosion is taking place for the last few years (Figure 3.11).

**Figure 3.11** Erosion sites of *Gamerighat*

***Palasbari (F)***

Among the 25 vulnerable and severe bank erosion sites as identified by the Water Resources Department, Govt. of Assam, *Palashbari* of Kamrup district is one of the most severely affected areas (Figure 3.12, Table 3.8) with erosion rate of 22 m/year. About 16,037 ha area of land has been eroded in *Palashbari* site alone since 1954, affecting 12,530 households (WRD, 2008).

**Figure 3.12** Erosion site of *Palasbari*

**Table 3.8** Extent of erosion in *Palasbari*

| | |
|---|---|
| Annual flood effected area | 3,340 Ha |
| Land area eroded (1967-2008), (bank line length 25 km) | 16,037 Ha |
| Rate of erosion | 22 m/year |
| Number of household lost (last 10 years) | 1,646 |
| Number of household affected | 12,530 |

Soil samples were collected at 10 cm depth and then at 30 cm intervals from vertical profile of exposed steep banks of erosion sites of the six locations. Multiple samples were collected from each location (Figure 3.13). Samples were collected from nearby non-erosion sites also.

**Figure 3.13** Collection of samples from *Palasbari* erosion site

All samples were brought to laboratory and preserved till analysis. pH, organic matter, carbonate content, Sodium Absorption Ratio, Exchangeable sodium percentage, Cation exchange capacity, mineralogy and particle size were estimated.

## 3.5 Evaluation of physico-chemical properties of sediments/ bank materials

### *3.5.1 Determination of pH*

Soil pH is a measure of the soil acidity or alkalinity and is sometimes called the 'soil water pH' since it is because it is a measure of the pH of the soil solution. The dried soil samples were mixed with distilled water (1:2.5 ratio) and then the mixture was stirred and the pH was measured using a pH meter.

### *3.5.2 Organic matter*

Two primary methods for the semi-quantitative estimation of organic matter in soils and sediments are: (1) loss on ignition and (2) hydrogen peroxide digestion. The hydrogen peroxide digestion method has several limitations including incomplete oxidation of the organic matter and varied extent of oxidation from one soil or sediment to another (Robinson, 1927). The loss-on-ignition (LOI) method was used for the determination of organic matter in the soil and sediment. Sequential loss on ignition is a common and widely used method to estimate the organic and carbonate content of sediments (Dean, 1974; Bengtsson & Enell, 1986). In a first reaction, organic matter is oxidized at 500–550°C to carbon dioxide and ash. In a second reaction, carbon dioxide is evolved from carbonate at 900–1000°C, leaving oxide (Heiri et al., 2001). The equations in the LOI method are given below:

$$LOI_{550} = \{(DW_{105}-DW_{550})/DW_{105}\}\times 100$$

Where

$LOI_{550}$ = LOI at 550°C (as percentage)

$DW_{105}$ = dry weight of the sample before combustion, g

$DW_{550}$ = dry weight of the sample after heating to 550°C, g

In a second step, carbon dioxide is evolved from carbonate, leaving oxide and LOI is calculated as:

$$LOI_{950} = \{(DW_{550}-DW_{950})/DW_{105}\}\times 100$$

Where

$LOI_{950}$ = LOI at 950°C (as percentage)

$DW_{550}$ = dry weight of the sample after combustion of organic matter at 550°C, g

$DW_{950}$ = dry weight of the sample after heating to 950°C, g

$DW_{105}$ = initial dry weight of the sample before combustion, g

Assuming 44g $mol^{-1}$ for carbon dioxide and 60g $mol^{-1}$ for carbonate, the weight loss by LOI at 950°C multiplied by 1.36 should then theoretically equal the weight of the carbonate in the organic sample (Bengtsson & Enell, 1986).

### *3.5.3 Heavy metal*

Heavy metals in suspended sediment samples were analyzed using the USEPA 3050B method and an atomic absorption spectrophotometer. For digestion of sediment, 0.5 g of sun dried sediment was mixed with 4 ml conc. HCl, 9 ml conc. $HNO_3$ and 5 ml conc. HF

acid in PTFE beaker with hood. The reagent mixture was heated till boiling for 1 hour and 2 ml of $H_2O_2$ was added and again heated for 30 minutes. Then it was allowed to cool. The final volume was adjusted with distilled water to 50 ml.

### *3.5.3.1 Geochemical fractionation of metals*

Mobility of trace metals, as well as their bioavailability and related eco-toxicity to a river system critically depends upon the chemical forms in which metals are present in sediments (Davidson et al., 1998). Sequential extraction procedure is frequently used to evaluate metal distribution into different chemical forms present in solid phase. Conceptually, sequential extraction categorizes metal associated with chemically homogenous fractions that ultimately affect metal availability. Modified BCR sequential extraction method (Rauret et al. 1999) was applied to understand the geochemical association and to predict the probable mobile fraction. Table 3.9 shows association of different metal fractions. The extractants used, extraction condition are outlined in Table 3.10. The different extracts were analyzed for their heavy metal concentration in AAS.

**Table 3.9** Association of different metal phases extracted

| Metal fraction | Association |
|---|---|
| Exchangeable (available fraction) | Metal sorbed on the surface, carbonate bound |
| Reducible | Metal associated with Fe-Mn oxides |
| Oxidizable | Metal bound with organics/ Sulfide associated metals |
| Residual | Metals fixed in crystalline phase |

**Table 3.10** Extractants used and extraction condition of modified BCR protocol

| Step | Fraction | Extracting agent | Extraction condition | |
|---|---|---|---|---|
| | | | Shaking time | Temperature ($^oC$) |
| 1 | Exchangeable and acid-soluble | 40 mL $CH_3COOH$ (0.1M, pH=7) | 16 h | 25--30 |
| 2 | Reducible | 40 mL $NH_2OH.HCl$ (0.5 M, pH=1.5) | 16 h | 25--30 |
| 3 | Oxidizable | 10 mL $H_20_2$ (30%, pH=2) and then 50 mL $CH_3COONH_4$ (1 M, pH=2) | 1, 2, 16 h | 30, 85, 30 |

#### *3.5.3.2 Quality control and quality assurance*

The analytical procedure quality control and assurance measures were implemented by analyzing blanks and replicates. Additional Certified Reference Material of Japanese Geological Survey, JSd-3 and JLk-1 were used for calibration and intermediate check in analytical procedure to evaluate the effectiveness of the digestion procedure.

### *3.5.4 Sodium Absorption Ratio (SAR), Exchangeable Sodium Percentage (ESP) and Cation Exchange Capacity (CEC)*

SAR: 4 g sediment was mixed with 40 mL of distilled water, followed by a consecutive 12 h shaking, centrifugation and filtering. The supernatant was analyzed to determine the amounts of Mg, Ca, Na and K to calculate SAR using the following equation (Sumner, 1993; Rengasamy and Churchman, 1999; Quirk, 2001):

$$SAR = [Na^{+}] / [(Ca^{2+} + Mg^{2+}) /2]^{0.5}$$

ESP and CEC: ESP was estimated for each sample by using residual sediments and adding 40 mL of 1.0 M ammonium acetate solution. The resulting suspension was shaken for 2 h, centrifuged and then filtered through a 0.45 μm membrane filter. The supernatant was analyzed with Flame photometer and AAS in order to determine the amounts of Na, K, Ca and Mg and the results obtained were used to calculate ESP and CEC.

### *3.5.5 Elemental and mineral composition*

Elemental composition of sediments was studied using Scanning Electron Microscope at Centre for Instrumentation Facility (CIF) at IIT Guwahati. Morphological investigations were carried out on a scanning microscopy analyzer (SEM, JOEL JSM-6300F), coupled with an energy dispersive X-ray analyzer (EDX, OXFORD 50 INCA ENERGY 400). The sample to be analyzed with Scanning Electron Microscope – Energy Dispersive X-Ray Spectroscopy (SEM-EDX) was mounted on Aluminium stub 2.5 cm in diameter using a double sided carbon tape. It was then placed in sputter coater and coated with thin layer of gold (Au) to make the sample electrically conductive. The typical accelerating voltage of SEM was kept at 30 kV, and the EDX was run with a lithium drifted silicon detector at a resolution of 133 keV.

Mineral composition was studied using X-ray diffraction (Bruker axs, model: D8 Advance). XRD is the primary, non-destructive tool for identifying and quantifying the mineralogy of crystalline compounds in rocks, soils and particulates. When monochromatic X-rays are projected onto a crystalline material at an angle (θ), diffraction occurs when the distance traveled by the rays reflected from successive planes differs by an integer *(n)* of wavelengths (λ). According to Bragg's Law:

$$n\lambda = 2d \sin\theta$$

where, d is the distance between atomic planes,

Approximate relative abundance ratios of major minerals were estimated from the relative intensities of the most intense and specific peak of each mineral from the XRD chart. The two theta (2θ) values for some individual minerals are shown in Table 3.11. The JCPDS database supplied with the diffractometer was used to identify the peaks of minerals in the diffractograms.

**Table 3.11** Minerals and their 2θ values

| Primary minerals | | Secondary minerals | |
|---|---|---|---|
| Mineral name | 2θ (degree) | Mineral name | 2θ (degree) |
| Quartz | 26.6 | Smectite | 5.1 |
| Feldspar | 27.5 | Illite | 8.9 |
| Calcite | 29.6 | Chlorite | 9.1 |
| Dolomite | 31 | Gypsum | 11.7 |
| Siderite | 31.8 | Kaolinite | 12.5 |
| Pyrite | 33.1 | Barite | 28.9 |
| Clays | 19.9, 34.6, 61.9 | Halite | 31.7 |

### *3.5.6 Particle size distribution*

Laser particle size analyzer (Mastersizer 2000) was used to find the grain size distribution of samples of sediments and bank materials. Laser diffraction particle size analyzers have proved to be an effective tool for providing particle size distributions of poorly coherent rocks and soils for last three decades (Weiss and Frock, 1976; McCave et al., 1986; de Boer et al., 1987; Wanogho et al., 1987; Agrawal et al., 1991; Loizeau et al., 1994; Pye and

Blott, 2004; Blott and Pye, 2006). They require little time for analysis, cover a wide size range, and require small size samples (Beuselinck et al., 1998), thus facilitating very detailed studies of particle size distributions in geological structures. It is based on the principle that particles of a given size diffract light through a given angle that increases logarithmically with decreasing size (Beuselinck et al., 1998). The 'wet procedures' involves dispersion of a few grams of material into a liquid that circulates across a quartz measurement cell illuminated by a laser beam (Storti and Balsamo, 2010).

## 3.6 Analysis of data

Role of individual bank material properties in erosion were studied with binary logistic regression using SPSS. The goal of logistic regression is to find the best model to describe the relationship between a dependent variable and multiple independent variables (Ohlmacher and Davis, 2003; Lee, 2005). The dependent variable of a logistic regression could be binary or categorical and the independent variables of a logistic regression could be a mixture of continuous and categorical or binary variables. General form of logistic regression is

$$y = a + b_1x_1 + b_2x_2 + b_3x_3 + \ldots + b_mx_m \quad (1)$$

$$y = \log_e [P/(1- P)] = \text{logit } (P) \quad (2)$$

$$P = e^y/ (1 + e^y) \quad (3)$$

where $x_1, x_2, \ldots, x_m$ are explanatory variables and y is a linear combination function of the explanatory variables representing a linear relationship. The parameters $b_1, b_2, \ldots, b_m$ are the regression coefficients to be estimated. P refers to the probability of the occurrence of an event **(**Ozdemir, 2011). Logistic Regression appears to be one of the most popular methods for landslide susceptibility assessment and has been applied in different geographical areas and various scales (Dai and Lee 2003, Yesilnacar and Topal, 2005). Ioannidou et al. (2015) determined river bank erosion by a regression model using independent variables that are considered to affect the erosion process. Detailed descriptions of the logistic regression technique can be found in Hosmer and Lemeshow (2000) and Kleinbaum and Klein (2002).

## 3.7 **Braiding indices and land use and land cover analysis**

Landsat images from NASA's USGS website (https://glovis.usgs.gov/) were utilized in the present study (Table 3.12).

**Table 3.12** Satellite dataset used in the present study

| Sl. No. | Sensor | Path / Row | Date of acquisition | Spatial resolution |
|---|---|---|---|---|
| 1 | MSS | 145 / 41 | 15-11-1973 | 60 m |
| 2 | MSS | 146 / 41 | 16-11-1973 | |
| 3 | MSS | 147 / 41 | 05-12-1973 | |
| 4 | MSS | 147 / 42 | 22-11-1973 | |
| 5 | MSS | 148 / 42 | 21-02-1973 | |
| 6 | TM | 135 / 41 | 20-11-1994 | 30 m |
| 7 | TM | 136 / 41 | 26-10-1994 | |
| 8 | TM | 136 / 42 | 26-10 -1994 | |
| 9 | TM | 137 / 42 | 01-10-1994 | |
| 10 | TM | 138 / 42 | 11-12-1994 | |
| 11 | OLI | 135 / 41 | 27-11-2014 | |
| 12 | OLI | 136 / 41 | 18-11-2014 | |
| 13 | OLI | 136 / 42 | 18-11-2014 | |
| 14 | OLI | 137 / 42 | 09-11-2014 | |
| 15 | OLI | 138 / 42 | 02-12-2014 | |

Images were procured for the same season of the year to minimize inconsistencies in data. Post-monsoon data were used due to low cloud cover and proper channel and sandbar definition available during this season. Raw data consisting of individual bands of each satellite image were combined in ERDAS Imagine image processing software to create a composite image. The images were then pre-processed for image enhancement techniques like haze reduction, brightness and contrast to make the process of information extraction easier. Images were then stitched to create a single seamless mosaic image for the entire stretch of the river which was utilized to visually interpret and extract the bank line, river center line, main channel, braided channels and sandbars as vector data created by ArcGIS 10.1 with the earth model and datum WGS84. The data was converted into planner coordinates system using UTM projection with earth model WGS84 and zone 46 North.

Brahmaputra River in Assam at three different years, i.e., 1973, 1994 and 2014 was divided into 16 reaches with equal length of 40 km and the reaches were numbered from 1 in the upstream to 16 in the downstream as shown in Figure 3.14.

Erosion and deposition during 1973 – 2014 was studied using overlay analysis in GIS. Braiding values for different reaches of Brahmaputra in 1973 and 2014 were calculated for sixteen reaches by seven different established methods and one new method suggested in this study.

Land use and land cover analysis for 1994 – 2014 was carried out by categorizing the satellite images into different classes, i.e., river/ water, sandbar, vegetation (including natural grass land) and agriculture (including human settlement), using unsupervised classification in image processing software (ERDAS Imagine).

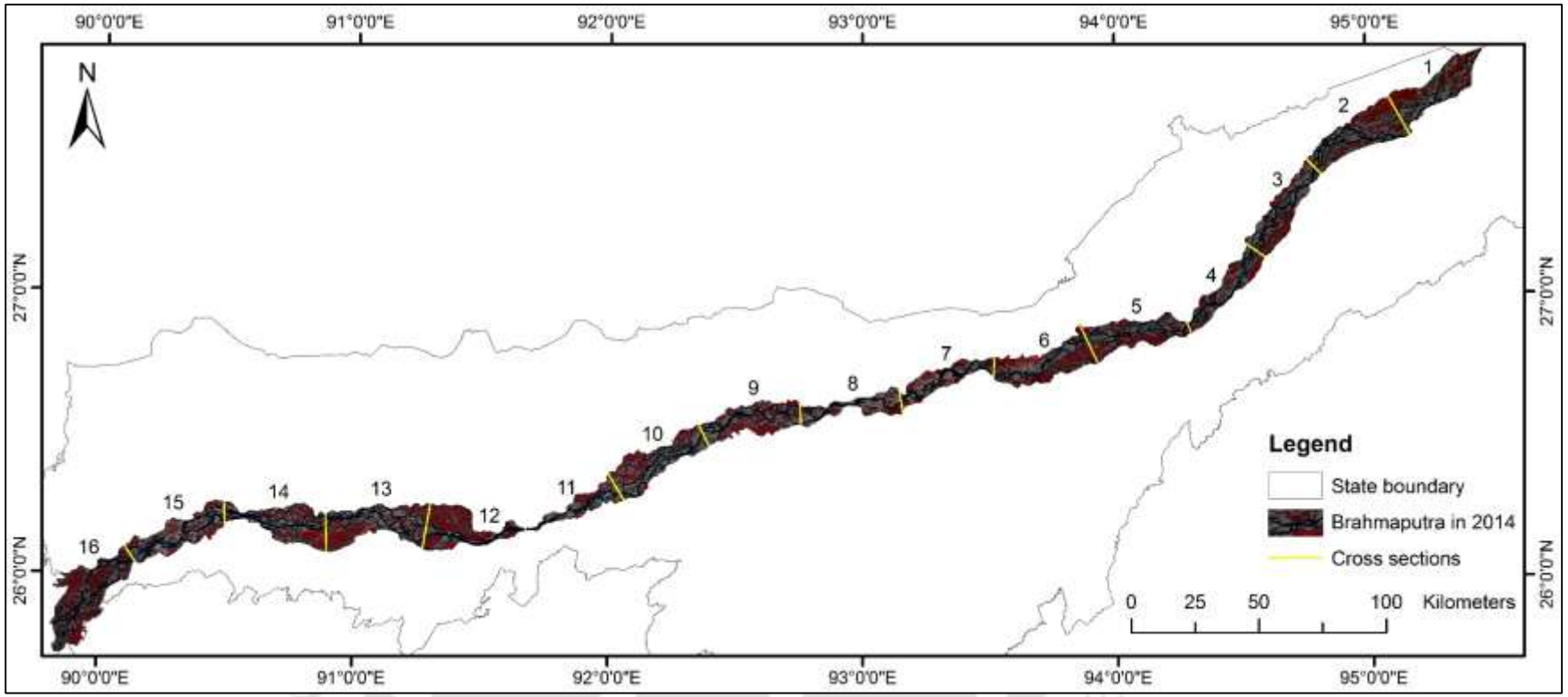


**Figure 3.14** Sixteen reaches of Brahmaputra River in Assam

Chapter 4

# Genesis and deposition of sediments in Brahmaputra

This chapter discusses the causes and sources of sediments of Brahmaputra River. Sediment inputs from tributaries, scouring and bank erosion along with sediment sinks are discussed. Physical properties of bed and bank materials are also highlighted. River bank erosion of Brahmaputra in Assam during 1973 – 2014 is studied using GIS. Finally, a sediment budget for Brahmaputra in Assam is presented.

## 4.1 Causes of high sediment load in Brahmaputra

The Brahmaputra alone supplies 1000 million ton of suspended material to the Bay of Bengal (Milliman and Meade, 1983; Milliman and Syvitski, 1992; Hay, 1998). Sediment yield of Brahmaputra (852.4 t/km$^2$/y) is the highest in the world (Latrubesse, 2008). Main reasons of high sediment load in Brahmaputra River are:

*i) Young lithology*

Geologically Brahmaputra is a young river whose present configuration took place only during Pleistocene and recent period (Datta and Singh, 2004), i.e., between 0.0117 and 2.58 million years ago. Table 4.1 shows age of a few large rivers of the world and the Brahmaputra is younger than most of the large rivers. The Brahmaputra valley evolved during the last two million years through subsidence and alluviation of the foreland depression in between the young mountain chains of the Eastern Himalayas and Indo-Burmese (Myanmar) mobile belts, and the block-uplifted plateau of Meghalaya (Nandi,

2001). The Himalaya is the youngest and tallest mountain system, which includes world's most erosion prone region (Pandey et al., 1999). The collision of the Indian and Tibetan plates, initiated ~55 Ma ago, resulted in the formation of the Himalayan orogeny (Kundu et al., 2012). Exposure of the geologically young rocks forming the Himalayan mountain range is responsible for the high sediment flux of the Himalayan rivers. Dissolved material fluxes carried by rivers are regulated by chemical weathering of rocks and minerals, whereas particulate transport is determined by physical weathering (Krishnaswami and Singh, 2005).

**Table 4.1** Age of a few large rivers

| River | Age |
|---|---|
| Amazon | 11 million years |
| Nile | 3 million years |
| Mississippi | 10,000 years |
| Yangtze | 45 million years |

(Four Rivers Reality, 1996)

*ii) Seismicity*

Brahmaputra is located in a tectonically complex and seismically active region. Occurrences of large and small frequent earthquakes reflect long-range interactions of mega tectonic units such as north-south convergence of the Indian-Eurasian plate along the Himalayas and east-west convergence in the Indo-Burma mountain and under thrusting of the Indian plate below the Eurasian plate (Tiwari et al., 2004). The Brahmaputra basin frequently experiences a number of earthquakes and landslides and slips occur owing to such earthquakes resulting in high sediment load in rivers. Between 1920 and 1980, as many as 455 earthquakes of magnitude higher than 5 on the Richter scale were recorded in the Northeast region of India. Magnitude-wise distribution of earthquakes for the period of 1920-1980 and beyond 1980 up to 1988 is noteworthy (Table 4.2).

**Table 4.2** Magnitude-wise distribution of earthquakes for the period of 1920 –1988

| 1920--1980 | | 1980--1988 | |
|---|---|---|---|
| Magnitude (Richter scale) | Number of occurrence | Magnitude (Richter scale) | Number of occurrence |
| 5 to 6 | 270 | 5.5 to 6 | 6 |
| 6 to 7 | 167 | 6 to 7 | 2 |
| 7 to 8 | 15 | 7 to 8 | 1 |
| 8 and above | 3 | 8 and above | NIL |
| Total | 455 | Total | 9 |

The earthquakes of 1762, 1822, 1865, 1869, 1897 and 1950 were notable. Particularly, by the impact of the 1950 earthquake (epicenter in China at about 50 km from north-east border of India, magnitude 8.6 in the Richter scale), the river bed of Brahmaputra and all other tributaries have been raised considerably owing to heavy deposit of silts (Krishna, 2004). The most dramatic feature of 1950 earthquake was the landslides (Gupta and Gahalaut, 2014). The liquefaction features formed by this earthquake were observed in the alluvial fans and fluvial deposits of Brahmaputra River and its tributaries (Poddar, 1952). As a result of the earthquake, the bed of Brahmaputra silted up by about 3 metres at *Dibrugarh* within a period of 10 years; prior to 1950, the annual average silting rate at *Dibrugarh* was 3 cm only (WRD, 2004). The abrupt change in water levels (yearly observed lowest water levels) of Brahmaputra at *Dibrugarh* after 1950 is discernible (Figure 4.1).

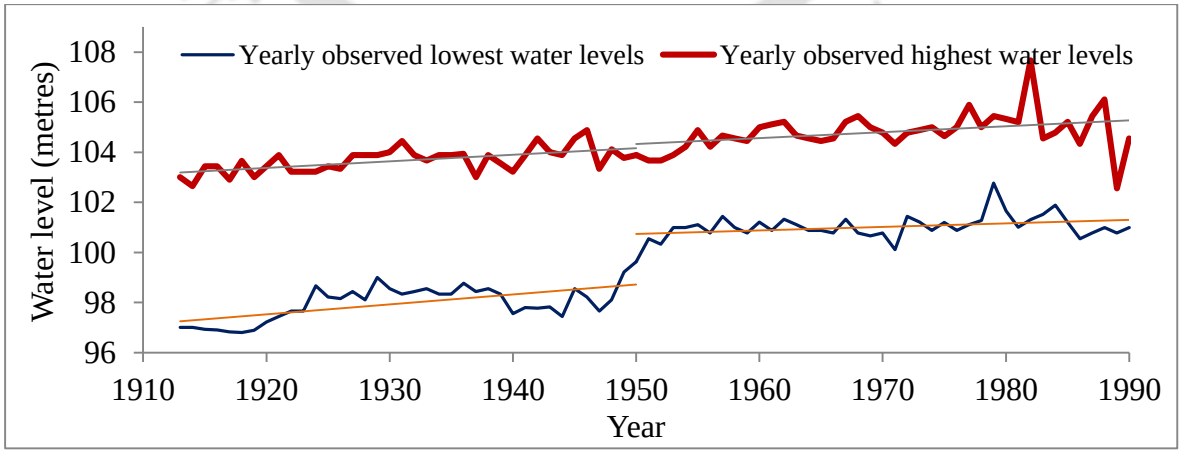


**Figure 4.1** Water levels of Brahmaputra at *Dibrugarh* during 1913--1990

*iii) Unconsolidated sedimentary rocks of the Himalayas*

There are three different tectonomorphic provenances in the Brahmaputra River Basin: Northwestern and northern provenance along the eastern Himalayas and the southern part which situated close to Naga-thrust belt (Indo–Burmese range). Tectonically, these regions are parts of the eastern continuity of the Indo–Gangetic–Brahmaputra foreland basin (Verma et al., 2016). The Brahmaputra River and its north bank tributaries traverse through unconsolidated sedimentary rocks of the Himalayas. High amount of sediment are washed down by the monsoon rains.

*iv) Heavy rainfall in monsoon*

Prolonged and heavy rainfall ranging from 2,480 mm in the Brahmaputra valley to 6,350 mm or more in the North Eastern Hill is largely concentrated during four to five monsoon months (WRD, 2004). High intensity of rainfall erodes the topsoil and mobilizes subsoil; landslides and slips, which occur in many places add high sediment load in the river. During monsoon period, sediment transport increases nearly 100 fold for a 10 fold increase of discharge (FAP24, 1996).

In the Eastern Himalaya, where heavy rainfall and earthquakes are frequent, the incidence of landslide is very high. Rain water percolates through joints, fractures, foliations and pores of rocks and soils making them loose and heavy, which caused the whole slope to slump down. Landslide susceptibility of the sub-Himalayan or lower-Himalayan region of Arunachal Pradesh at elevation 100 – 3000 m, characterized by very high relief, severe sandstone, shale alternations, schist, phyllite, is very high.

*v) Steep slope of Brahmaputra and its tributaries*

Slope of Brahmaputra is steep when it crosses the Himalayas. Steepness of Brahmaputra River is high compared to most of the large rivers of the world. Gradients measured over 50 km on adjacent floodplain using GoogleEarth for a few large rivers are shown in Table 4.3 (Lewin and Ashworth, 2014). Among the Tibetan rivers, although the gradient of the Mekong river is higher, much of its length the Mekong flows through bedrock channels, i.e. channels that are confined or constrained by bedrock or old alluvium in the bed and

riverbanks (MRC, 2010). The Mekong reach is an example of 'bedrock anastomosis' where the river divides up into multiple channels etched into bedrock. In case of the Ganges, with low relief and limited height differences over long distances, the surface of the plain appears as a rather flat alluvial plain (Singh, 1996). Slope of Brahmaputra River (Figure 4.2) created by using data of 175 points along the channel taken from Google Earth demonstrates a much clear picture with marked differences compared to the earlier figure proposed by other researchers based on a few points (Goswami, 1985; Lewin and Ashworth, 2014), e.g., slope near *Pasighat* and *Guwahati* are 1.52 m $km^{-1}$ and 0.13 m $km^{-1}$ respectively, whereas the corresponding values in the earlier finding were 0.62 m $km^{-1}$ and 0.1 m $km^{-1}$ respectively. Average gradient of Brahmaputra River is 1.52 m $km^{-1}$. In the entire course of the river, ~100km reach known as Tsangpo gorge where the river abruptly bends southward is a locus of extremely rapid and focused erosion (e.g., Finlayson et al., 2002; Finnegan et al., 2008; Stewart et al., 2008; Larsen and Montgomery, 2012).

North bank tributaries like *Subansiri, Ranganadi, Jia Bharali, Noa Nadi, Moridhal, Jiadhal,* and *Pagladiya* also have very steep slopes and shallow braided channels for a considerable distance from the foothills and in some cases right up to the outfall. Steep slopes of river and tributaries in the mountainous reaches led to high amount of sediment generation and transportation. The sediment transporting capacity of a flow is highly sensitive to the velocity. Theoretical considerations have shown that the rate of sediment transport is proportional to the fourth to sixth power of velocity. 10% decrease in flow velocity would result in the reduction of 30% to 40% of its original transport capacity (Oak, 2014). Sudden decrease in slope of Brahmaputra results in a large amount of sediment deposition developing a prominent braided pattern near *Pasighat* in Arunachal Pradesh, where slope is abruptly decreased (slope of the river in the reach between *Pi* in Tibet and India border is 8.27 m $km^{-1}$, whereas the slope in the reach between entry to India and *Pasighat* is 1.52 m $km^{-1}$). The slope is further decreased during the course of the river in Assam plains, e.g., from 0.81 m $km^{-1}$ between *Pasighat* and *Dibrugarh* at upstream to 0.09 m $km^{-1}$ between *Guwahati* and Bangladesh border at downstream (Table 4.4.). More prominent braided pattern of Brahmaputra near *Pasighat, Dibrugarh* (upstream), *Palasbari* and *Dhubri* (downstream) are shown in Figure 4.3. Average braided width of

Brahmaputra through Assam has increased from 6 km in 1912-28 to 9 km in 2006 (FAP24, 1996).

**Table 4.3** Gradients of a few large rivers of the world (From Lewin and Ashworth, 2014)

| River | Mean annual runoff ($10^9 m^3$) | Gradient (m $km^{-1}$) | Valley width (km) | Channel width (km) |
|---|---|---|---|---|
| Amazon | 6246 | 0.10 | 50 | 2.5 |
| Congo | 1292 | 0.14 | 10-26 | 2.5 |
| Yangtze | 872 | -- | 15 | 2.5 |
| **Brahmaputra** | **574** | **0.22** | **20** | **12.0+** |
| Volga | 560 | 0.08 | 18 | -- |
| Zambezi | 546 | 0.22 | 9 | 0.80 |
| Mississippi | 495 | 0.06 | 50+ | 1.5 |
| Mekong | 466 | 0.46 | 10 | 1.8 |
| Ganges | 380 | 0.08 | 10 | 1.00 |
| Indus | 238 | 0.14 | 90+ | 1.10 |

**Table 4.4** Slope of Brahmaputra River

| Reach | Elevation difference (m) | Length (km) | Slope (m $km^{-1}$) |
|---|---|---|---|
| Source and Lhasa | 1696 | 1194 | 1.42 |
| Lhasa and Pi (Pe) | 679 | 535 | 1.27 |
| Pi (Pe) and Great Bend | 1497 | 113 | 13.19 |
| Great bend and India border | 852 | 170 | 5.01 |
| India border and Pashighat | 420 | 276 | 1.52 |
| Pasighat and Dibrugarh | 36 | 44 | 0.81 |
| Dibrugarh and Tezpur | 55 | 280 | 0.19 |
| Tezpur and Guwahati | 18 | 137 | 0.13 |
| Guwahati and Bangladesh border | 20 | 209 | 0.09 |
| Indo-Bangladesh border and Bay of Bengal | 21 | 494 | 0.04 |
| **Entire length** | **5291** | **3452** | **1.52** |

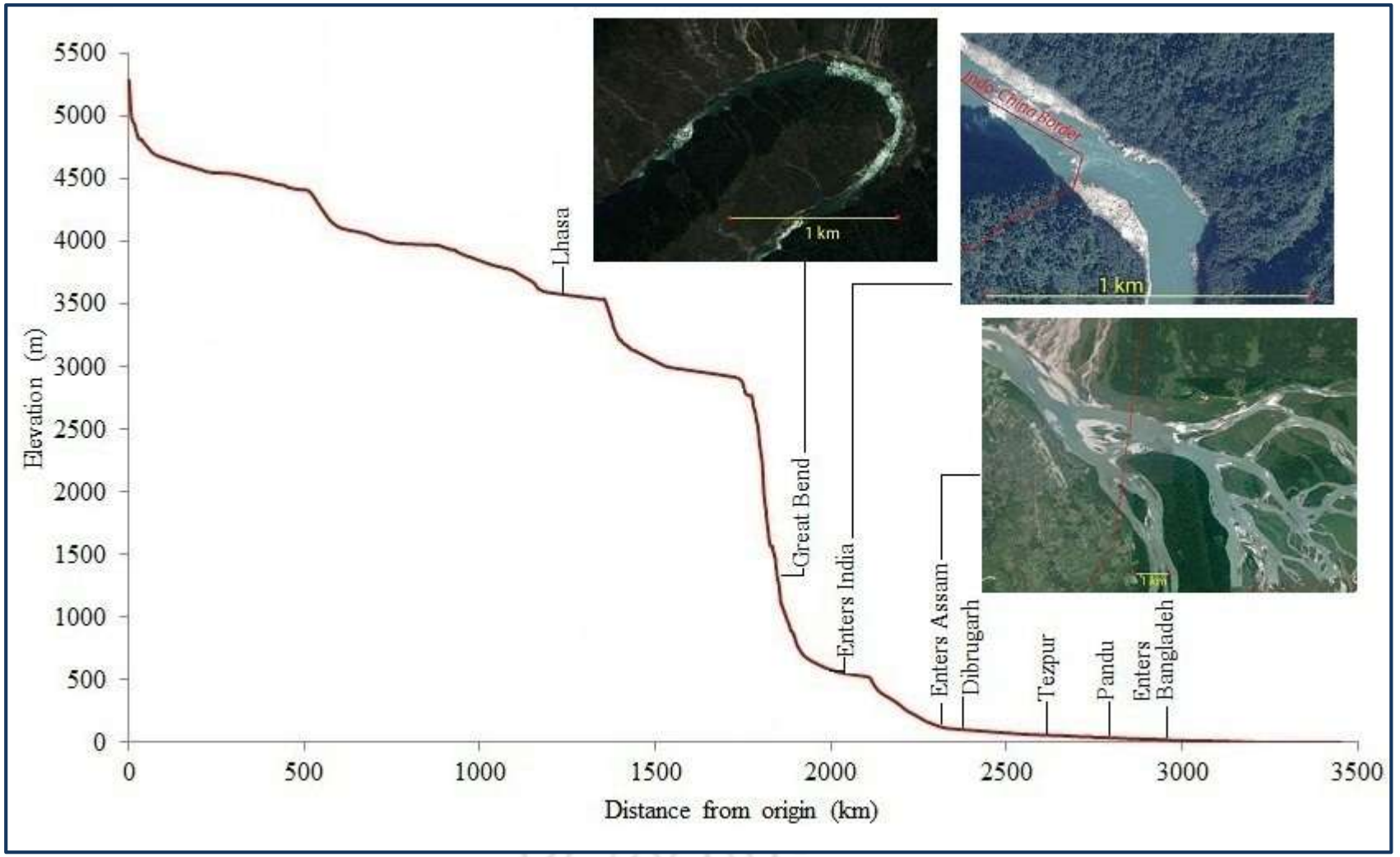


**Figure 4.2** Slope of Brahmaputra River

*Source of data and images: 2013 DigitalGlobe [Google Earth]*

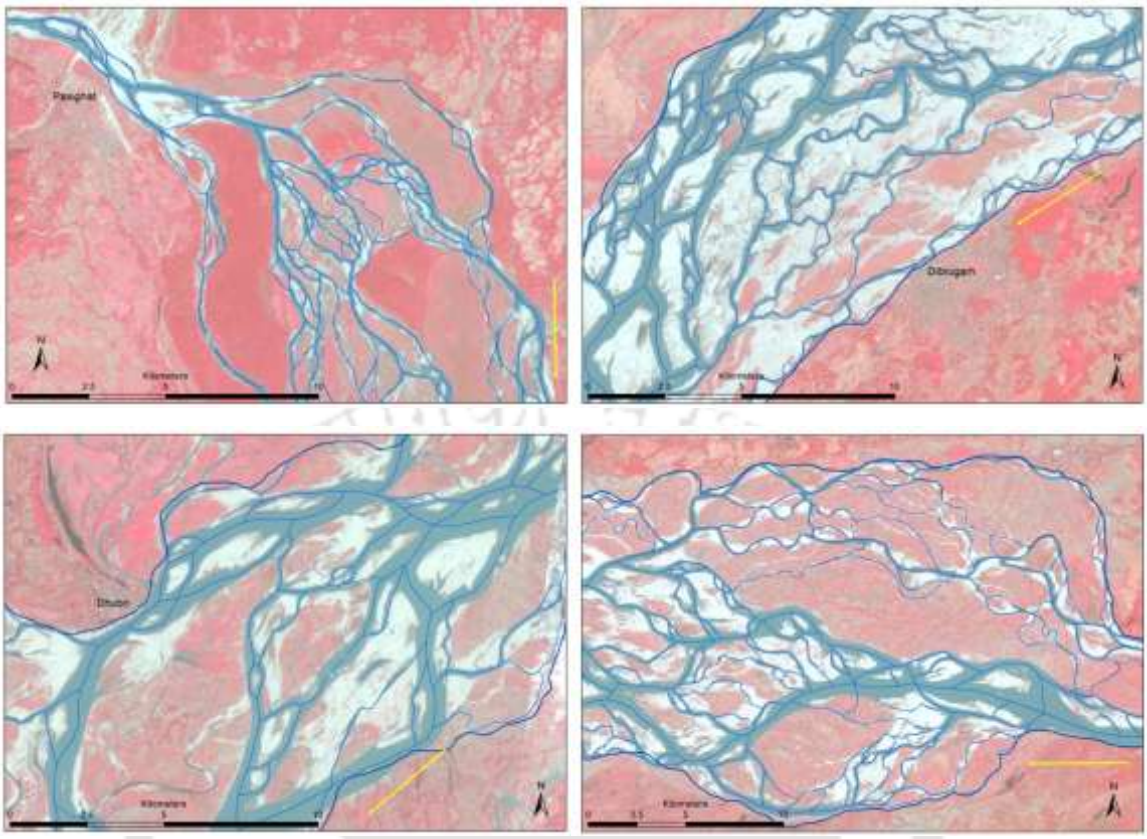


**Figure 4.3** Braided pattern of Brahmaputra near (clockwise) *Pasighat, Dibrugarh, Palasbari* and *Dhubri* in 2014

*vi) Deforestation, jhum cultivation, forest fire*

About half a million families in northeastern region annually cultivate in 10,000 $km^2$ forests, whereas total area affected by *jhumming* is believed to be 44,000 $km^2$ (Singh, 1990). It has been estimated that in North-Eastern region of India about 40 tones per hectre or 2.5 mm top soil is lost annually due to soil erosion from the areas where *jhuming* is frequently resorted to and no soil conservation measures have been taken. Heavy pressure on land due to unscientific and commercial exploitation of forest wealth including hills and hillocks, grazing, shifting cultivation, forest fires, faulty land use practices are significant factors contributing to high sediment load in the tributaries as well as Brahmaputra River. Annual soil loss from water induced erosion in some specific catchments of Northeast India (Table 4.5) points towards major impact.

**Table 4.5** Annual soil loss estimates from water erosion in Northeast India

| Sl no | Details of land resource regions | Area ($km^2$) | % to total area of the country | Area ($km^2$) with erosion | Soil loss in $t/km^2$ |
|---|---|---|---|---|---|
| 1 | North-Eastern Himalayan Alpine grass and Meadow region | 16,000 | 0.5% | 4,000 (25%) No erosion<br>12,000 (75%) Medium erosion | Nil<br>50 |
| 2 | North-Eastern forest region | 1,61,000 | 4.97% | 40,000 (25%) No erosion<br>81,000 (50%) medium erosion<br>40,000 (25%) Shifting cultivation | Nil<br>287<br>4,095 |
| 3 | Assam valley | 88,500 | 2.73% | | 2,815 |

(NEC, 1993)

Sediment concentration at *Pandu* (Guwahati) site for the period of 1955 – 1983 (Figure 4.4) showed that the sediment concentration was more and almost constant up to 1958. It followed a linearly decreasing trend between 1958 to 1974 due to clearing of sediment deposits and debris deposited during the 1950 earthquake. Increase in sediment concentration after 1974 may be due to excessive precipitation, afforestation and erosion.

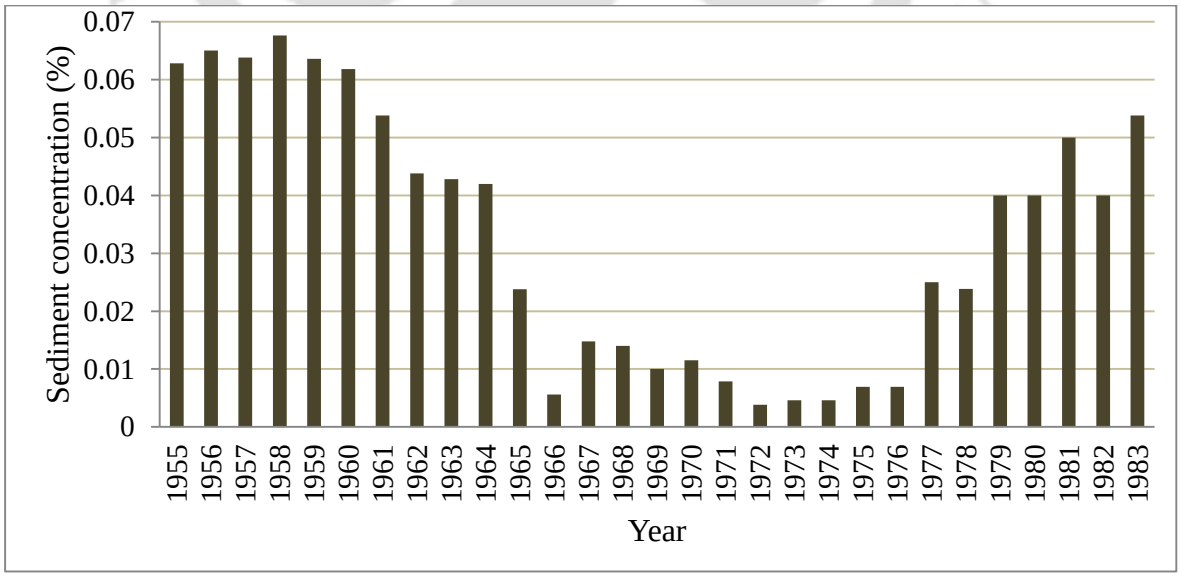


**Figure 4.4** Sediment concentration of Brahmaputra at *Pandu* site during 1955 – 1983

## 4.2 Sources of sediments in Brahmaputra

Based on material balance calculations, Singh and France-Lanord (2002) estimated that contribution from Tibet, Eastern Syntaxis, Eastern drainage/Mishmi Hills and the Himalayan sub-basins to the Brahmaputra sediments are 5%, 45%, 10% and 40% respectively. The Eastern Syntaxis, with an area of ~4% of the Brahmaputra basin, supplies about half of the total sediments to Brahmaputra and this can be attributed to rapid erosion in the region. The tributaries joining from the Himalaya in the Assam plain drain crystallines and sedimentaries of the higher and lesser Himalaya (Kumar, 1997).

### 4.2.1 Tributaries of Brahmaputra

Three main branches Dihang, Dibang and Lohit contribute the highest share of sediment load to Brahmaputra in Assam. 63% of annual average sediment load of the river is contributed by these three rivers. Contribution of suspended sediment load by other tributaries to Brahmaputra (Figure 4.5) is relatively lesser.

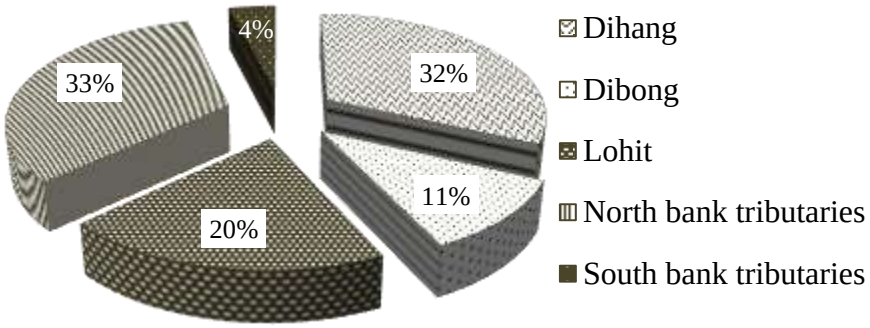


**Figure 4.5** Contribution of suspended sediment load by tributaries to Brahmaputra

Of the north bank tributaries, four major ones, i.e., *Subansiri, Jia Bharali*, *Manas* and *Sankosh* together contribute more than 90% sediment load of all north bank tributaries. The south bank tributaries contribute only 4% of total sediment load. Annual average sediment load of the major tributaries of Brahmaputra (Figure 4.6) is thus affected by differential loads from either banks.

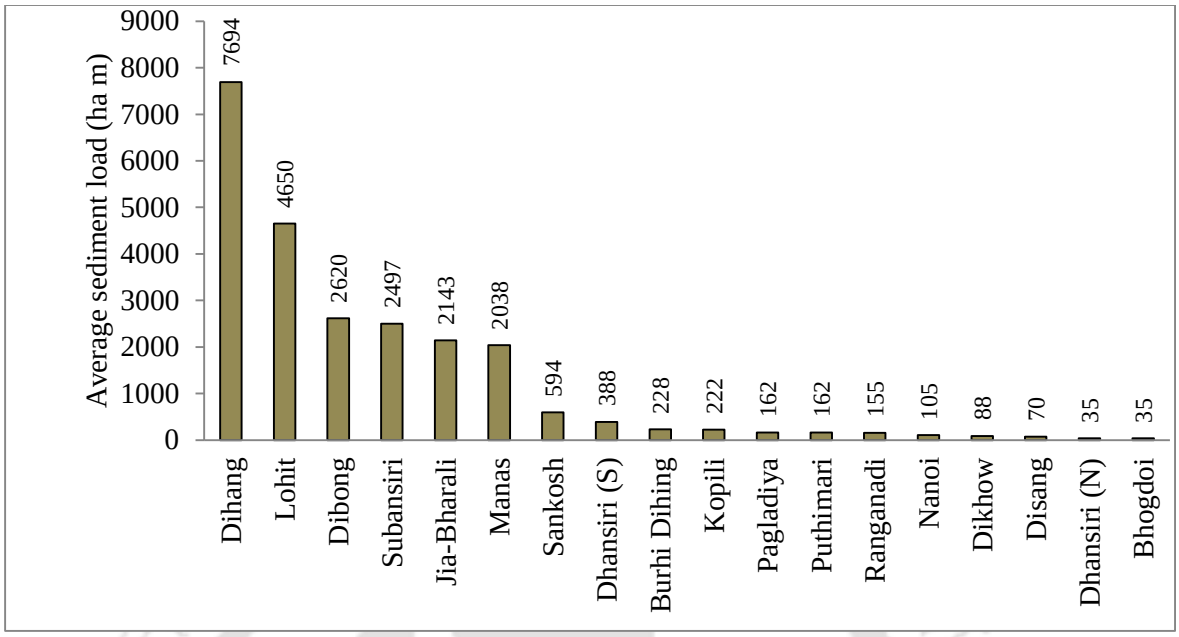


**Figure 4.6** Average sediment load of the major tributaries of Brahmaputra

In spite of input from tributaries, scouring of river bed and bank erosion are other sources of sediments to Brahmaputra. These two factors are discussed in the following sections.

### 4.2.2 Scour and deposition of sediments in Brahmaputra

Scouring of bed is a significant source of sediments in an alluvial river, whereas deposition in the bed is a sink, which may be temporary or permanent. Mainstream sediment exchange with floodplains/ islands by erosion and accretion dominate on some actively meandering and braided rivers like Amazon (Mertes et al., 1996), Orinoco (Meade, 2007), Fly and Strickland (Swanson et al., 2008) including the Brahmaputra–Jamuna (Best et al., 2007), but very little on others like the Congo or Magdalena (Lewin and Ashworth, 2014). Scour can be developed for many reasons such as local flow condition, secondary currents, presence of bedforms and natural or man-made structures.

Aggradation and degradation in the river bed of Brahmaputra were studied considering data from six reaches as mentioned in Table 4.6 (Figure 4.7).

**Table 4.6** Average width, length and area of reaches

| Sl no | Cross section to cross section | Average width of River (km) | Length of reach (km) | Area ($km^2$) |
|---|---|---|---|---|
| 1 | 2 to 11 | 11.46 | 83.64 | 958.85 |
| 2 | 11 to 21 | 12.35 | 88.23 | 1088.41 |
| 3 | 21 to 31 | 9.62 | 83.14 | 799.47 |
| 4 | 31 to 41 | 11.22 | 117.31 | 1316.22 |
| 5 | 41 to 51 | 10.40 | 109.14 | 1134.73 |
| 6 | 51 to 61 | 13.04 | 103.02 | 1343.38 |
| Total | 61 to 2 | 11.25 | 584.38 | 6574.28 |

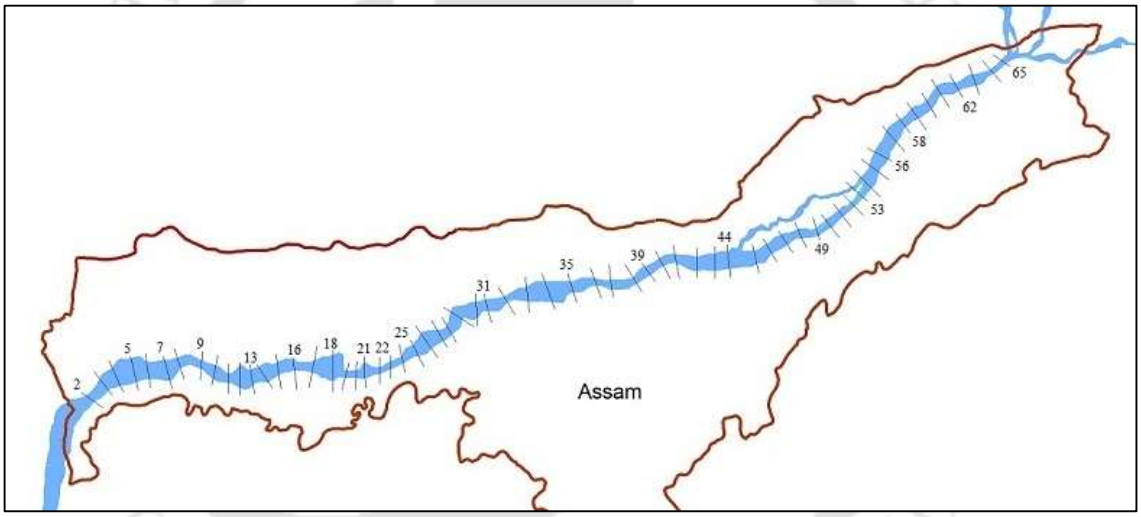


**Figure 4.7** Twenty cross-sections of Brahmaputra River identified for present study

Amount of total deposition and scour in the six reaches during 1957-71, 1971-77, 1977-81 and 1981-89 is shown in Figure 4.7.

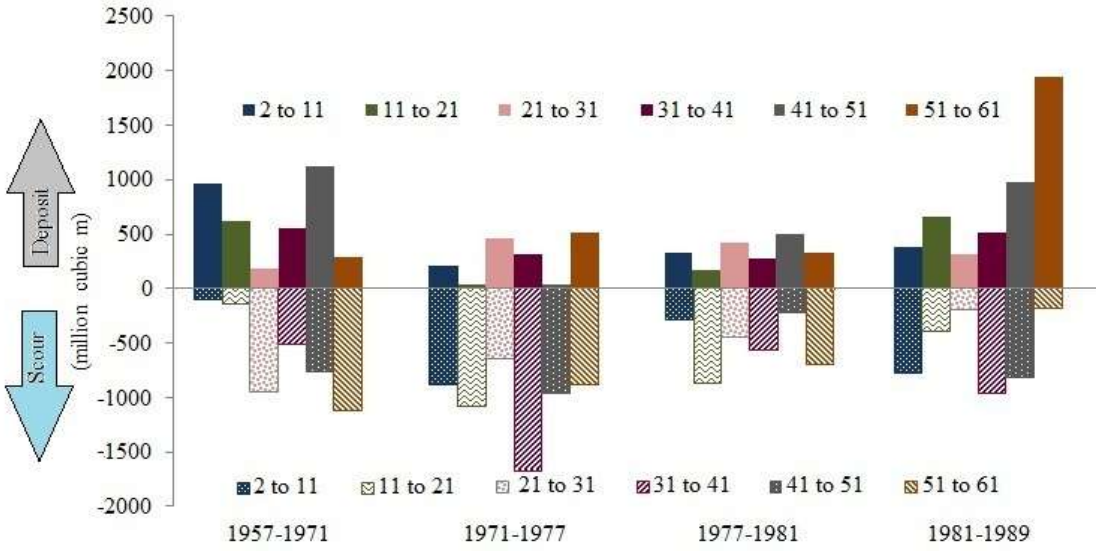


**Figure 4.8** Scour and deposition in Brahmaputra

During 1957–71, scouring was the highest in the middle reaches and upstream of the river (cross-sections 21–31, 41–51 and 51–61) with consequent deposition in downstream reaches (cross-sections 2–11, 11–21) including cross-section 41–51. During 1971–77 and 1977–81, scouring was dominant in all the reaches (exception: cross-sections 41–51) with maximum scouring in the cross-sections 31–41.

Comparison of net deposition/ scour in different reaches from 1957 to 1971 (Figure 4.9–4.11) showed relatively lesser deposition or scour along the river, although the scouring and deposition at different reaches were not uniform. During 1957–71, aggradation of about 6 cm per year and a scour of 7 cm per year were taken place. Beyond 1971, however, scour was more pronounced and approximately 11 cm per year was observed from 1971 to 1977. During 1977–1981, scour of about 4 cm per year occurred. During 1981 – 1989, aggradation of 2.5 cm per year was noticed. Considerably higher aggradation in the head reaches upstream at the rate of 17 cm per year was recorded. Considering the period of 1957 to 1989 for which cross sections data were available, average scour of 2 cm per year was noticed with maximum scouring of 5 cm per year in the middle reaches (Cross sections 31–41) except for aggradation of 0.5 cm per year in the upper most reaches (Cross sections 51–61) (Figure 4.10).

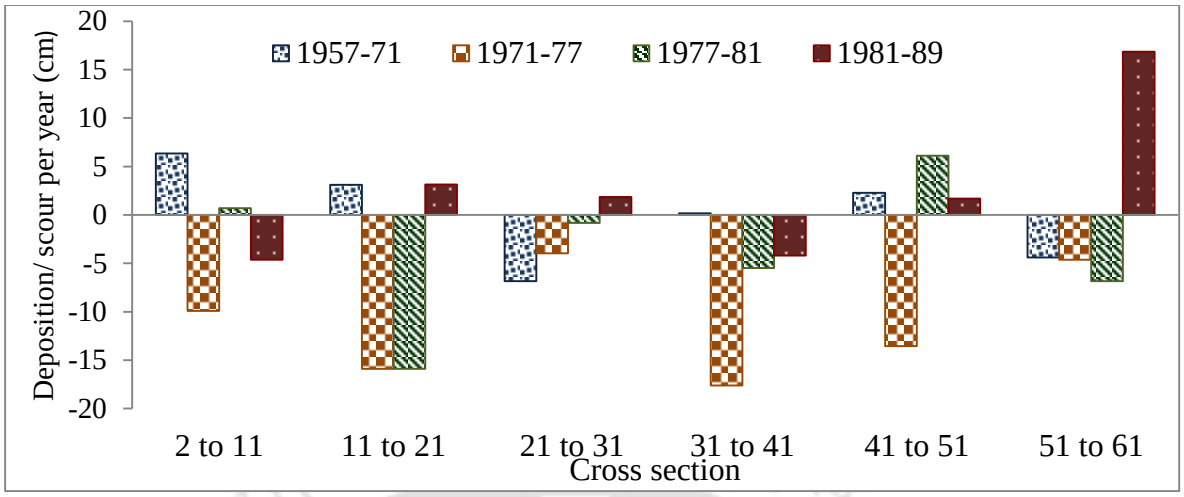


**Figure 4.9** Deposition/ scour in different reaches in different periods

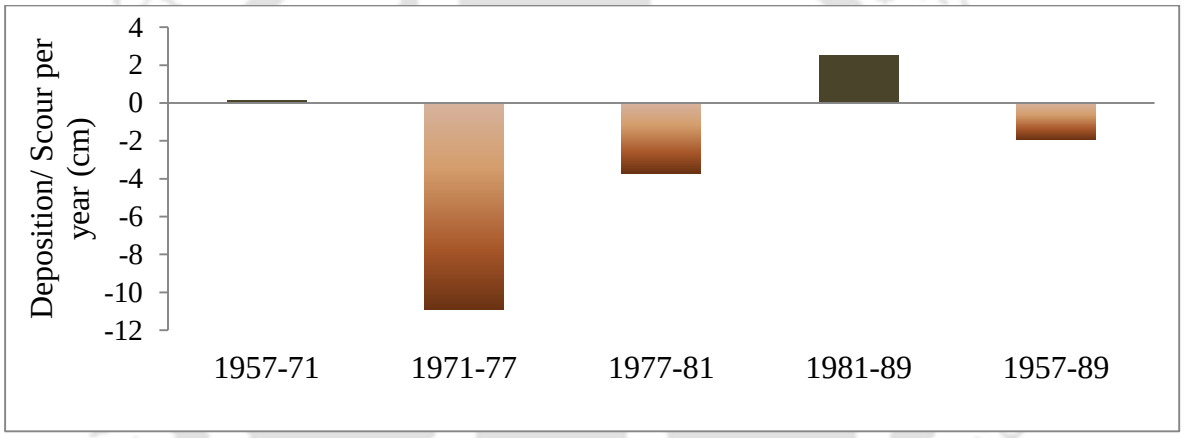


**Figure 4.10** Net deposition/ scour in all the reaches in different periods

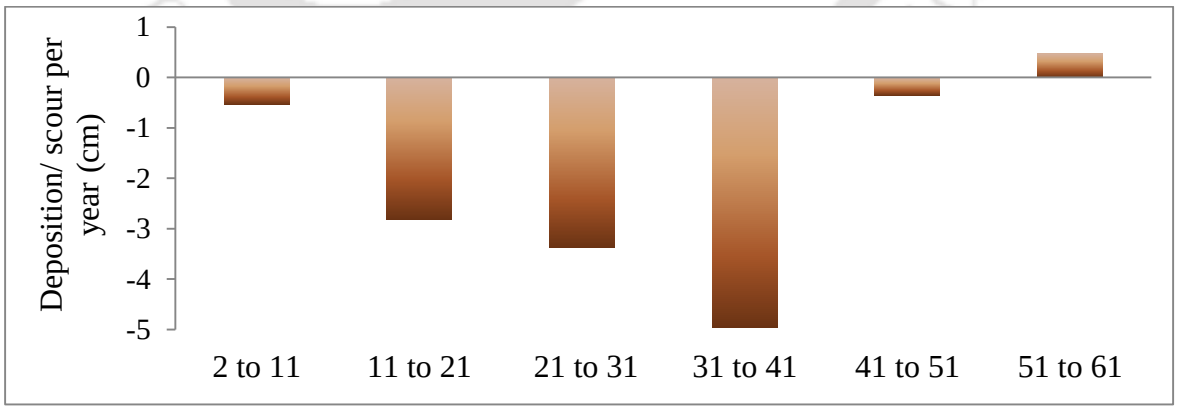


**Figure 4.11** Net deposition/ scour in different reaches during 1957–89

Deposition of sediments results in stable island formation and unstable bar development. Size, shape and position of bars change radically both seasonally and annually (Coleman, 1969; Bristow, 1987). Large scale bedforms (bars and islands) and micro-scale bedforms (ripples and dunes) are probably the most important river bed features inducing resistance to flow, and thus influences bed shear stress (Hassan and Galapati, 2014). Ripples and dunes exist in abundance in Brahmaputra. Sand dunes, with heights ≤ 6m, wavelengths ≤ 330 m, and migration rates ≤ 17 m/h (Garzanti et al., 2010) exist through the entire course of the monsoon in Brahmaputra. Dunes remain as major driving forces for friction and turbulence to the flow. The distribution of flow is the most complicated in Brahmaputra due to presence of braid bars, ripples and dunes. Dunes are the main driver of bed load transports, and responsible for the formation of local bed morphology.

### 4.2.3 Shifting of Brahmaputra and river bank erosion

Alluvial courses are very sensitive indicators of channel change and can readjust to variation in hydrology, sediment load and active tectonics (Schumm et al., 2000). Rivers like Ganga (Singh, 1996; Srivastava and Singh, 1999; Harijan et al., 2003; Swamee et al., 2003; Roy and Sinha, 2005), Kosi (Geddes, 1960; Mookerjea, 1961; Wells and Dorr, 1987), Gandak (Mohindra et al., 1992), Meghna (Rahman et al., 2004), Indus (Harbor et al., 1994), Madison, USA (Leeder and Alexander, 1987) and many others show spatio-temporal shifting of their channels. Kotoky et al. (2005) studied shifting of Brahmaputra River. Contemporary mainstream sediment exchanges with floodplains/ islands by erosion and accretion dominate on some actively meandering and braided rivers like Amazon (Mertes et al., 1996), Orinoco (Meade, 2007) and Brahmaputra–Jamuna (Best et al., 2007).

Based on data from NEC (1993) and Brahmaputra Board (1995), shifting of Brahmaputra in Assam from 1911–1928 to 1961–1970 and 1971–1972 is shown in Figure 4.12. Both the bank lines were shifted outward from base line of 1911-28 in the upstream of Brahmaputra in Assam. There was continuous erosion in the reach with length of 120 km and 137 km in left bank and right bank respectively at upstream between 1911-28 and 1971-72. For next 300 km from upstream, the bank lines were oscillated from the base line with erosion and deposition on both the banks. The north (right) bank shifted to

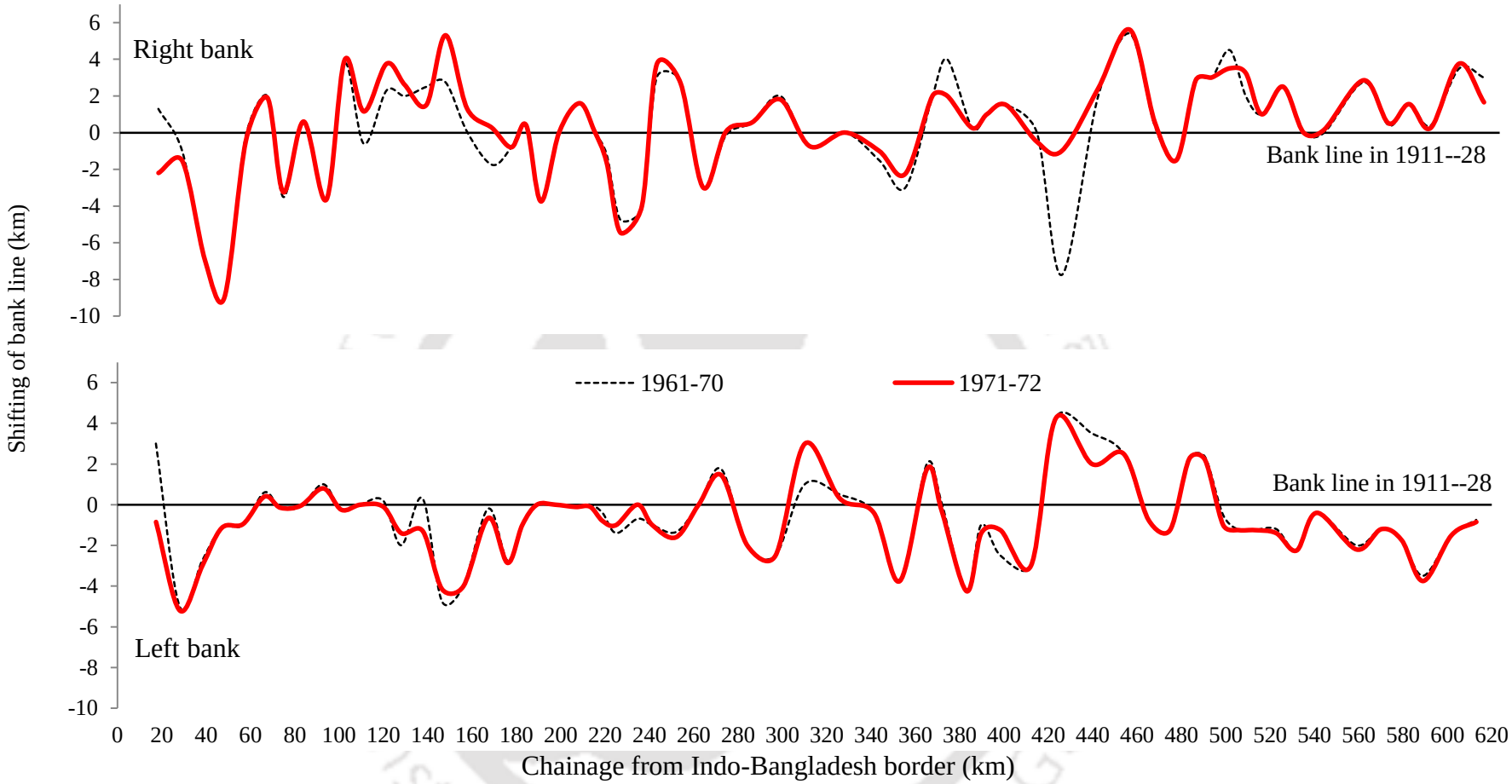


**Figure 4.12** Shifting of bank line of Brahmaputra (in Assam) from 1911—28

maximum 5.6 km outward at distance of 454 km from India-Bangladesh border. The north bank shifted to maximum 9 km inward and the south (left) bank shifted maximum 5.2 km outward with deposition in the north bank and erosion in south bank at downstream of the river. Thus the river was shifted to southward in the reach of 46 km length at downstream.

Erosion and deposition during 1973 – 2014 was studied using overlay analysis in GIS. Brahmaputra River in Assam was divided into 16 reaches (Reach no 1 at upstream and reach no 16 at downstream) of 40 km length. Erosion and deposition during 1973 – 2014 at different reaches are shown in Figure 4.13 – 4.20.

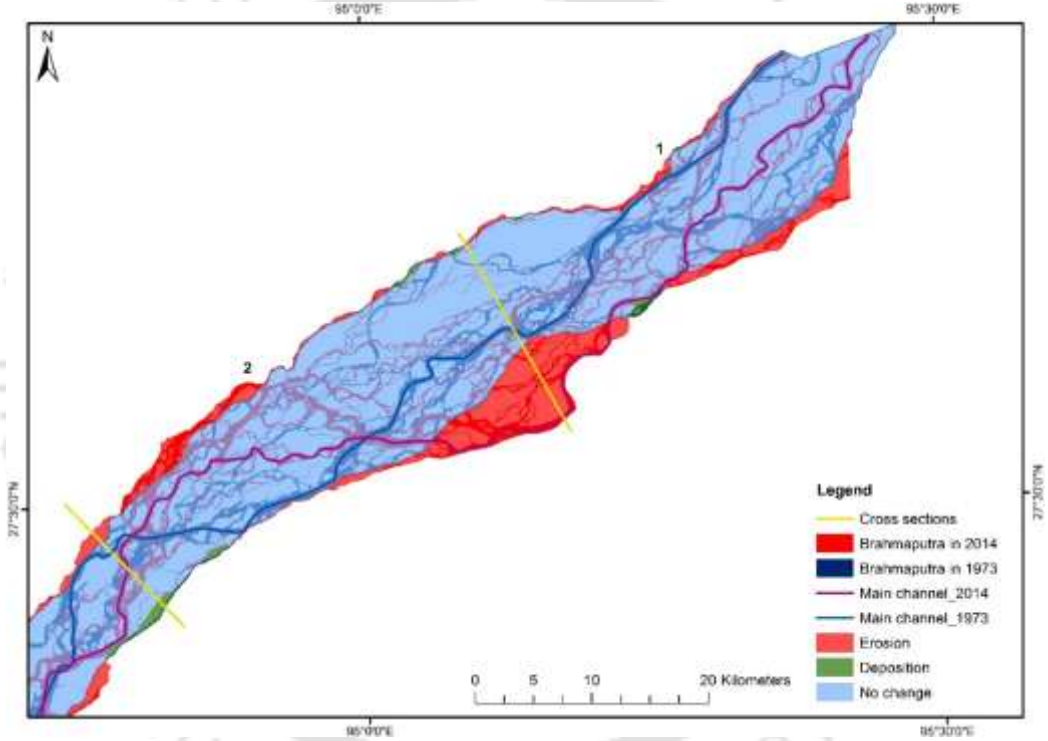


**Figure 4.13** Erosion/ deposition in Brahmaputra during 1973 – 2014 at reach no 1 & 2

Although the river was widened to both the banks at upstream in earlier years, i.e., during 1911–28 and 1971–71, there was severe erosion in the south (left) bank of the river during 1973 – 2014 with downward shifting of the main channel in the first two reaches. Erosion in the first two reaches (Reach no 1 and 2) was 128 $km^2$ of which 101 $km^2$ was in the south bank. Place like *Rohmoria* (mentioned in Chapter 2) is highly affected from erosion problem. Compared to erosion (128 $km^2$), there was low deposition (6 $km^2$) in the first two reaches during 1973 – 2014.

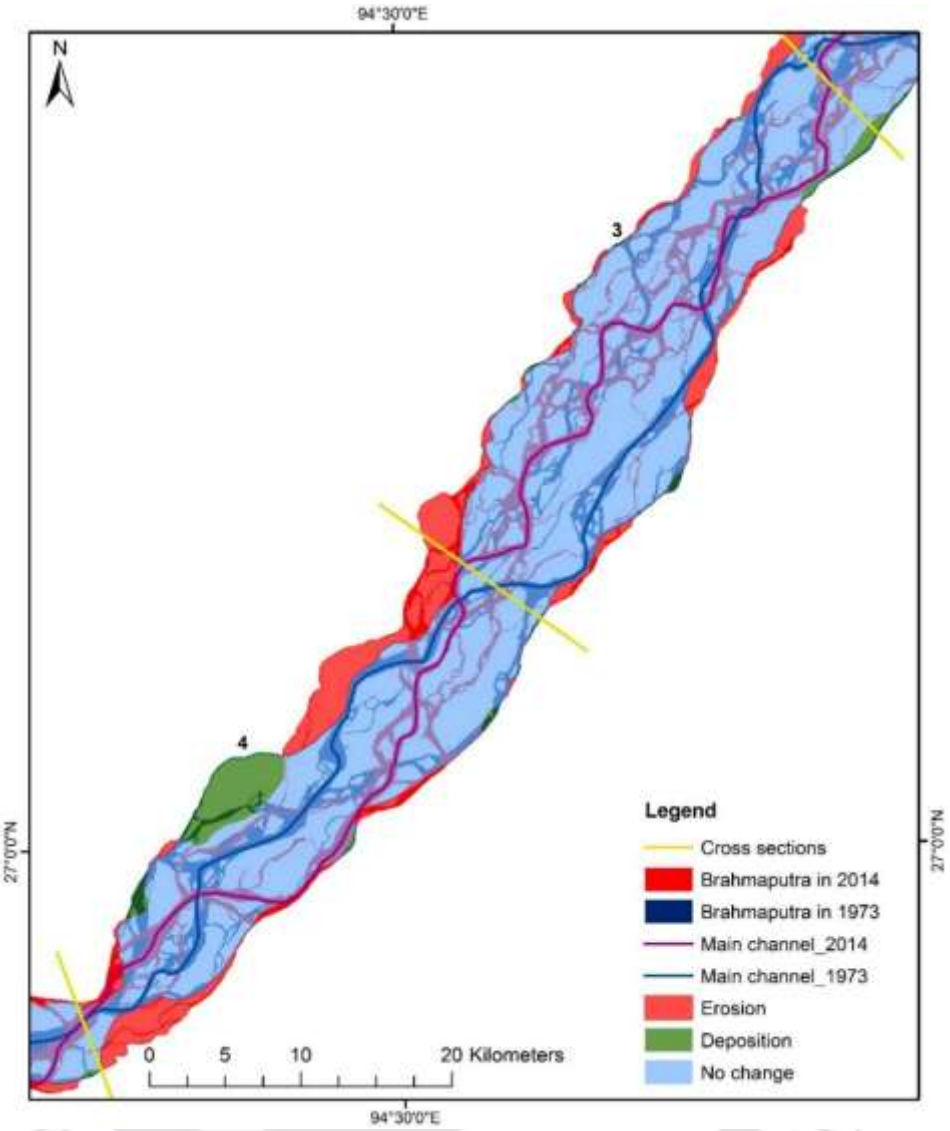


**Figure 4.14** Erosion/ deposition in Brahmaputra during 1973 – 2014 at reach no 3 & 4

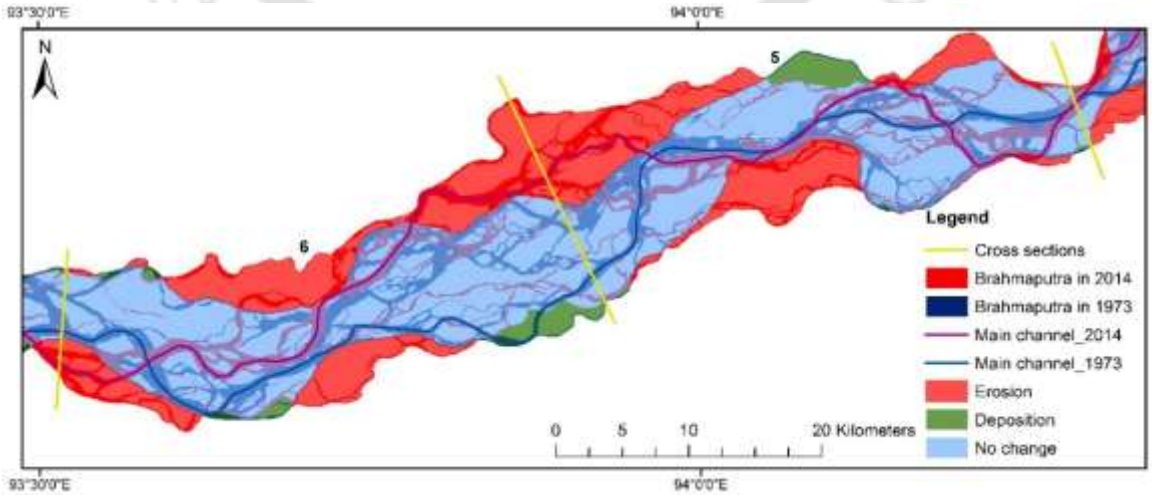


**Figure 4.15** Erosion/ deposition in Brahmaputra during 1973 – 2014 at reach no 5 & 6

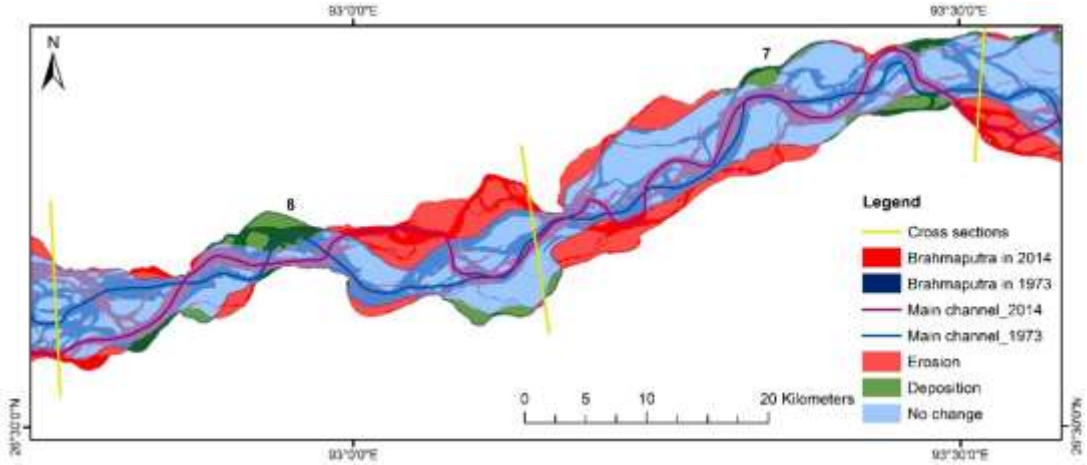


**Figure 4.16** Erosion / deposition in Brahmaputra during 1973 – 2014 at reach no 7 & 8

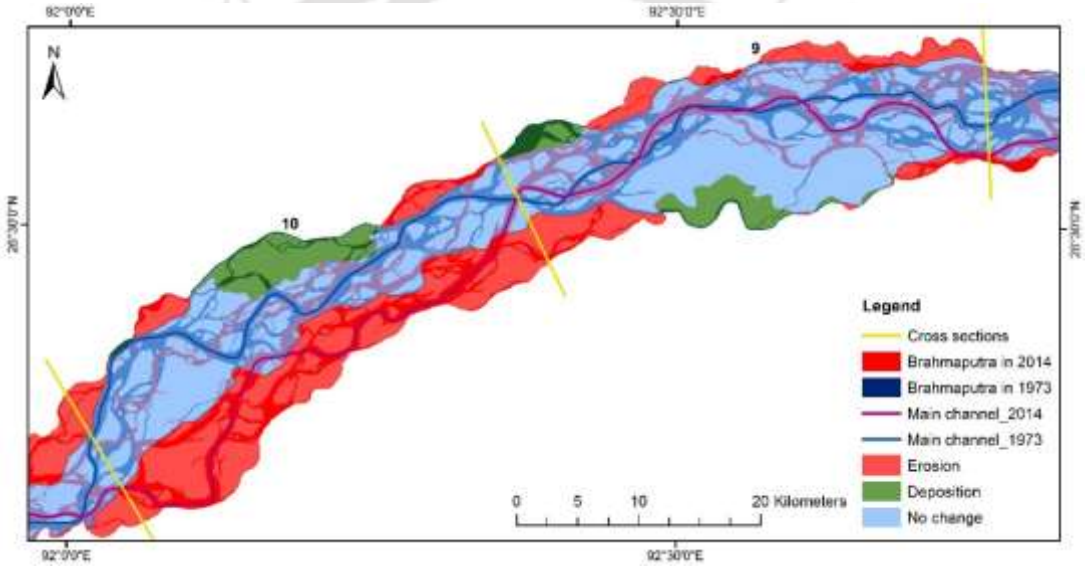


**Figure 4.17** Erosion / deposition in Brahmaputra during 1973 – 2014 at reach no 9 & 10

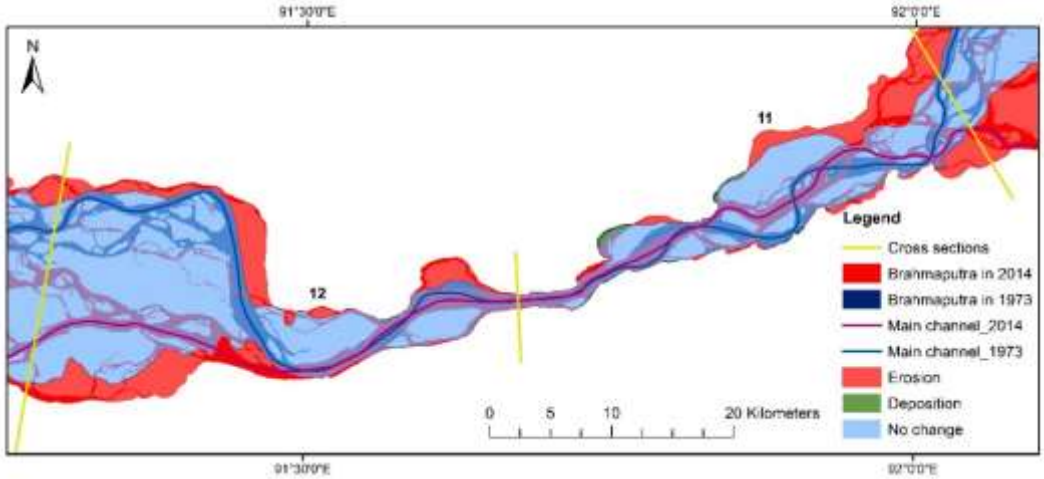


**Figure 4.18** Erosion / deposition in Brahmaputra during 1973 –2014 at reach no 11 & 12

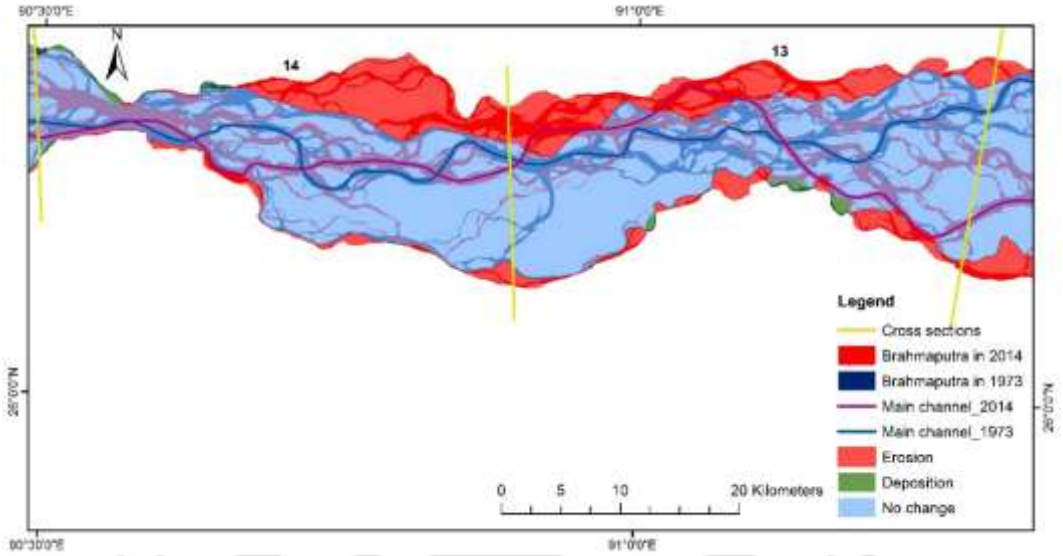


**Figure 4.19** Erosion / deposition in Brahmaputra during 1973 –2014 at reach no 13 & 14

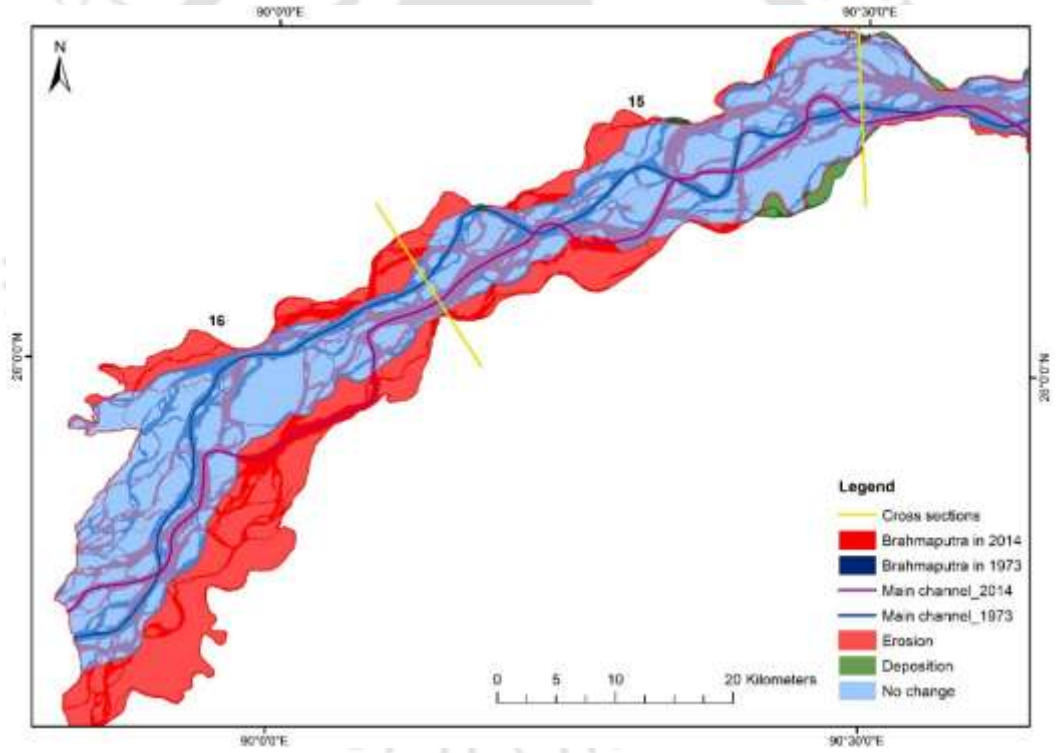


**Figure 4.20** Erosion/ deposition in Brahmaputra during 1973 –2014 at reach no 15 & 16

Reach no 3 experienced the least erosion (35 $km^2$) among all the reaches. High erosion was observed in the north bank than the south bank at reach no 3, 4, 5, 6, 8, 9, 11, 13, 14, 15 and 16. However, extent of erosion was more in south bank at reach no 1, 2, 7, 10 and 12. More than 100 $km^2$ area was affected by erosion in reach no 5, 6, 10, 13 and 16 (Figure 4.21). High erosion area in these reaches was mainly due to two factors:

i) Migration of the main channel with loss of land in reaches 1, 2, 5, 6, 7, 8, 10, 12, 13, 14, 15 and 16

ii) Bifurcation of distributaries or migration of mid-channels with development of sandbars or islands in reach no 3, 4, 9, 11 and 16.

Deposition was comparatively lesser in all the reaches. No deposition was observed in reach no 12 and 16. Total area of erosion during 1973 – 2014 was 1557 $km^2$ out of which 728 $km^2$ was in north bank and 829 $km^2$ in the south bank of the river. Total deposition area during the period was 204 $km^2$ with 122 $km^2$ in the north bank and 82 $km^2$ in the south bank. Thus the south bank experienced higher erosion whereas deposition was more prominent in the north bank.

Unequal erosion in both banks of Brahmaputra is unique compared to other Tibetan rivers like the Yellow. Bank retreat on both sides of the Yellow River from 1958 to 2008 were almost equal as erosional area on the left bank and the right bank was 257.3 $km^2$ and 261.09 $km^2$ respectively (Yao et al., 2011). But in Brahmaputra, higher erosion in the south bank is mainly due to downward shifting of the main channel in most of the reaches (Figure 4.22). Maximum shifting of the main channel took place during 1973 – 1994 compared to 1994 – 2014. Average shift of the main channel was 3 km during 1973 – 1994 and 2 km during 1994 – 2014. Total erosion during 1973 – 1994 was 1166 $km^2$ with 564 $km^2$ in the north bank and 602 $km^2$ in the south bank. Total deposition during 1973 -- 1994 was 172 $km^2$ with 96 $km^2$ in the north bank and 76 $km^2$ in the south bank. Compared to 1973 – 1994, there was less erosion (589 $km^2$) and more deposition (197 $km^2$) during 1994 – 2014. Total erosion during 1973 – 2014 (1557 $km^2$) was not numerically equal to erosional area of 1973 – 1994 (1166 $km^2$) and 1994 – 2014 (589 $km^2$) since some area eroded during 1973 – 1994 was deposited in 1994 – 2014. Similarly, some area deposited during 1973 – 1994 was affected by erosion in later period (e.g., reach no 2, 6, 7, 8, 11, 13 and 14).

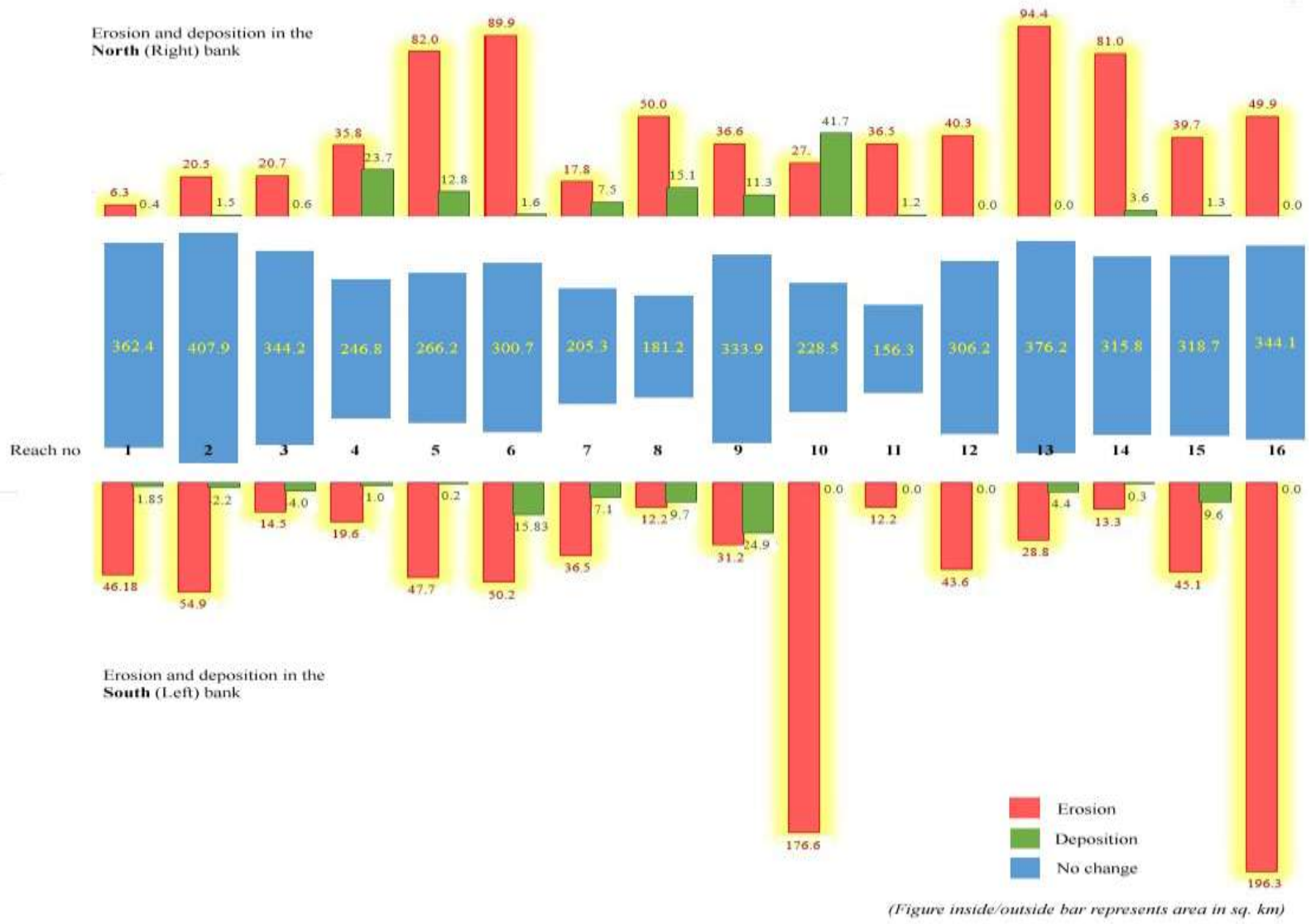


**Figure 4.21** Erosion/ deposition in different reaches (1 at upstream, 16 at downstream) of Brahmaputra during 1973 – 2014

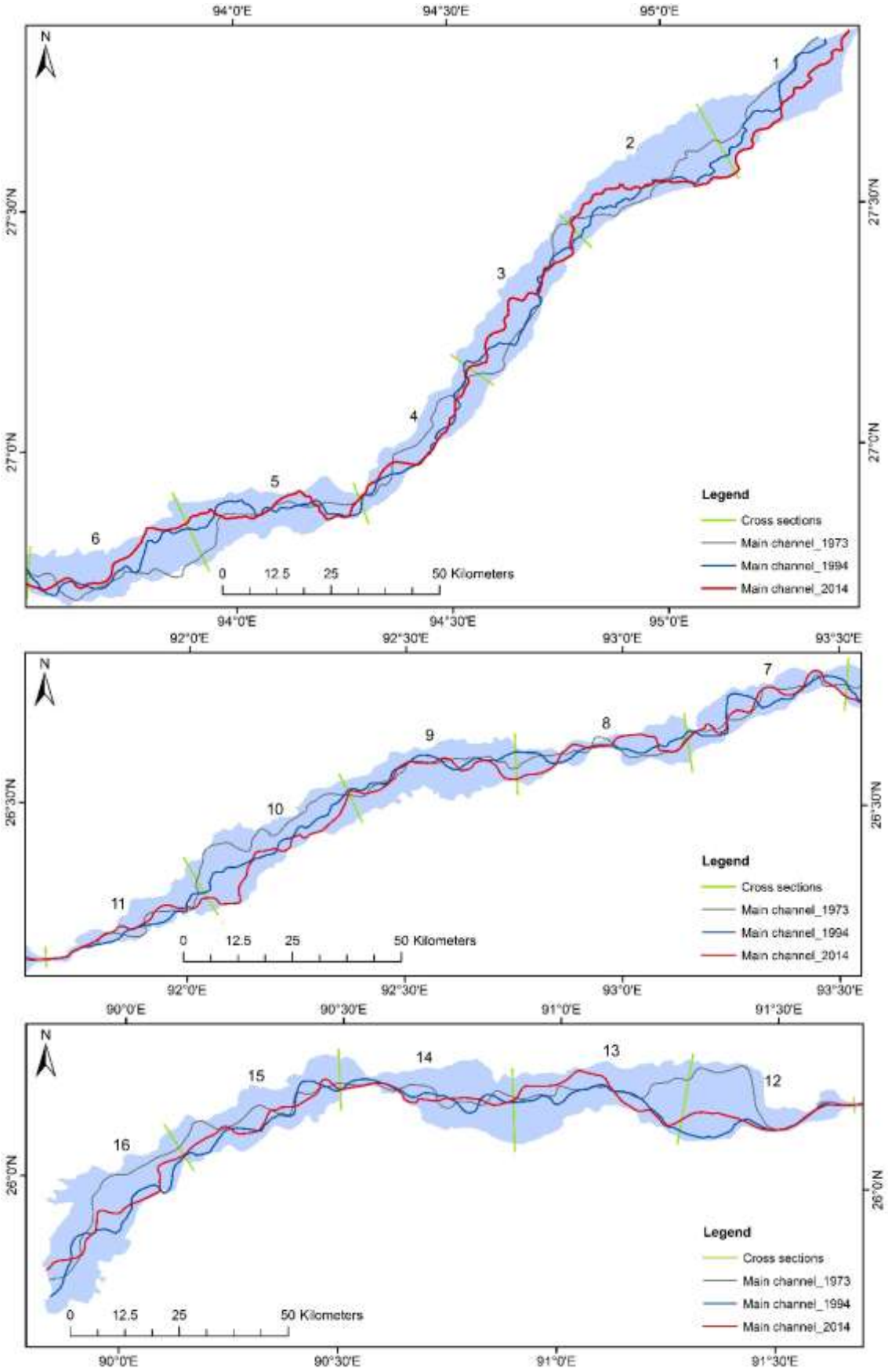


**Figure 4.22** Main channel of Brahmaputra in 1973, 1994 and 2014

### 4.3 Slope variation

Secondary data on slope of Brahmaputra collected from River Research Station was used to study slope variation of the River. Average bed slope and deepest bed slope in three years of 1971, 1977 and 1981 along with average of average bed levels in six sections are shown in Table 4.7. Bed slope variation during different years is shown in Figure 4.23.

**Table 4.7** Average bed levels of Brahmaputra

| Cross sections | 1971 | | 1977 | | 1981 | | Average of Avg. bed slope $\times 10^{-4}$ |
|---|---|---|---|---|---|---|---|
| | Average bed slope $\times 10^{-4}$ | Deepest slope $\times 10^{-4}$ | Average bed slope $\times 10^{-4}$ | Deepest slope $\times 10^{-4}$ | Average bed slope $\times 10^{-4}$ | Deepest slope $\times 10^{-4}$ | |
| 2 to 12 | 0.534 | 1.060 | 0.792 | 0.096 | 0.608 | 1.510 | 0.645 |
| 12 to 22 | 0.815 | 0.266 | 1.040 | 1.120 | 0.922 | 0.342 | 0.926 |
| 22 to 32 | 1.500 | 2.040 | 1.520 | 1.490 | 1.480 | 1.480 | 1.500 |
| 32 to 42 | 1.430 | 1.600 | 1.570 | 1.940 | 1.670 | 1.560 | 1.557 |
| 42 to 52 | 1.360 | 1.840 | 1.360 | 2.130 | 1.440 | 1.480 | 1.387 |
| 52 to 60 | 1.670 | 2.140 | 2.080 | 1.770 | 2.070 | 1.790 | 1.940 |

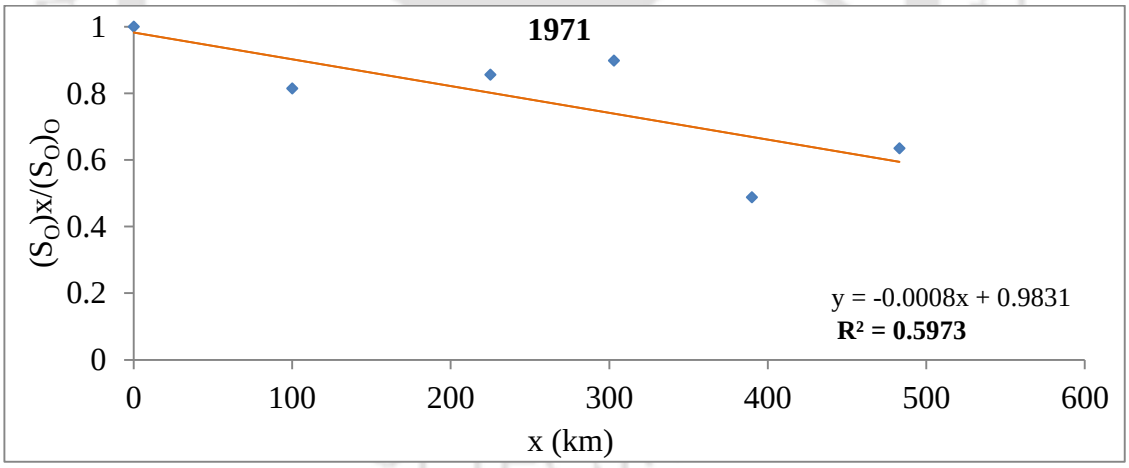


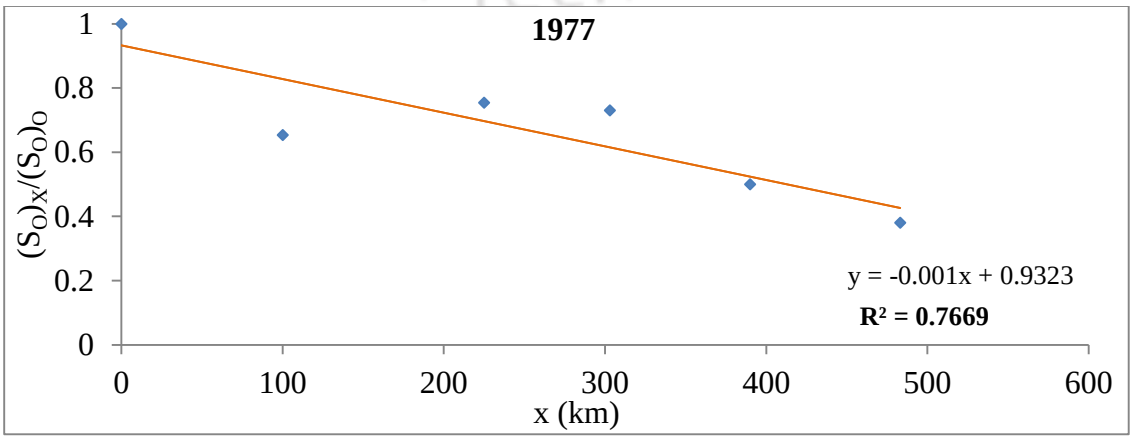

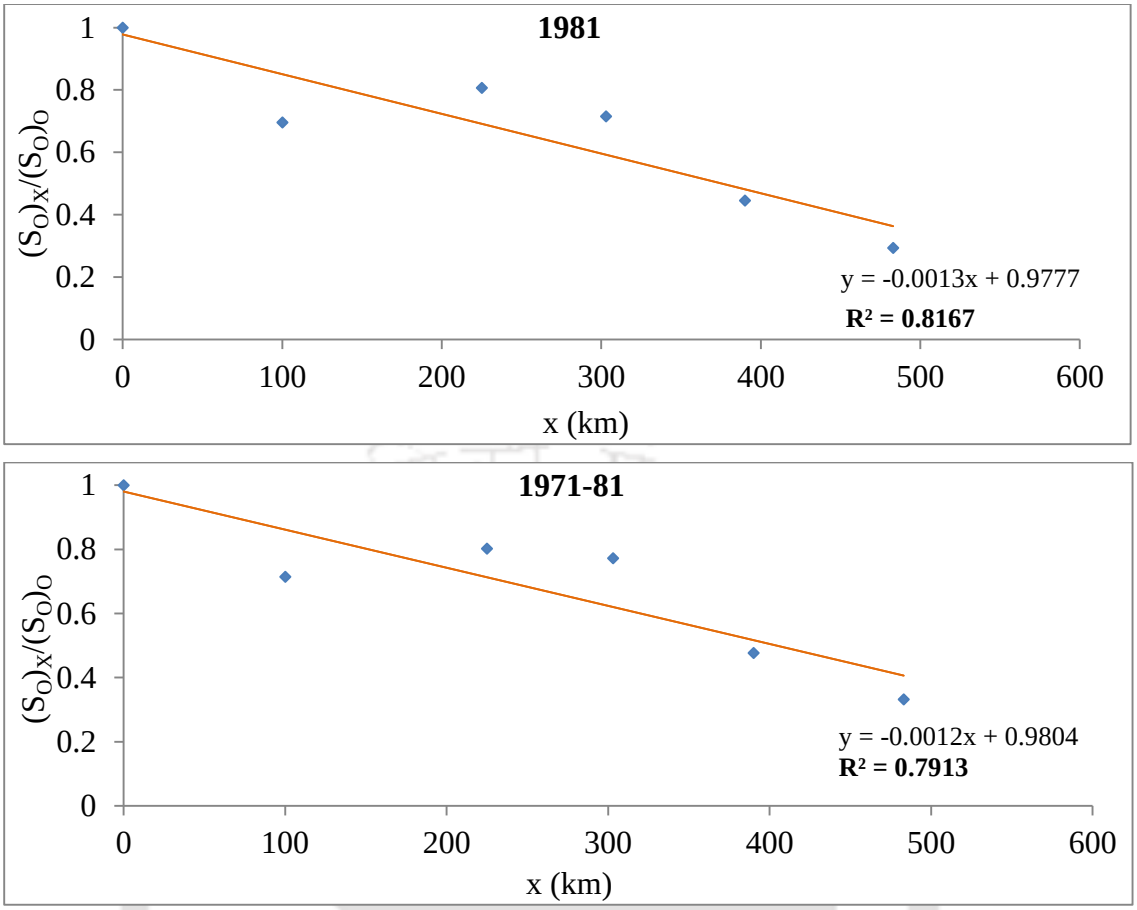


**Figure 4.23** Bed slope variation in Brahmaputra in 1971, 1977, 1981 & 1971-81

There is overall decrease in slope with increase in distance. Topographic decrease resulting decrease in the main stream water velocity and increased sediment deposition as observed in the Mekong, which flows through bedrock channels, is applicable to the alluvial river Brahmaputra. Since 1971, slope is increased in the observed reaches, suggesting more erosion from river bed. Variation of slope in different cross-sections were maximum in 1971 ($R^2$= 0.5973). Decrease in average bed slope at the second reach (cross-sections 42–52) and then increase in the third and fourth reaches (cross-sections 32–42, 22–32) favored more erosion in the cross-sections 42–52 with widening of the river and deposition in other reaches. Similar results were observed in the lower Yellow River where sedimentation caused channel bed to rise continuously as a 'hanging river', exerting great pressure on flood protection (Xu, 2002).

## 4.4 A sediment budget of Brahmaputra River in Assam

Construction of an approximate sediment budget for the Ganga-Brahmaputra catchment was first attempted by Wasson (2003) based on published data and Nd/Sr tracer results.

Subramanian and Ramanathan (1996) estimated highly variable sediment load of Brahmaputra ranging from 402 to 710 million $t/y^{-1}$. Islam et al. (1999) reported suspended load flux ranging from 402 to 1157 million $t/y^{-1}$ for Brahmaputra to the Bay of Bengal. Generic conclusions on sediment load transported by Brahmaputra River system is near to impossible due to wide diurnal, seasonal and annual variations in the sediment-carrying capacity of the river (Subramanian and Ramanathan, 1996). Paucity of dependable data for the main stem and tributaries also bring lot of uncertainty to sediment quantification for Brahmaputra.

An attempt was made to construct a sediment budget for Brahmaputra in Assam using a broad mass balance approach:

*Total in channel sediment at a downstream cross section = Sediment contribution from main stream and tributaries + sediment contribution from river bank erosion + sediment contribution from scouring – sediment deposition in bed/bank/ floodplains*

In the calculation process,

1) Annual sediment load of tributaries were considered from work of Pahuja and Goswami (2006).
2) 60% sediments of the tributaries was considered to contribute to sediments of Brahmaputra (after Goodbred and Kuehl, 1998; Goodbred and Kuehl, 1999; Liu et al., 2009)
3) Sediment input from bank erosion and sediment sink due to deposition in banks were calculated from erosion and deposition data for the period 1973 – 2014.
4) Annual inputs from scouring and sediment deposition in river bed were calculated from aggradation and degradation data of Brahmaputra for the period 1957 – 1989.

Similar mass - balance equation with variety of data sources was used in the Yangtze River for quantitative estimation of the contribution of the river mouth reach to the sediment load before and after impoundment of the Three Gorges Dam (Wang et al., 2015).

***Sediment input from tributaries***

The major rivers/ tributaries within Assam with high sediment load are shown in Figure 4.24.

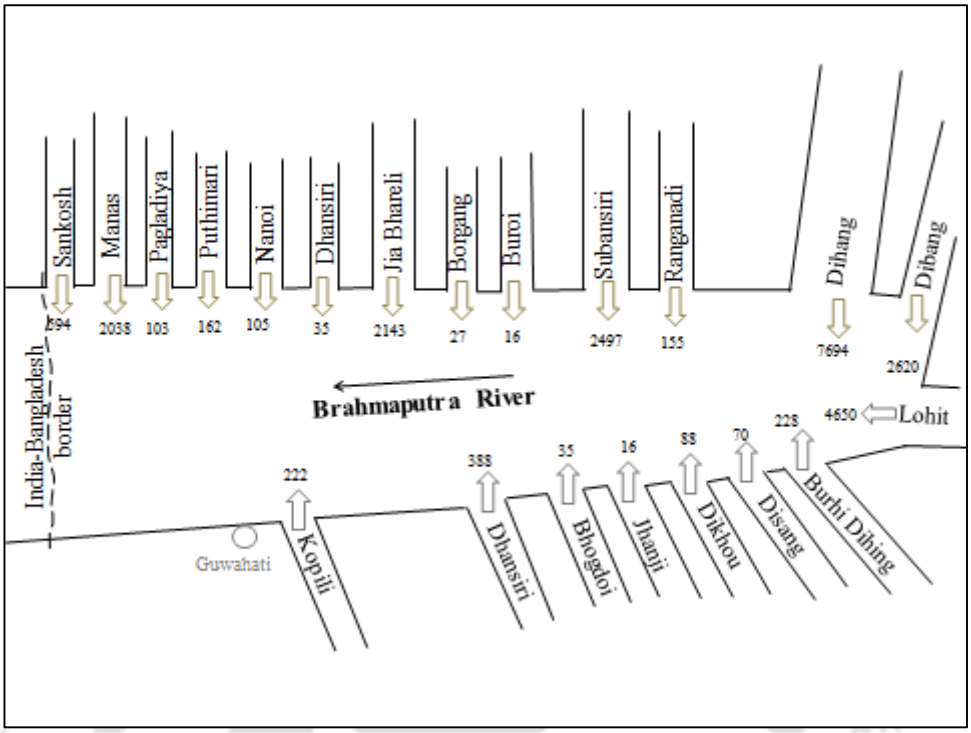


**Figure 4.24** Rivers/ tributaries within Assam with high sediment load

*(The numbers indicate annual average suspended sediment load in ha m)*

Volume of sediments to Brahmaputra from tributaries in a year (from Pahuja and Goswami, 2007) = 51,316 ha m

= $513.16 \times 10^6$ $m^3$.

Considering sediment density 1.36 $g/cm^3$ (Agarwal and Singh, 2007), mass of suspended sediments collectively contributed by tributaries in a year = $698 \times 10^6$ t.

Floodplains are known to be important sites for sediment storage in fluvial systems (Phillips, 1992; Steiger et al., 2001; Noe and Hupp, 2009). Approximately one third of the annual sediment load of the Ganges-Brahmaputra is deposited in the river flood-plains (Goodbred and Kuehl, 1998; Goodbred and Kuehl, 1999). Liu et al. (2009) reported that 30-50% river-derived sediments of the Tibetan rivers like Yellow, Yangtze, Brahmaputra, Ganges, Indus, Mekong and Irrawaddy are trapped in the river's low reaches and contribute to extensive floodplain and delta plain development. Considering trapping of 40% of riverine sediments of Brahmaputra in river bed and floodplain, $279 \times 10^6$ t (40% of $698 \times 10^6$ t) was estimated to be deposited along river bed and floodplains. Hence, mass of suspended sediment at downstream from all rivers/ tributaries is $419 \times 10^6$ t (60% of total sediments).

***Sediment contribution from scouring***

The development and movement of scour holes have significant influence on the total sediment transports in Brahmaputra; they may equate up to 25% of total sediment transports in Brahmaputra (FAP24, 1996).

Total scour during 1957 – 1989 = 5649.6 × $10^6$ $m^3$

Volume of scour in a year = 5649.6×$10^6$ $m^3$/32 =177×$10^6$ $m^3$

Mass of sediment from scouring = 241×$10^6$ t

*Sediment deposition on river bed*

Deposition in bed during 1957–1989 = 1625×$10^6$ $m^3$

Volume of deposition in a year = 1625×$10^6$ $m^3$/32 = 51×$10^6$ $m^3$

Mass of deposited sediment in a year = 69×$10^6$ t

***Sediment contribution from river bank erosion***

In calculation of sediment input from erosion, bank erosion in Brahmaputra in Assam during 1973 – 2014 was considered.

Bank erosion in 41 years (1973 – 2014) = 1557 $km^2$

Thus, bank erosion in a year = 1557 $km^2$/41 = 38 $km^2$ = 38×$10^6$ $m^2$

Average difference of yearly observed highest and the lowest water levels of Brahmaputra for the period 1914 – 1990 was 4.7 m (from Figure 4.1). Assuming depth of bank erosion as 4.7 m, volume of bank erosion in a year = 179×$10^6$ $m^3$

Mass of eroded materials = 243×$10^6$ t

*Deposition in banks/ floodplains*

Total deposition in banks/ floodplains in Brahmaputra (Between *Dibrugarh* and *Dhubri* in Assam) during 1973–2014 = 204 $km^2$

Bank deposition in a year = 204 $km^2$/41 = 4.97 $km^2$ = 4.97×$10^6$ $m^2$

Garzanti et al. (2010) suggested that dominant bedform in Brahmaputra are sand dunes with heights ≤6 m and wavelengths (λ) ≤330 m. Considering sandbars as spherical domes of height 6 m and radius of base 82.5 m (half of λ/2), average height of deposition is 3 m.

Volume of deposition = 15×$10^6$ $m^3$

Mass of deposited sediments = 20×$10^6$ t

Now, Total in channel sediment at a downstream cross section

= Sediment contribution from main stream and tributaries + sediment contribution from river bank erosion + sediment contribution from scouring – sediment deposition in bed/bank/floodplains

$= 419\times10^6$ t + $243\times10^6$ t + $241\times10^6$ t – $69\times10^6$ t – $20\times10^6$ t

$= 814\times10^6$ t

Lane and Borland (1951) postulated that suspended load of a river carries 90% of the sediment, while bed load transport accounts for approximately 10% of sediment. Thus, 90% of the total suspended sediment load at a catchment outlet may be explained by the total amount of sediments coming from upstream nested catchments (Gay et al., 2014). Considering 10% of sediment load of Brahmaputra as bed load, suspended sediment load at downstream is $733\times10^6$ t (90% of $814\times10^6$ t).

Based on these estimates, a schematic sediment budget for Brahmaputra within Assam can be arrived at (Figure 4.25).

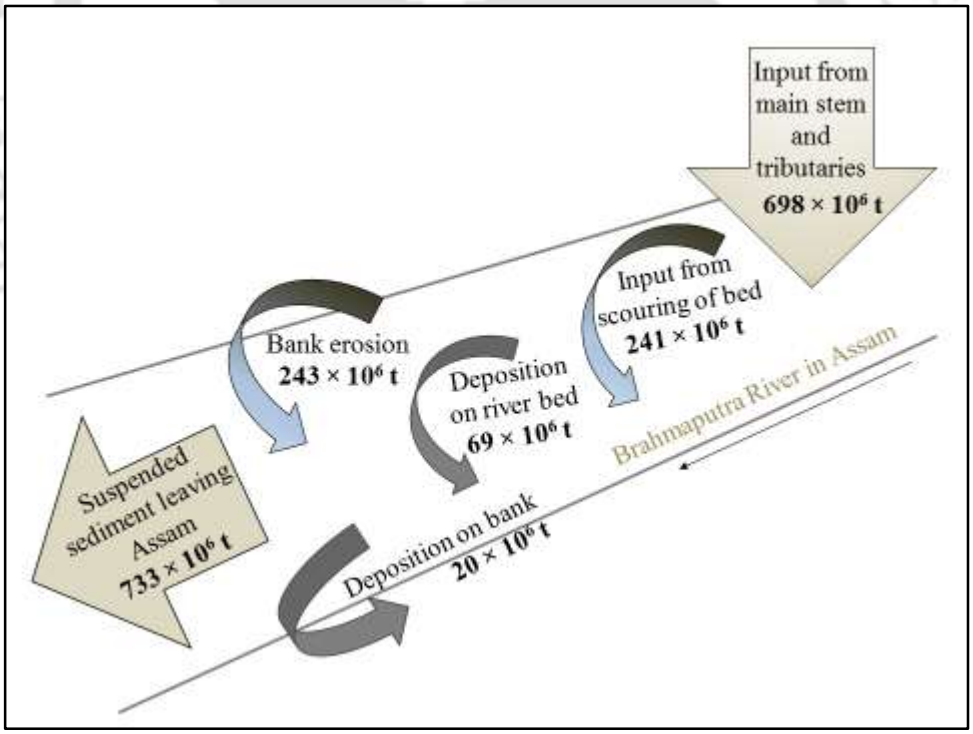


**Figure 4.25** A sediment budget for Brahmaputra River in Assam

Calculated sediment load of $733\times10^6$ t $y^{-1}$ at downstream of Brahmaputra (India-Bangladesh border) is comparable with findings from earlier studies (Table 4.8).

**Table 4.8** Sediment load of Brahmaputra from different studies

| Suspended sediment load ($10^6$ t $y^{-1}$) | Reference | Gauging stations/ sampling locations | Period of measurement |
|---|---|---|---|
| 617 | Coleman (1969) | Bahadurabad, Bangladesh | 1958 – 1962 |
| 541 | BWDB (1972) | Bahadurabad, Bangladesh | 1967 – 1969 |
| 1157 | Milliman and Meade (1983) | Bahadurabad, Bangladesh | 1966 – 1967 |
| 402 | Goswami (1985) | Pandu, Assam | 1955 – 1979 |
| 650 | Hossain (1992) | Bahadurabad, Bangladesh | 1982 – 1988 |
| 721 | Islam et al. (1999) | Bahadurabad, Bangladesh | 1989 – 1994 |
| **733** | **Present study** | Secondary data compiled from multiple sources for the river in Indian part | Different period for different data |

Contribution to suspended sediment of Brahmaputra at Indo-Bangladesh border:

Tributaries: 52%,

Bank erosion: 27% and

Scouring: 21%.

Thus, tributaries including the main stem is major contributor of sediment in Brahmaputra. More than half of total sediment of Brahmaputra at downstream (52%) comes from the main stem and the tributaries. Calculated mass of eroded materials from bank erosion in a year was $243\times10^6$ t. Amount of yearly deposition on river bank and floodplains was $20\times10^6$ t. Thus $223\times10^6$ t sediments (27%) were contributed to annual sediment load of the river from bank erosion. However, major contribution (about 50%) of sediment loads from bank erosion is common in most of the rivers (Bull, 1997; Church and Slaymaker, 1989; Grimshaw and Lewin, 1980; Imeson and Jungerius, 1977; Imeson et al., 1984; Lawler et al., 1999; Simon, 1989). But sediment load of Brahmaputra can't be compared with that of other Tibetan rivers like Yellow and Yangtze in case of sediment input from bank erosion. In Yellow river, bank-to-channel sediment transfer process was found to cause the overall increase in channel deposition with little influences on the down-stream suspended sediment load and transport (Ta et al., 2013). A remote sensing investigation on a 1479 km-long reach of Yangtze River for the period of 1970 – 1998 indicated that volume of bank failure ($267\times10^6$ $m^3$) and volume of bed deposition ($291\times10^6$ $m^3$) was almost same (Xu et al., 2001). But, in case of Brahmaputra, volume of bank erosion in a year ($243\times10^6$ $m^3$) was more than ten times of volume of deposition ($20\times10^6$ $m^3$).

However, sediment budget for a particular reach of Brahmaputra is different from that of another reach due to difference in sediment input from different sources. This phenomenon can be verified considering data (collected by WRD, Govt. of Assam) of two reaches as mentioned below:

i) Reach from *Bhurbandha* (upstream) to *Pandu* (downstream)

Sediment load at *Bhurbandha* site = 6202 ha m

Input from tributaries (between *Bhurbandha* and *Pandu*) = 1008 ha m

Total sediment at *Pandu* site = 7210 ha m

Observed sediment at *Pandu* site = 10426 ha m

Surplus sediment at *Pandu* site = 3216 ha m

Sediment contribution from tributaries, bank erosion and scouring = 4224 ha m

% contribution from tributaries = 24%

ii) Reach between *Pandu* and *Jogighopa*

Observed total sediment load at *Jogighopa* = 16949 ha m

Input from tributaries (within *Pandu* and *Jogighopa*) = 2362 ha m

% contribution from tributaries = 36%

In the entire reach from *Bhurbandha* to *Jogighopa*,

Sediment input from tributaries = 3370 ha m

% contribution from tributaries = 31%

Thus, 69% sediment is picked up from bank erosion or channel degradation process. But there was no evidence of significant channel degradation in the reach from C/S 11 to C/S 31, while there were considerable aggradations (Figure 4.8). Hence, remaining sediment contribution can be assumed from bank erosion.

Major limitation of the present sediment budget is that, data for different components were from different sources and different periods and have different reliabilities, which might lead to the uncertainty associated with the results presented herein. Apart from the above limitations, climate change impact (ICIMOD, 2009) and hydropower dam initiative in upstream of Brahmaputra, i.e., Arunachal Pradesh (The Ecologist Asia, 2003), has added further complexity in the sediment flux regime of Brahmaputra.

Chapter 5

# Physico-chemical properties of sediments of Brahmaputra

This chapter investigates different physico-chemical properties of sediments including particle size distribution, heavy metal concentration and mineralogical components. Size distribution of bed sediments has been studied based on data collected from River Research Station, Guwahati, Assam, and data generated at IIT Guwahati. Studies on chemical properties are on the basis of analysis of collected bed sediments and suspended sediments of Brahmaputra.

## 5.1 Size distribution of bed materials

The River Research Station, Guwahati, Assam collected and tested bed sediment samples from different cross sections of Brahmaputra River in Assam. Bed material samples were collected from 20 cross sections (numbered from 2 to 65, Figure 4.7, p. 65). Samples were collected, (six at each section), from a depth ranging from 0.30 m to 0.60 m below the bed level. Table 5.1 summarizes the characteristics of bed materials in terms of $d_{50}$, $d_{84.1}$ and $d_{15.9}$ sizes and its geometric standard deviation is given by

$$\sigma = ½ (d_{84.1}/d_{50} + d_{50}/d_{15.9})$$

where $d_{50}$, $d_{84.1}$ and $d_{15.9}$ are such sediment sizes that 50%, 84% and 16% of the materials are finer than these sizes respectively.

**Table 5.1** Characteristics of bed materials at different cross sections of Brahmaputra River (Based on data obtained from River Research Station, Guwahati)

| Cross section no | Chainage in km | $d_{50}$ mm | $d_{84.1}$ mm | $d_{15.9}$ mm | $\sigma_g$ |
|---|---|---|---|---|---|
| 2 | 17.34 | 0.223 | 0.274 | 0.134 | 1.446 |
| 5 | 46.92 | 0.205 | 0.240 | 0.131 | 1.368 |
| 7 | 66.30 | 0.159 | 0.201 | 0.120 | 1.295 |
| 9 | 82.62 | 0.138 | 0.188 | 0.091 | 1.439 |
| 13 | 119.85 | 0.181 | 0.243 | 0.122 | 1.413 |
| 16 | 146.37 | 0.155 | 0.241 | 0.089 | 1.648 |
| 18 | 167.28 | 0.146 | 0.228 | 0.092 | 1.574 |
| 21 | 189.21 | 0.113 | 0.210 | 0.054 | 1.976 |
| 22 | 197.37 | 0.085 | 0.169 | 0.041 | 2.031 |
| 25 | 218.79 | 0.125 | 0.190 | 0.075 | 1.593 |
| 31 | 272.35 | 0.214 | 0.305 | 0.117 | 1.627 |
| 35 | 325.91 | 0.122 | 0.184 | 0.072 | 1.601 |
| 39 | 371.81 | 0.146 | 0.207 | 0.096 | 1.469 |
| 44 | 423.31 | 0.148 | 0.218 | 0.076 | 1.710 |
| 49 | 483.49 | 0.168 | 0.235 | 0.083 | 1.711 |
| 53 | 513.08 | 0.150 | 0.196 | 0.098 | 1.419 |
| 56 | 541.13 | 0.156 | 0.202 | 0.094 | 1.477 |
| 58 | 570.20 | 0.176 | 0.221 | 0.114 | 1.400 |
| 62 | 613.04 | 0.220 | 0.284 | 0.140 | 1.431 |
| 65 | 640.07 | 0.161 | 0.230 | 0.112 | 1.433 |

In most of the alluvial rivers, the median size of the bed materials shows a decrease in the downstream direction. This is partly due to abrasion and partly due to the sorting action. Abrasion involves rubbing, grinding and crushing of sediment particles as they move on the bed. Sorting takes place due to variation in transport capacity of stream for different sediment sizes. Two laws are available for predicting variation of $d_{50}$ along the length. Sternberg (1875) assumed the change in weight of the sediment particle to be proportional to the weight of the particle itself and the distance travelled. He gave the equation

$$d = d_o e^{-cx}$$

where $d_o$ is the size of sediment at the beginning and d at distance x, and c is a constant with dimension $L^{-1}$. Figure 5.1 shows variation of $(d_{50})_x/(d_{50})_o$ with x. Another equation given by Schaffernak (1922) according to which $(d_{50})_x/(d_{50})_o$ decreases linearly with $x/(d_{50})_o$. Variation of $(d_{50})_x/(d_{50})_o$ with $x/(d_{50})_o$ is shown in Figure 5.2. Even though in

the first 300 km, there is some decrease in $(d_{50})_x/(d_{50})_o$ with increase in x, overall, the ratio seems to be nearly equal to unity indicating that size of bed materials has not decreased. This is primarily due to the fact that these sediments are very fine, and is primarily transported as suspended load.

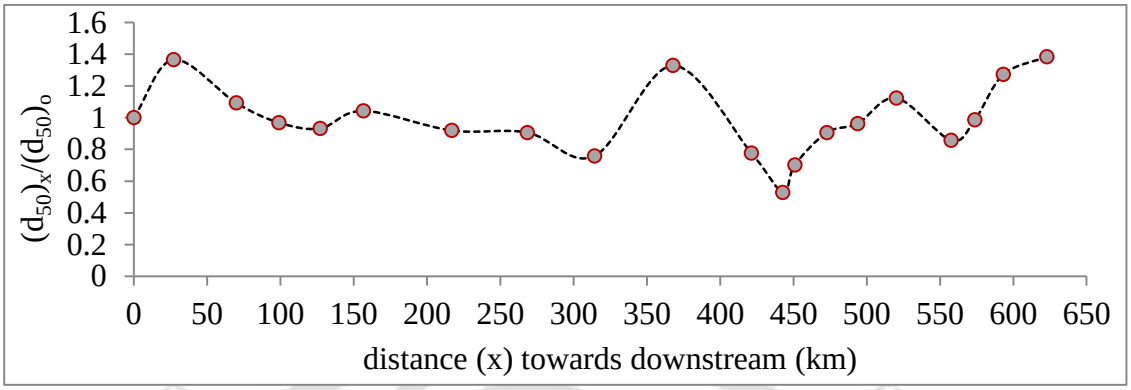


**Figure 5.1** Variation of $(d_{50})_x/(d_{50})_o$ with x

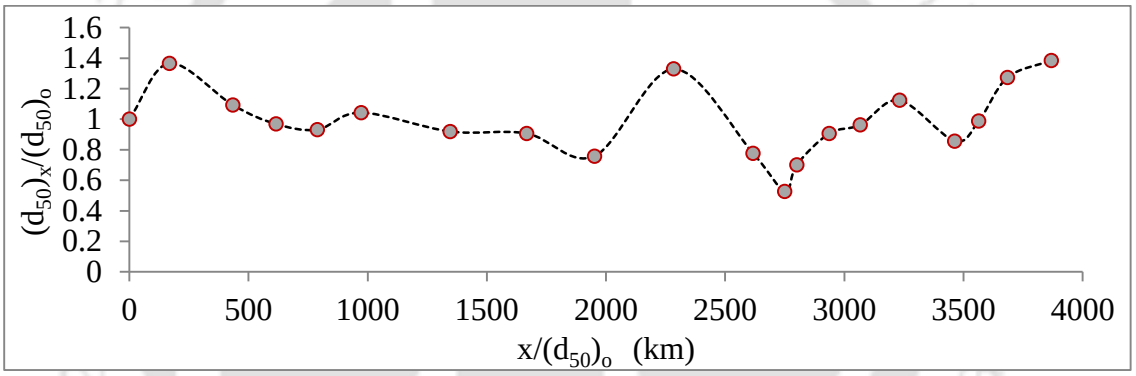


**Figure 5.2** Variation of $(d_{50})_x/(d_{50})_o$ with $x/(d_{50})_o$

Variation of standard deviation ($\sigma_g$) with $d_{50}$ is shown in Figure 5.3. Even though $\sigma_g$ increases with increase in $d_{50}$ for coarser materials, for material finer than 0.20 mm, it remains constant at about 1.40. In case of very finer material, $\sigma_g$ seems to be increasing with decrease in $d_{50}$.

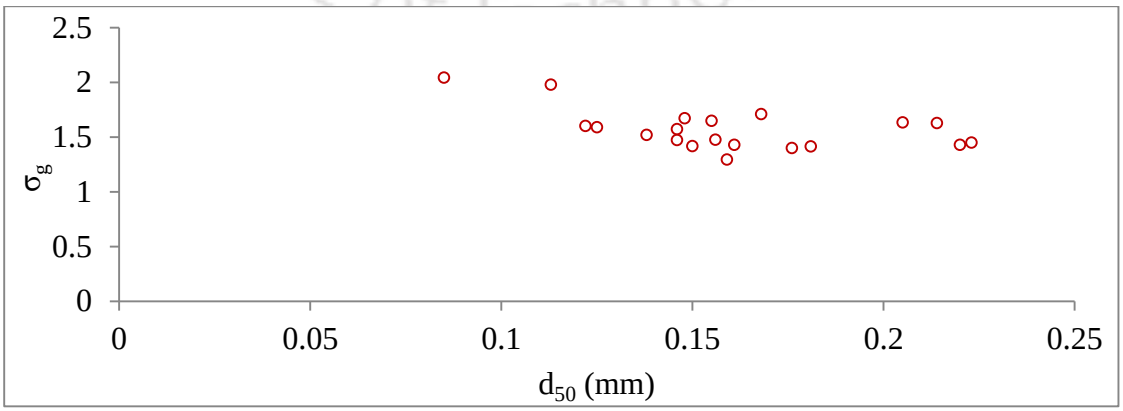


**Figure 5.3** Variation of $\sigma_g$ with $d_{50}$

## 5.2 Heavy metal concentrations in suspended sediments

Total concentrations of Fe, Mn, Cu, Pb, Zn and Ni in suspended sediments of Brahmaputra during pre-monsoon, monsoon and post-monsoon seasons in different locations are shown in Figure 5.4. Six locations are denoted by Station 1-6, where 1 represents *Dibrugarh* (upstream) and 6 represents *Guwahati* (Downstream).

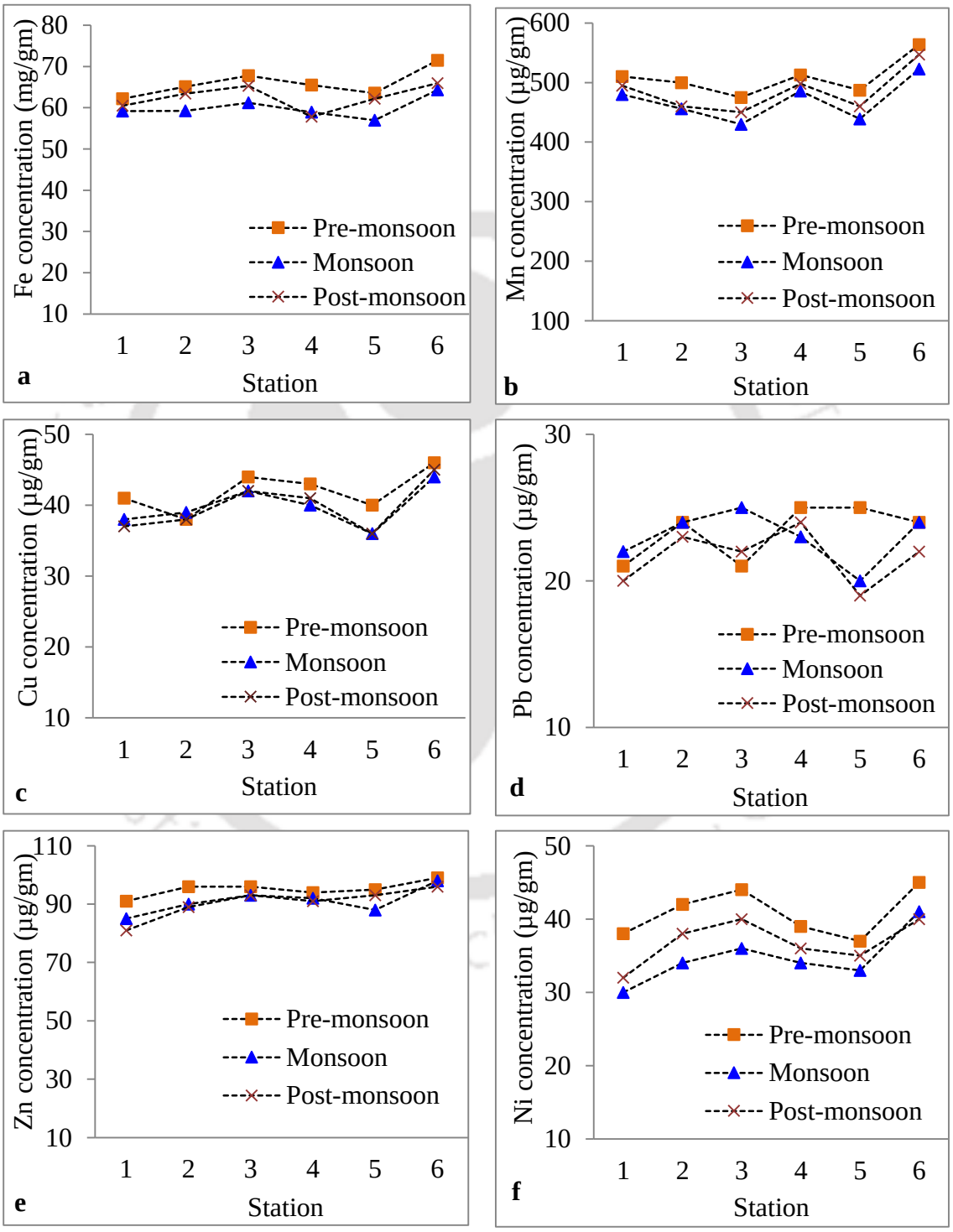


**Figure 5.4** Concentrations of Fe, Mn, Cu, Pb, Zn and Ni and in suspended sediments during pre-monsoon, monsoon and post-monsoon months

Maximum metals are in higher concentration in pre-monsoon season compared to monsoon and post-monsoon seasons. All the metals in suspended sediments have an almost uniform concentration along downstream. Less concentration of heavy metals in sediments during monsoon season may be due to dilution and much physical weathering than chemical weathering associated with less industrial inputs compared to other rivers.

Particle size distribution of suspended sediments (Location 1 during monsoon season) reveals dominance of silt (3.9 – 62.5µm), very fine sand (62.5 – 125µm) and fine sand (125 – 250µm) fractions (Figure 5.5). XRD analysis reveals dominance of silt sized Quartz, Kaolinite, Illite and Albite (Figure 5.6 and 5.7). Dominance of silt sized quartz, kaolinite, montmorrillonite in suspended sediments also suggest less adsorbing capacity of metals.

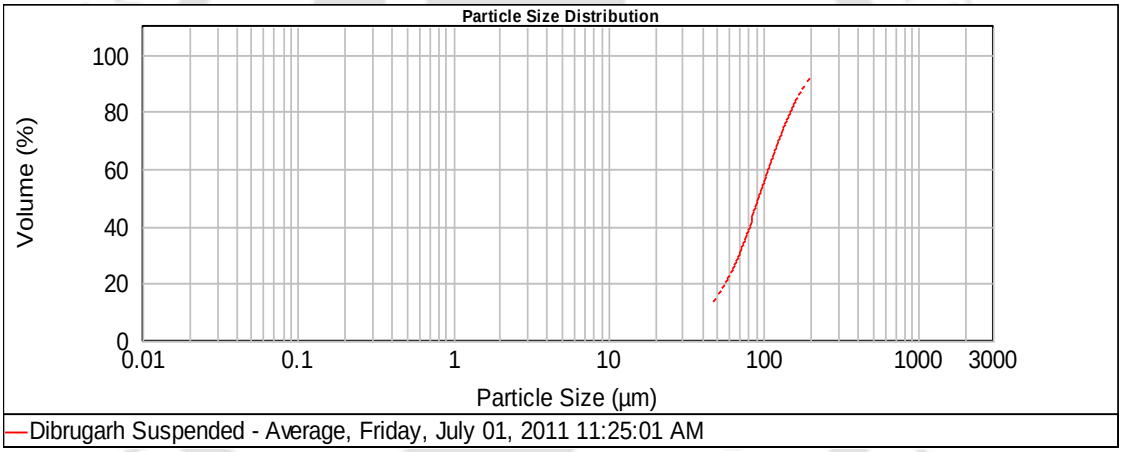


**Figure 5.5** Particle size distribution of suspended sediments in location 1

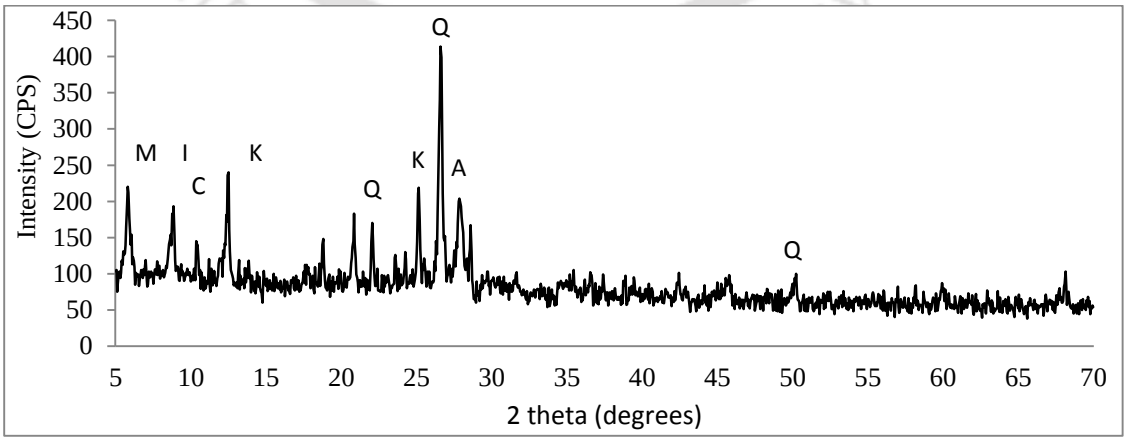


**Figure 5.6** X-Ray diffractogram of suspended sediment at location 1

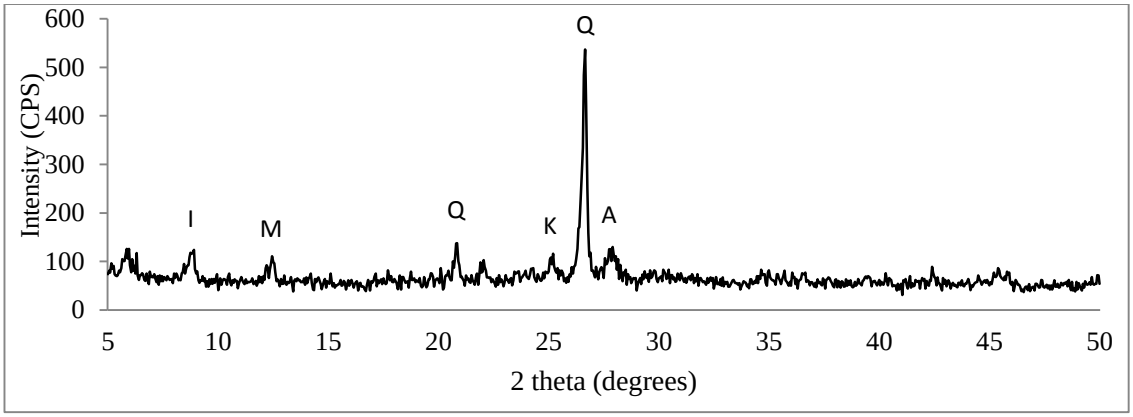


**Figure 5.7** X-Ray diffractogram of suspended sediment at location 6

Elemental composition of suspended sediments during monsoon and non-monsoon seasons are shown in Figure 5.8 and 5.9 respectively (in terms of weight %). Figure 5.8 and 5.9 are based upon EDX which does not represent the whole sediment population and based upon some selected grains. Prolate, oblate and bladed shape of suspended sediments (Figure 5.10 and Figure 5.11) suggested immature sediments coming from bank erosion or scouring with short transportation history.

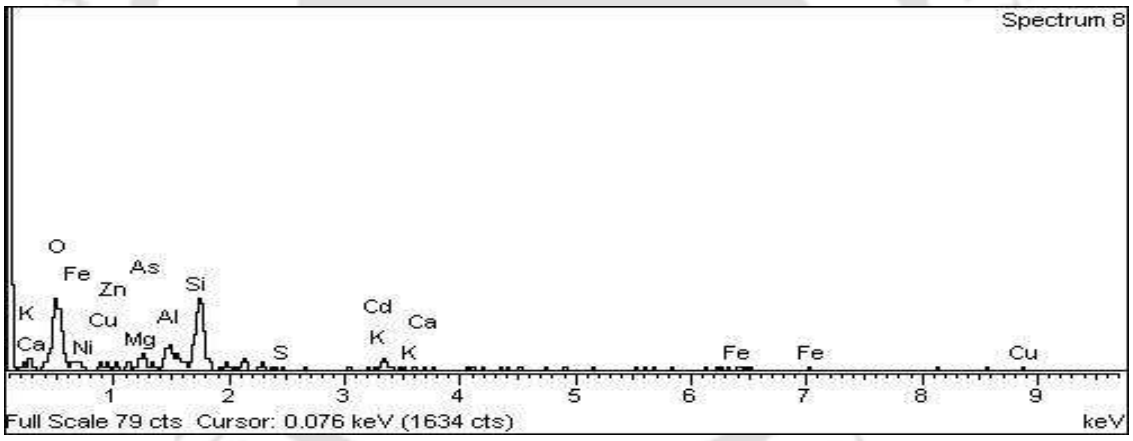


**Figure 5.8** EDX of suspended sediments during monsoon

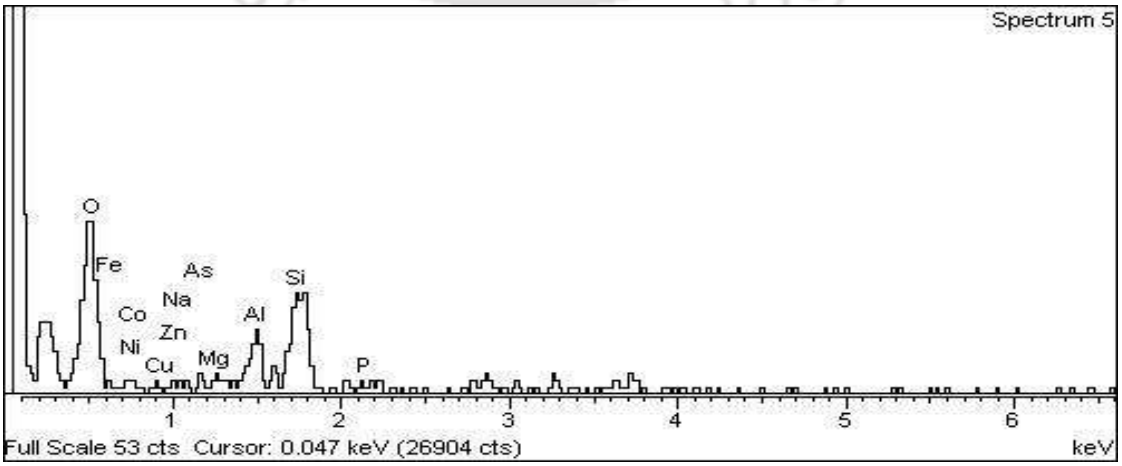


**Figure 5.9** EDX of suspended sediments during non-monsoon

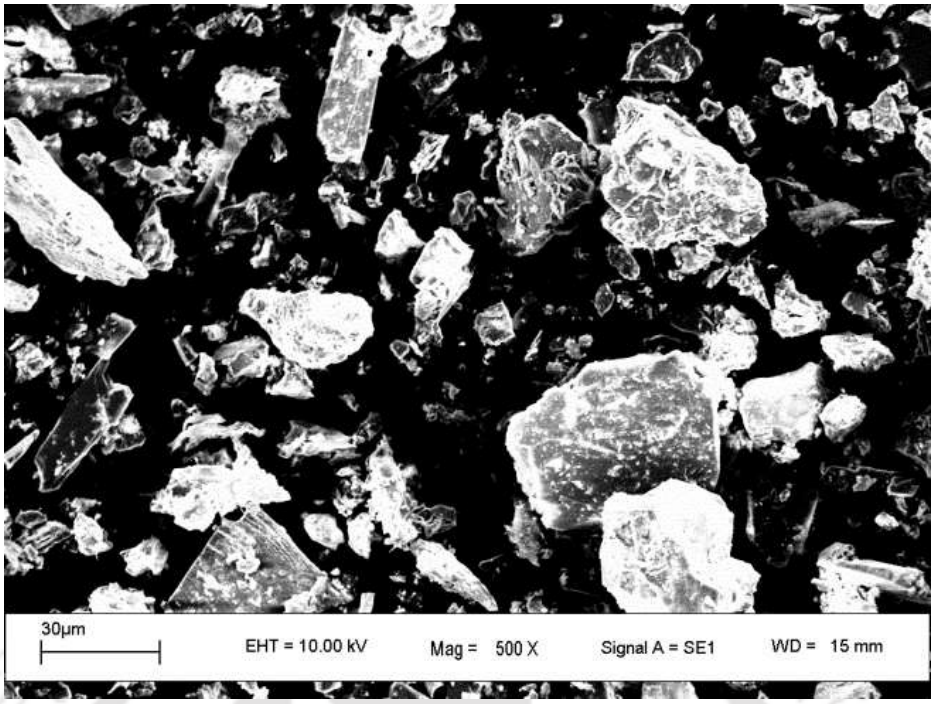


**Figure 5.10** SEM image of suspended sediment of location 3

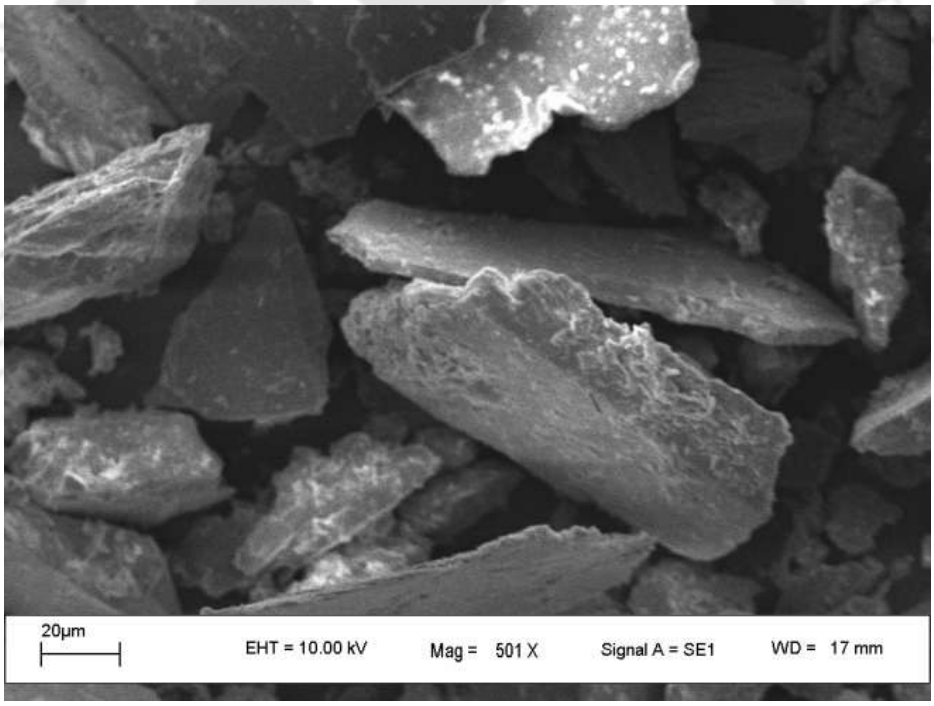


**Figure 5.11** SEM image of suspended sediment of location 5

Comparison of studied metal concentration (average) in suspended sediments of Brahmaputra River with that of world average (from two data sets), Indian river sediment, Bay of Bengal, World surface rock and average shale are presented in Table 5.2. Except Fe, concentration of other heavy metals are lower in Brahmaputra river compared to world's average suspended sediment as presented by Martin and Meybeck

(1979) and Viers et al. (2009). All metal concentrations except Mn are in higher concentrations in Brahmaputra river compared to that of Indian average river and Bay of Bengal.

**Table 5.2** Metal concentration (average) in suspended sediments
(Fe in %, other values in µg/gm)

| **Metal** | **Suspended sediment of Brahmaputra** (present study) | | | **Word's average suspended sediment** | | **Indian average river sediment** (Subramanian et al., 1985) | **Bay of Bengal** (Sarin et al, 1979) | **World surface rock** (Martin and Meybeck, 1979) | **Average shale** (Turkian and Wedephol, 1961) |
|---|---|---|---|---|---|---|---|---|---|
| | Pre-monsoon | Monsoon | Post-monsoon | (Martin & Meybeck, 1979) | (Viers et al., 2009) | | | | |
| Fe | 6.5% | 5.9% | 6.2% | 4.8% | 5.81% | 2.9% | 3.9% | 3.6% | 4.7% |
| Cu | 41.3 | 39.3 | 39.5 | 100 | 75.9 | 28 | 26 | 32 | 45 |
| Pb | 23.3 | 23 | 21.7 | 150 | 61.1 | 15 | -- | 16 | 20 |
| Zn | 94 | 90.7 | 90.2 | 350 | 208 | 16 | -- | 129 | 95 |
| Mn | 503.2 | 469 | 485 | 1050 | 1679 | 605 | 529 | 720 | 850 |
| Ni | 40.3 | 34.3 | 36.8 | 90 | 74.5 | 37 | 64 | 49 | 50 |

### *5.2.1 Geochemical fractionation of metals*

Different fractions of metals in bed sediments are shown in Figure 5.12.

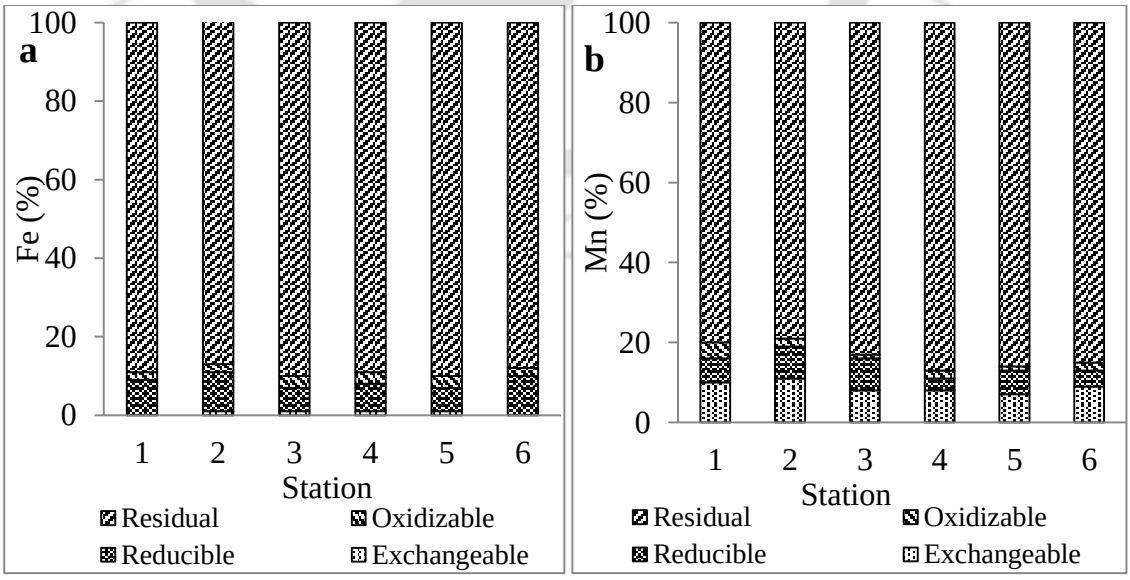

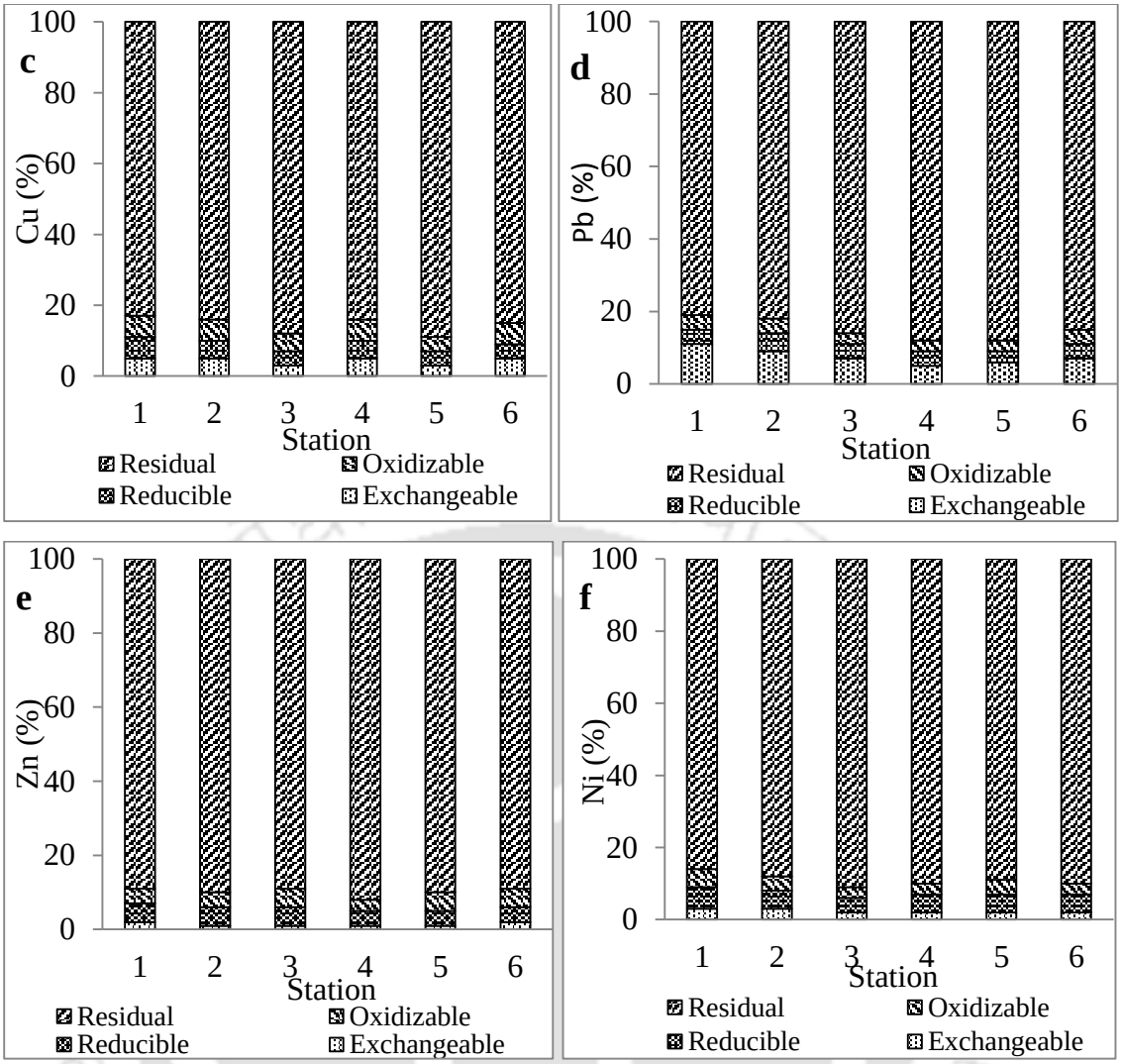


**Figure 5.12** Percentage of different fractions of metals at different locations

Based on the geochemical characteristics of the samples (Figure 5.12a) the concentration of Iron in different fractions shows the trend:

*Residual* > *Reducible* > *Oxidizable* > *Exchangeable*

Presence of Fe as residual fraction contributes > 85%. Thus, it is the most dominant phase, while, rest other fractions i.e. Reducible, Available and Oxidizable together contributes <15%. The presence of Fe as residual fraction depicts that it is bound to the silicate and detrial material of the sediments. Heavy metals in this form are not soluble under experimental conditions. The second most dominant fraction is Reducible phase. This phase accumulates metals from the aqueous system by the mechanism of adsorption and co-precipitation (Bordas and Bourg, 2001) and acts as a significant sink for heavy metals. The third most dominant fraction is Oxidizable phase; it is the phase, which includes organics and sulfides.

Abundance of Manganese in different phases exhibits the trend (Figure 5.12b):

Residual > Exchangeable > Reducible > Oxidizable

The most abundant phase for Mn observed is residual, which is due to absorption of Mn to the crystal lattice of minerals. The abundance of Mn in the available phase in BCR sequential extraction is due to the occurrence of both exchangeable as well as Carbonate bound fraction. In calcareous soils, chemisorption onto $CaCO_3$ and precipitation of $MnCO_3$ may play an important role (Norvell and Lindsay, 1972). Relatively high concentration of exchangeable manganese suggests that the metal exists in the reduced form (Tessier et al., 1979). $Mn^{2+}$ can easily be adsorbed on the surface of fine granules than other ions; the oxidation of $Mn^{2+}$ is more relaxed than $Fe^{2+}$, and at lower pH (<8) $Mn^{2+}$ can be easily associated with carbonates (Liu et al., 1984). Another feature is that the radius of $Mn^{2+}$ (0.91) is similar to that of $Ca^{2+}$ (1.08) and $Mg^{2+}$ (0.8), so the replacement of $Ca^{2+}$ and $Mg^{2+}$ by $Mn^{2+}$ is easier (Enfeng, 2005). Mn is a mobile trace metal that has great affinity to mix up with oxygen (Karbassi and Amirnezhad, 2004). All the above properties may be the reason for higher Mn content in the exchangeable/carbonate form in the sediments, while its abundance in the residual fraction suggests that the metal is bound within the mineral matrix and remains attached to the silicate or detrital materials of the sediments.

The fractionation profile of Zn shows the trend (Figure 5.12c):

Residual > Reducible > Oxidizable > Exchangeable

Residual fraction is the most abundant and thus is bound to the silicates and detrial materials in the sediments and cannot be remobilized under normal conditions. The second most abundant fraction is reducible. Zn associated with the Fe-Mn (hydr) oxide bound fraction is caused by the adsorption of the metal by Fe-Mn colloids (Jenne, 1968). The oxidizable and exchangeable fractions are the least abundant fractions for Zn.

Copper exhibits the following trend in different fractions (Figure 5.12d):

Residual > Oxidizable > Reducible > Exchangeable

The dominance of Cu in residual fraction depicts that it is bound to the silicate and detrial material of the sediments. The concentration in the crystalline fraction is largely controlled by the mineralogy and the extent of weathering. Cu shows a strong affinity

for soil organic matter and therefore organic fraction Cu is high compared to that of other metals, even though the absolute amounts are low.

The fractionation profile of Pb shows the trend (Figure 5.12e):

Residual > Exchangeable > Reducible > Oxidizable

Fractionation trend for Ni (Figure 6.12f):

Residual > Reducible > Oxidizable > Exchangeable

Pb and Ni also show their maximum concentration in the residual phase and thus are found to be bound to the silicates and remain in the mineral matrix. They are not easily available to biota.

Dominance of residual fraction and less amount of bioavailable portion of heavy metals may be attributed to low organic matter, dominant coarser fraction in sediments coupled with low pollution in the river from low industrial activities in the region. The organic matter content in bed sediments of Brahmaputra is less than 1.5% (Figure 5.13), which may be due to dominance of coarser fraction in sediments. From particle size distribution of bed sediments (Figure 5.14), it is observed that $d_{50}$ is 300 µm. Mineralogy of bed sediments of Brahmaputra is characterized by dominance of Quartz and Muscovite (Figure 5.15 & 5.16). Dominance of very fine sand (62.5-125 µm), fine sand (125-250 µm) and medium sand (0.25-0.5 mm) particles and absence of clay (< 3.9 µm) percentage (<10%) suggest less metal scavenging capacity of sediments supplemented by less chemical inputs.

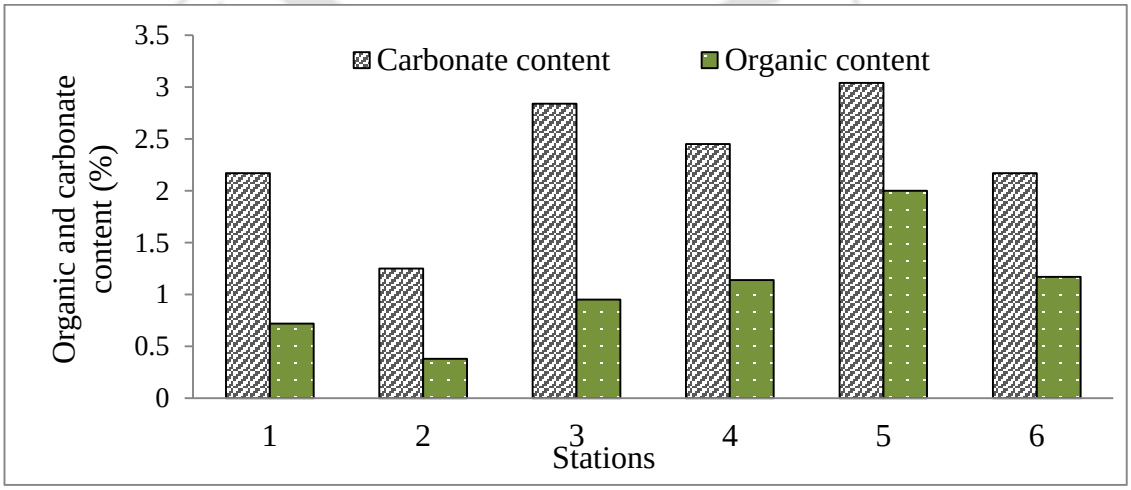


**Figure 5.13** Organic content and carbonate content in bed sediments

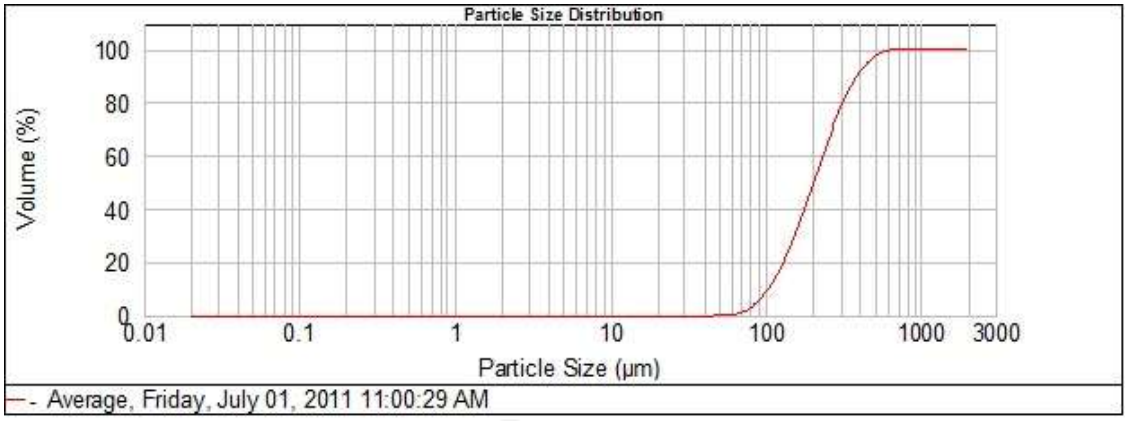


**Figure 5.14** Particle size distribution of bed sediments

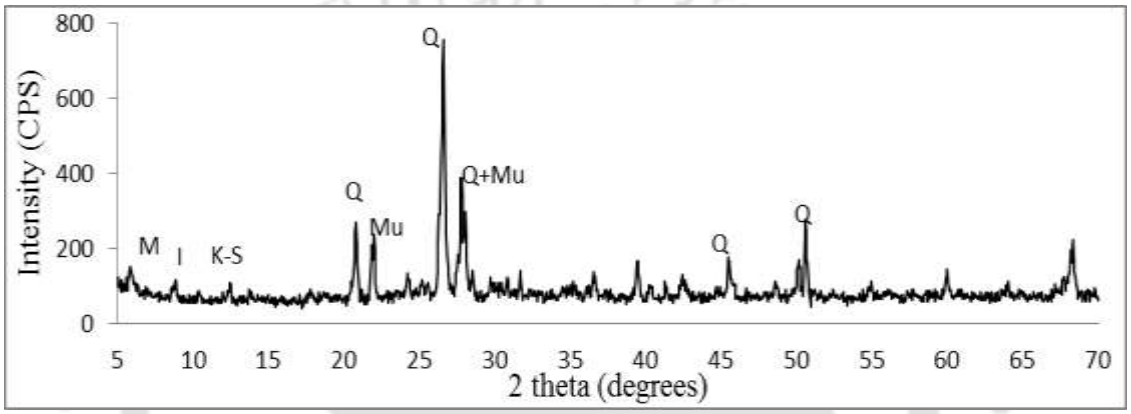


**Figure 5.15** X-Ray diffractogram of bed sediment at location 1

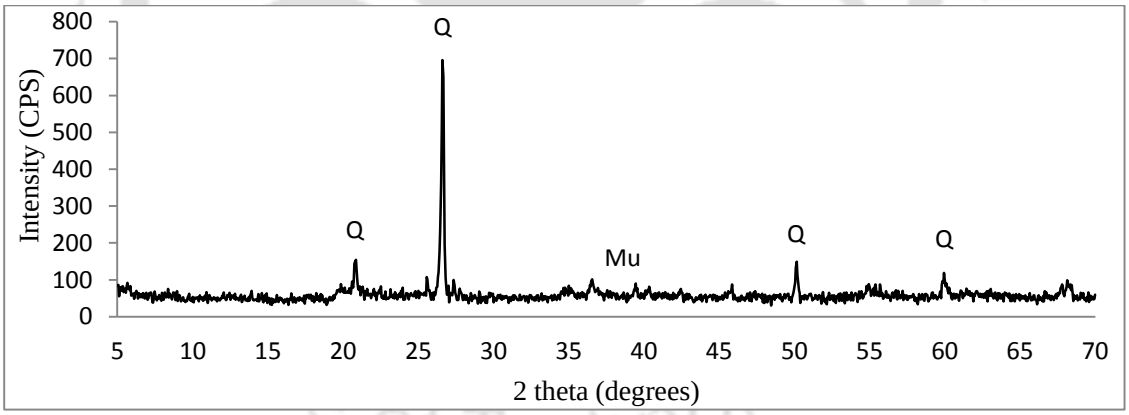


**Figure 5.16** X-Ray diffractogram of bed sediment at location 6

### *5.2.2 Geo-accumulation Indices*

To understand the level of enrichment with respect to heavy metals, geo-accumulation indices were computed. The index of geo-accumulation ($I_{geo}$) has been widely applied to the assessment of soil and sediment contamination (Santos Bermejo et al., 2003). While calculating the geo-accumulation index of bed sediments, world average concentrations of these elements reported for shale (Turkian and Wedephol, 1961) were

taken as the background values. Possible sediment enrichment of metals was evaluated in terms of the $I_{geo}$ of Muller (1979). The formula used for calculation of

$$I_{geo} = \log_2 (Cn/1.5Bn)$$

where Cn is the measured content of element 'n', and Bn is the element's content in the average shale. The geoaccumulation index was originally defined by Muller (1979) for a quantitative measure of the metal pollution in aquatic sediments (Ridgway and Shimmield, 2002).

**Table 5.3** $I_{geo}$ values and assessment of sediment quality

| Description of sediment quality | $I_{geo}$ |
|---|---|
| Extremely contaminated | >5 |
| Strongly to extremely strongly contaminated | 4 to 5 |
| Strongly contaminated | 3 to 4 |
| Moderately to strongly contaminated | 2 to 3 |
| Moderately contaminated | 1 to 2 |
| Uncontaminated to moderately contaminated | 0-1 |
| Uncontaminated | <0 |

Geo-accumulation indices for all analyzed metals at different locations are shown in Figure 5.17.

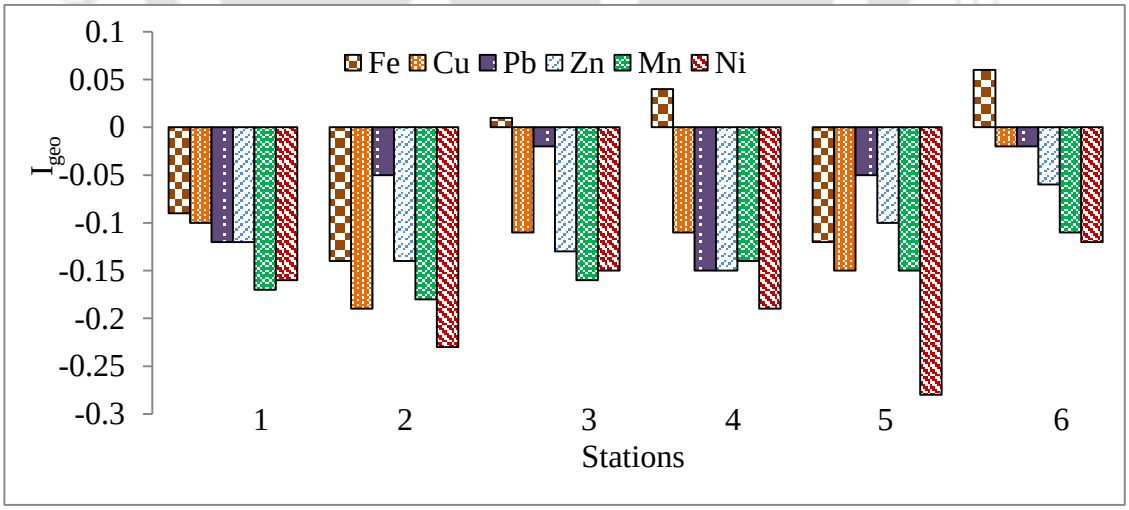


**Figure 5.17** Geo-accumulation indices of different metals at different locations

Geo-accumulation indices showed uncontaminated sediment quality for all the metals except for Fe in locations 3, 4 and 6 (Table 5.4). Nystrand et al (2012) studied metal

speciation in rivers affected by enhanced soil erosion in Finland and from their findings it can be concluded that high Fe concentrations and dominant solid fractions in Brahmaputra may be associated with river bank erosion of metal bearing phyllosilicates. Hence, enrichment of Fe is also non-anthropogenic.

Chapter 6

# Geochemical evaluation of bank materials of Brahmaputra

This chapter discusses results of geochemical analysis of bank materials collected from six locations namely *Rohmoria*, *Dibrugarh*, *Nematighat*, *Majuli*, *Gamerighat*, and *Palasbari* (Figure 3.6, p. 40). In this chapter, these six sampling locations are mentioned as *A*, *B*, *C*, *D*, *E* and *F* respectively.

## 6.1 Geochemical properties of bank materials

### 6.1.1 Analysis of bank materials of erosion site *A*

Results of analysis of different parameters for bank materials of erosion site *A* are shown in Figure 6.1(a-i). In the figure showing particle size distribution (Figure 6.1f) *A*-2, 4, 5, 6 and 7 represent samples at depth of 40 cm, 100 cm, 130 cm, 160 cm and 190 cm respectively.

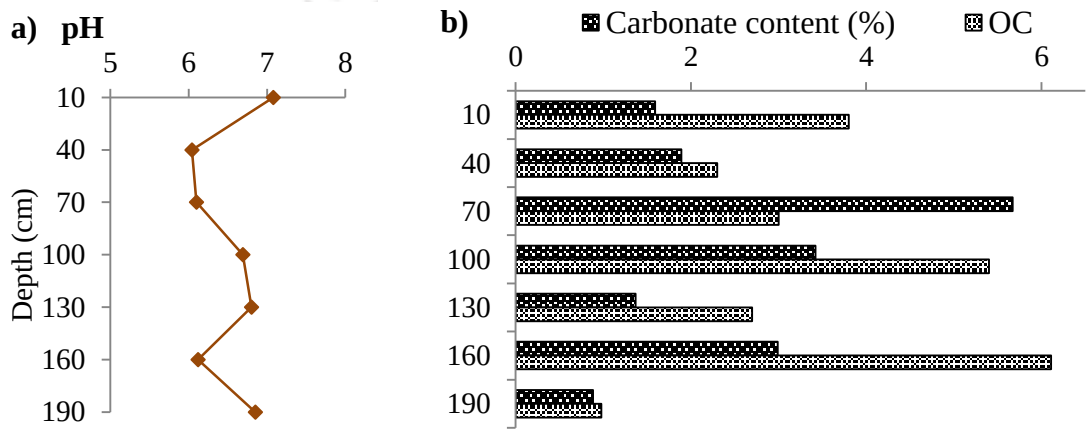


**Figure 6.1(a-b)** pH, OC and CC of bank materials of erosion site *A*

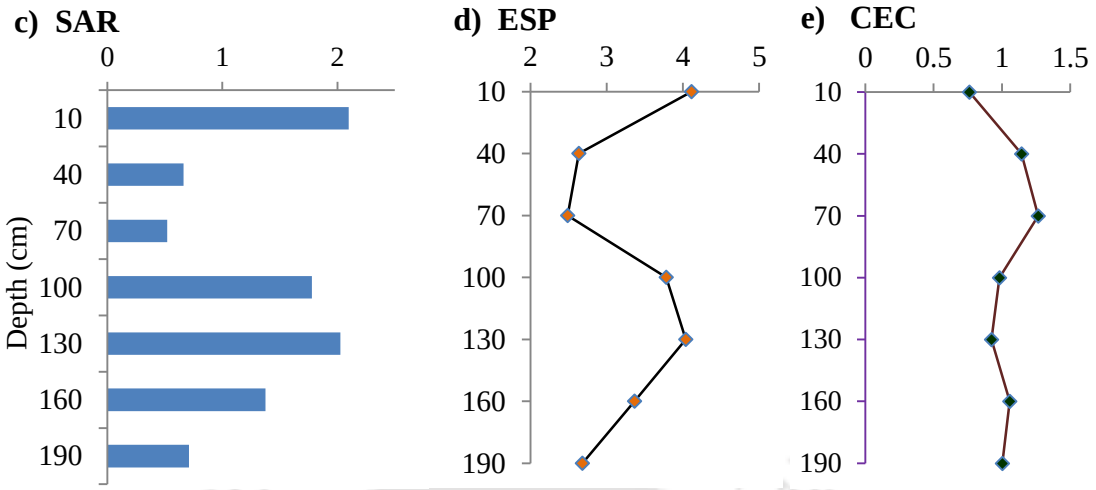


**Figure 6.1(c-e)** SAR, ESP and CEC of bank materials of erosion site *A*

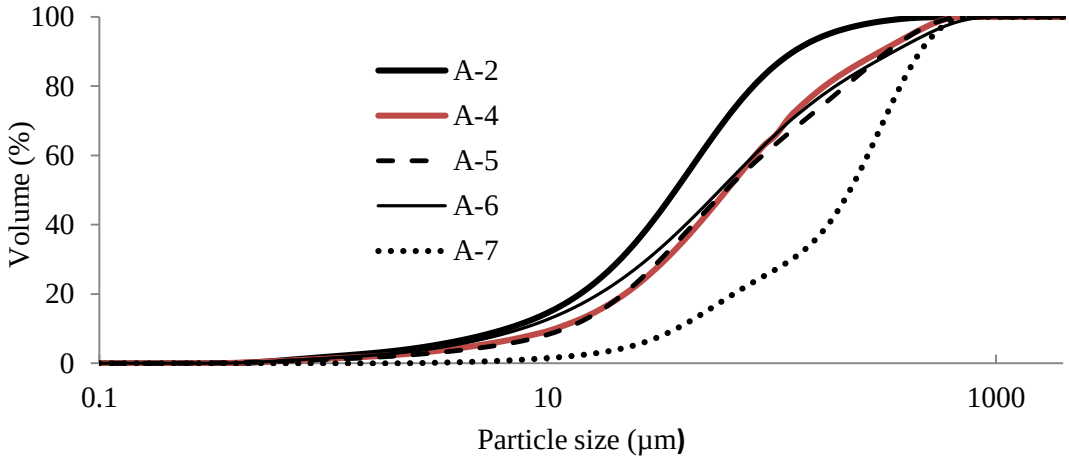


**Figure 6.1f** Particle size distribution of bank materials of erosion site *A*

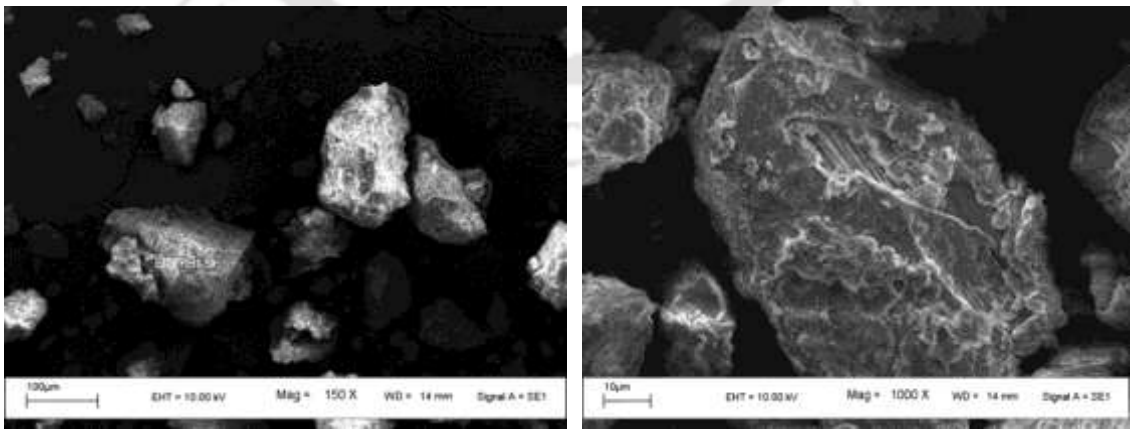

**Figure 6.1g** SEM images of bank materials of erosion site *A*

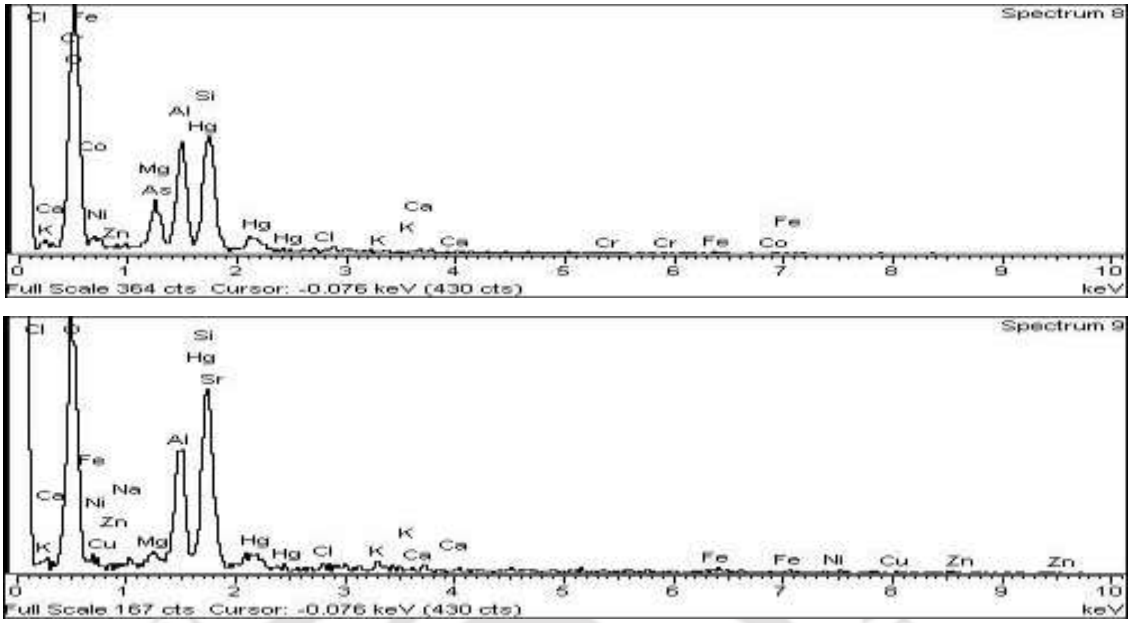


**Figure 6.1h** EDX of bank materials of erosion site *A*

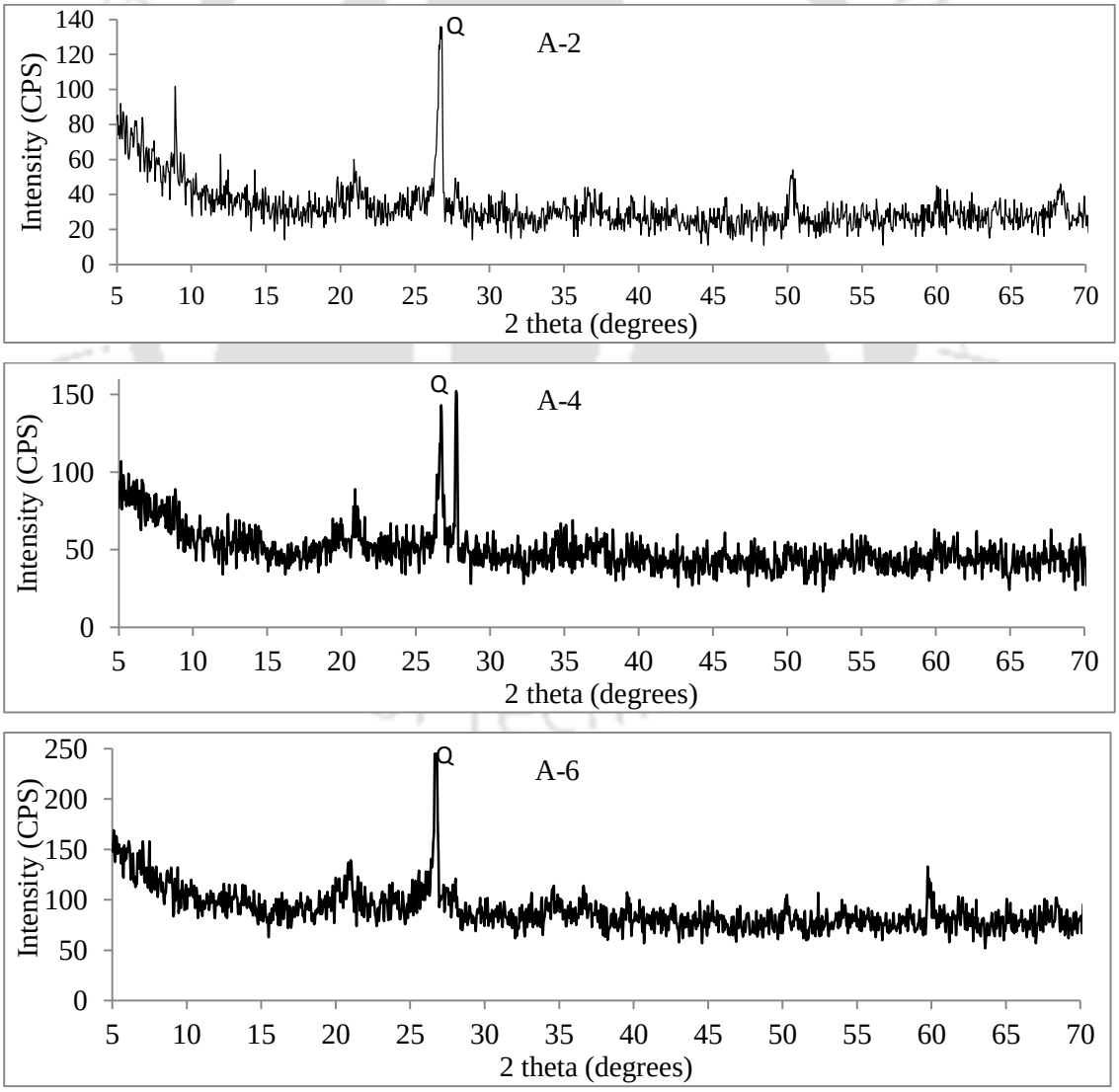


**Figure 6.1i** XRD of bank materials of erosion site *A*

pH of the bank materials (Figure 6.1a) was neutral to mild acidic with values ranging from 6.04 to 7.08. Although average organic content was 3.47%, its value at 190 cm depth is 0.98% only (Figure 6.1b). Similarly, carbonate content was very low at the layers of depth 130 cm and 190 cm (1.37% and 0.88% respectively). Values of SAR, ESP and CEC were found to be fluctuating with depth; however, continuous decrease at lower layers was distinct (Figure 6.1c-e). This continuous decrease has similarity with findings of Santis et al. (2010) for eroded profiles of Aliano area (Southern Italy). Grain size distribution showed dominance of silts (3.9--62.5 µm) and medium sands (250-500 µm) in the bank profile with layered structures having particle size ranging from 7µm to 460 µm. Presence of a loose layer of medium grained sand at 190 cm depth with $d_{50}$ and $d_{90}$ values of 224 µm and 460 µm respectively was the main geochemical cause of erosion in the study area. During high flow, the river current undermines the loose sand layer; as a result the overhanging soil layers lose support and tumble down and carried away easily by strong current of the river. Although abundance of soluble metals like Fe and Al in the study area as observed from EDX (Figure 6.1h), could reduce the double layer thickness of clay particles, theoretically increasing cohesion and reducing sediment erodibility, such results were not observed due to absence of clay particle and dominance of silt and medium sand particle.

### 6.1.2 Analysis of bank materials of erosion site *B*

Results of analysis of different parameters for bank materials of erosion site *B* are shown in Figure 6.2. In the figure showing particle size distribution (Figure 6.2f), *B*-2, 3, 4, 5 and 6 represent samples at depth of 40 cm, 70 cm, 100 cm, 130 cm and 160 cm respectively.

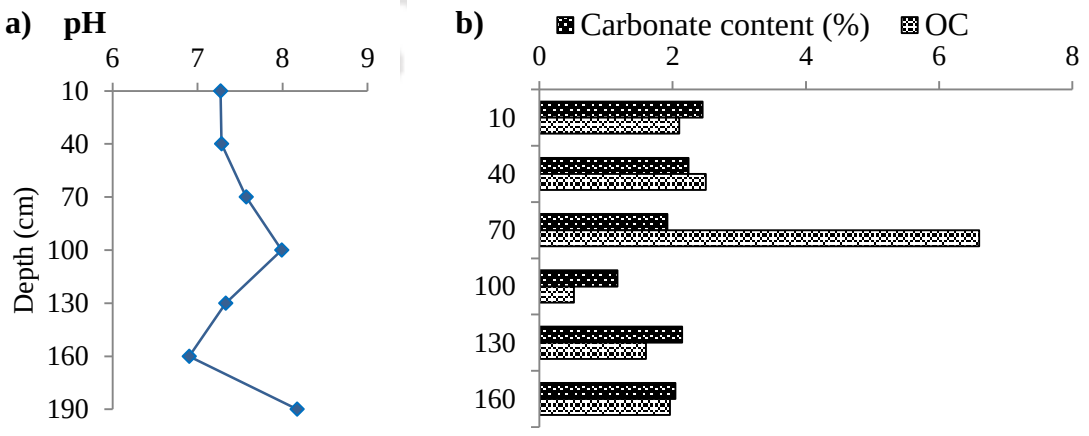


**Figure 6.2 (a-b)** pH, OC and CC of bank materials of erosion site *B*

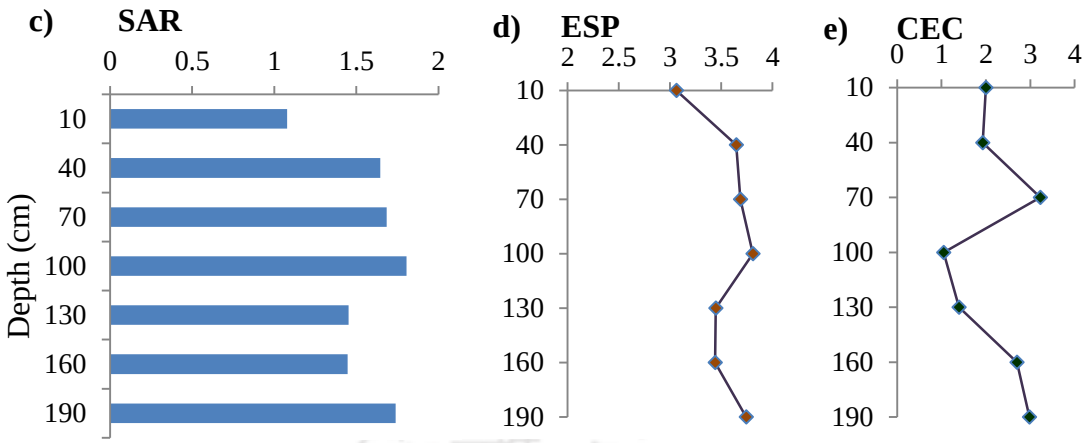


**Figure 6.2(c-e)** SAR, ESP and CEC of bank materials of erosion site *B*

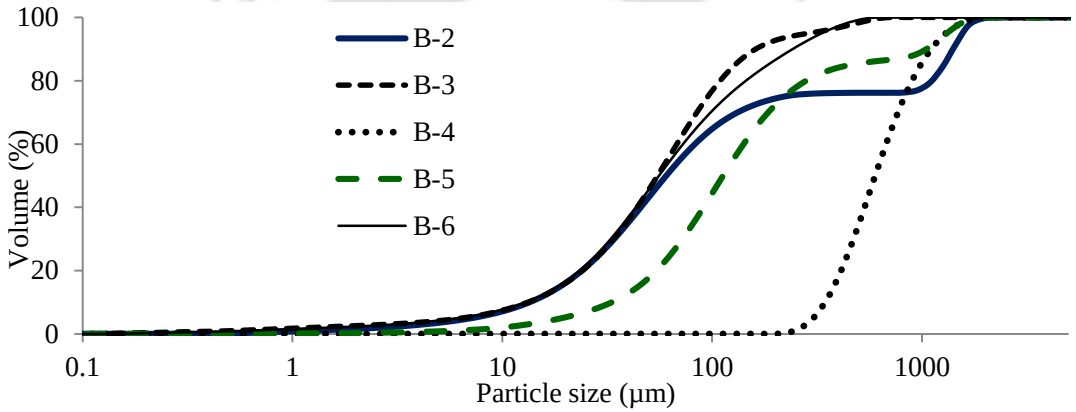


**Figure 6.2f** Particle size distribution and XRD of bank materials of erosion site *B*

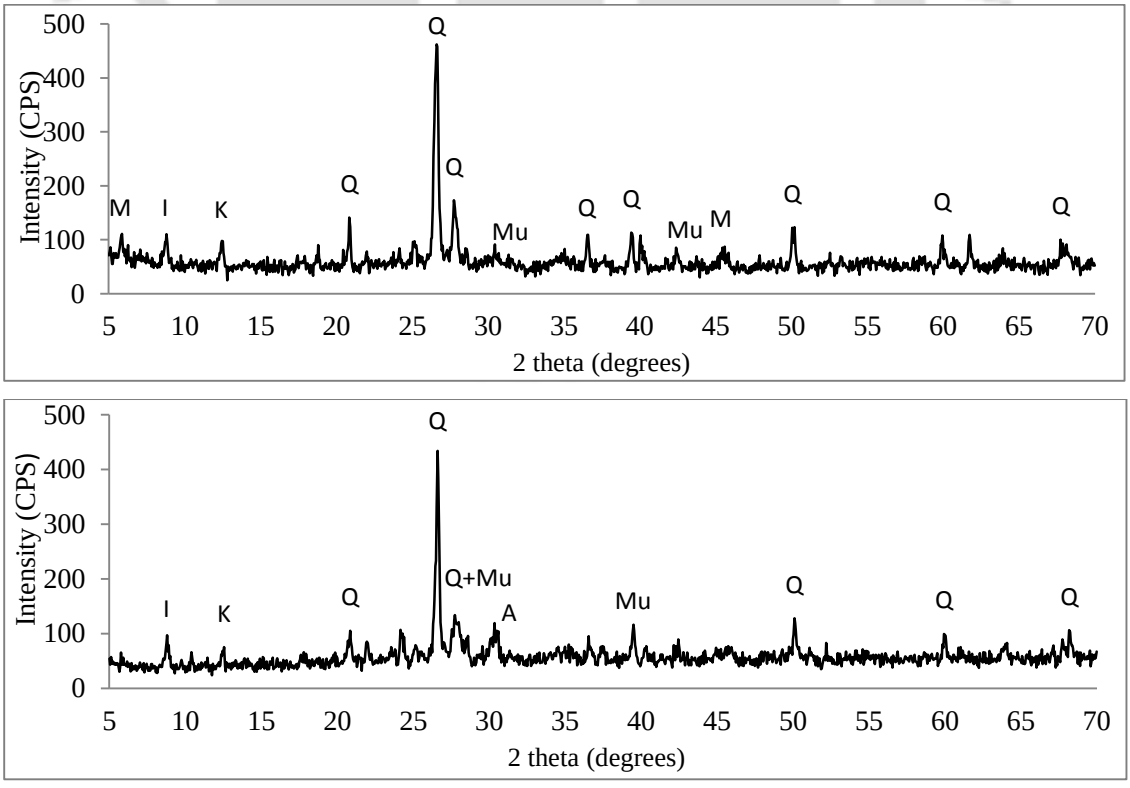

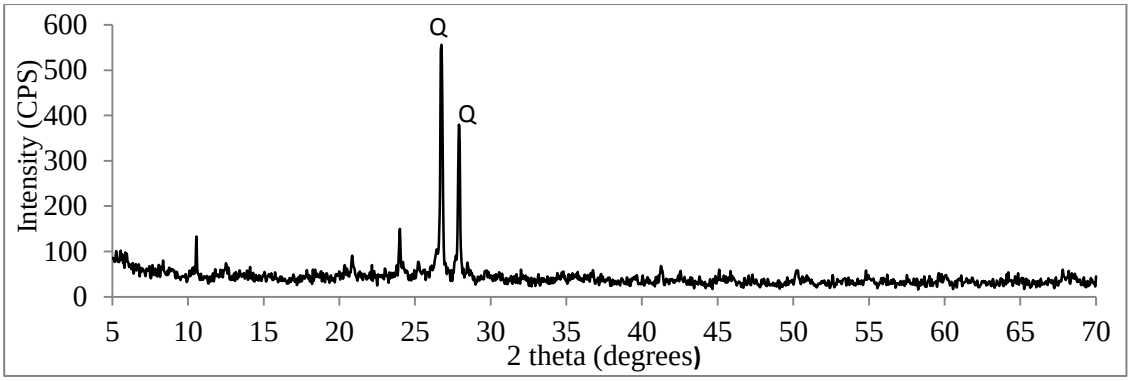


**Figure 6.2g** XRD of bank materials of erosion site *B*

pH of the bank materials was alkaline with values ranging from 6.9 to 8.1 (Figure 6.2a). Average OC was more than 2% at upper layers, but its value was quite low at bottom layers of the sediment profile (0.52% at 100 cm, 1.6% at 130 cm and 1.96% at 160 cm depth). Similarly carbonate content was low at all layers with average value of 01.99% (Figure 6.2b). Fluctuating SAR and ESP values and decreasing CEC values were observed. From grain size distribution, $d_{50}$ values for different layers were 60, 55, 598, 113 and 60 µm respectively. Dominance of silts (3.9-62.5 µm), medium sands (250-500 µm) and coarse sands (500-1000 µm) in the bank profile, particularly presence of a loose layer of coarse grained sand at 100 cm depth with $d_{10}$ and $d_{90}$ values of 345.6 µm and 1106.5 µm respectively were the main geochemical variables affecting erosion in the studied location. Bank profile in *B* erosion site was distinct with composite structure of silts and sands as shown in Figure 6.3.


**Figure 6.3** Composite structure of river bank in erosion site *B*

### 6.1.3 Analysis of bank materials of erosion site *C*

In location *C*, river bank is made up of loose unconsolidated alluvium soil (Figure 6.4).

**Figure 6.4** Loose structure of river bank in *erosion site C*

Results of analysis of different parameters for bank materials of location *C* are shown in Figure 6.5. In the figure showing particle size distribution (Figure 6.5f), *C*-2, 3, 4, 5, 7 represent samples at depth of 40 cm, 70 cm, 100 cm, 130 cm and 190 cm respectively.

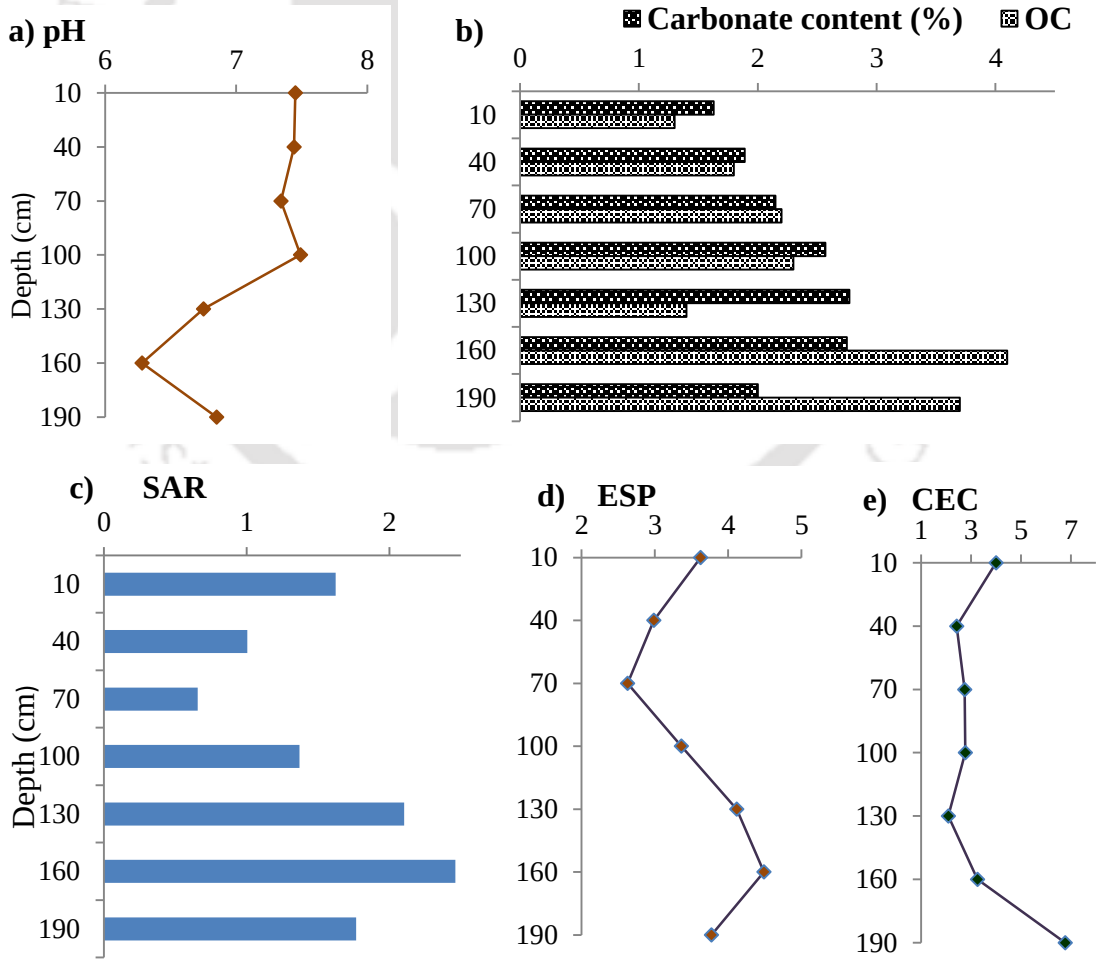


**Figure 6.5(a-e)** pH, OC, CC, SAR, ESP and CEC of bank materials of erosion site *C*

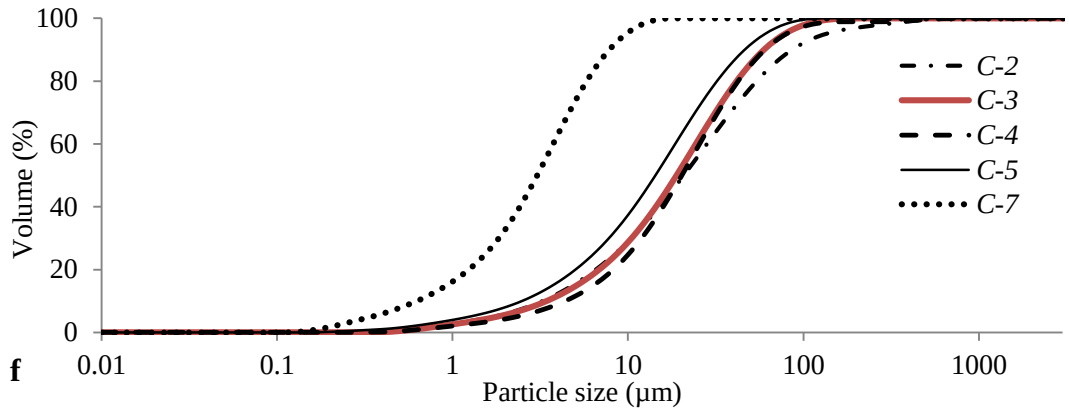


**Figure 6.5f** Particle size distribution of bank materials of erosion site *C*

pH of bank materials were alkaline at upper layers but slightly acidic at bottom layers. Although organic content was high at bottom layers, there was no typical trend. SAR and ESP values were decreased at bottom layer while CEC values were increasing. From grain size distribution, uniform particles of silt size were observed with $d_{50}$ values of 21 µm, 19 µm, 20 µm & 14 µm at depth of 40 cm, 70 cm, 100 cm and 130 cm respectively. Abundance of clay particles (with $d_{50}$ value of 3 µm) was observed at depth of 190 cm. However, role of the clay pocket was not significant due to dominance of silt particles.

### 6.1.4 Analysis of bank materials of location *D*

Samples were collected from both eroded and non-eroded locations of *D*. Results of analysis of different parameters for bank materials of non-erosion sites of two locations (named as *D1* and *D5*) are shown in Figure 6.6. *D1-3*, *D1-7* and *D1-10* in the figure showing particle size distribution, represent samples at depth of 70 cm, 190 cm and 280 cm respectively.

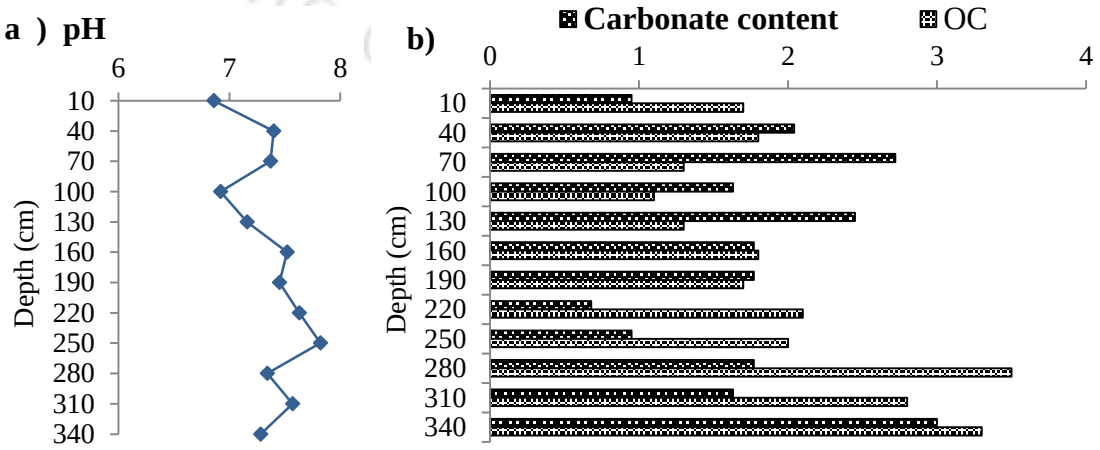


**Figure 6.6(a-b)** pH, OC and CC of bank materials of non-eroded site of *D1*

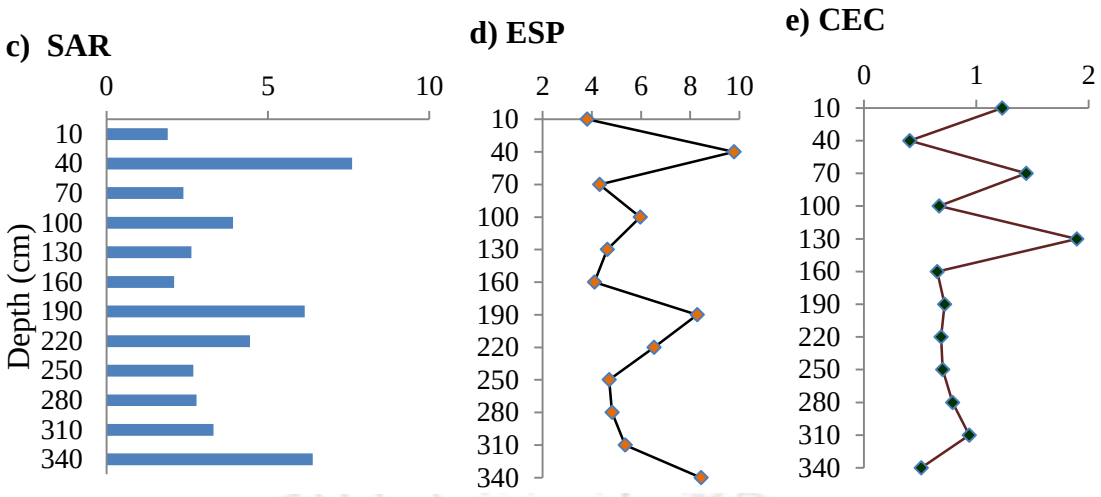


**Figure 6.6(c-e)** SAR, ESP and CEC of bank materials of non-eroded site of *D1*

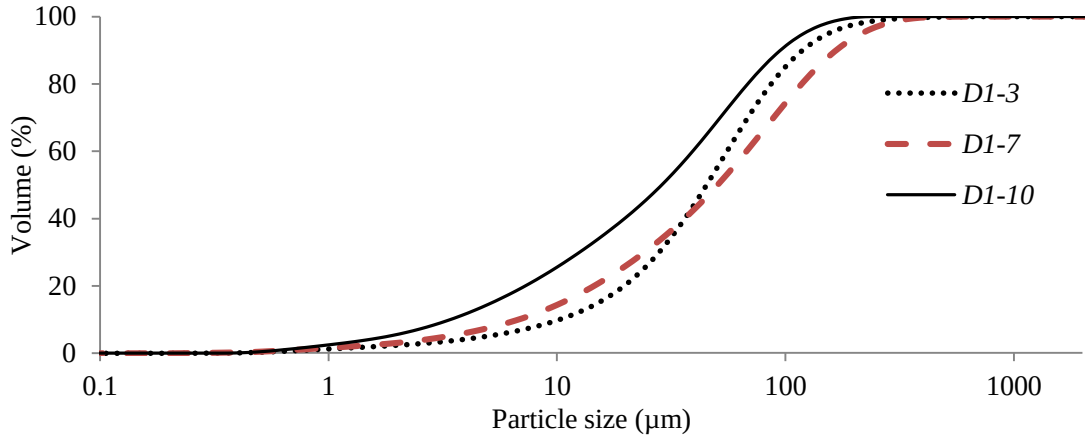


**Figure 6.6f** Particle size distribution of bank materials of non-eroded site of *D1*

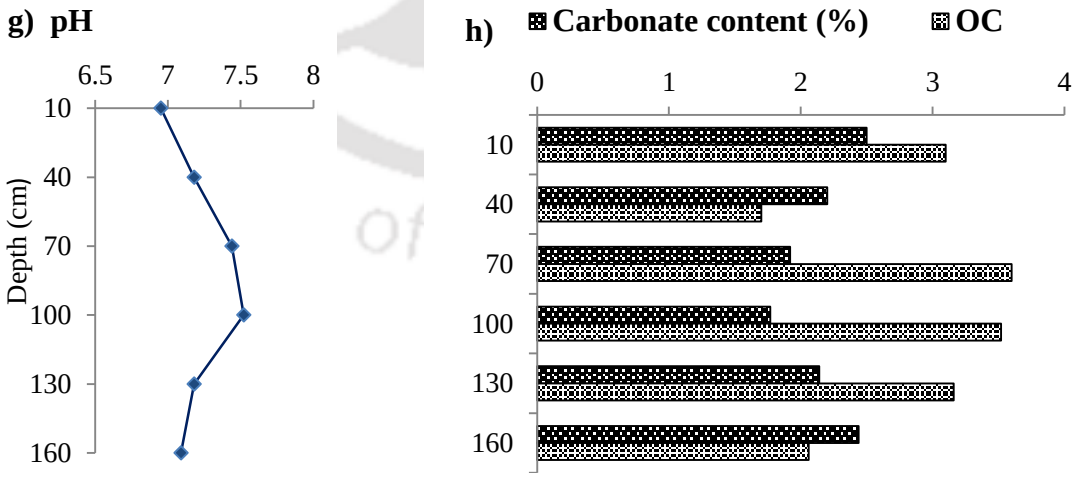


**Figure 6.6(g-h)** pH, OC and CC of bank materials of non-eroded sites of *D5*

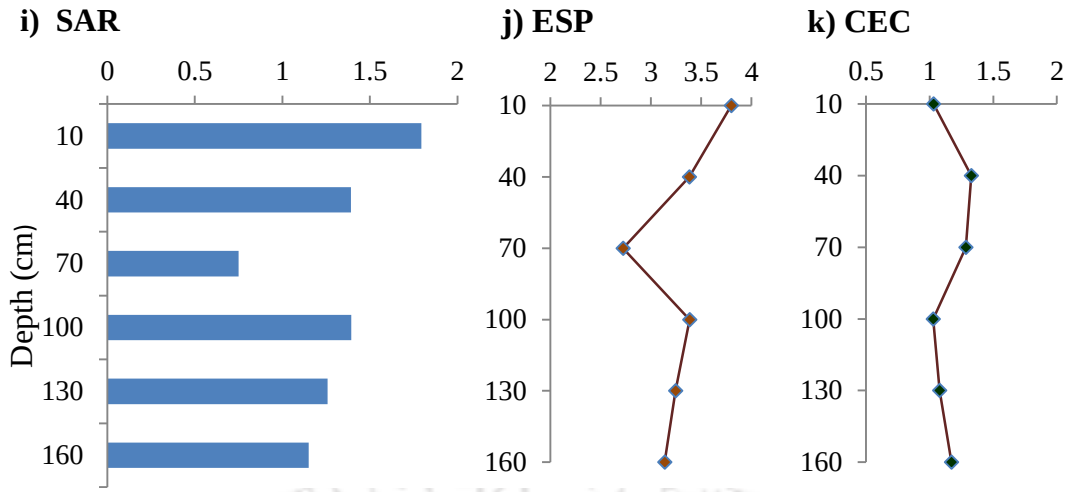


**Figure 6.6(i-k)** pH, OC, CC, SAR, ESP, CEC and particle size distribution of bank materials of non-eroded sites of *D5*

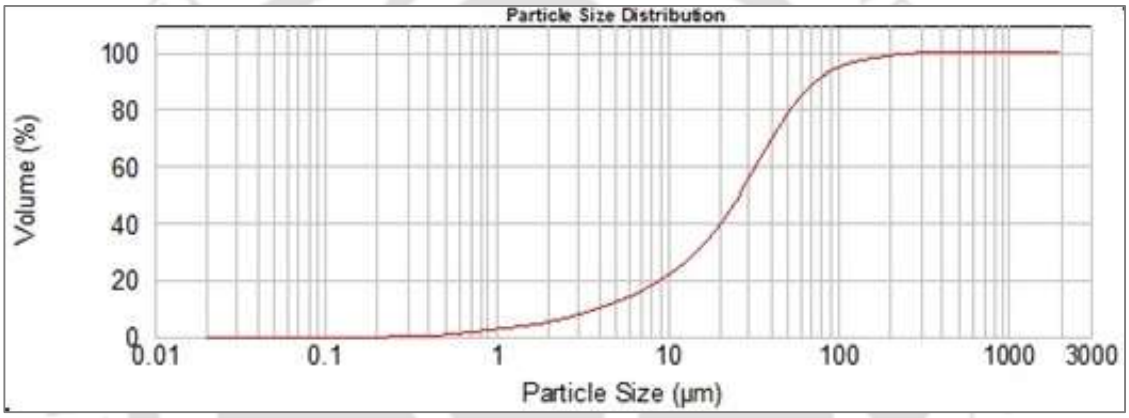


**Figure 6.6l** Particle size distribution of bank materials of non-eroded sites of *D5*

pH of both the non-eroded sites was slightly alkaline. Average organic content was more than 2% in five out of six samples of sediment profile. SAR, ESP and CEC values fluctuated with depth. Particle size distribution showed dominance of silt particles but a homogenous structure in both the two locations. $d_{50}$ values for samples at depth of 70 cm, 190 cm and 280 cm of location *D1* are 45, 51 and 29 µm respectively; the value at 90 cm depth of the other location (D5) is 26 µm. Homogenous structure of bank profile with high organic content are likely to be responsible for non-erodibility of those two locations.

Findings of analysis of different parameters for bank materials of erosion sites named as *D3*, *D6* and *D8* are shown in Figure 6.7.

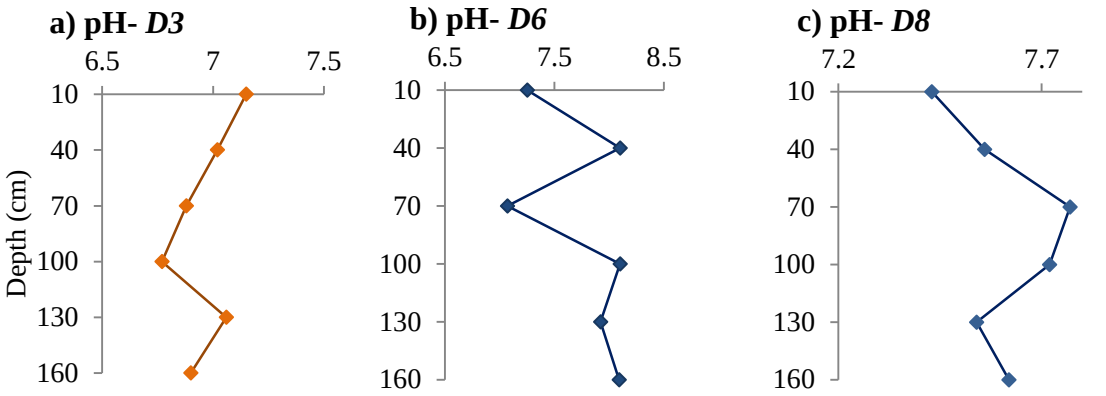


**Figure 6.7(a-c)** pH of bank materials of erosion sites of *D3*, *D6* and *D8*

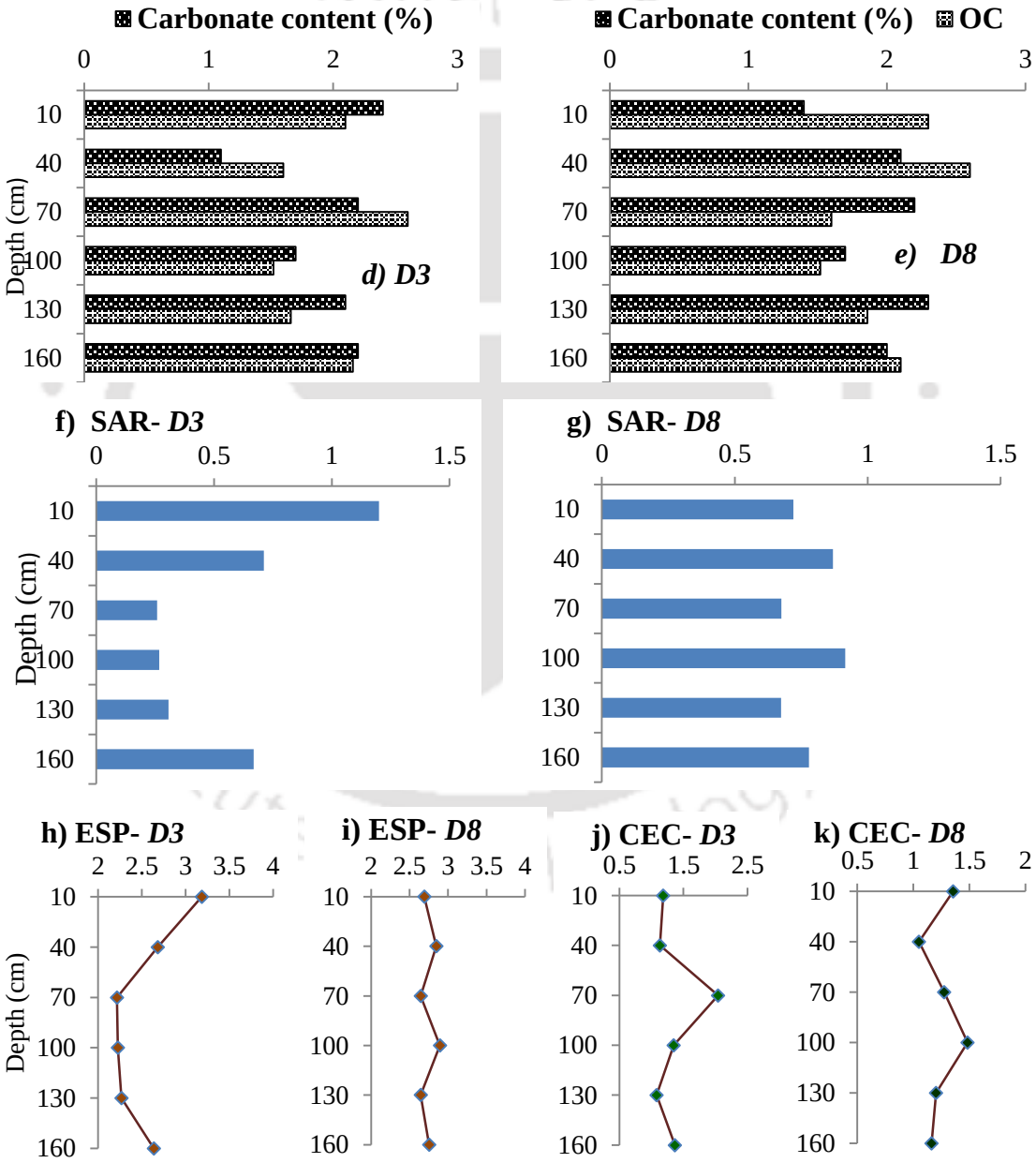


**Figure 6.7(d-k)** OC, CC, SAR, ESP and CEC of bank materials of erosion sites of *D* (*D3* and *D8*)

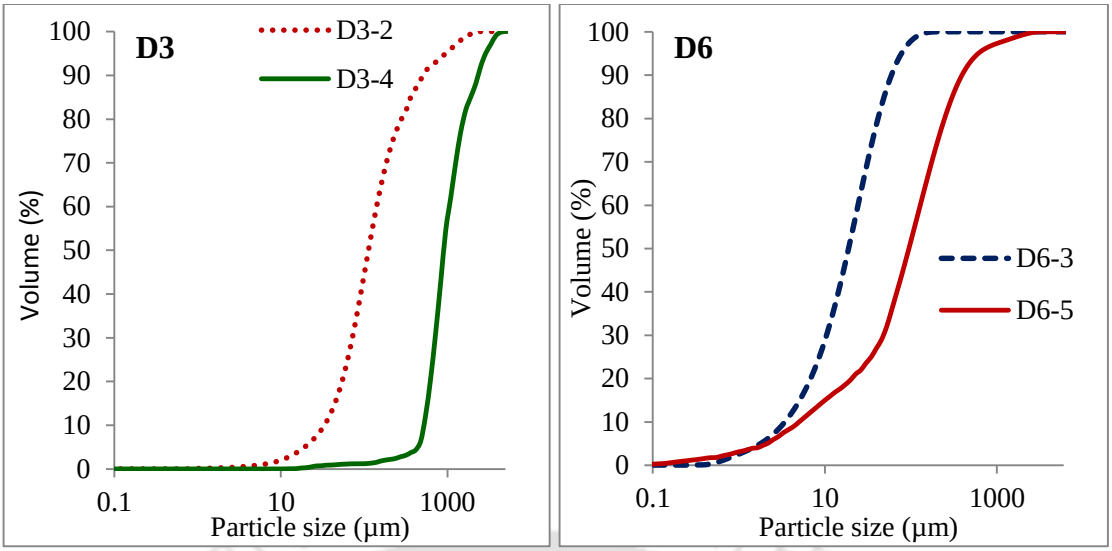


**Figure 6.7l** Particle size distribution of bank materials of erosion sites of *D* (*D3* and *D6*)

At lower layers of sediment profile, pH was slightly acidic in D3, but alkaline at other two locations. Values of average OC and CC were less than 2% at *D3* and *D8* which suggested vulnerability to erosion. SAR was decreasing at *D3* but it was almost constant at D8. Both ESP and CEC increased with respect to the lower portions of the sediment profiles in *D3* while these values were fluctuating in *D8*. Particle size analysis (Figure 6.7l) suggested composite bank materials. Dominance of sand layers in both the locations indicated susceptibility to erosion. Bank failure of a composite bank is shown in Figure 6.8.

**Figure 6.8** Bank failure of a composite bank in erosion site *D*

### 6.1.5 Analysis of bank materials of erosion site *E*

Findings of analysis of different parameters for bank materials are shown in Figure 6.9.

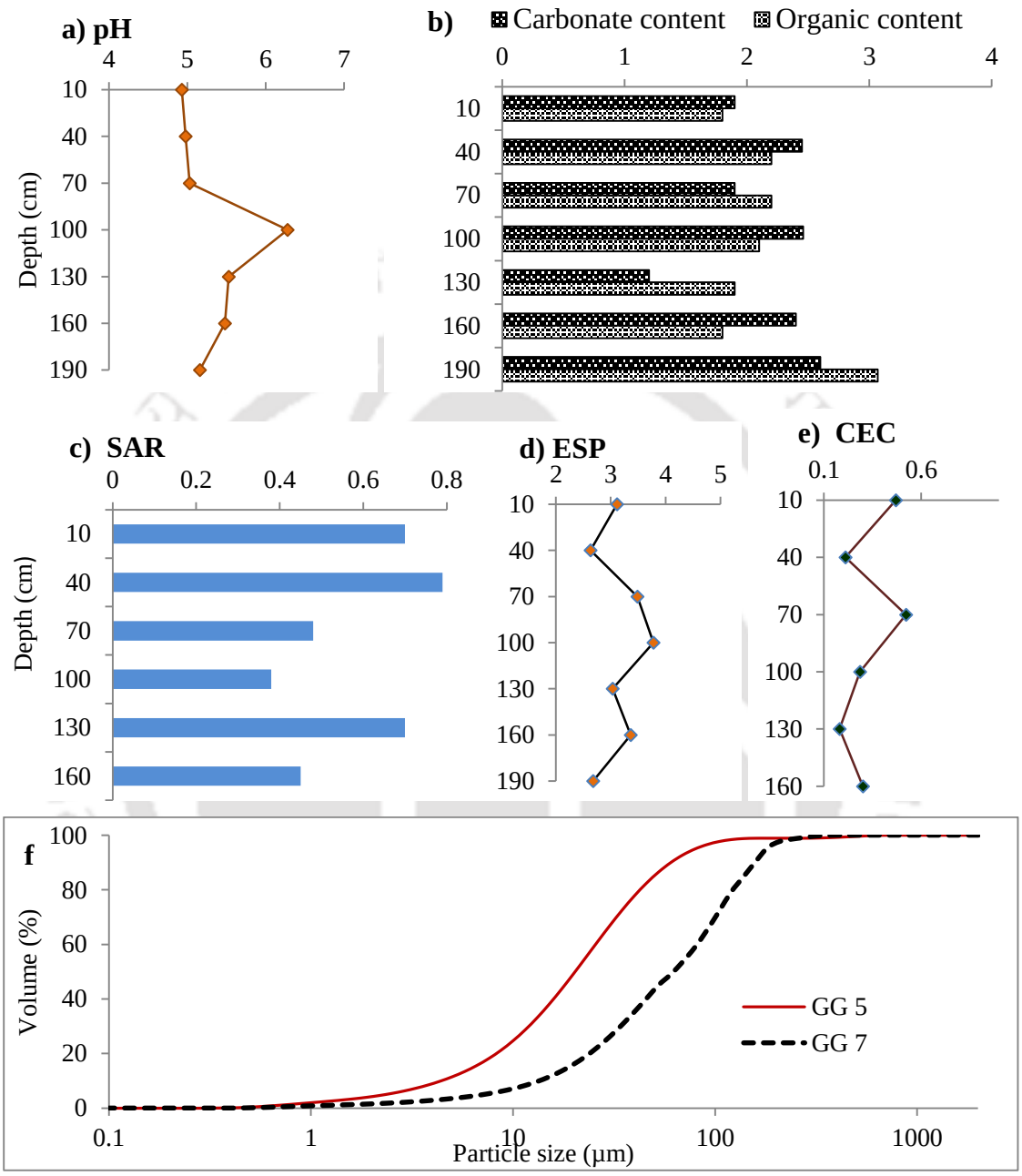


**Figure 6.9(a-f)** pH, OC, CC, SAR, ESP, CEC and particle size distribution of bank materials of erosion site *E*. (*E5* and *E7* in particle size distribution represent samples at depth of 130 cm and 190 cm respectively)

Soil pH was continuously decreasing at the lower profile of erosion site *E*. Although average value of OC was 2.15% and SAR and ESP showed no typical trend, dominance of silt particles with $d_{50}$ values of 18 µm and $d_{90}$ values of 65µm suggested vulnerability to river bank erosion.

### 6.1.6 Analysis of bank materials of erosion site *F*

Results of analysis of different parameters for bank materials of *F* erosion site are shown in Figure 6.10.

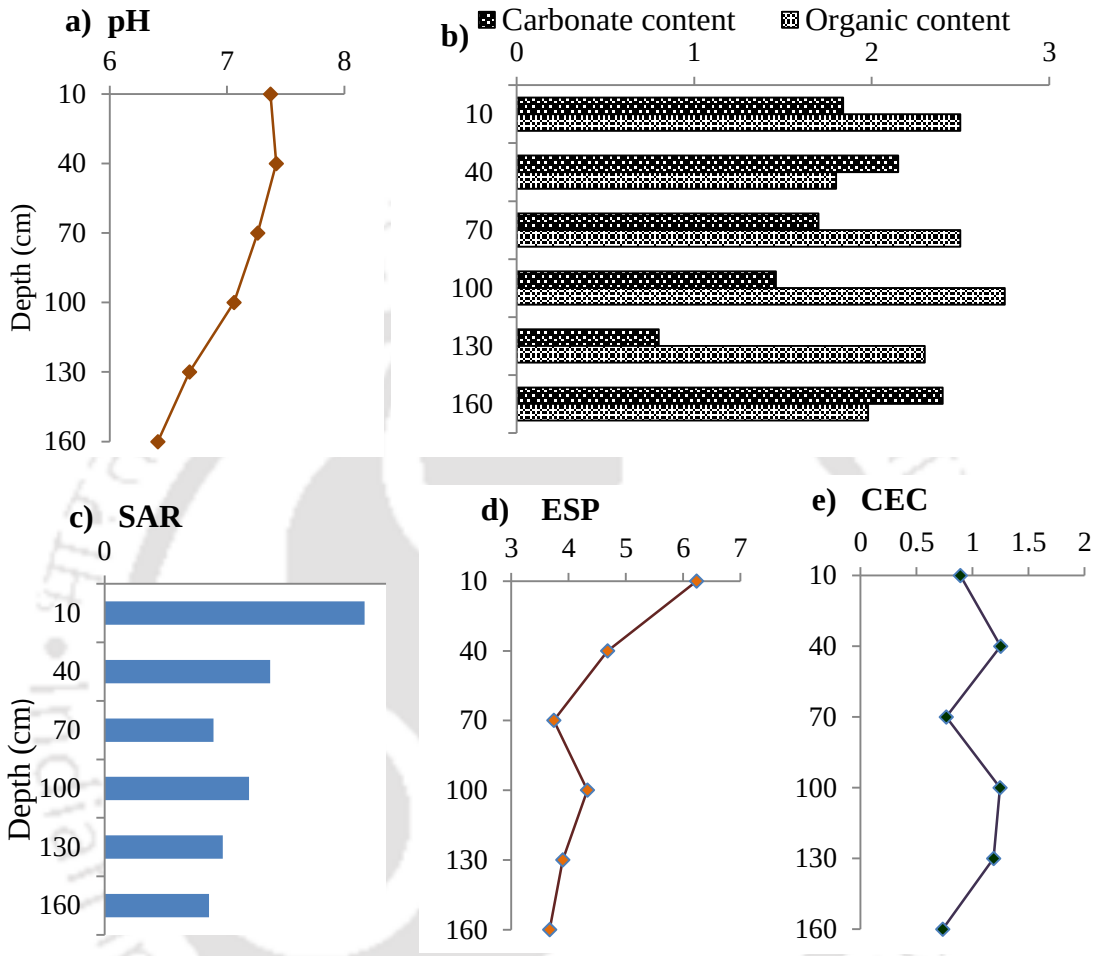


**Figure 6.10(a-e)** pH, OC, CC, SAR, ESP and CEC of bank materials of erosion site *F*

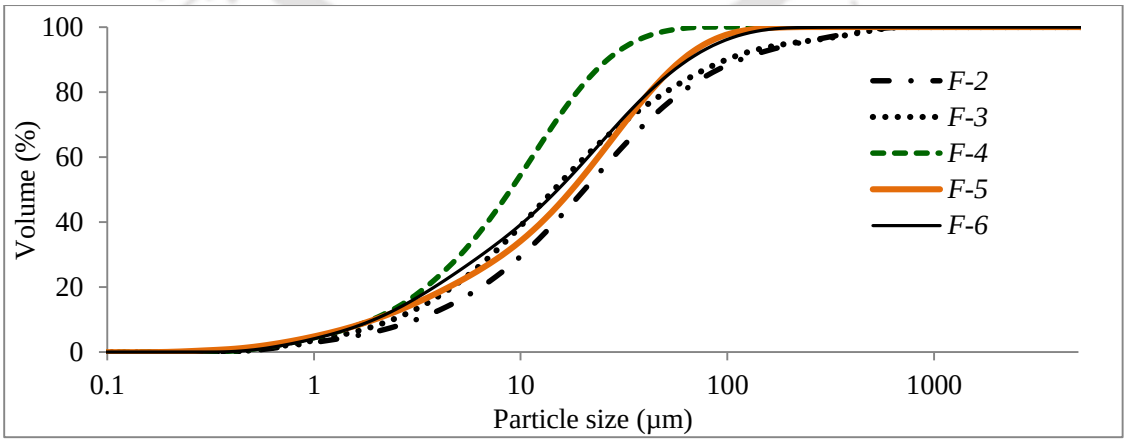


**Figure 6.10f** Particle size distribution of bank materials of erosion site *F* (*F-2*, *F-3*, *F-4*, *F-5* and *F-6* represent samples at depth of 40 cm, 70 cm, 100 cm, 130 cm and 160 cm respectively)

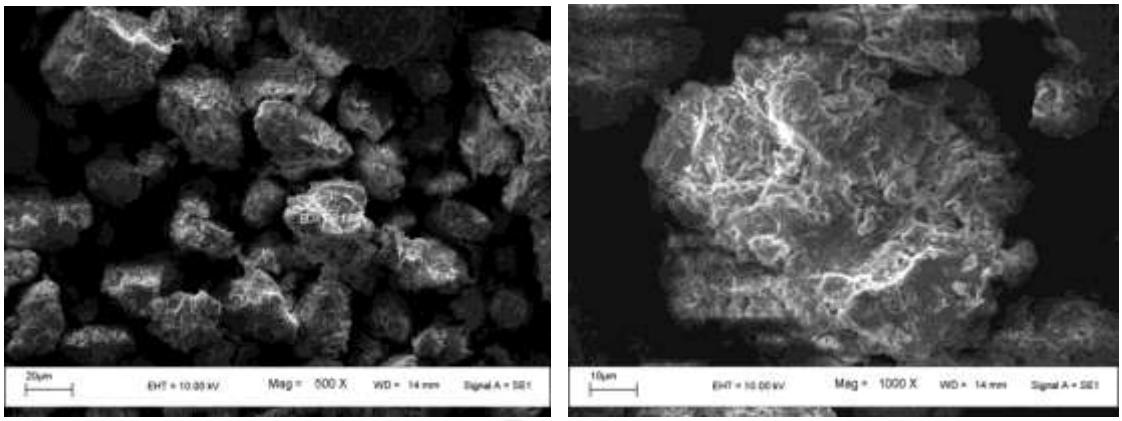

**Figure 6.10g** SEM images of bank materials of erosion site *F*

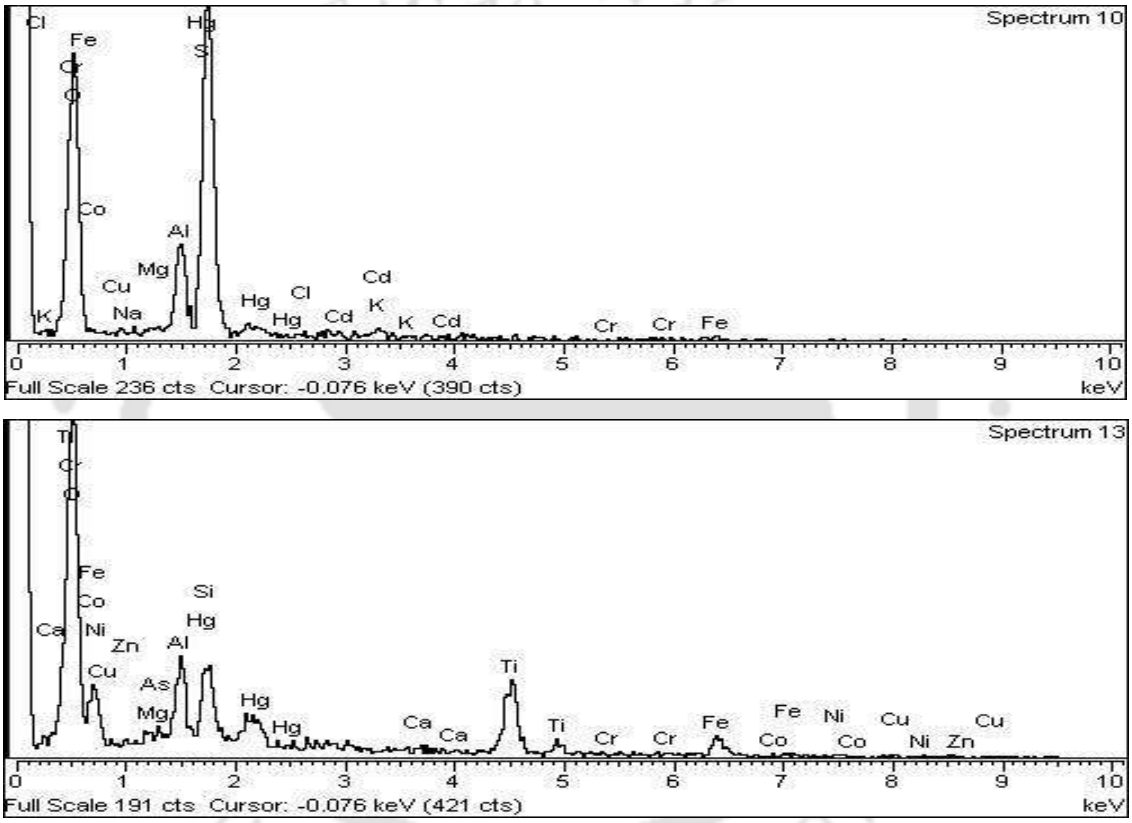


**Figure 6.10h** EDX of bank materials of erosion site *F*

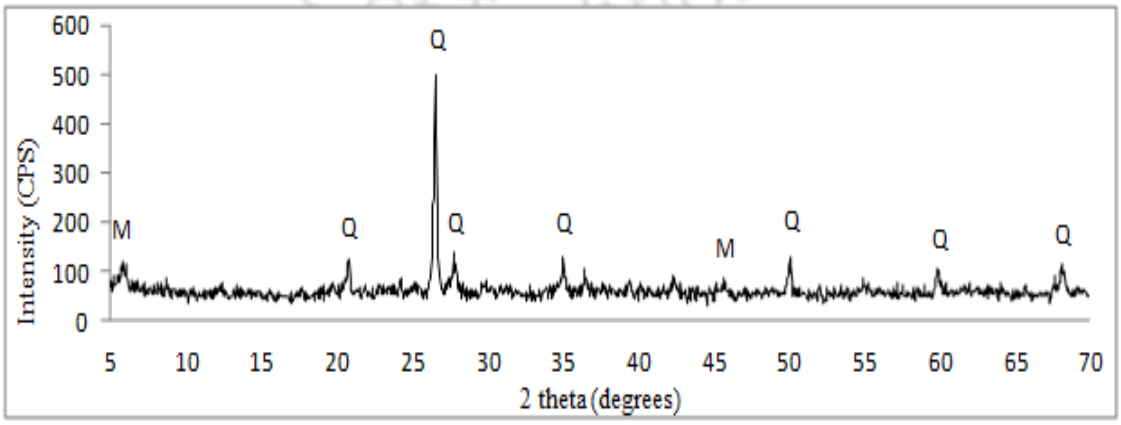

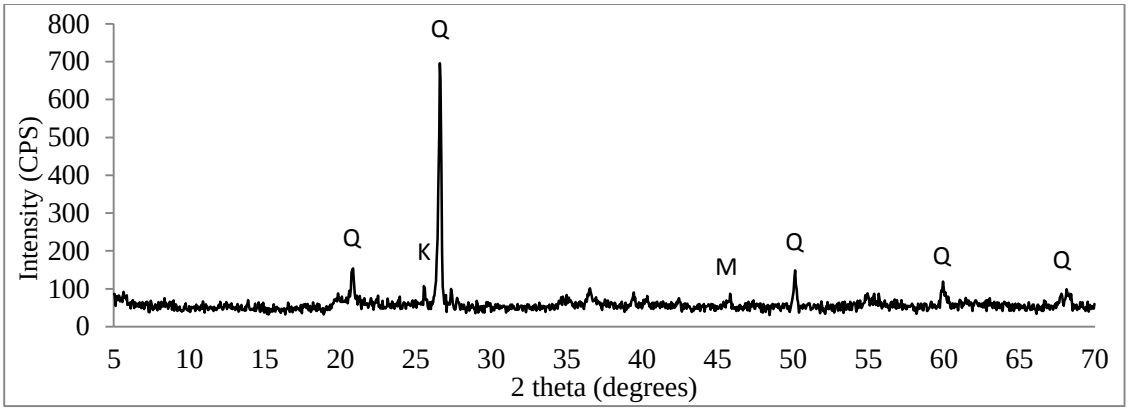


**Figure 6.10i** XRD of bank materials of erosion site *F*

pH value was decreased in the study area. Average OC and average CC values were found to be 2.56% and 1.85% respectively. Although the average value of organic content was higher than 2% which was considered as lower value for non-erodible soils, organic content less than 2%, was observed at lower depths, i.e., at a depth of 70 cm and 190 cm. Organic content and carbonate content, varying along vertical profile of bank materials, suggested differential erosion potential of different layers.

SAR, ESP and CEC values were decreasing downwards. From particle size distribution, $d_{50}$ values at depth of 40 cm, 70 cm, 100 cm, 130 cm and 160 cm were 20 µm, 15 µm, 9 µm, 18 µm and 15 µm respectively. The corresponding $d_{90}$ values were 120, 99, 26, 61 and 65 µm. Dominance of silt (3.9-62.5 µm ) and very fine sand (62.5-125 µm ) and less abundance of clay (< 3.9 µm) percentage (<10%) widely favoured erosion in the area.

Mineral composition of bank materials at different depths (100 cm and 160 cm) of vertical profile are shown in the XRD (Figure 6.10i). Quartz along with Montmorrilonite and Muscovite were dominant minerals in bank materials.

## 6.2 Synthesis of observations and interpretation from different experiments and test results

Among the analyzed geochemical parameters pH, OC, CC, CEC, ESP, $d_{10}$, $d_{50}$ and $d_{90}$, were more fluctuating in erosion sites than those of non-erosion sites, as revealed from range and standard deviation values (Table 6.1 and Table 6.2).

**Table 6.1** Descriptive statistics of different parameters of soil samples from erosion sites (N = 36)

| | Range | Minimum | Maximum | Mean | SD |
|---|---|---|---|---|---|
| pH | 3.17 | 4.93 | 8.10 | 6.81 | .93 |
| OC | 6.48 | .12 | 6.60 | 1.74 | 1.75 |
| CC | 5.45 | .22 | 5.67 | 1.30 | 1.15 |
| SAR | 3.90 | .26 | 4.16 | 1.12 | .765 |
| CEC | 3.97 | .24 | 4.22 | 1.32 | .96 |
| ESP | 14.41 | 1.26 | 15.67 | 4.15 | 3.15 |
| $d_{10}$ | 343.10 | 1.90 | 345.00 | 35.22 | 75.35 |
| $d_{50}$ | 605.00 | 15.00 | 620.00 | 105.98 | 133.65 |
| $d_{90}$ | 1340.90 | 59.10 | 1400.00 | 343.21 | 346.81 |

**Table 6.2** Descriptive statistics of different parameters of samples from non-erosion sites (N = 34)

| | Range | Minimum | Maximum | Mean | SD |
|---|---|---|---|---|---|
| pH | 2.13 | 6.67 | 8.80 | 7.34 | .38 |
| OC | 5.50 | 1.10 | 6.60 | 2.49 | 1.13 |
| CC | 2.32 | .68 | 3.00 | 1.82 | .69 |
| SAR | 6.85 | .75 | 7.60 | 2.61 | 1.62 |
| CEC | 3.54 | .64 | 4.19 | 1.48 | .71 |
| ESP | 4.42 | 1.47 | 5.89 | 3.22 | 1.25 |
| $d_{10}$ | 32.10 | 2.10 | 34.20 | 7.25 | 6.23 |
| $d_{50}$ | 84.08 | 10.72 | 94.80 | 36.78 | 17.43 |
| $d_{90}$ | 272.62 | 34.38 | 307.00 | 110.17 | 54.96 |

Bank materials of erosion site E had the lowest pH (acidic, mean value 5.3). Less amount of exchangeable Na, K, Ca and Mg was observed in all locations including non-erosion site of *D*, which resulted in very low value of CEC in all locations. This may be attributed to less amount of clay and high amount of silt and sand particles in soil. Comparatively, more varied as well as high values of Ca and Mg were observed in erosion site of *C*. Increasing soluble Ca and Mg improves aggregate stability in soils. However, impact of high Ca and Mg was not observed in loose unconsolidated bank materials of *C* location in spite of having clay pockets. This may be attributed to high amount of silt particles (mean value 71%) in the bank materials. Low amount of exchangeable Na (8%) in bank materials of erosion site *C* is one geochemical factor contributing to loose structure of bank.

Low value of SAR in erosion sites could be due to low available Na in soils. Although comparatively high values of SAR were observed in non-erosion sites of *D*, only 4 samples out of 12 samples had higher SAR values than the mean value. High variation of SAR with depth along with high clay content and less variation of sand particles have been observed as significant geochemical properties contributing to non-erosion in the locations of *D*.

Erosion site *A* had comparatively high sand content and the lowest value of minimum clay content (0.3%) among the study areas. Erosion sites of *B, D, E* and *F* also had high sand content (52%, 44%, 36% and 31% respectively) with very low amount of clay sized particles (3 – 8%). These two factors including low organic content are likely to be considered as significant geochemical factors for low cohesion in the studied locations as revealed from direct shear test results (Figure 6.11).

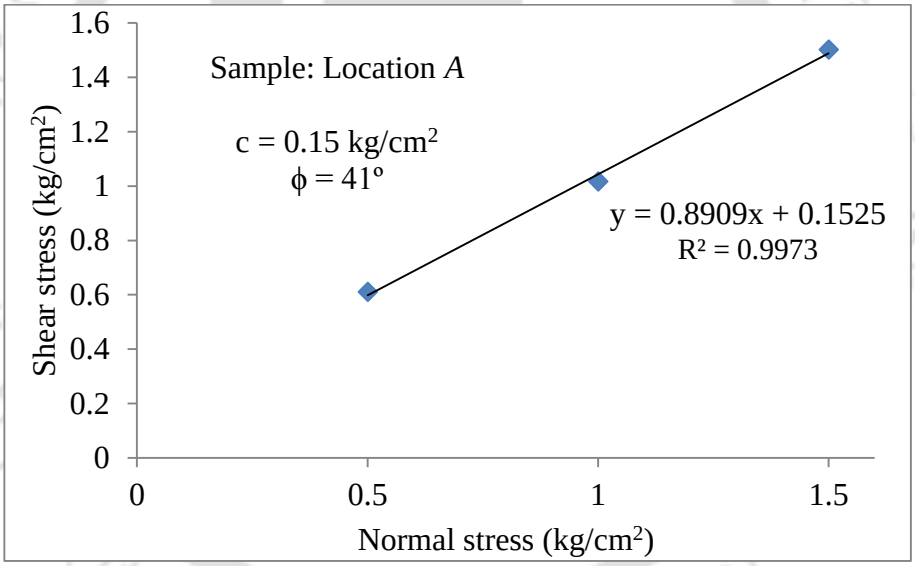


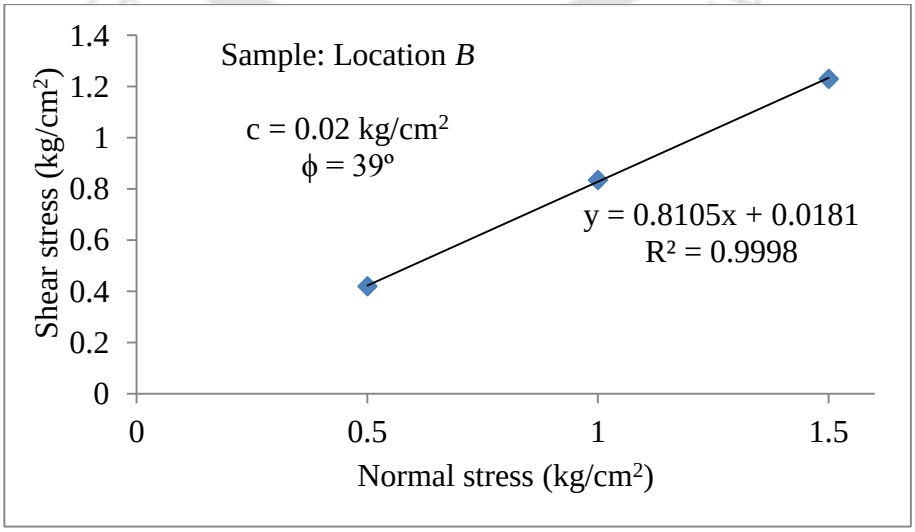

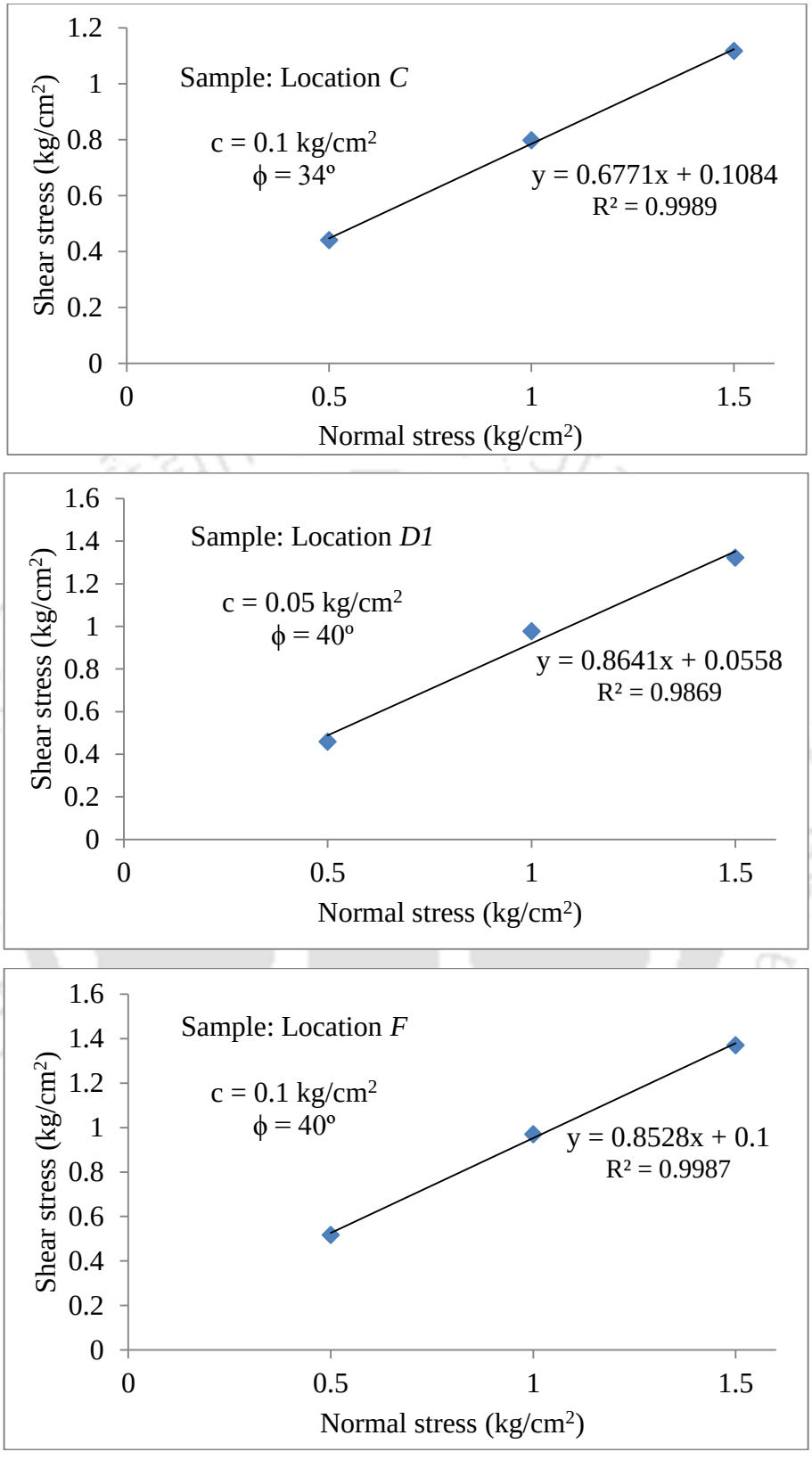


**Figure 6.11** Direct shear test results of bank materials

High angle of internal friction of samples in spite of low cohesion could be explained by aggregation of soil particles (Lebert and Horn, 1991). The aggregates were strong

enough to resist the stresses and the soil acted like very dense sand with high angle of internal friction (Lebert and Horn, 1991). Lohnes and Handy (1968) suggested that unconsolidated sediments with low cohesion can stand temporarily at steep angles. Steep river banks in erosion sites of Brahmaputra might be due to high angle of internal friction resulting from aggregation of cohesion less soil particles.

Brahmaputra at erosion sites A, B and F is extremely braided. So, section average velocity at A, B and F are comparatively low than that of single channel in other location. However, the average velocities corresponding to a pre-monsoon discharge and peak monsoon discharge are two to hundred folds higher than that required for threshold movement of sediment (Table 6.3), as obtained from Hjulström diagram.

**Table 6.3** Particle size and corresponding velocities for threshold movement of sediments

| Location *B*<br>Pre-monsoon discharge = 15000 $m^3/s$<br>Monsoon peak discharge = 64619 $m^3/s$<br>Pre monsoon velocity = 0.82 m/s<br>Monsoon velocity = 1.01 m/s | | | | Location *F*<br>Pre-monsoon discharge = 15000 $m^3/s$<br>Monsoon peak discharge = 76303 $m^3/s$<br>Pre monsoon velocity = 0.80 m/s<br>Monsoon velocity = 0.86 m/s | | | |
|---|---|---|---|---|---|---|---|
| $d_{50}$ | *TV* | $d_{90}$ | *TV* | $d_{50}$ | *TV* | $d_{90}$ | *TV* |
| 0.06 | 0.07 | 0.16 | 0.40 | 0.01 | 0.009 | 0.03 | 0.03 |
| 0.06 | 0.07 | 0.24 | 0.50 | 0.02 | 0.02 | 0.07 | 0.09 |
| 0.06 | 0.07 | 1.40 | 3 | 0.02 | 0.02 | 0.10 | 0.35 |
| 0.11 | 0.35 | 1.10 | 2.7 | 0.02 | 0.02 | 0.06 | 0.07 |
| 0.62 | 0.80 | 1.10 | 2.7 | 0.02 | 0.02 | 0.12 | 0.38 |

*TV*: velocities for threshold movement of sediments

### *6.2.1 Role of geochemical properties of bank materials in erosion*

The first preliminary step was to see potential correlation between predictor variables (different geochemical properties of bank materials) and the outcome, i.e., erosion. Correlation matrices (Table 6.4) showed that pH, organic content, carbonate content, SAR had negative correlation with erosion and particle size ($d_{50}$ and $d_{90}$) had positive correlation with erosion.

**Table 6.4** Correlation matrices of different parameters of all samples

| | Erosion | pH | OC | CC | SAR | CEC | ESP | $d_{10}$ | $d_{50}$ | $d_{90}$ |
|---|---|---|---|---|---|---|---|---|---|---|
| Erosion | 1 | | | | | | | | | |
| pH | -.35** | 1 | | | | | | | | |
| OC | -.25* | .07 | 1 | | | | | | | |
| CC | -.27* | .05 | .51** | 1 | | | | | | |
| SAR | -.52** | .27* | .21 | .29* | 1 | | | | | |
| CEC | -.09 | .17 | .34** | .47** | .13 | 1 | | | | |
| ESP | .19 | -.48** | -.24* | -.38** | -.10 | -.56** | 1 | | | |
| $d_{10}$ | .25 | .21 | -.27* | -.22 | -.15 | -.15 | .13 | 1 | | |
| $d_{50}$ | .34** | .07 | -.22 | -.26* | -.21 | -.20 | .22 | .93** | 1 | |
| $d_{90}$ | .43** | .04 | -.21 | -.13 | -.22 | .01 | .10 | .63** | .68** | 1 |

** *correlation is significant at 0.01 level*
* *correlation is significant at 0.05 level*

Among different geochemical properties, negative correlation (0.48) was observed between pH and ESP. Increasing pH of soil will lead to decrease in ESP and decreasing ESP will lead to increase in CEC (Sumner, 1993; Rengasamy and Churchman, 1999; Quirk, 2001). OC had significant positive correlation with carbonate content (.51) and CEC (0.34) and negative correlation with particle size, i.e., $d_{50}$ and $d_{90}$. SAR had positive correlation with carbonate content (0.29). $d_{10}$, $d_{50}$, and $d_{90}$ are strongly correlated to each other. $d_{10}$ had significant positive correlation with $d_{50}$ (0.93) and $d_{90}$ (0.63). With increase in finer fraction of soil particles, there was increase of coarse particles in the study area. Presence of coarse particles was dominant in erosion sites, although a few sites had clay pockets.

### *6.2.2 Results of analysis of data using logistic regression in SPSS*

To evaluate contribution of selected geochemical properties to erosion event, binary logistic regression in SPSS was used with 'Erosion' ('Yes' or 'No') as dependent variable. Two sets of potential predictor variables were considered from correlation matrices:

i) OC, SAR, $d_{50}$

ii) OC, SAR, $d_{90}$

Outputs of the Binary logistic model for the first set of predictor variables (OC, SAR and $d_{50}$) are shown in Table 6.5.

**Table 6.5a** Variables in the equation (for the first set of variables)

| | B | S.E. | Wald | Sig. | Exp(B) |
|---|---|---|---|---|---|
| OC | -.049 | .192 | .065 | .799 | .952 |
| SAR | -1.344 | .461 | 8.515 | .004 | .261 |
| $d_{50}$ | .021 | .011 | 3.410 | .065 | 1.021 |
| Constant | 1.283 | .939 | 1.867 | .172 | 3.607 |

**Table 6.5b** Model Summary (for the first set of variables)

| -2 Log likelihood | Cox & Snell R Square | Nagelkerke R Square |
|---|---|---|
| 62.276[a] | .391 | .521 |

a. Estimation terminated at iteration number 6 because parameter estimates changed by less than .001.

Nagelkerke's $R^2$ of .521 (Table 6.5b) indicated a moderate relationship between prediction and grouping. The Wald criterion demonstrated that only SAR made a significant contribution to prediction (p = .004).

Outputs of the Binary logistic model for the second set of predictor variables (OC, SAR and $d_{90}$) are shown in Table 6.6.

**Table 6.6a** Variables in the equation (for the second set of variables)

| | B | S.E. | Wald | Sig. | Exp(B) |
|---|---|---|---|---|---|
| OC | -.073 | .199 | .135 | .713 | .929 |
| SAR | -1.321 | .485 | 7.405 | .007 | .267 |
| $d_{90}$ | .010 | .004 | 5.888 | .015 | 1.010 |
| Constant | .796 | .951 | .701 | .402 | 2.217 |

**Table 6.6b** Model Summary (for the second set of variables)

| -2 Log likelihood | Cox & Snell R Square | Nagelkerke R Square |
|---|---|---|
| 56.520[a] | .439 | .586 |

a. Estimation terminated at iteration number 6 because parameter estimates changed by less than .001.

Nagelkerke's $R^2$ of .586 (Table 6.6b) indicated a moderate relationship between prediction and grouping. The Wald criterion demonstrated that SAR and $d_{90}$ made a significant contribution to prediction (p = .007 and .015 respectively).

Higher value of Nagelkerke's $R^2$ of .586 for the second set of predictor variables (OC, SAR and $d_{90}$) suggested the variables more suitable for analysis. The odd ratio was .929 for an additional unit in OC, which suggested that for one unit increase of OC, the odds of erosion was lowered by a factor of 0.929. For one unit increase of OC, the odds of erosion was lowered by 7% (=.929×100 – 100).

The odd ratio was .267 for an additional unit in SAR, which suggested that for one unit increase of SAR, the odds of erosion was lowered by a factor of 0.267. For one unit increase of SAR, the odds of erosion was lowered by 73% (=.267×100 – 100). Brady and Weil (2002) suggested that SAR and erodibility were positively correlated for clay soils. The anomaly in our study might be due to abundance of sand content as clay size particles were responsible for expansion and dispersion at high SAR.

The odd ratio was 1.010 for an additional unit in $d_{90}$ values, which suggested that for one unit increase of $d_{90}$, the odds of erosion was increased by a factor of 1.010. For one unit increase of $d_{90}$, the odds of erosion was increased by 1% (=1.010×100 – 100). The resistance of a bank to fluvial erosion and mass failures tends to increase with increasing silt–clay content (Thorne and Tovey, 1981; Osman and Thorne, 1988), i.e., decrease in particle size. Thus, with increase in particle size, susceptibility of erosion increases. Now, considering geochemical properties of bank materials, probability of erosion (P) can be measured as follows (using equation 3 from Chapter 3):

$$P = \frac{e\{0.796 + (-.073)OC + (-1.321)SAR + (.010)d90\}}{1 + e\{0.796 + (-.073)OC + (-1.321)SAR + (.010)d90\}}$$

For example, in a site with soil OC= 2.4, SAR= 1.7 and $d_{90}$= 200µm, probability of bank erosion,

$$P = \frac{e\{0.796 + (-.073)2.4 + (-1.321)1.7 + (.010)200\}}{1 + e\{0.796 + (-.073)2.4 + (-1.321)1.7 + (.010)200\}}$$

$$= \frac{e\{0.796 - 0.175 - 2.246 + 2\}}{1 + e\{0.796 - 0.175 - 2.246 + 2\}}$$

$$= \frac{e\{0.375\}}{1 + e\{0.375\}}$$

$$= \frac{1.455}{2.455}$$

= 0.593

Hence, probability of erosion in a location with soil OC = 2.4, SAR = 1.7 and $d_{90}$ = 200µm is 59%.

Particle size and OC were the most important geochemical factors of river bank erosion in Brahmaputra, holding other parameters constant. Role of particle size (Wolman, 1959; Schumm, 1960; Walker et al., 1987; Dade et al., 1992) and OC (Wischmeier and Mannering, 1969; Robinson and Phillips, 2001; Brady and Weil, 2002; Morgan, 2005) in erosion was already documented. The above equation can be used for rapid assessment of vulnerability to bank erosion in alluvial rivers like Brahmaputra.

Chapter 7

# Braiding and land use and land cover of Brahmaputra River

This chapter discusses braiding (in 1973 and 2014) and land use and land cover (LULC) of Brahmaputra River in Assam (in 1994 and 2014) using remote sensing (ERDAS Imagine) and GIS (ArcGIS 10.1) techniques. Details of satellite images used in the study are mentioned in Chapter 3 (Materials and methods), Section 3.7, p. 51.

## 7.1 Braiding indices of Brahmaputra River

Several indices have been proposed to describe braiding intensity based on different characteristics, i.e., bar dimensions and frequency (e.g. Brice, 1960, 1964; Rust, 1978); the number of channels in the network (e.g. Howard et al., 1970, Ashmore, 1982); and the total channel length in a given river length (e.g. Mosley, 1981; Friend and Sinha, 1993). Sharma (2004) developed Plan Form Index (PFI) ratio for identifying the degree of braiding of highly braided river utilizing flow top width of mid-channels, overall width of the channel and number of braided channels. All indices consider one or two parameters from different parameters of a braided channel, e.g., length of bars, mid-channels, main-channel or center line and number of channels in a cross section. Braiding index (BI) of Brahmaputra River in Assam was estimated using formula suggested by Brice (1960, 1964) using information collected from topographic maps, prepared from aerial photographs of 1963—1975 and IRS satellite images of December 1996 (Sarma, 2004). In the present study, braiding indices of Brahmaputra in Assam during 1973 and 2014 is studied by a few widely used approaches (Table 7.1).

**Table 7.1** Different approaches for calculation of braiding indices

| Sl. no. | Braiding index (BI) or Braiding Parameter (B) | Reference |
|---|---|---|
| 1 | BI = 2 (Sum of length of all the islands or bars in a reach) / Center line reach length | Brice (1964) |
| 2 | BI = Average number of channels in several cross-valley transects | Howard et al. (1970) |
| 3 | B = Sum of the braid lengths between channel thalweg divergences and confluences / Mean of the meander wavelength in a reach of the channel belt | Rust (1978) |
| 4 | BI = Total length of the channels / Length of main channel | Mosley (1981) |
| 5 | BI = Average number of active channels per cross-valley transect | Ashmore (1982) |
| 6 | B = Sum of the mid-channel lengths of all the segments of primary channels in a reach / Mid-channel length of the widest channel through the reach | Friend & Sinha (1993) |
| 7 | Plan Form Index (PFI) = (T/B) ×100/N where, T = flow top width; B = overall width of the channel; N = number of braided channel | Sharma (2004) |

Different approaches for measurement of braiding indices can be grouped in to two types: (i) counting the number of active channels or braid bars per transect across the channel belt, and (ii) calculating the ratio of the sum of channel lengths in a reach to a measure of reach length (the ratio being called the total sinuosity). The first approach is more desirable since it is related to mode of the river, or the average number of sinuous channels that occur laterally adjacent to each other and the total sinuosity is a combined measure of channel segment sinuosity and degree of braiding (Bridge, 2009).

The lengths of the center line, main channel, sand bars and mid-channels in the sixteen reaches, mentioned in Section 3.7, p. 51, needed for calculation of braiding parameters were obtained for two different years, i.e., 1973 and 2014 (Figure 7.1 and 7.2, Table 7.2) from Landsat images using GIS tools. Main stem of Brahmaputra was considered and riverine island *Majuli* was not included in the study.

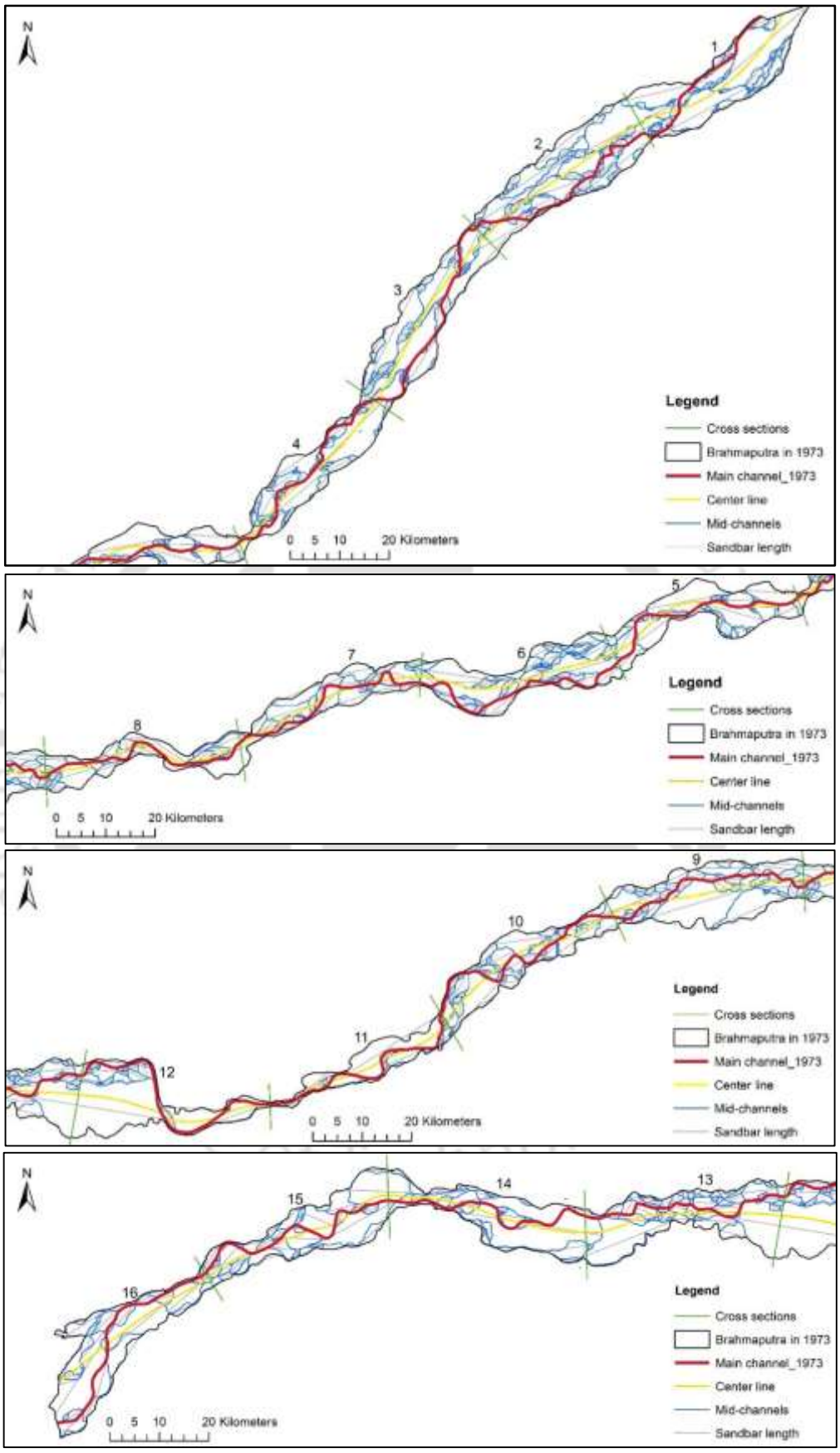


**Figure 7.1** Main channel, center line, mid-channels and sandbar length in different reaches in 1973

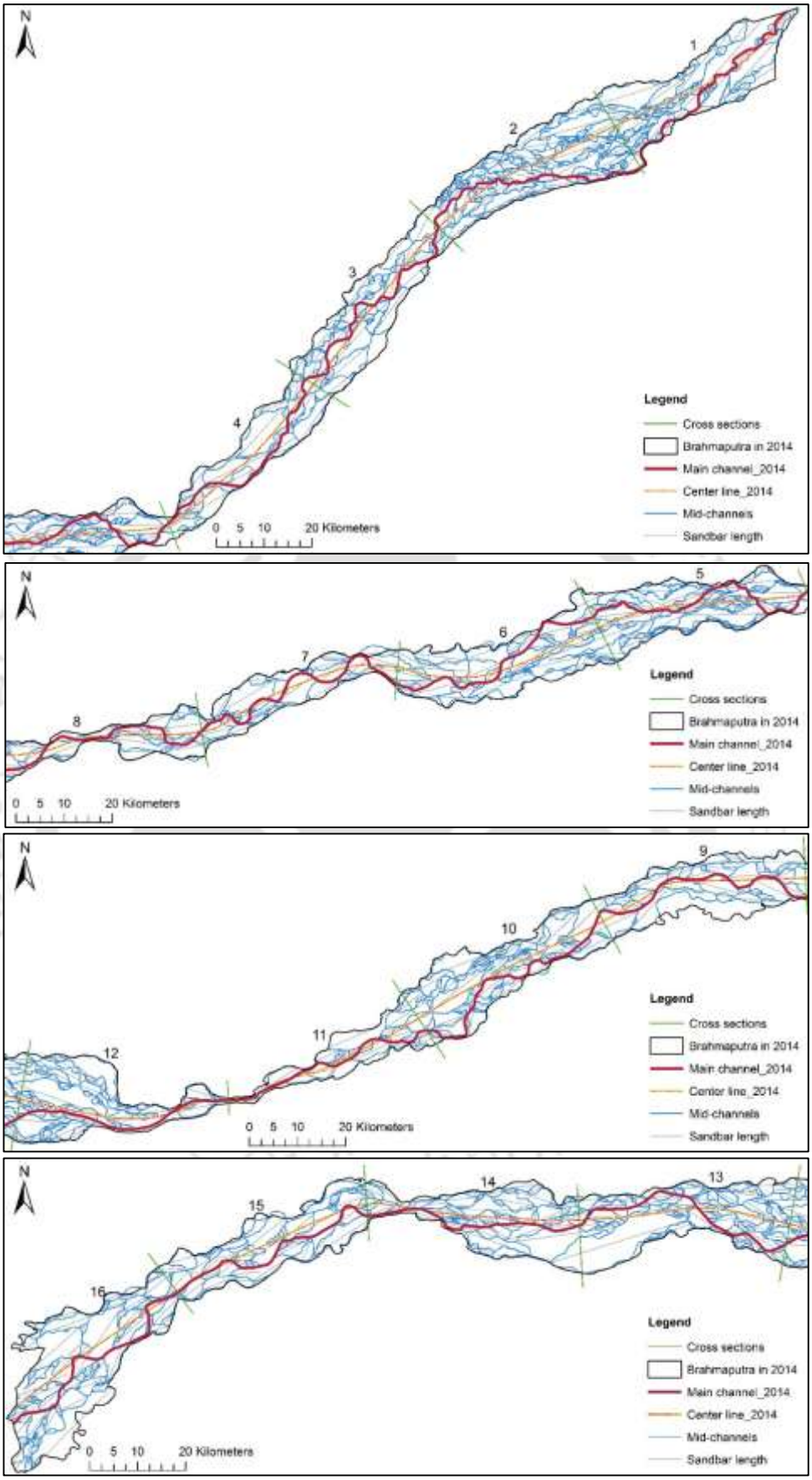


**Figure 7.2** Main channel, center line, mid-channels and sandbar length in different reaches in 2014

**Table 7.2** Length of the center line, the widest channel, mid-channels and sandbars

| Reach no. | Length in km | | | | | | | |
|---|---|---|---|---|---|---|---|---|
| | Center line (*C*) | | Widest (main) channel (*M*) | | All mid-channels (*s*) | | Sandbars (*b*) | |
| | **1973** | **2014** | **1973** | **2014** | **1973** | **2014** | **1973** | **2014** |
| 1 | 33.4 | 40 | 35 | 52 | 314 | 377 | 175 | 272 |
| 2 | 40.5 | 40 | 46 | 47 | 406 | 616 | 223 | 391 |
| 3 | 40 | 40 | 46.5 | 50 | 294.5 | 358 | 183 | 210 |
| 4 | 40.3 | 40 | 45.4 | 46 | 285.4 | 248 | 139 | 150 |
| 5 | 41 | 40 | 45 | 50 | 247 | 461 | 109 | 295 |
| 6 | 40.3 | 40 | 49.3 | 47 | 323.3 | 382 | 152 | 254 |
| 7 | 39.6 | 40 | 45.3 | 52 | 233.3 | 255 | 104 | 133 |
| 8 | 41.9 | 40 | 46.1 | 47 | 202.1 | 245 | 78 | 129 |
| 9 | 39.6 | 40 | 43.5 | 47 | 315.5 | 301 | 154 | 173 |
| 10 | 40.9 | 40 | 49 | 50 | 279 | 455 | 148 | 257 |
| 11 | 40.6 | 40 | 47.7 | 43 | 153.7 | 168 | 58 | 91 |
| 12 | 39.9 | 40 | 52.2 | 43 | 181.2 | 412 | 83 | 240 |
| 13 | 40.1 | 40 | 45.2 | 47 | 328.2 | 486 | 159 | 306 |
| 14 | 40.7 | 40 | 45.9 | 42 | 259.9 | 390 | 112 | 261 |
| 15 | 40.7 | 40 | 47.8 | 46 | 286.8 | 374 | 137 | 192 |
| 16 | 36.6 | 38 | 48.1 | 48 | 237.1 | 454 | 143 | 275 |
| Whole River | 636 | 638 | 738 | 757 | 4347 | 5225 | 2157 | 3629 |

It is observed that, none of the methods to determine braiding index used number of mid-channel bar, which is a key factor of a braided channel. Hence, a new braiding index has been introduced incorporating fraction of area covered by sandbars, number of mid-channel bars and maximum width of the reach (Table 7.3 and 7.4) using the formula:

$$\text{Braiding, } B = X \times N \times W/L$$

where, $X$: fraction of area covered by bars

$N$: number of mid-channel bars

$L$: length of reach

$W$: maximum width of the reach

In the formulation of the method, following points are considered:

(i) River or reach with more fraction of area by bars has more braiding value.

(ii) In case of same fraction of area by bars, number of mid-channel bars will influence braiding value.

(iii) Braiding of rivers or reaches with same fraction of area by bars and same number of mid-channel bars will differ by maximum width.

(iv) Length is used in denominator to get a dimensionless braiding index.

**Table 7.3** Fraction of area covered by bars, number of mid-channel bars and maximum width and length of reaches in 1973

| Reach no | Total area of the reach or river in km$^2$ ($R$) | Area of bars ($B$) | Fraction of area covered by bars ($X = R/B$) | No of mid-channel bars ($N$) | Max. width in km ($W$) | Reach length in km ($L$) | Braiding, $B = X \times N \times W/L$ |
|---|---|---|---|---|---|---|---|
| 1 | 365.4 | 281.7 | 0.8 | 77 | 11.4 | 33.4 | 20.3 |
| 2 | 411.0 | 322.0 | 0.8 | 92 | 13.1 | 40.5 | 23.3 |
| 3 | 349.3 | 265.2 | 0.8 | 58 | 9.7 | 40 | 10.7 |
| 4 | 271.9 | 187.2 | 0.7 | 66 | 9.5 | 40.3 | 10.7 |
| 5 | 280.6 | 156.9 | 0.6 | 48 | 9.5 | 41 | 6.2 |
| 6 | 317.4 | 216.0 | 0.7 | 79 | 10.8 | 40.3 | 14.4 |
| 7 | 222.6 | 118.7 | 0.5 | 38 | 7.9 | 39.6 | 4.0 |
| 8 | 206.3 | 100.7 | 0.5 | 37 | 7.0 | 41.9 | 3.0 |
| 9 | 370.2 | 251.9 | 0.7 | 61 | 13.3 | 39.6 | 13.9 |
| 10 | 270.2 | 167.1 | 0.6 | 62 | 9.5 | 40.9 | 8.9 |
| 11 | 159.0 | 101.3 | 0.6 | 22 | 6.6 | 40.6 | 2.3 |
| 12 | 306.1 | 225.9 | 0.7 | 25 | 15.8 | 39.9 | 7.3 |
| 13 | 381.0 | 270.0 | 0.7 | 68 | 12.4 | 40.1 | 14.9 |
| 14 | 320.3 | 235.3 | 0.7 | 48 | 11.1 | 40.7 | 9.6 |
| 15 | 330.1 | 246.3 | 0.7 | 51 | 11.5 | 40.7 | 10.8 |
| 16 | 344.0 | 251.6 | 0.7 | 46 | 11.6 | 36.6 | 10.6 |
| Whole river | 4905.6 | 3397.7 | 0.7 | 878 | 15.8 | 41.9 | 10.7 |

**Table 7.4** Fraction of area covered by bars, number of mid-channel bars and maximum width and length of reaches in 2014

| Reach no | Total area of the reach or river in km$^2$ ($R$) | Area of bars ($B$) | Fraction of area covered by bars ($X = R/B$) | No of mid-channel bars ($N$) | Max. width in km ($W$) | Reach length in km ($L$) | Braiding, $B = X \times N \times W/L$ |
|---|---|---|---|---|---|---|---|
| 1 | 418.2 | 316.6 | 0.8 | 203 | 12.6 | 40 | 48.6 |
| 2 | 480.3 | 357.9 | 0.7 | 246 | 17.6 | 40 | 80.7 |
| 3 | 379.4 | 286.4 | 0.8 | 104 | 11.0 | 40 | 21.5 |
| 4 | 302.4 | 230.2 | 0.8 | 69 | 10.7 | 40 | 14.0 |
| 5 | 396.6 | 286.3 | 0.7 | 133 | 12.1 | 40 | 29.1 |
| 6 | 440.0 | 334.1 | 0.8 | 74 | 11.9 | 40 | 16.7 |
| 7 | 264.9 | 185.3 | 0.7 | 56 | 8.5 | 40 | 8.3 |
| 8 | 243.7 | 154.2 | 0.6 | 36 | 11.0 | 40 | 6.3 |
| 9 | 401.9 | 306.4 | 0.8 | 62 | 13.8 | 40 | 16.3 |
| 10 | 430.6 | 296.6 | 0.7 | 124 | 15.9 | 40 | 34.0 |

| Reach no | Total area of the reach or river in km$^2$ (*R*) | Area of bars (*B*) | Fraction of area covered by bars (*X* = *R/B*) | No of mid-channel bars (*N*) | Max. width in km (*W*) | Reach length in km (*L*) | Braiding, *B* = *X*×*N*×*W*/*L* |
|---|---|---|---|---|---|---|---|
| 11 | 205.4 | 121.9 | 0.6 | 37 | 8.6 | 40 | 4.7 |
| 12 | 389.9 | 254.3 | 0.7 | 48 | 17.6 | 40 | 13.8 |
| 13 | 500.3 | 365.5 | 0.7 | 114 | 14.6 | 40 | 30.4 |
| 14 | 411.3 | 281.8 | 0.7 | 110 | 16.0 | 40 | 30.1 |
| 15 | 403.3 | 250.8 | 0.6 | 72 | 11.7 | 40 | 13.1 |
| 16 | 590.1 | 372.4 | 0.6 | 148 | 20.5 | 38 | 50.3 |
| Whole river | 6258.3 | 4400.4 | 0.7 | 1636 | 20.5 | 638 | 36.9 |

Braiding values obtained for different reaches of Brahmaputra are shown in Table 7.5 and Figure 7.3. In spite of variations of braiding values in different approaches, almost similar trend of braiding values has been observed in all the reaches. Lower values of PFI are observed in braided reaches due to the fact that PFI value and braiding are inversely proportional to each other. Ten reaches, i.e., reach no 1, 2, 3, 4, 6, 9, 10, 13, 15 and 16, had greater braiding values in 1973 than the average value for the entire Brahmaputra River in Assam. Similarly, during 2014, nine reaches, i.e., reach no 1, 2, 5, 6, 10, 12, 13, 15 and 16, were observed to have greater braiding values than the average value for the river in Assam. Higher braiding in those reaches were due to greater channel width with

i) more distributaries, i.e., increased mid-channel lengths, e.g., in reach no 2, 5, 6, 12, 13, 14 and 16 in 1973 and reach no 1, 2, 3, 4, 6, 9, 13 and 15 in 2014.
ii) more mid-channel bars, i.e., increased sandbar lengths, e.g., reach no 1, 2, 3, 4, 6, 9,10, 13, 15 and 16 in 1973 and reach no 1, 2, 5, 6, 10, 12, 13, 14 and 16 in 2014.

Low braiding in three reaches, i.e., reach no 7, 8 and 11 was due to comparatively narrower channel width with lesser number of distributaries and mid-channel bars. The values of the new braiding index suggested in the present study revealed higher braiding (than average) in reach no 1, 2, 3, 4, 6, 13, 15 and 16 in 1973, and only in reach no 1, 2 and 16 in 2014.

**Table 7.5** Braiding parameters of Brahmaputra River from different approaches

| Reach | Brice (1964) *BI = 2 b/C* | | Howard et al. (1970) *BI* = Average number of channels | | Maximum number of channels | | Rust (1978) *B = b/M* | | Mosley (1981) *B = s/ M* | | Friend & Sinha (1993) *B = (s-M)/M* | | Sharma (2004) *PFI = (T/B*) ×100/N* | | Present work ***B = X×N×W/L*** | |
|---|---|---|---|---|---|---|---|---|---|---|---|---|---|---|---|---|
| | **1973** | **2014** | **1973** | **2014** | **1973** | **2014** | **1973** | **2014** | **1973** | **2014** | **1973** | **2014** | **1973** | **2014** | **1973** | **2014** |
| 1 | 10.5 | 13.6 | 7 | 8 | 8 | 11 | 5 | 5.2 | 9 | 7.3 | 8 | 6.3 | 4.7 | 2.6 | 20.3 | 48.6 |
| 2 | 11 | 19.6 | 9 | 11 | 10 | 16 | 4.8 | 8.3 | 8.8 | 13.1 | 7.8 | 12.1 | 2.8 | 2.6 | 23.3 | 80.7 |
| 3 | 9.2 | 10.5 | 7 | 7 | 8 | 8 | 3.9 | 4.2 | 6.3 | 7.2 | 5.3 | 6.2 | 4.3 | 4.3 | 10.7 | 21.5 |
| 4 | 6.9 | 7.5 | 5 | 5 | 5 | 6 | 3.1 | 3.3 | 6.3 | 5.4 | 5.3 | 4.4 | 8.1 | 6.3 | 10.7 | 14.0 |
| 5 | 5.4 | 14.8 | 4 | 11 | 5 | 14 | 2.4 | 5.9 | 5.5 | 9.2 | 4.5 | 8.2 | 9.6 | 6.7 | 6.2 | 29.1 |
| 6 | 7.6 | 12.7 | 6 | 9 | 7 | 11 | 3.1 | 5.4 | 6.6 | 8.1 | 5.6 | 7.1 | 4.6 | 4 | 14.4 | 16.7 |
| 7 | 5.3 | 6.7 | 4 | 4 | 5 | 5 | 2.3 | 2.6 | 5.2 | 4.9 | 4.2 | 3.9 | 8.5 | 4.9 | 4.0 | 8.3 |
| 8 | 3.7 | 6.5 | 4 | 4 | 6 | 7 | 1.7 | 2.7 | 4.4 | 5.2 | 3.4 | 4.2 | 24.5 | 7.7 | 3.0 | 6.3 |
| 9 | 7.8 | 8.7 | 6 | 6 | 7 | 7 | 3.5 | 3.7 | 7.3 | 6.4 | 6.3 | 5.4 | 7.5 | 4.8 | 13.9 | 16.3 |
| 10 | 7.2 | 12.9 | 5 | 7 | 6 | 9 | 3 | 5.1 | 5.7 | 9.1 | 4.7 | 8.1 | 12.7 | 2.8 | 8.9 | 34.0 |
| 11 | 2.9 | 4.6 | 3 | 3 | 4 | 7 | 1.2 | 2.1 | 3.2 | 3.9 | 2.2 | 2.9 | 25.6 | 18.6 | 2.3 | 4.7 |
| 12 | 4.2 | 12 | 3 | 8 | 5 | 16 | 1.6 | 5.6 | 3.5 | 9.6 | 2.5 | 8.6 | 6.8 | 6.6 | 7.3 | 13.8 |
| 13 | 7.9 | 15.3 | 5 | 11 | 6 | 13 | 3.5 | 6.5 | 7.3 | 10.3 | 6.3 | 9.3 | 4.8 | 3.9 | 14.9 | 30.4 |
| 14 | 5.5 | 13.1 | 5 | 6 | 6 | 8 | 2.4 | 6.2 | 5.7 | 9.3 | 4.7 | 8.3 | 11 | 10 | 9.6 | 30.1 |
| 15 | 6.7 | 9.6 | 5 | 6 | 6 | 9 | 2.9 | 4.2 | 6 | 8.1 | 5 | 7.1 | 5 | 8 | 10.8 | 13.1 |
| 16 | 7.8 | 14.5 | 4 | 7 | 6 | 10 | 2.9 | 5.7 | 4.9 | 9.5 | 3.9 | 8.5 | 8 | 3.3 | 10.6 | 50.3 |
| River | 6.8 | 11.3 | 5 | 7 | 10 | 16 | 2.9 | 4.8 | 5.9 | 7.9 | 4.9 | 6.9 | 9.3 | 6.1 | 10.6 | 36.9 |

*b*: length of sandbars, *C*: length of center line, *M*: length of main (widest) channel, *s*: length of mid-channels
*T*: flow top width, *B**: overall width of the channel, *N*: number of braided channels
*X*: fraction of area covered by bars
*N*: no of mid-channel bars
*L*: length of reach
*W*: maximum width of the reach

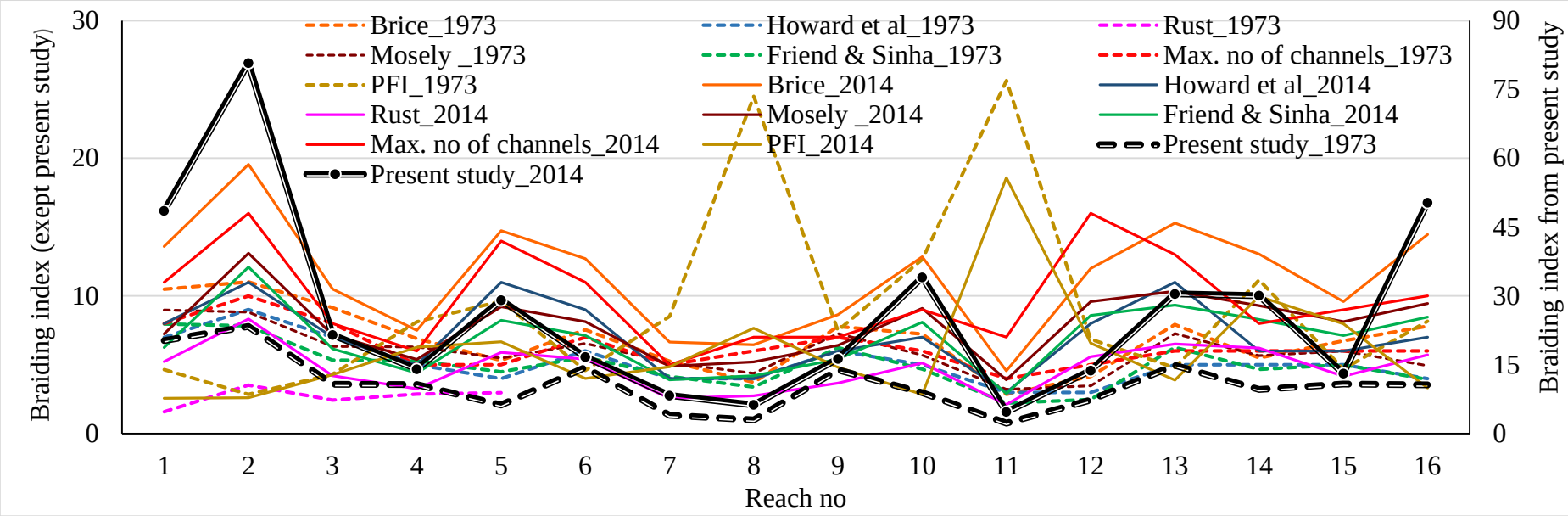


**Figure 7.3** Braiding index of Brahmaputra River at different reaches calculated by different approaches

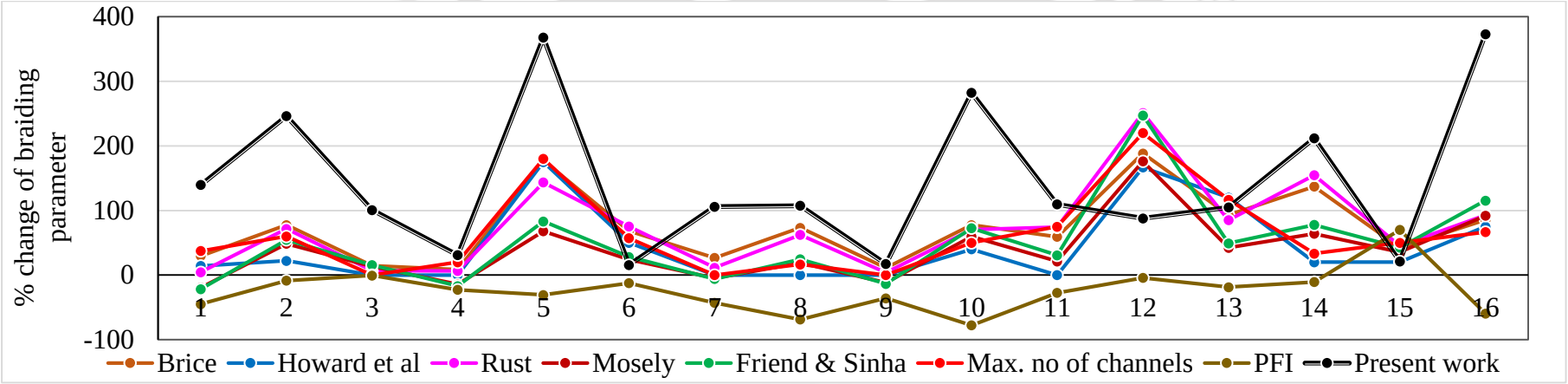


**Figure 7.4** % change of braiding parameters of Brahmaputra River during 1973 – 2014 at different reaches

The newly suggested index has showed comparable result with other approaches. Moreover, the new parameter has very good correlation (0.97) with number of sandbars. The new index also showed relatively better correlation with sinuosity than braiding values obtained from other approaches (Table 7.6).

**Table 7.6** Correlation matrix of different braiding parameters

| | No of sandbars | Sinuosity | Brice | Howard | Rust | Mosley | Friend & Sinha | Sharma | Present work |
|---|---|---|---|---|---|---|---|---|---|
| No of sandbars | 1 | | | | | | | | |
| Sinuosity | 0.36 | 1 | | | | | | | |
| Brice | 0.87 | 0.12 | 1 | | | | | | |
| Howard | 0.74 | 0.12 | 0.91 | 1 | | | | | |
| Rust | 0.82 | -0.01 | 0.97 | 0.90 | 1 | | | | |
| Mosley | 0.77 | -0.12 | 0.94 | 0.88 | 0.96 | 1 | | | |
| Friend & Sinha | 0.77 | -0.12 | 0.94 | 0.88 | 0.96 | 1 | 1 | | |
| Sharma | -0.50 | -0.23 | -0.62 | -0.56 | -0.59 | -0.58 | -0.59 | 1 | |
| Present work | 0.97 | 0.25 | 0.88 | 0.72 | 0.84 | 0.81 | 0.81 | -0.50 | 1 |

With reference to braiding values for different reaches from different approaches, following threshold values can be provided from the new braiding index ($B$) for a broad range of classification of braiding phenomenon:

Highly braided: $B > 30$

Moderately braided: $5 < B < 30$

Low braided: $B < 5$

On the basis of this classification, braiding pattern of different reaches of Brahmaputra in Assam during 1973 and 2014 can be summarized (Table 7.7).

**Table 7.7** Braiding pattern of different reaches of Brahmaputra in Assam

| Braiding range | Reaches | | Number of reaches | |
|---|---|---|---|---|
| | 1973 | 2014 | 1973 | 2014 |
| Highly braided | NIL | 1,2,10,13,14,16 | 0 | 6 |
| Moderately braided | 1,2,3,4,5,6,9,10, 12,13,14,15,16 | 3,4,5,6,7,8,9,12,15 | 13 | 9 |
| Low braided | 7, 8, 11 | 11 | 3 | 1 |

The reaches which were only low and moderately braided in 1973, became moderately braided and highly braided during 40 years' period (1973 – 2014). Braiding value was increased by more than 50% in reach no 2, 5, 6, 8, 10, 11, 12, 13, 14 & 15 during 1973 – 2014. Even, more than 100% increase of braiding was observed in the reach no 5, 12 and 14 (Figure 7.4). Increase of braiding was due to development of more sandbars and distributaries resulting increased mid-channel lengths and sandbar lengths. Area of Brahmaputra River in Assam has been increased from 4906 $km^2$ in 1973 to 6258 $km^2$ in 2014. Widening of the river has resulted in loss of huge land area by bank erosion in many locations. But, increased area of Brahmaputra in Assam is not linked solely to river bank erosion. Increase in area (28%) of Brahmaputra during 1973 – 2014 was also due to bifurcation of streams without loss of land in addition to river bank erosion.

## 7.2 Land use and land cover of Brahmaputra River

Changed braiding from altered channel course has resulted in different land use and land cover of the river including the floodplains. The dynamic nature of Brahmaputra and its tributaries modifies the floodplains frequently, at times to an undesired magnitude (Das et al., 2012; Goswami et al., 1999; Kotoky et al., 2005; Lahiri and Sinha, 2012; Sarma and Phukan, 2004). Associated changes in LULC (linking it with river dynamics) are rarely documented in quantitative terms (Kotoky et al., 2012; Mondal et al., 2013) which are essential preconditions for the formulation of floodplain management programme. Land use and land cover change analysis is helpful in understanding the current environmental status of an area and ongoing changes (Raj and Azeez, 2010). LULC change has emerged as one of the key independent themes in the global change, climate change, earth systems, and sustainability research programs (Gutman et al., 2004). Land use and land cover analysis for 1994 – 2014 was carried out by catgorizing the Landsat images into different classes using unsupervised classification in image processing software. The river during post monsoon months was categorized into four types: river/ water, sandbar, vegetation (including natural grass land) and agriculture including human settlement (Figure 7.5, Table 7.8 – 7.9).

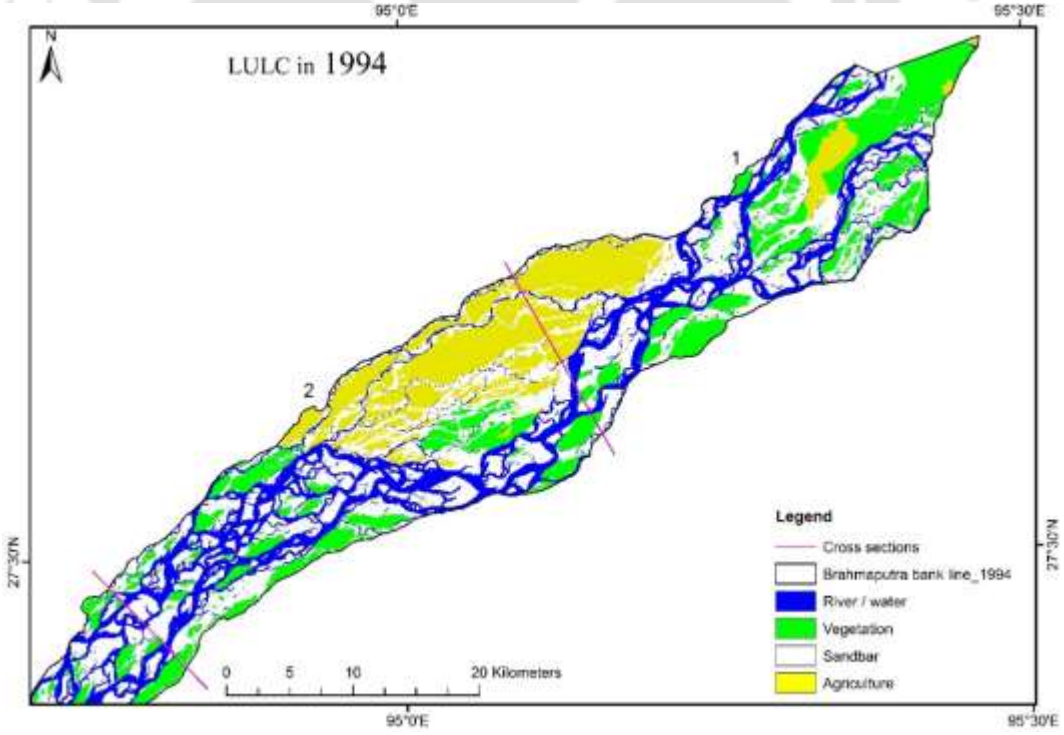

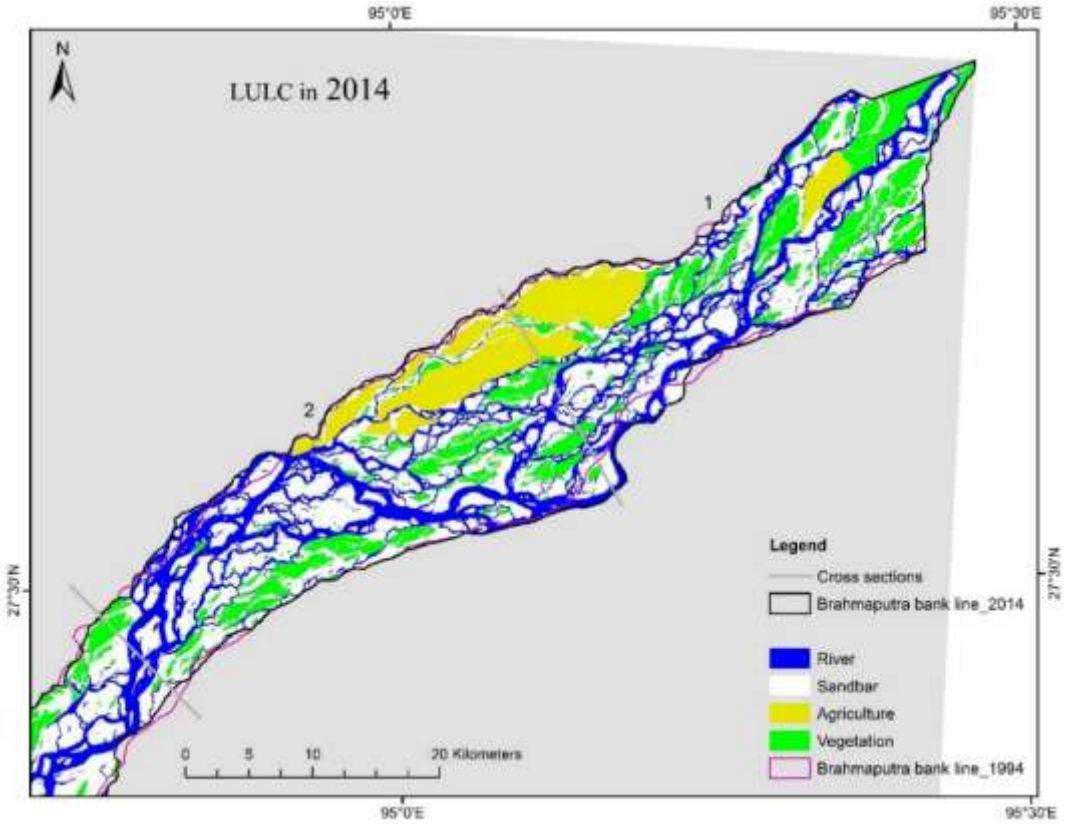


**Figure 7.5a** LULC of Brahmaputra in reach no 1 and 2 during post-monsoon months of 1994 and 2014

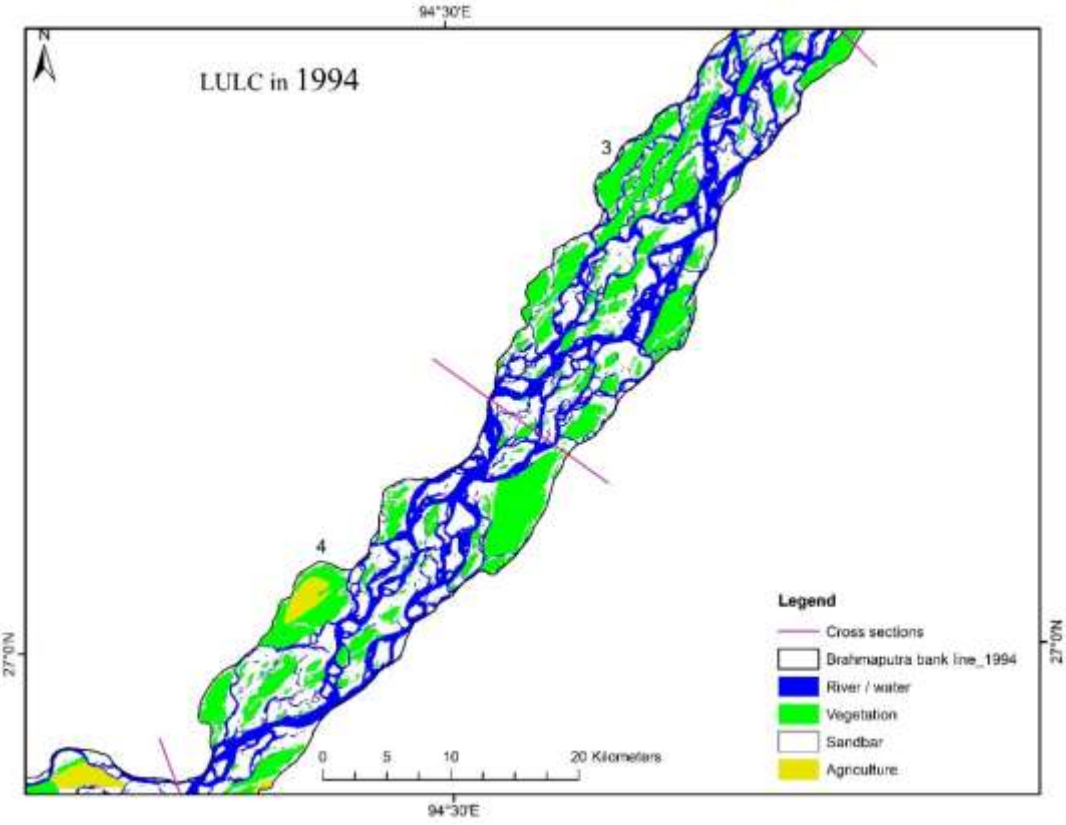

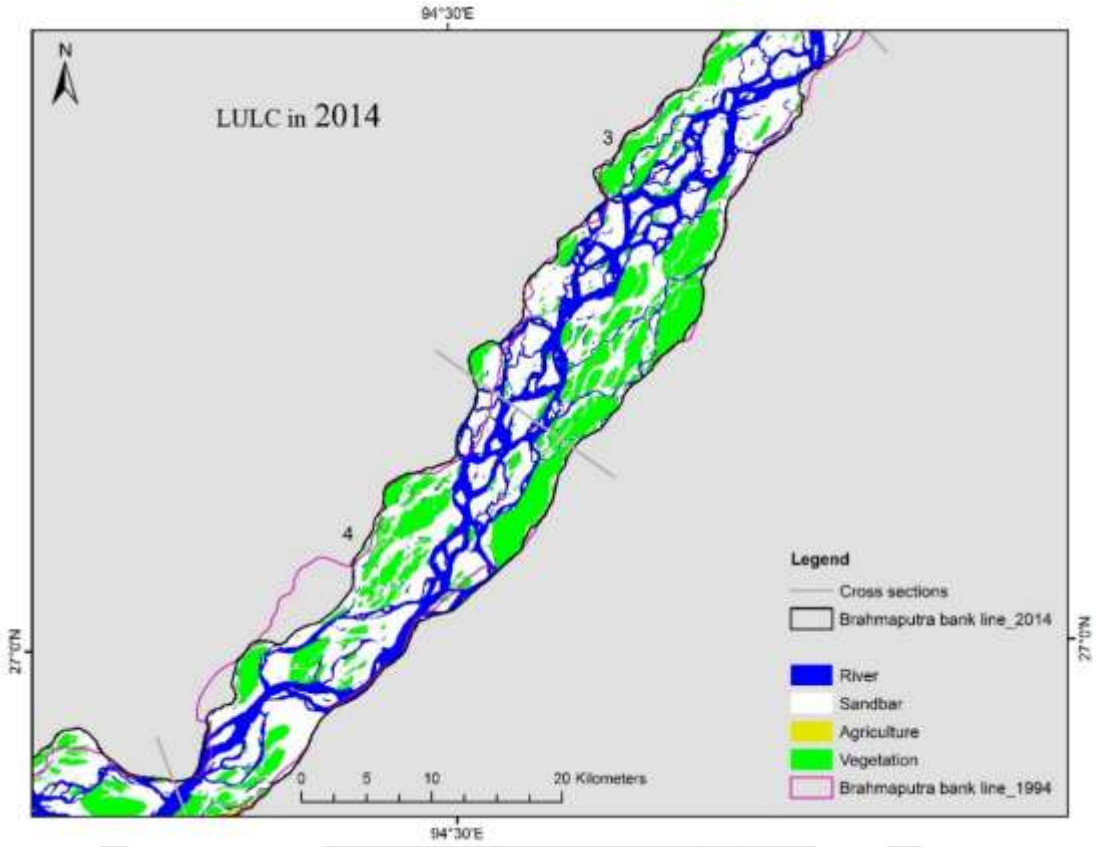


**Figure 7.5b** LULC of Brahmaputra in reach no 3 and 4 during post-monsoon months of 1994 and 2014

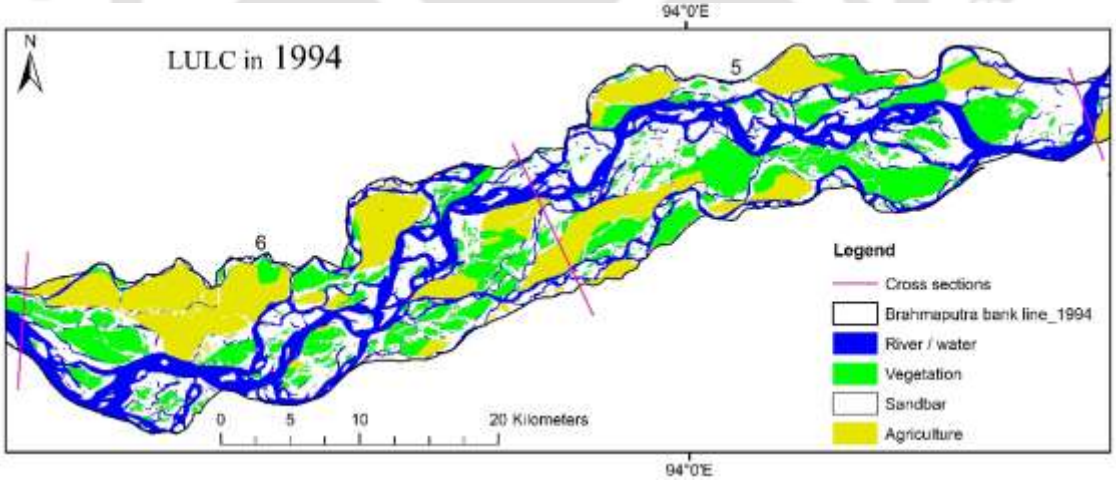

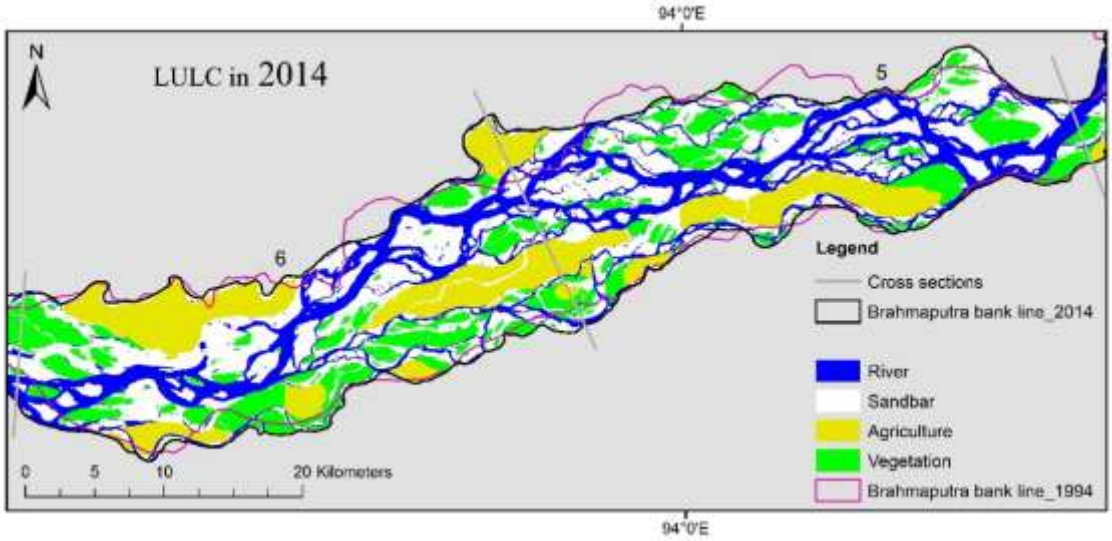


**Figure 7.5c** LULC of Brahmaputra in reach no 5 and 6 during post-monsoon months of 1994 and 2014

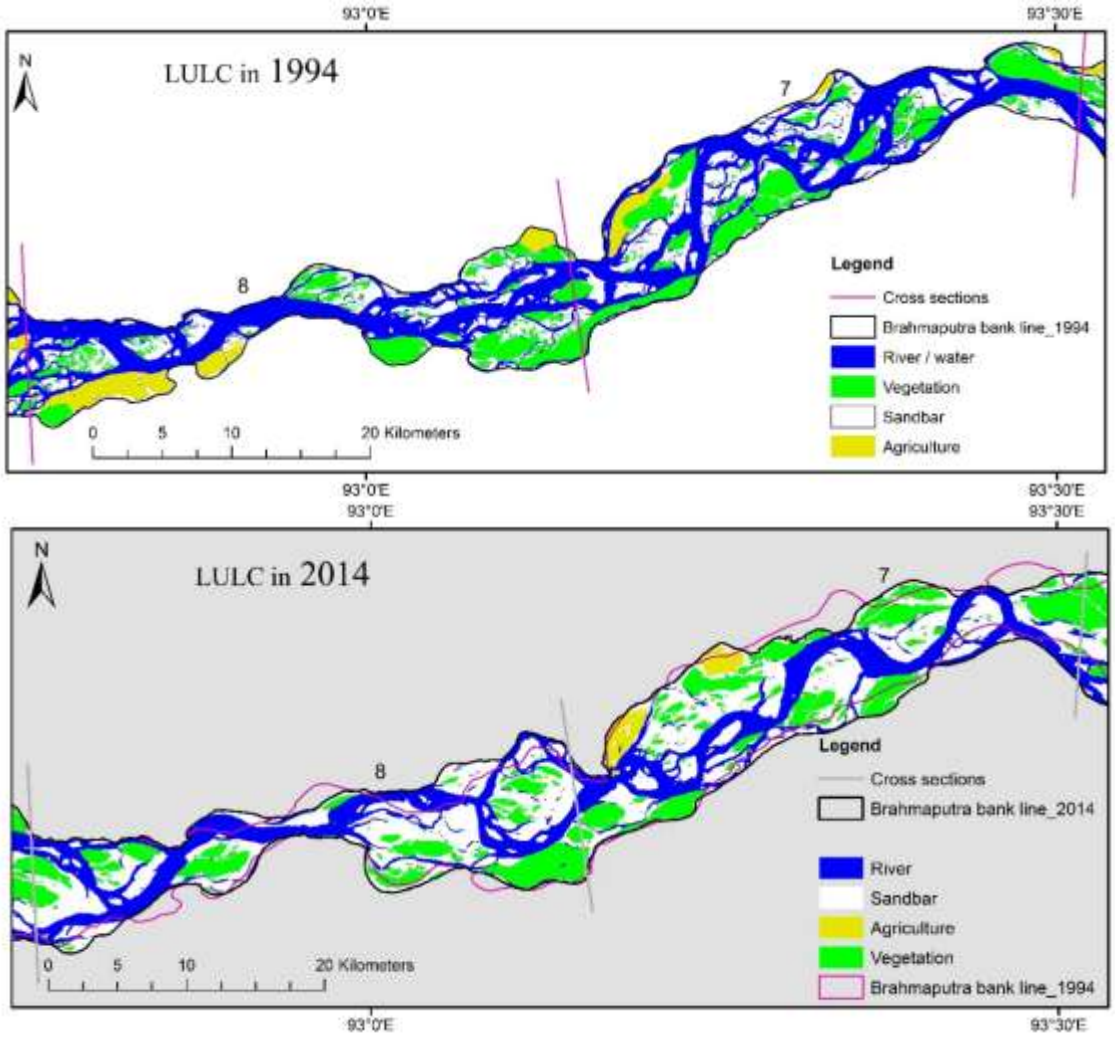


**Figure 7.5d** LULC of Brahmaputra in reach no 7 and 8 during post-monsoon months of 1994 and 2014

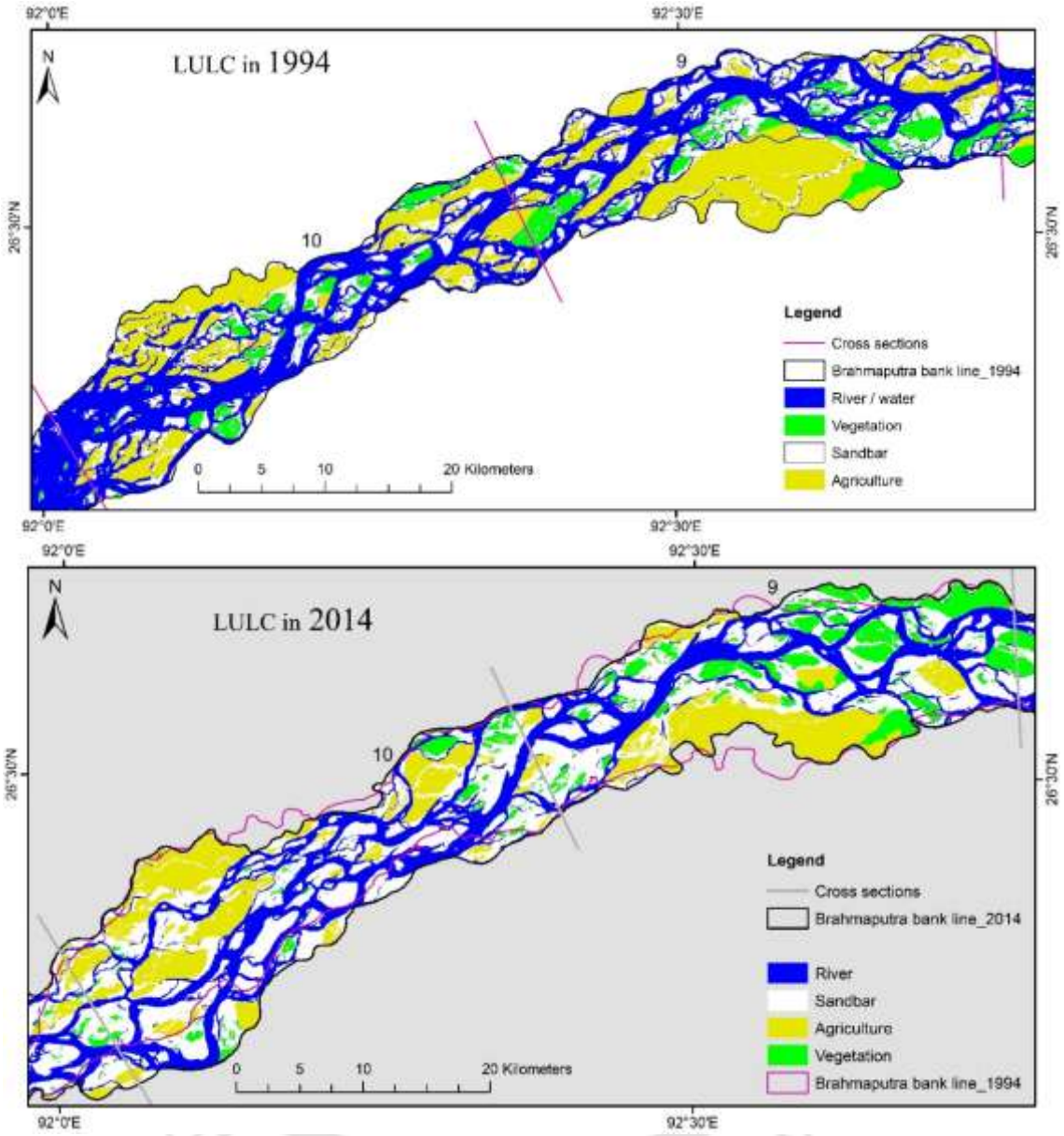


**Figure 7.5e** LULC of Brahmaputra in reach no 9 and 10 during post-monsoon months of 1994 and 2014

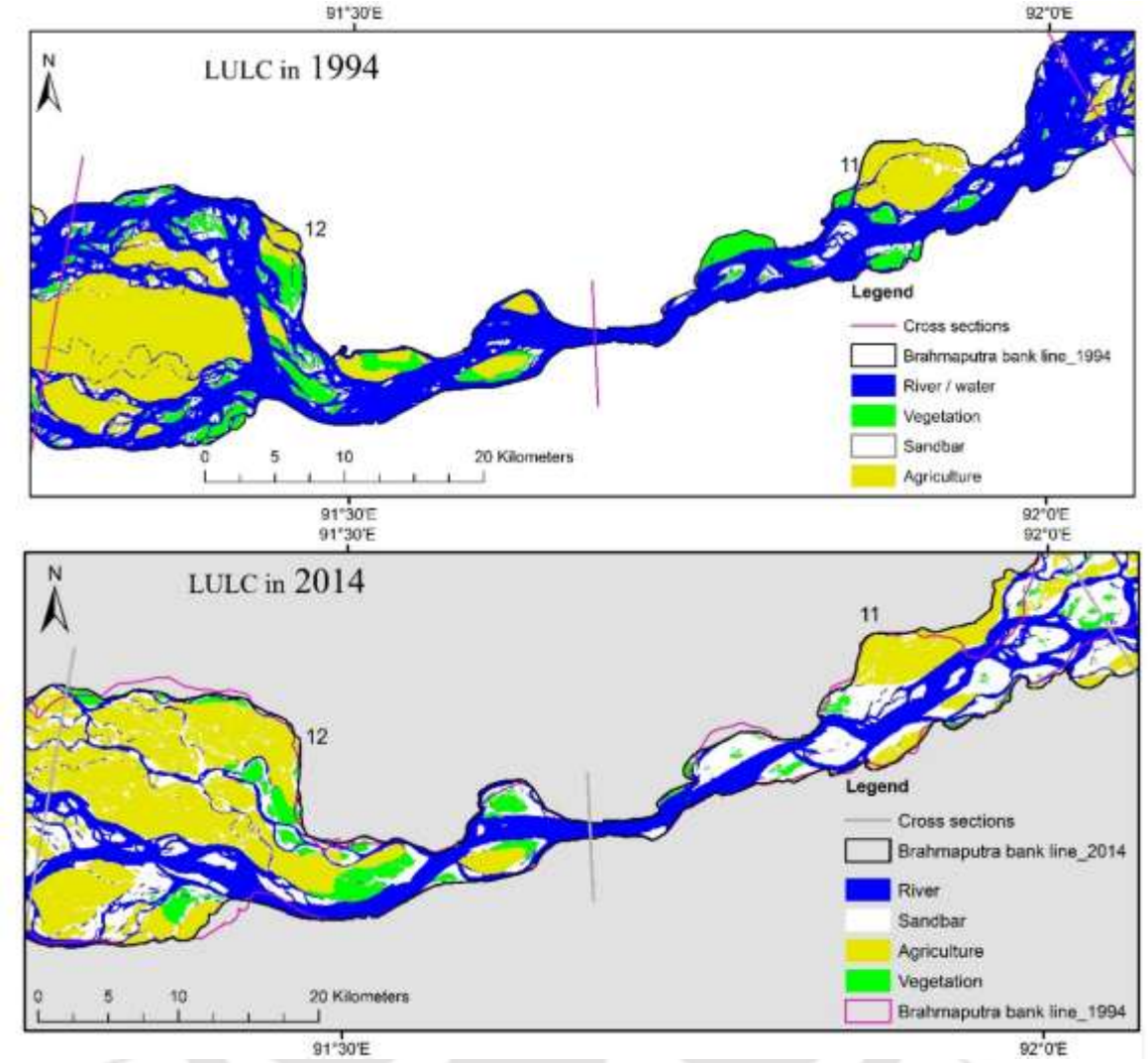


**Figure 7.5f** LULC of Brahmaputra in reach no 11 and 12 during post-monsoon months of 1994 and 2014

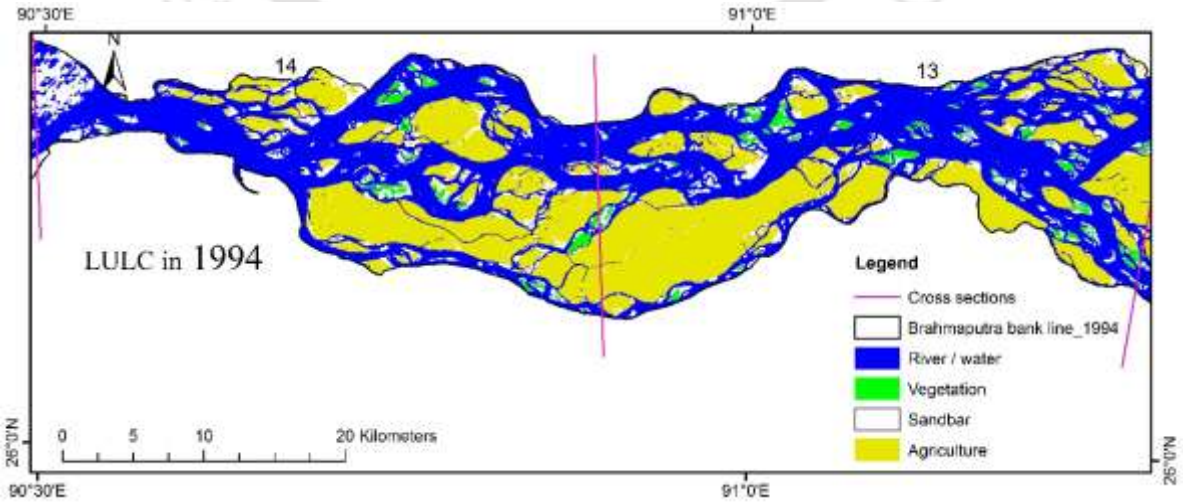

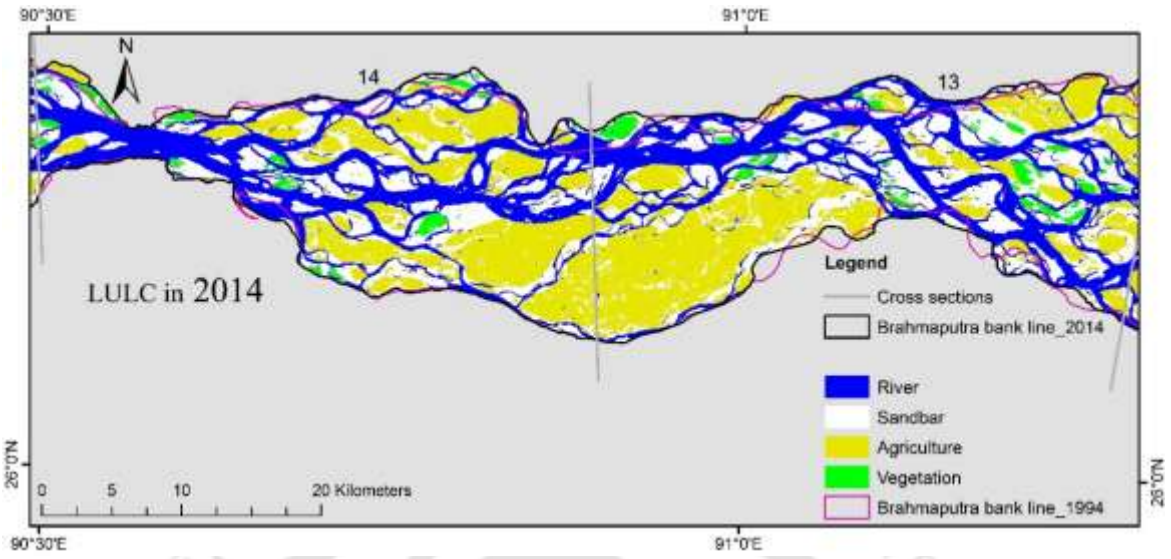


**Figure 7.5g** LULC of Brahmaputra in reach no 13 and 14 during post-monsoon months of 1994 and 2014

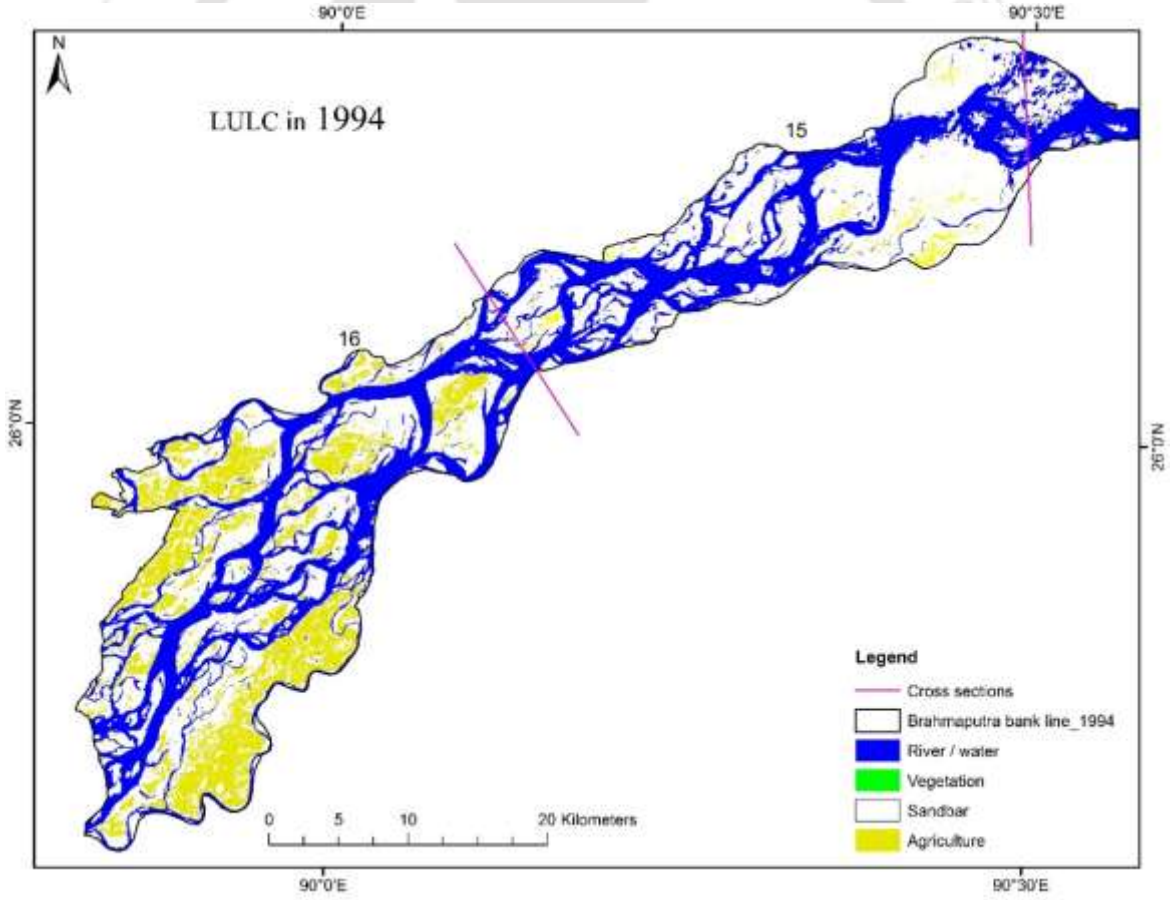

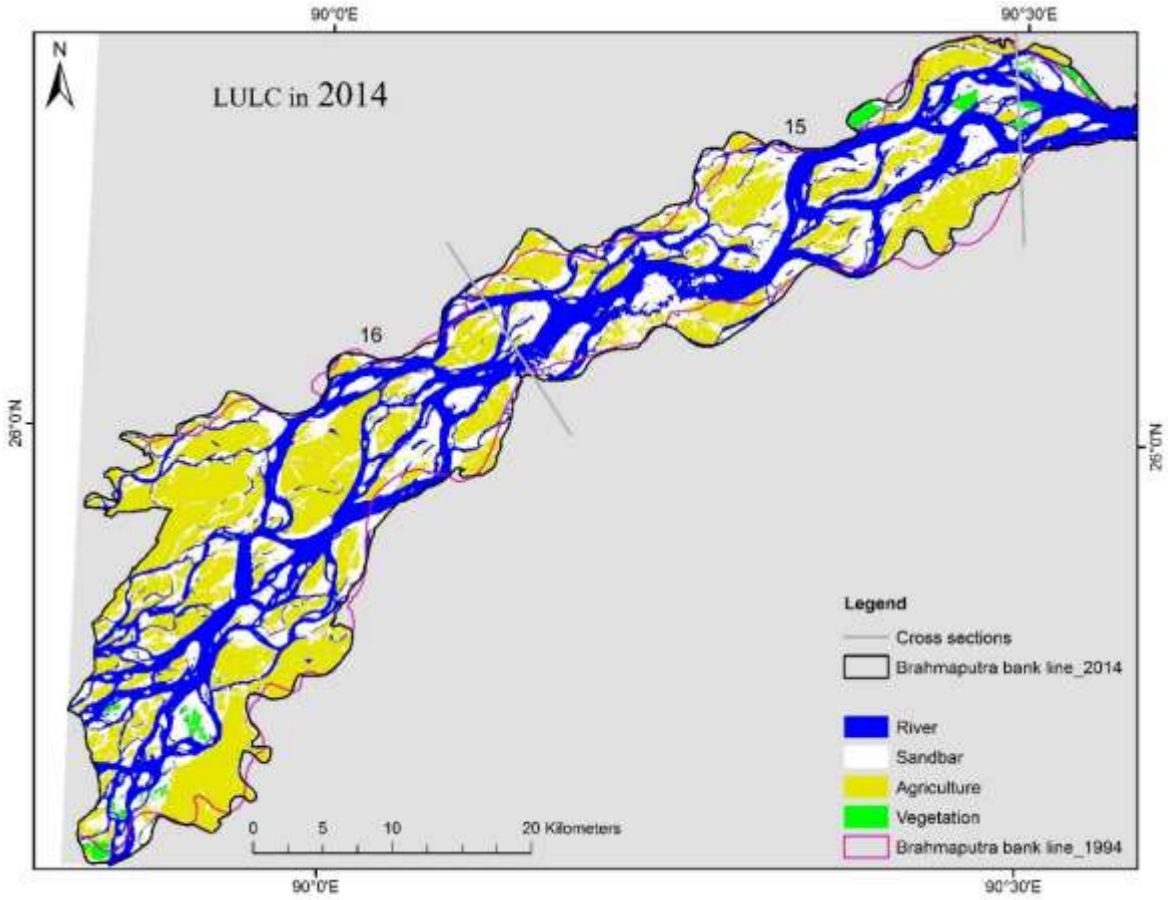


**Figure 7.5h** LULC of Brahmaputra in reach no 15 and 16 during post-monsoon months of 1994 and 2014

Land use and land cover of entire Brahmaputra River during post-monsoon season in 1994 and 2014 is shown in Figure 7.6. Land use and land cover change of Brahmaputra River during the two decades is shown in Figure 7.7. In 1994, 37% area of the river was occupied by water, i.e., live channels and 63% area was bars out of which 30% was sand and 33% was under agricultural practice and vegetation (Table 7.8). Thus, more than 60% of Brahmaputra was covered by temporary sandbars and permanent islands in the post-monsoon months. However, different reaches had varied amount (range 34% – 79%) of sandbars and islands.

**Table 7.8** LULC of Brahmaputra River in 1994

| Reach no | Area in km$^2$ | | | | | % of area covered | | | |
|---|---|---|---|---|---|---|---|---|---|
| | Water | Sandbar/ island | | | Total | Water | Sand | Agriculture | Vegetation |
| | | Sand | Agriculture | Vegetation | | | | | |
| 1 | 84 | 149 | 63 | 103 | 398 | 21 | 37 | 16 | 26 |
| 2 | 112 | 184 | 94 | 65 | 455 | 25 | 40 | 21 | 14 |
| 3 | 115 | 151 | 0 | 104 | 371 | 31 | 41 | 0 | 28 |
| 4 | 88 | 126 | 14 | 86 | 313 | 28 | 40 | 4 | 27 |
| 5 | 93 | 140 | 57 | 95 | 385 | 24 | 36 | 15 | 25 |
| 6 | 106 | 122 | 100 | 74 | 401 | 26 | 30 | 25 | 18 |
| 7 | 110 | 72 | 8 | 60 | 250 | 44 | 29 | 3 | 24 |
| 8 | 100 | 54 | 20 | 45 | 218 | 46 | 25 | 9 | 20 |
| 9 | 144 | 93 | 125 | 42 | 404 | 36 | 23 | 31 | 10 |
| 10 | 168 | 72 | 93 | 22 | 355 | 47 | 20 | 26 | 6 |
| 11 | 114 | 16 | 29 | 16 | 176 | 65 | 9 | 16 | 9 |
| 12 | 187 | 28 | 141 | 35 | 390 | 48 | 7 | 36 | 9 |
| 13 | 237 | 40 | 172 | 14 | 464 | 51 | 9 | 37 | 3 |
| 14 | 203 | 44 | 132 | 8 | 386 | 52 | 11 | 34 | 2 |
| 15 | 137 | 225 | 7 | 0 | 370 | 37 | 61 | 2 | 0 |
| 16 | 177 | 261 | 122 | 0 | 559 | 32 | 47 | 22 | 0 |
| Whole river | 2174 | 1776 | 1178 | 768 | 5896 | 37 | 30 | 20 | 13 |

**Table 7.9** LULC of Brahmaputra River in 2014

| Reach no | Area in km$^2$ | | | | | % of area covered | | | |
|---|---|---|---|---|---|---|---|---|---|
| | Water | Sandbar/ island | | | **Total** | Water | Sand | Agriculture | Vegetation |
| | | Sand | Agriculture | Vegetation | | | | | |
| 1 | 100 | 177 | 52 | 90 | 420 | 24 | 42 | 12 | 21 |
| 2 | 136 | 221 | 58 | 69 | 484 | 28 | 46 | 12 | 14 |
| 3 | 94 | 189 | 0 | 100 | 383 | 24 | 49 | 0 | 26 |
| 4 | 76 | 149 | 3 | 77 | 305 | 25 | 49 | 1 | 25 |
| 5 | 110 | 162 | 54 | 72 | 397 | 28 | 41 | 14 | 18 |

| | | | | | | | | | |
|---|---|---|---|---|---|---|---|---|---|
| 6 | 91 | 160 | 101 | 89 | 442 | 21 | 36 | 23 | 20 |
| 7 | 81 | 109 | 12 | 63 | 265 | 30 | 41 | 4 | 24 |
| 8 | 83 | 110 | 0 | 51 | 244 | 34 | 45 | 0 | 21 |
| 9 | 104 | 150 | 77 | 71 | 402 | 26 | 37 | 19 | 18 |
| 10 | 131 | 189 | 94 | 15 | 429 | 30 | 44 | 22 | 4 |
| 11 | 74 | 83 | 41 | 9 | 207 | 36 | 40 | 20 | 4 |
| 12 | 103 | 83 | 171 | 32 | 389 | 27 | 21 | 44 | 8 |
| 13 | 147 | 168 | 165 | 17 | 498 | 30 | 34 | 33 | 3 |
| 14 | 143 | 129 | 126 | 11 | 409 | 35 | 31 | 31 | 3 |
| 15 | 140 | 150 | 106 | 4 | 401 | 35 | 37 | 27 | 1 |
| 16 | 170 | 176 | 234 | 5 | 585 | 29 | 30 | 40 | 1 |
| Whole river | **1783** | **2404** | **1295** | **776** | **6258** | **29** | **38** | **21** | **12** |

In 2014, 29% area was occupied by channels and 71% area was occupied by sandbar, vegetated bars and agriculture (Table 7.9). Thus amount of water in post monsoon months has been decreased (from 37% to 29%) during 1994 – 2014. All the reaches except reach no 1, 2 and 5 experienced reduction of water in 2014 compared to 1994. Again, different reached had almost uniform (range: 65% – 76%) area covered by bars with sand, vegetation and agriculture. Vegetation has been decreased and agricultural practices have been increased in the different bars and islands of Brahmaputra during 1994 – 2014. Agricultural activity has been increased in lower reaches of Brahmaputra, i.e., reach no 15 (25%) and 16 (18%). Socio-political factor is a major driving force of land use and land cover change in upper reaches of Yangtze River during 1980 – 2000 (Wu et al., 2008) and same factor is responsible for LULC change in Brahmaputra River bed particularly in lower reaches.

The mid-channel bars are locally known as *char* and the *chars* account for about 5 percent of the total area of the state spreading across 14 districts, 55 blocks and around 2,300 villages [Directory of Char Areas 2007-08, Government of Assam; from Chakraborthy, (2010)]. *Char* area is home to 9.37 per cent of the population in Assam but has only 4 per cent of the State's agricultural land. Population in *char* areas has increased from 16,00244 in 1992 – 1993 to 24,90,397 in 2003 – 2004 with maximum population in Dhubri district in the lowest reach (reach no 16). Agriculture is the main activity in those areas. Cultivable land has increased from 1,67,300 ha in 1992 – 1993 to 2,42,277 ha in 2003 – 2004

(CADA, 1994; CADA, 2004). Lack of occupational diversification and absence of non-farm activities does not help in the process of transfer of population from agriculture to non-agricultural activities (Chakraborthy, 2010).

Area covered by sandbars generally increase from October with decrease in discharge and drying of small streams in post monsoon months. Agriculture is becoming less remunerative in char areas due to interplay of several factors like erosion, lack of better inputs, erratic use of chemical fertilizer, improper marketing linkages along with skewed pattern of land ownership (Chakraborthy, 2010). Identification of sandbars/ islands is necessary for better agricultural utilization or other activities in post-monsoon months. Improved regulation and management strategies are necessary to enhance the retention of land resources in changed socio-political scenario.

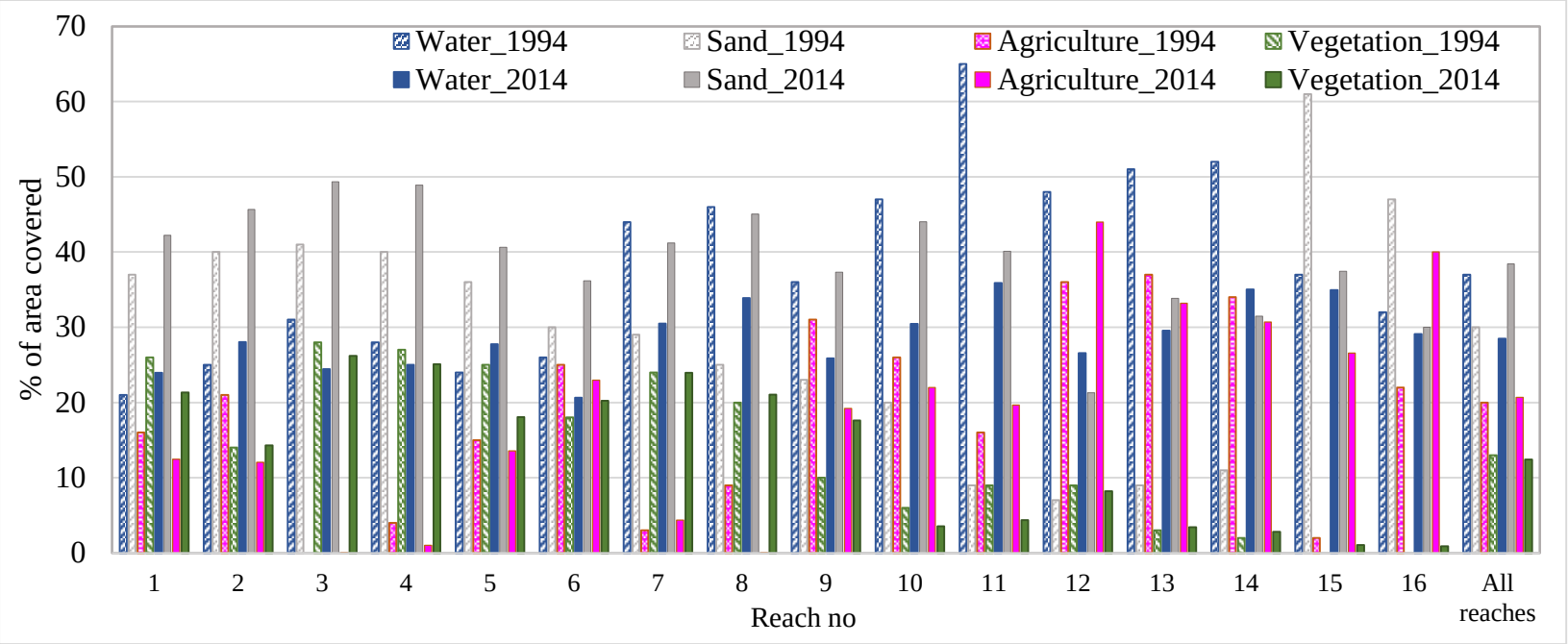


**Figure 7.6** LULC of Brahmaputra River in post monsoon months of 1994 and 2014

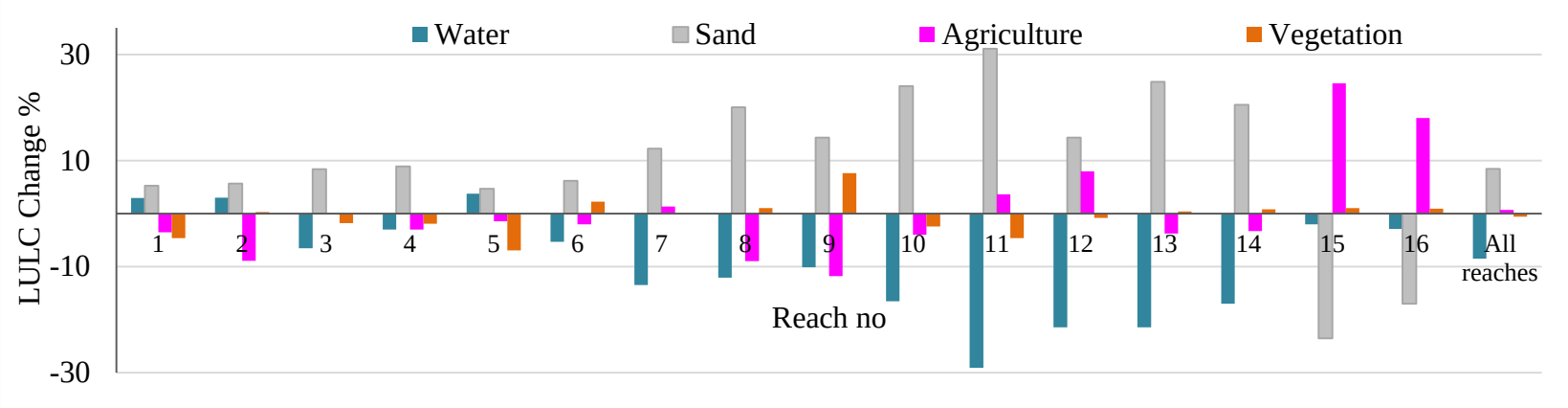


**Figure 7.7** LULC change of Brahmaputra River during 1994 – 2014

Chapter 8

# Bank erosion management

This chapter discusses existing flood and erosion management measures in Brahmaputra River. Based on understanding of sediment properties and river processes of Brahmaputra (from previous chapters), a few options are suggested for sustainable solution of bank erosion.

## 8.1 Existing flood and erosion management practices in Brahmaputra

The flood and erosion management measures started in Assam after the declaration of National Policy in 1954. Accordingly, a huge network of flood embankments along Brahmaputra and its tributaries was erected across the state. Most of the embankments were constructed during the first five year plan (1951-1956) and the second five year plan (1956-1961) periods. The embankments were apparently constructed and planned on inadequate hydrological and hydro-meteorological data, sub-surface information and were designed on specifications short of what is actually required. Extensive riverbank protection or anti-erosion measures were initiated only when the existing embankments became more and more vulnerable to breaches from erosion. Different protection works/ technologies taken up in different erosion affected reaches of Brahmaputra since 1970 are

- *Construction of boulder revetment with launching apron*

  Water Resources Department (WRD) of Govt. of Assam has extensively used chiseled and blasted boulders as one of the chief material for erosion protection.

Conventionally used boulder for anti-erosion works of WRD has become scarce, time consuming to procure at site due to distance from source and cost thereof. Large scale excavation of river boulders also invites threatens the ecology and environment.

- *Construction of deflector/ bull head along with up-stream and down-stream protection work.*
- *Construction of spurs/ land spurs.*

Sediment inducing devices performs satisfactorily in river Brahmaputra by inducing siltation in the channels. High sediment load and comparatively lower velocity of the river provides favourable conditions for the sediment inducing devices. RCC porcupine has been used as pro-siltation devices. Porcupines have pole-like projections in all directions, resembling a porcupine with its quills sticking into the air. They are used as flood control structures, and for river bank and bed protection. Porcupines can be used in a line, forming a spur into a river, as silting aprons for larger spurs, and in a longitudinal line along an embankment. Originally, such devices were made of timber or bamboo, but these have a limited lifespan. It has been observed that in rivers having the silt factor from 0.7 to 1.50 (grain size 0.158 mm to 0.725 mm), the porcupine performs very satisfactorily as silt inducing device. The Silt factor of Brahmaputra ranges from 0.9 to 1.0, as such the silt inducing performance of porcupines is excellent.

Recently WRD has started use of geo-textile technology in the form of geo-tubes and geotextile scour aprons tubes in selected areas. Advantages of geotextiles are:

- Usage of sand filled geotextiles in different forms, size, shape is found to perfect replacement for boulder.
- Tubular mattress filled with sand serve dual purposes of preventing bank erosion and bank sloughing due to seepage of C/S water as the seepage water is filtered out by the sand filled mattress.
- They can be manufactured at factories according to site requirements
- Geo tubular mattress coupled with bio-engineering techniques provides solution for erosion control.

- Sand for filling and installing the geo-textile bags/ mattresses/tubes, is abundantly available at site. Unskilled labours for filling are locally available.

However, performance of geotextile technology in Assam is yet to seen at site for the designed life period of 50 years. Effectiveness of the technology in upper reaches of Brahmaputra, where physical environment vary to a great extent is not well known. Again, stability of recently introduced geo bags against ultra violet rays is not fully tested for suitability for use in bank revetment works.

## 8.2 Promising erosion management options for Brahmaputra

Specific bank protection measures in Brahmaputra have yielded satisfactory results by solving erosion problem of particular reaches. But one measure cannot be considered as a complete solution to the problem of the whole river because causes and mechanisms of erosion differ at different parts of the river due to variations in flow direction of the main channel, water velocity, topography and bank material properties. It is necessary to identify the underlying causes and erosion mechanisms in different sites. Common erosion mitigation method for all effected sites is ineffective and this is the main reason of failure of many existing erosion protection measures. A field survey conducted among 80 families of erosion effected areas of *Sonitpur, Barpeta, Goalpara* and *Dhubri* districts has revealed that there was no consultation with effected people regarding erosion protection works. Again, there was no compensation for land lost in erosion. It is essential to include public consultation component in policy for better understanding of the river and the erosion problem. Rehabilitation of erosion effected people is another important issue which is lacking in current erosion management policies.

It is essential to study the whole river to identify effected and erosion prone areas based on severity of the problem and probability of occurrence. Site specific erosion protection measures considering causes and mechanisms of erosion and impact assessment studies for protection of other vulnerable reaches is important. Loss in erosion can be reduced if protective measures are taken up immediately after signs of erosion of the banks.

Different reaches of the river can be categorized into two major groups based on braiding, shifting of the main channel and bank material properties to select appropriate river training works. Some river training works for two types of reaches are highlighted below:

*a) Reach with main channel(s) towards the bank(s)*

For places eroded by direct attack of the main channel, e.g., *Rohmoria* at upstream, revetments along with flow deflectors at immediate upstream areas can be suitable option. Revetment is a protective structure with stony material, usually natural stone or concrete. The negative effect of concrete blocks is very limited and they have almost no considerable effect on river hydro-system (Maritime Navigation Commission, 2011). Articulated concrete block mattress has an appropriate flexibility that can be installed on different conditions of slope revetments (Yamini et al., 2017).

*b) Braided reach with secondary channels towards the bank(s)*

Bank revetment, spurs etc. have proved to be highly capital intensive and hence can't be applied to long reaches seeking erosion protection. In erosion sites of highly braided area where secondary channels attack the banks, pro-siltation devices can be applied to induce siltation in banks and channelization of the main channel. RCC Jack Jetty and bamboo submerged vanes can be considered as a semi-permanent cost effective approach of river management for sedimentation along with arresting erosion (Sharma and Nayak, 2015). Due to abundance of bamboo in Assam, bamboo porcupines are cost effective option with less environmental impacts. Low slope banks with loose structure having relatively more organic content, e.g., erosion site of *Nematighat* (from Chapter 5), can be managed with geo bags/ tubes coupled with bioengineering tools, e.g., vetiver plantation for its effective bank stabilization with cost effective nature, low maintenance, longevity and little environmental impacts. The vetiver is a special type of grass having longer roots of length up to 3 m. These roots have an average tensile strength of 75MPa (CWC, 2012). Massive plantation with vetiver, bamboo etc. along the banks of vulnerable reaches can provide protection from threat of erosion.

A braided reach can be narrowed by using submerged vanes which are small flow-training structures designed and installed on the riverbed to modify the near-bed flow pattern and redistribute flow and sediment transport within the channel cross section (Odgaard, 2017). Vanes have been used in the past to successfully close off secondary branches of a river (Chabert et al. 1961). Odgaard (2017) have showed that submerged vanes are effective in managing braided rivers like Brahmaputra to close off selected secondary branches and reduce the lateral extent.

Existing embankments under direct attack of the river need erosion protection. Erosion is one cause of embankment breach in many cases along with other factors, e.g., sudden settlement, overtopping, seepage and leakage (WRD, 2016). Erosion protection measures for embankments may be revetment/ mattressing, spurs/ groynes, grade control measures or improvement of shear strength (by growing shallow rooted vegetation). Recently in 2016, state government of Assam has decided to start dredging of Brahmaputra with objectives of erosion control, sediment management and flood control (NDTV, 2016). Although, dredging is practiced in different rivers of the world for navigation, remediation and flood protection; there are evidences of negative impacts from dredging, e.g., increasing risk downstream, ecological risks affecting physical habitat, disrupting riverine processes and reduced connectivity with the floodplain (Barbe et al., 2000; Gob et al., 2005; Freedman and Stauffer, 2013). Channels which have been artificially deepened by dredging silt-up more frequently as they return to their pre-dredged state. In these situations, dredging will be an unsustainable activity since it needs to be repeated regularly (Environment Agency, 2013). Sediment budget of Brahmaputra River is likely to be changed after dredging operation since 21% suspended sediment of the river is contributed from scouring (from Chapter 4). Dredging will alter this figure and it may have other implications including increased aggradation and changed river morphology at downstream.

Land use and land cover study of the river will be helpful in site/ route selection for dredging of the river bed. Dredged material, i.e., sands, can be used to fill geo-tubes and to strengthen existing embankments to super levee as developed in Japan (Takahasi and

Uitto, 2004). Super levee is a high standard river embankment with a broad width (Stalenberg and Kikumori, 2008) having mild slope of 1:30 (Arakawa – Karyu River Office and MLIT, 2006) and is resistant to earthquake, overflow and seepage. The mild slope of the super levee prevents sliding of the top layer. The great width of the super levee also reduces seepage (Arakawa – Karyu River Office and MLIT, 2006). Super levee concept will overcome the drawbacks of existing embankment system.

From above discussions, it can be concluded that understanding of river processes and underlying causes are necessary for solution of erosion problem of Brahmaputra and river training works should be site specific with little environmental impacts. All approaches related to bank erosion management should be carried out in line with the hydrological character of Brahmaputra.

Chapter 9

# Summary and conclusions

The research attempted to evaluate key sediment properties and processes of a large alluvial river the Brahmaputra in Assam, India. Both secondary and primary data were used to evaluate causal factors, sources and processes involved with high sediment concentration and sediment transport, along with physical and geochemical status, bank line shifting and river bank erosion of Brahmaputra. Combining available secondary data with primary data, a sediment budget for Brahmaputra was estimated using mass-balance approach. The physico-chemical properties of the sediments were evaluated based on analysis of samples collected over different seasons, supplemented by relevant secondary data collected from agencies and departments like Brahmaputra Board, NEC and WRD Assam. A major part of the work was constituted of comprehensive geochemical analysis of bank materials collected systematically from selected erosion sites to evaluate the role of the bank material properties in erosion. Remote sensing and GIS tools were used in studying erosion-deposition, braiding and LULC of Brahmaputra River in Assam. One objective of the research was to understand geoenvironmental changes of Brahmaputra in Assam and seeking solution to the bank erosion problem. The results and interpretations were summarized to draw major conclusions and also to prepare ground for further research.

## 9.1 Genesis and deposition of sediments in Brahmaputra

The first chapter deals with factors and sources of sediment generation, bank line shifting due to sediment dynamics and bank erosion as a function of sediment properties in Brahmaputra. The hydrological factors of sediment transport and bank erosion is quite well established and the attempt of the current work was to throw light on properties other than those connected to hydrology, such as texture, morphology and geochemical properties. It was demonstrated that young lithology, seismicity, unconsolidated sedimentary rocks of the Himalayas, steep slope of Brahmaputra and its tributaries in the Himalayas, heavy monsoon rainfall, deforestation and sediment generating cultivation were the major causes of sediment generation in the river catchment, whereas a sudden decrease of slope in Assam plains was the main cause of sediment deposition.

Steepness of Brahmaputra is high compared to most of the large rivers of the world like Amazon, Congo, Volga, Mississippi, Ganges and Indus (Lewin and Ashworth, 2014). Slope of Brahmaputra created for the current study by using data of 175 points along the channel taken from Google Earth demonstrated a clear picture with marked departure from the earlier figures proposed by other researchers based on fewer points.

Average gradient of Brahmaputra was found to be 1.52 m $km^{-1}$. Steep slope of river (slope of Brahmaputra in the reach between PE and India border is 8.27 m/km) and tributaries in the mountainous reaches led to high amount of sediment generation and transportation whereas a sudden decrease in slope (slope in the reach between entry to India and *Pasighat* was 1.52 m/km) has resulted in a large amount of sediment deposition, developing a prominent braided pattern. There was considerable aggradation in the head reaches (C/S 51 – 61) of Brahmaputra at the rate of 16.85 cm per year during the period 1957 – 1989. Slope was further decreased during the course of the river in Assam plains (from 0.81 m $km^{-1}$ between *Pasighat* and *Dibrugarh* at upstream to 0.09 m $km^{-1}$ between *Guwahati* and Bangladesh border at downstream), causing more prominent braided pattern and river instability in terms lateral shifting and erosion of non-cohesive banks. Slope variation in different cross-sections was maximum in 1971. Decrease in average bed slope at the

second reach (C/S 42 – 52) and then increase in the third and the fourth reaches (C/S 32 – 42, 22 – 32) favored more erosion in C/S 42 – 52 and deposition in other reaches.

Studies on erosion and deposition of Brahmaputra in Assam at sixteen reaches has revealed erosion of 1166 $km^2$ during 1973 – 1994 with 564 $km^2$ in the north bank and 602 $km^2$ in the south bank of the river. Total deposition during 1973 – 1994 was 172 $km^2$ with 96 $km^2$ in the north bank and 76 $km^2$ in the south bank. Compared to 1973 – 1994, there was less erosion (589 $km^2$) and more deposition (197 $km^2$) during 1994 – 2014. Total erosion during 1973 – 2014 (1557 $km^2$) was not numerically equal to erosional area of 1973 – 1994 (1166 $km^2$) and 1994 – 2014 (589 $km^2$) since some area eroded during 1973 – 1994 was deposited by sediments during 1994 – 2014. Similarly, some area deposited during 1973 – 1994 was affected by erosion in later period (e.g., reach no 2, 6, 7, 8, 11, 13 and 14). Total amount of deposition during 1973 – 2014 was 204 $km^2$ with 122 $km^2$ in the north bank and 82 $km^2$ in the south bank. There was more erosion in the south bank and more deposition in the north bank.

High erosion (more than 100 $km^2$ area) was taking place in many reaches like reach no 5, 6, 10, 13 and 16. High erosion area in those reaches was mainly due to two factors:

i) Migration of the main channel towards the banks (particularly in left bank) with loss of land.

ii) Bifurcation of distributaies or migration of mid-channels with development of sandbars or islands.

***A sediment budget for Brahmaputra River in Assam***

Generic conclusions on sediment behaviour in a complex river system like Brahmaputra is near to impossible due to wide diurnal, seasonal and annual variations in local sediment-carrying capacities of the river braids. Paucity of dependable data for the main stem and tributaries also bring lot of uncertainty to sediment quantification for Brahmaputra. Yet, an attempt was made to construct a sediment budget for Brahmaputra in Assam using a broad mass balance approach involving the following equation:

Total sediment in channel at a downstream cross section = Sediment contribution from main stream and tributaries + sediment contribution from river bank erosion + sediment contribution from scouring – sediment deposition in bed/bank/floodplains

In the calculation process,

1) Annual sediment load of tributaries were considered from work of Pahuja and Goswami (2006).
2) An estimate that 60% sediments of the tributaries contribute to sediments of Brahmaputra was considered.
3) Sediment input from bank erosion and sediment sink due to deposition in banks were calculated from erosion and deposition for the period 1973 – 2014.
4) Annual inputs from scouring and sediment deposition in river bed were calculated from aggradation and degradation data of Brahmaputra for the period 1957 – 1989.

The tributaries were found collectively to contribute $698\times10^6$ t suspended sediment annually to Brahmaputra. Since a large portion of river-derived sediments of Tibetan rivers are trapped in low reaches, considering an estimated 40% of riverine sediments trapped in the river bed and flood-plains, $419\times10^6$ t sediments (60% of $698\times10^6$ t) were estimated to be at downstream, i.e., at India-Bangladesh Border, whereas $279\times10^6$ t (40% of $698\times10^6$ t) was estimated to be deposited along river bed and floodplains. From scouring and deposition data, mass of deposited sediment on river bed was estimated to be $69\times10^6$ t in a year. Average annual land area lost due to bank erosion during 1973 – 2014 was found to be 38 $\times10^6$ $m^2$. Considering depth of bank erosion as 4.7 m (which was the average difference of yearly observed the highest and the lowest water levels of Brahmaputra for the period 1914 – 1990), mass of eroded soil was found to be 243 $\times10^6$ t. It was earlier suggested that dominant bed form in Brahmaputra were sand dunes with heights $\leq$6 m and wavelengths ($\lambda$) $\leq$330 m. Considering sandbars as spherical domes of height 6 m and radius of base 82.5 m (half of $\lambda/2$), average height of deposition was 3 m. Hence, mass of deposited sediments on $4.97 \times 10^6$ $m^2$ area with 3 m average uniform height, was $20\times10^6$ t. Total sediment load in the river at downstream (India-Bangladesh border) was estimated to be $814\times10^6$ t/year. Considering 10% of sediment load of Brahmaputra as bedload, suspended sediment load at downstream was estimated $733\times10^6$ t/year. Tributaries, bank

erosion and scouring of river bed were found to contribute 52%, 27% and 21% respectively to sediment load of Brahmaputra at downstream. Thus, the main stem including tributaries was the major contributor of sediments in Brahmaputra. More than half of total sediments of Brahmaputra at downstream (52%) comes from the main stem and the tributaries. River bank erosion has contributed 27% suspended sediments to Brahmaputra River. However, 50% suspended sediment load contribution from bank erosion was common in most of the large rivers (Bull, 1997; Church and Slaymaker, 1989; Grimshaw and Lewin, 1980; Imeson and Jungerius, 1977; Imeson et al., 1984; Lawler et al., 1999; Simon, 1989), sediment load of Brahmaputra couldn't be compared with that of other Tibetan rivers, e.g., Yellow and Yangtze in case of sediment input from bank erosion. As revealed from other studies (Ta et al., 2013), bank-to-channel sediment transfer process was found to cause overall increase in channel deposition in Yellow river with little influence on the down-stream suspended sediment load and transport. Similarly, volume of bank erosion and volume of bed deposition in Yangtze river was almost same during 1970 – 1998. But, in case of Brahmaputra, volume of bank erosion in a year ($243 \times 10^6$ $m^3$) was more than ten times of volume of deposition ($20 \times 10^6$ $m^3$). Comparatively less contribution of sediments from scouring (i.e., 16%) in Brahmaputra (present study) is due to less scouring of river bed for less and almost constant slope of the river in Assam plains.

## 9.2 Physico-chemical properties of sediments of Brahmaputra

Investigation of sediment properties was done which has the scope of understanding of sediment behavior in rivers. Based on experimental analysis, particle size, mineralogy and metal content of both bed sediments and suspended sediments of Brahmaputra at longitudinally spread locations were investigated. Revealed useful information is narrated briefly below:

***Particle size and mineralogy***

In most alluvial rivers, the median sizes of the bed materials demonstrate a decrease in downstream direction. In case of Brahmaputra, there was decrease in (d50)x/(d50)o with corresponding increase in x for the first 300 km (of the river in Assam). The ratio seems to

be nearly equal to unity indicating that size of bed materials has not decreased. This is primarily due to transport of sediment as suspended load and continuous input from bank erosion.

Particle size distribution of suspended sediments revealed dominance of silt (3.9– 62.5µm), very fine sand (62.5 – 125µm) and fine sand (125 – 250µm) fractions. XRD analysis revealed dominance of silt sized Quartz, Kaolinite, Illite and Albite. Dominance of silt sized Quartz, Kaolinite, Montmorrillonite in suspended sediments suggested less adsorbing capacity of metals. Prolate, oblate and bladed shape of suspended sediments suggested immature sediments coming from erosion with short transportation history.

***Metal content in sediments***

Concentrations of Fe, Mn, Cu, Zn and Ni content in suspended sediment during pre-monsoon season were higher compared to that of monsoon (3% – 19%) and post-monsoon seasons (4%– 9%). All metal concentrations except Mn were in higher concentrations in Brahmaputra River (Fe: 6.5%, Cu: 41.3 µg/gm, Pb: 23.3 µg/gm, Zn: 94 µg/gm, Mn: 503.2 µg/gm, Ni: 40.3 µg/gm) compared to that of Indian average river (Fe: 2.9%, Cu: 28 µg/gm, Pb: 15µg/gm, Zn: 16µg/gm, Mn: 605 µg/gm, Ni: 37 µg/gm) and that of Bay of Bengal (Fe: 3.9%, Cu: 26 µg/gm, Mn: 529 µg/gm, Ni: 64 µg/gm).

Geo-accumulation indices showed uncontaminated sediment quality with respect to all the metals except moderate Fe enrichment in three locations. Dominance of residual fraction and less amount of bioavailable portion of heavy metals may be attributed to low organic matter, dominant coarser fraction in sediments coupled with low pollution in the river due to less industrial activities in the region. Less organic matter content in bed sediments of Brahmaputra (<1.5%) is due to dominance of coarser fraction in sediments. High Fe concentrations and dominant solid fractions in Brahmaputra may be associated with non-anthropogenic river bank erosion of metal bearing phyllosilicates.

## 9.3 Geochemical evaluation of bank materials

This part of the research attempted to examine the geochemical properties of bank materials collected from six key locations, i.e., *Rohmoria (A), Dibrugarh (B), Nematighat (C), Majuli (D), Gamerighat (E) and Palasbari (F)* including their implications to erodibility of bank materials and metal flux through sediments.

Among the analyzed parameters, pH, organic content (OC), carbonate content (CC), cation exchange capacity (CEC), exchangeable sodium percentage (ESP), and particle size ($d_{10}$, $d_{50}$ and $d_{90}$) were found to be more heterogeneous in erosion sites than those of non-erosion sites. Low (<2%) organic content, dominance of silt and sand sized particles, particularly in lower layers of sediment profile were found to be the major geochemical properties of bank materials contributing to bank erosion in sites like A, B, E and F. Decrease of SAR, ESP and CEC towards deeper depth showed consistency of results over erodible areas at different locations. Presence of clay pocket and high organic content at lower layer of sediment profile had little role in stability of bank profile in location C due to overall dominance of silt sized particles over the bank.

Low amount of exchangeable Na, K, Ca and Mg were observed in all locations including non-erosion site of D, which resulted in very low value of CEC in all locations. Low value of SAR in erosion sites could be due to low available Na in soils. High variation of SAR with depth along with high clay content and less variation of sand particles had been observed as significant geochemical properties contributing to resistance to erosion in the locations of D. Although abundance of soluble metals like Fe and Al in the study area as revealed from EDX studies could reduce the double layer thickness of clay particles, theoretically increasing cohesion and reducing sediment erodibility (Winterwerp and Kesteren, 2004), such results were not observed due to absence of clay particle and dominance of silt and medium sand sized particles.

Erosion site A had comparatively high sand content (particle size range: 7µm – 460 µm) and the lowest value of minimum clay content (0.3%) among the study areas. Erosion sites of B, D, E and F also had higher sand content (52%, 44%, 36% and 31% respectively) with very low amount of clay sized particles (3 – 8%). These two factors including low organic

content are likely to be considered as significant geochemical factors for low cohesion (c = 0.02 – 0.15 Kg/cm$^2$,) in the studied locations as obtained from direct shear test results.

High angle of internal friction of samples ($\phi = 34^0 – 40^0$) in spite of low cohesion could be explained by aggregation of soil particles (Lebert and Horn, 1991). The aggregates were strong enough to resist the stresses and the soil acted like very dense sand with high angle of internal friction. Thus, steep river banks in erosion sites of Brahmaputra might be due to high angle of internal friction resulting from aggregation of cohesion less soil particles.

Brahmaputra River at erosion sites *A, B* and *F* (Figure 3.6, p. 40) is wide and highly braided. So, section average velocity at *A, B* and *F* are comparatively low than that of single channel in other locations (*C, D* and *E*). However, these average velocities corresponding to a pre-monsoon discharge (e.g., 0.82 m/s and 0.80 m/s at sites *B* and *F* respectively) and peak monsoon discharge (e.g., 1.01 m/s and 0.86 m/s at sites *B* and *F* respectively) are two to hundred folds higher than that required for threshold movement of sediment (e.g., 0.40 m/s and 0.03 m/s at sites *B* and *F* respectively) as obtained from Hjulström diagram. (Table 6.3, p. 118).

***Role of geochemical properties of bank materials in erosion***

Correlation matrices showed that pH, OC, Carbonate content, SAR had negative correlation with erosion. Particle size ($d_{50}$ and $d_{90}$) had positive correlation with erosion (Table 6.4, p. 119). To evaluate contribution of selected geochemical properties to erosion event, binary logistic regression in SPSS was used with 'Erosion' ('Yes' or 'No') as dependent variable and OC, SAR and particle size ($d_{50}$ and $d_{90}$) as predictor variables. Moderate relationship of 59% between prediction and grouping was observed with predictor variables OC, SAR and $d_{90}$. Experimental and statistical analysis revealed that probability (P) of bank erosion in Brahmaputra is related to geochemical parameters OC, SAR and $d_{90}$ by the equation:

$$P = \frac{e\{0.796 + (-.073)\mathrm{OC} + (-1.321)\mathrm{SAR} + (.010)\mathrm{d90}\}}{1 + e\{0.796 + (-.073)\mathrm{OC} + (-1.321)\mathrm{SAR} + (.010)\mathrm{d90}\}}$$

Particle size and OC were the most important geochemical factors of river bank erosion in Brahmaputra, holding other parameters constant. Role of particle size and OC in erosion was already documented by different researchers. Values of OC, SAR and $d_{90}$ of bank materials could be used for rapid assessment of probability of erosion in Brahmaputra.

## 9.4 Braiding and LULC of Brahmaputra river

Braiding of Brahmaputra River in Assam during 1973 & 2014 was studied using Landsat images and GIS tools. Methodologies suggested by Brice (1960, 1964), Rust (1978), Howard et al. (1970), Mosley (1981), Ashmore (1982), Friend and Sinha (1993), Sharma (2004) were used to calculate braiding indices of the river in sixteen reaches. Those indices consider one or two parameters a braided channel, e.g., length of bars, mid-channels, main-channel or center line and number of channels in a cross section. But number of mid-channel bars, which is a characteristic feature of a braided river, was not used in any indices. Hence, a new braiding index has been suggested incorporating fraction of area covered by sandbars, number of mid-channel bars, maximum width and length of the reach using the formula

$$\text{Braiding, } B = X \times N \times W/L$$

Where, $X$: fraction of area covered by mid-channel bars, $N$: number of mid-channel bars, $L$: length of reach, $W$: maximum width of the reach.

In spite of variations of braiding values in different approaches, almost similar trend of braiding values has been observed for all the reaches. Higher braiding in most of the reaches were due to greater channel width with

i) more distributaries, i.e., increased mid-channel lengths, e.g., in reach no 2, 5, 6, 12, 13, 14 and 16 in 1973 and reach no 1, 2, 3, 4, 6, 9, 13 and 15 in 2014.
ii) more mid-channel bars, i.e., increased sandbar lengths, e.g., reach no 1, 2, 3, 4, 6, 9,10, 13, 15 and 16 in 1973 and reach no 1, 2, 5, 6, 10, 12, 13, 14 and 16 in 2014.

Minimum braiding in three reaches, i.e., reach no 7, 8 and 11 was due to comparatively narrow channel width with less number of distributaries and mid-channel bars.

The newly suggested parameter has showed comparable result with other approaches. Moreover, the new parameter has very good correlation (0.97) with number of sandbars. The new index also showed relatively better correlation with sinuosity than braiding values obtained from other methods. With reference to braiding values for different reaches from different approaches, following threshold values can be suggested from the new braiding index for a broad range of classification of braiding phenomenon:

Highly braided: $B > 30$

Moderately braided: $5 < B < 30$

Low braided: $B < 5$

On the basis of above classification, thirteen reaches were moderately braided and three were low braided in 1973. But in 2014, six reaches became highly braided and nine reaches became moderately braided. The reaches which were only low and moderately braided in 1973, became moderately braided and highly braided during 1973 – 2014. Braiding value was increased by more than 50% in reach no 2, 5, 6, 8, 10, 11, 12, 13, 14 & 15 during 1973—2014. In some cases, more than 100% increase of braiding was observed (in reach no 5, 12 and 14). Increase of braiding was due to development of more sandbars and distributaries resulting in increased mid-channel lengths and sandbar lengths. Area covered by Brahmaputra River in Assam has increased from 4,906 $km^2$ in 1973 to 6,258 $km^2$ in 2014. Widening of the river has resulted in loss of land area by bank erosion process in many locations. However, increased area of Brahmaputra is not necessarily linked to bank erosion in every case. Increase in area (28%) of Brahmaputra River during 1973 – 2014, besides bank erosion is also due to bifurcation of streams without significant loss of land.

Brahmaputra River in post-monsoon months of 1994 and 2014 were studied for four types of land use and land cover, i.e., river/ water, sandbar, vegetation (including natural grass land) and agriculture (including human settlement). In 1994, 37% area of the river was occupied by water, i.e., live channels and 63% area was bars out of which 30% was sand and 33% was under agricultural practices and vegetation. However, reaches had varied amount (range 34% – 79%) of sandbars and island. In 2014, 29% area was occupied by channels and 71% area was occupied by sandbar, vegetated bars and agriculture. Thus,

amount of submerged part in post monsoon months has decreased (from 37% to 29%) during 1994 – 2014. A reduction in natural grassland and forest has been observed with corresponding increase in agricultural practices in different bars and islands of Brahmaputra in Assam during 1994 – 2014. Agricultural activity has increased in lower reaches of Brahmaputra, i.e., reach no 15 (25%) and 16 (18%). Socio-political factor is one factor for LULC change in Brahmaputra River floodplain particularly in lower reaches. Loss of agricultural land and homestead land from river bank erosion and growing population in the lower reaches has compelled the riverine people to explore agricultural activities in inter fluvial landmasses in post-monsoon months.

## 9.5 Understanding of geoenvironmental changes in Brahmaputra and solution to the bank erosion problem

Prominent dynamic nature of Brahmaputra in its valley part due to flat topography after high slope of the river in China and Arunachal Pradesh (India) facilitates sediment deposition and widening of the river (Chapter 4).

Dynamism with instability is distinct in terms of increased braiding, channel migration, bifurcation of the distributaries with development of temporary mid-channel bars, bank line shifting causing sever bank erosion in many areas besides annual flooding. Irregular decrease in average bed slope of the river particularly in the middle reaches triggers instability by channel migration and bank erosion. Causes and mechanisms of bank erosion differ at different parts of the river due to variations in flow direction of the main channel, topography and bank material properties. It is necessary to identify the underlying causes and erosion mechanisms in different sites.

Values of OC, SAR and $d_{90}$ of bank materials could be used for rapid assessment of probability of erosion. Common erosion mitigation method for all erosion sites is ineffective and this is the main reason of failure of many existing erosion protection measures. It is essential to identify effected and erosion prone areas based on severity of the problem and probability of occurrence. Site specific erosion protection measures considering causes and mechanisms of erosion and impact assessment studies for

protection of other vulnerable reaches is important. It is essential to include public consultation component in policy for better understanding of the river and the erosion problem. Rehabilitation with separate fund to compensate land loss is another important issue which is lacking in current erosion management policies.

Narrow reach or braided reach with direct attack of main channel(s) can be protected by revetments along with flow deflectors at immediate upstream areas. Articulated concrete block mattress has an appropriate flexibility that can be installed on different conditions of slope revetments.

Bank revetment, spurs etc. have proved to be highly capital intensive and hence can't be applied to long reaches seeking erosion protection. In erosion sites of highly braided area where secondary channels attack the banks, pro-siltation devices can be applied to induce siltation in banks and channelization of the main channel. RCC Jack Jetty, submerged vanes can be cost effective option of river management for sedimentation along with arresting erosion. A braided reach can be narrowed by using submerged vanes which are effective to close off selected secondary branches and reduce the lateral extent. Low slope banks with loose structure having relatively more organic content, e.g., erosion site of *Nematighat* (Chapter 5), can be managed with geo bags/ tubes coupled with bioengineering tools, e.g., vetiver plantation for its effective bank stabilization with cost effective nature, low maintenance, longevity and little environmental impacts. Massive plantation with vetiver, bamboo etc. along the banks of other reaches can increase resistance of the river banks against erosion.

Existing embankments under direct attack of the river need erosion protection and it may be revetment/ mattressing, spurs, grade control measures or improvement of shear strength (by growing shallow rooted vegetation). Recently state government of Assam has decided to start dredging of Brahmaputra with objectives of erosion control, sediment management and flood control. Land use and land cover study of the river will be helpful in site/ route selection for dredging of the river. Dredged material, i.e., sands, can be used to fill geo-tubes and to strengthen existing embankments to super levee as developed in Japan. Improved regulation and management strategies are necessary to enhance the retention of

land resources in changed socio-political scenario. Considering potential negatives impacts of different river training works, e.g., changed river morphology, increasing risk downstream, disrupting riverine processes, reduced connectivity, altered sediment budget; all approaches for bank erosion management should be carried out in line with the hydrological character of Brahmaputra.

### 9.6 Future scope of research

a) The present study has provided a scope to extend study on fate and transport of sediments in an alluvial river.

b) The present study has dealt with sediment geochemical properties to evaluate erodibility of a particular site. Inclusion of hydrological data along with sediment data as input parameters can give clear picture of vulnerability of erosion in a particular area.

c) Integration of bank material properties with erosion behavior will be helpful in site specific protection measures for the erosion problem

d) Identification of sandbars/ islands is necessary for better agricultural utilization or other activities in post-monsoon months.

e) The present study is based on erosion behavior and protection measures of a few selected locations. Integration of all findings and a strong R&D backup can be a base for a detailed survey of entire Brahmaputra for effectiveness of erosion management measures.

# References


Abowei J. F. N. and Sikoki F. D. (2005). *Water Pollution Management and Control*. Double Trust Publications Company, Port Harcourt, p. 236.

ADB (2007). *Technical Assistance Consultant's Report*, Northeastern Integrated Flood and Riverbank Erosion Management Project (Assam), TA (Phase 1) Workshop Materials.

Agarwal P. K. and Singh V. P. (2007). Brahmaputra and Barak Basin. In Agarwal P. K., Jain S. K. and Singh V. P. (Eds.), *Hydrology and Water Resources of India*, Springer, p. 437.

Agrawal Y. C., McCave I. N. and Riley J. B. (1991). Laser Diffraction Size Analysis. In Syvitski, J. P. M. (Ed.), *Principles, Methods and Application of Particle Size Analysis*, Cambridge University Press, Cambridge, pp. 119 – 128.

Ahmed A. A. and Fawzi A. (2009). Meandering and Bank Erosion of the River Nile and its Environmental Impact on the Area Between Sohag and El-Minia, Egypt. *Arabian Journal of Geosciences*, Vol. 4, No. 1, pp. 1 – 11.

Alagarsamy R. and Zhang Z. (2005). Comparative Studies on Trace Metal Geochemistry in Indian and Chinese Rivers. *Current Science*, vol. 89, no. 2, pp. 299 – 309.

Ali K. F. (2009). *Construction of Sediment Budgets in Large Scale Drainage Basins: the Case of the Upper Indus River*. University of Saskatchewan Library, Electronic Theses & Dissertations. Assessed from url: http://library2.usask.ca/theses/available/etd-12012009-234340/ on 09.06.2011.

Alonso Castillo M. L., Sanchez Trujillo I., Vereda Alonso E., Garcia de Torres A. and Cano Pavon J.M. (2013). Bioavailability of Heavy Metals in Water and Sediments from a Typical Mediterranean Bay (Malaga Bay, Region Of Andalucia, Southern Spain). *Mar Pollut Bull*, Vol. 76, No. 1 – 2, pp. 427 – 434.

Arakawa - Karyu River Office and MLIT (2006). The Arakawa: River of the Metropolis; *A comprehensive guide to the lower Arakawa, Arakawa - Karyu River Office*. Ministry of Land, Infrastructure and Transport.

Arulanandan K., Gillogley E. and Tully R. (1980). *Development of a Quantitative Method to Predict Critical Shear Stress and Rate of Erosion of Natural Undisturbed*

*Cohesive Soils.* Report GL-80-5, U.S. Army Engineers, Waterways Experiment Station, Vicksburg, Mississippi.

Ashmore P. E. (1982). Laboratory Modelling of Gravel Braided Stream Morphology. *Earth Surface Processes*, Vol. 7, Issue 3, pp. 201 – 225.

Ashmore P. E. (1991). Channel Morphology and Bed Load Pulses in Braided Gravel-Bed Streams. *Geografiska Annaler*, Vol. 73A, pp. 37 – 52

Ashworth P. J. and Lewin J. (2012). How Do Big Rivers Come to be Different? *Earth-Science Reviews*, Vol. 114, Issues 1 – 2, pp. 84 – 107.

Barbe D. E., Fagot K. and McCorquodale J. A. (2000). Effects on Dredging Due to Diversions from the Lower Mississippi River. *Journal of Waterway Port Coastal and Ocean Engineering*, Vol. 126, No. 3, pp. 121 – 129.

Baruah U. and Goswami R. K. (2013). River Bank Erosion Management in Assam. In Kakati H. and Changkakati P. P. (Eds.), *Proceedings of the Assam Water Conference 2013*, Water Resources Department, Govt. of Assam, Guwahati, p. 41.

Battarbee R., Anderson N., Appleby P., Flower R.J., Fritz S., Haworth E., Higgit S., Jones V., Kreiser A., Munro M. A., Natkanski J., Oldfield F., Patrick S. T., Richardson N., Rippey B. and Stevenson A. C. (1988). *Lake Acidification in The United Kingdom*, ENSIS, London. p. 68.

Bengtsson L. and Enell M. (1986). Chemical Analysis. In Berglund B. E. (Ed.), *Handbook of Holocene Palaeoecology and Palaeohydrology*, John Wiley & Sons Ltd., Chichester, pp. 423 – 451.

Best J. L., Ashworth P. J., Sarker M. H. and Roden J. E. (2007). The Brahmaputra–Jamuna River, Bangladesh. In Gupta, A. (Ed.), *Large Rivers: Geomorphology and Management*, Wiley, Chichester, pp. 395 – 433.

Best J. L. and Bristow C. S. (1993). Braided Rivers: Perspectives and Problems. In Best, J. L. and Bristow C. S. (Eds.), *Braided Rivers*, Vol. 75, Geological Society of London Special Publication, pp. 1–11.

Beuselinck L., Govers G., Poesen J., Degraer G., and Froyen L. (1998). Grain-size Analysis by Laser Diffractometry: Comparison With the Sieve-Pipette Method. *Catena*, Vol. 32, Issues 3 – 4, pp. 193 – 208.

Bhuyan D. K. (2013). Flood Management Activities in Assam. *Souvenir: Assam Water*

*Conference 2013*, Water Resources Department, Govt. of Assam, pp. 15 – 20.

Billi P. and Ali Omer el B. (2010). Sediment transport of the Blue Nile at Khartoum. *Quaternary International*, Vol. 226, No. 1 – 2, pp. 12 – 22.

Blott S. J. and Pye K. (2006). Particle Size Distribution Analysis of Sand Size Particles by Laser Diffraction: An Experimental Investigation of Instrument Sensitivity and The Effects of Particle Shape. *Sedimentology*, Vol. 53, Issue 3, pp. 671 – 685.

Bocco G., Mendoza M., and Velazquez A. (2001). Remote Sensing and GIS-Based Regional Geomorphological Mapping- A Tool For Land Use Planning in Developing Countries. *Geomorphology*, Vol. 39, pp. 211 – 219.

Boori M. S., Vozenilek V., Choudhary K. (2015). Land Use/ Cover Disturbance Due to Tourism in Jeseniky Mountain, Czech Republic: A Remote Sensing and GIS Based Approach. *The Egyptian Journal of Remote Sensing and Space Sciences*, Vol. 18, Issue 1, pp. 17–26.

Bordas F. and Bourg A. (2001). Effect of Solid/ Liquid Ratio on the Remobilization of Cu, Pb, Cd and Zn from Polluted River: Sediment Modeling of the Results Obtained and Determination of Association Constants Between the Metals and the Sediment. *Water Air Soil Pollution*, Vol. 128, pp. 391 – 400.

Bradl H. (2005). *Heavy Metals in the Environment: Origin, Interaction and Remediation*. Elsevier/ Academic Press, London.

Brady N. C. and Weil R. R. (2002). *The Nature and Properties of Soils*. Prentice Hall.

Brasington J., Rumsby B. T. and McVey R. A. (2000). Monitoring and Modelling Morphological Change in a Braided Gravel-Bed River Using High-Resolution GPS-Based Survey. *Earth Surface Processes and Landforms*, Vol. 25, pp. 973–990.

Brice J. C. (1960). Index for Description of Channel Braiding. *Geological Society of America Bulletin*, Vol. 71, pp. 1833.

Brice J. C. (1964). Channel Patterns and Terraces of the Loup Rivers in Nebraska. *Geological Survey* Professional Paper 422-D.

Bridge J. S. (2009). Alluvial Channels and Bars. *Rivers and Floodplains: Forms, Processes, and Sedimentary Record*. John Wiley & Sons, p. 151.

Bristow C. S. (1987). Brahmaputra River: Channel Migration and Deposition. In Ethridce

F.G., Flores R.M. & Harvey M.D. (Eds.), *Recent Developments in Fluvial Sedimentology*. Society of Economic Paleontologists and Mineralogists Special Publications, Vol. 39, pp. 63 – 74.

Bryant R. G. and Gilvear D. J. (1999). Quantifying Geomorphic Riparian Land Cover Changes Either Side of a Large Flood Event Using Airborne Remote Sensing: River Tay, Scotland. *Geomorphology*, Vol. 29, pp. 307–321.

Bull L. J. (1997). Magnitude and Variation in the Contribution of Bank Erosion to the Suspended Sediment Load of the River Severn, UK. *Earth Surface Processes Landforms*, Vol. 22, Issue 12, pp. 1109 – 1123.

BWDB (1972). *Sediment Investigations in Main Rivers of Bangladesh, 1968 & 1969*. BWDB Water Supply Paper No. 359. Bangladesh Water Development Board, Bangladesh.

CADA (1994). *Socio-Economic Survey Report, 1993-94*. Char Area Development Authority, Government of Assam, Dispur, Assam.

CADA (2004). *Socio-Economic Survey Report, 2003*. Char Area Development Authority, Government of Assam, Dispur, Assam.

Carson M. A. and Kirby M. J. (1972). *Hillslope, Form and Process*. Cambridge University Press.

Chabert J., Remillieux M. and Spitz I. (1961.) Application de la circulation transversal a la correction des rivieres et a la protection des prises d'eau. *Proceeding of the Ninth Convention of IAHR, Dubrovnik, Yugoslavia*, pp 1216–1223. {in French, from Odgaard (2017)}

Chakraborthy G. (2010). Victims of 'Suspicious' Identity: the Char Dwellers of Assam. In Deb B. J. (Ed.), *Population and Development in North East India*, Concept Publishing Company Pvt. Ltd.

Chang H. H. (1988). *Fluvial Processes in River Engineering*. John Wiley & Sons, p. 5.

Changxing S. and Qingchao Y. (1997). Bank Breach Hazards in the Lower Yellow River, Destructive Water: Water-Caused Natural Disasters, their Abatement and Control, Proceedings of the Conference (held at Anaheim, California, June 1996), IAHS Publ. no. 239, p. 391.

Charlton R. (2008). Process of Erosion, Transport and Deposition. *Fundamentals of*

*Fluvial Geomorphology*, Routledge, p. 97.

Chaudhuri S., Stille P. and Clauer N. (1992). Isotopic Signatures and Sedimentary Records. *Springer*, pp. 287 – 319.

Chu Z. (2014). The Dramatic Changes and Anthropogenic Causes of Erosion and Deposition in the Lower Yellow (Huanghe) River since 1952. *Geomorphology*, Vol. 216, pp. 171 – 179.

Church M. (2006). Bed Material Transport and the Morphology of Alluvial River Channels. *Annual Review of Earth and Planetary Sciences*, Vol. 34, pp. 325 – 354.

Church M. and Slaymaker O. (1989). Disequilibrium of Holocene Sediment Yield in Glaciated British Columbia. *Nature*, Vol. 337, pp. 452 – 454.

Clark M. K., Schoenbohm L. M., Royden, L. H., Whipple, K. X., Burchfiel, B. C., Xhang, X., Tang W., Wang E. and Chen L. (2004). Surface uplift, tectonics, and erosion of eastern Tibet from large-scale drainage patterns. *Tectonics*, p. 23.

Coleman J. M. (1969). Brahmaputra River: Channel Processes and Sedimentation. *Sediment Geology*, Vol. 3, Issue 2 – 3, pp. 129 – 239.

Collins A. L.,Walling D. E. and Leeks G. J. L.(1997). Finger Printing Suspended Sediment Sources in Larger River Basins: Combining Assessment of Spatial Provenance and Source Type. *Geografiska Annaler*, Vol. 79A, pp. 239 – 254.

CWC (2012). *Handbook for flood protection, anti erosion & river training works*. Central Water Commission, Govt. of India, p. 36.

Czuba J. A., Magirl C. S., Czuba C. R., Grossman E. E., Curran C. A., Gendaszek A. S. and Dinicola R. S. (2011). Comparability of Suspended-Sediment Concentration and Total Suspended Solids Data: Sediment Load from Major Rivers into Puget Sound and its Adjacent Waters. *USGS Fact Sheet 2011–3083*. Tacoma, WA: U S Geological Survey.

Dade W. B., Nowell A. R. M. and Jumars P. A. (1992). Predicting Erosion Resistance of Muds. *Marine Geology*, Vol. 105, Issues 1 – 4, pp. 285 – 297.

Dai F. C. and Lee C. F. (2003). A Spatiotemporal Probabilistic Modelling of Storm-Induced Shallow Landsliding Using Aerial Photographs and Logistic Regression. *Earth Surface Processes and Landforms*, Vol. 28, Issue 5, pp. 527– 545.

Dai S. B. and Lu X. X. (2010). Sediment Deposition and Erosion During the Extreme

Flood Events in the Middle and Lower Reaches of the Yangtze River. *Quaternary International*, Vol. 226, Issues 1 – 2, pp. 4 – 11.

Dai S. B. and Lu X. X. (2014). Sediment Load Change in the Yangtze River (Changjiang): a Review. *Geomorphology*, Vol. 215, pp. 60 – 73.

Dalai T. K., Krishnaswami S. and Sarin M. M. (2002). Major Ion Chemistry in the Headwaters of the Yamuna River System: Chemical Weathering, its Temperature Dependence and $CO_2$ Consumption in the Himalaya. *Geochimica et Cosmochimica Acta*, Vol. 66, pp. 3397 – 3416.

Das A. K., Sah R. K., and Hazarika N. (2012). Bankline Change and the Facets of Riverine Hazards in the Floodplain of Subansiri-Ranganadi, Brahmaputra Valley, India. *Natural Hazards*, Vol. 64, pp. 1015 – 1028.

Datta B. and Singh V. P. (2004). Hydrology. In Singh V., Sharma N. and Ojha C. S. P. (Eds.), *The Brahmaputra Basin Water Resources*, Springer Netherlands, pp. 139 – 195.

Datta D. K. and Subramanian V. (1997a). Nature of Solute Loads in the Rivers of the Bengal Basin, Bangladesh. *Journal of Hydrology*, Vol. 198, pp. 196 – 208.

Datta D. K. and Subramanian V. (1997b). Texture and Mineralogy of Sediments from the Ganges- Brahmaputra-Meghna River System in the Bengal Basin, Bangladesh and their Environmental Implications. *Environmental Geology*, Vol. 30, Issues 3 – 4, pp. 181 – 188.

Davidson C. M., Duncan A. L., Littlejohn D., Ure A. M. and Garden L. M. (1998). A Critical Evaluation of three Stage BCR Sequential Extraction Procedure to Assess the Potential Mobility and Toxicity of Heavy Metals in Industrially Contaminated Land. *Anal. Chem. Acta*, Vol. 363, pp. 45 – 55.

Dean W. E. Jr. (1974). Determination of Carbonate and Organic Matter in Calcareous Sediments and Sedimentary Rocks by Loss on Ignition: Comparison with Other Methods. *J. Sed. Petrol*, Vol. 44, No. 1, pp. 242 – 248.

de Boer G. B. J., de Weerd C., Thoenes D., and Goossens H. W. J. (1987). Laser Diffraction Spectrometry: Fraunhofer Diffraction versus Mie Scattering. *Particle Characterization*, Vol. 4, Issues 1 – 4, pp. 138 – 146.

Dingzhong D. and Ying T. (1996). Soil Erosion and Sediment Yield in the Upper Yangtze

River Basin, Erosion and Sediment Yield: Global and Regional Perspectives. *Proceedings of the Exeter Symposium*, IAHS Publ. no. 236, p. 191.

Dunne T., Mertes L. A. K., Meade R., Richey J. E. and Forsberg B. R. (1998). Exchanges of Sediment Between the Flood Plain and Channel of Amazon River in Brazil. *GSA Bulletin*, Vol. 110, No. 4, pp. 450 – 467.

Dunnivant F. M. and Anders E. (2006). *A Basic Introduction to Pollutant Fate and Transport*. John Wiley & Sons, Inc., pp. 76 – 79.

Eisma D. (1993). *Suspended Matter in the Aquatic Environment*. Springer, pp. 29 – 30.

El Bouraie M. M., El Barbary A. A., Yehia M. M. and Motawea E. A. (2010). Heavy Metal Concentrations in Surface River Water and Bed Sediments at Nile Delta in Egypt. *Suoseura* — Finnish Peatland Society, Suo, Vol. 61, No. 1, pp. 1 – 12.

Eljarrat E. and Barcelo D. (2009). Chlorinated and Brominated Organic Pollutants in Contaminated River Sediments. In Kassim T. A. and Barcelo D. (Eds.), *Handbook of Environmental Chemistry*, Vol. 5, Part-T, Springer, p. 21.

Enfeng L. I. U., Ji S. and Xingqi L. (2005). Geochemical Features of Heavy Metals in Core Sediments of Northwestern Taihu Lake, China. *Chinese J. Geochem*, Vol. 24, pp. 73 – 81.

Environment Agency (2013). *Evidence: Impacts of Dredging*. Environment Agency, Bristol, U. K.

EPA (2003). River Morphology. *Low land River Bank Stability and Erosion Assessment*, pp. 6 – 52.

EPA (2014). Sediments. In *Water: Pollution Prevention & Control*. Assessed from http://water.epa.gov/polwaste/sediments on 09/03/2014

Evans D. J., Gibson C. E. and Rossell R. S. (2006). Sediment Loads and Sources in Heavily Modified Irish Catchments: A Move Towards Informed Management Strategies. *Geomorphology*, Vol. 79, pp. 93 – 113.

Fan F., Weng Q. and Wang Y. (2007). Land Use and Land Cover Change in Guangzhou, China, from 1998 to 2003, based on Landsat TM/ ETM+ imagery. *Sensors*, Vol. 7, pp. 1323 – 1342.

Fan W. H., Zhang B. and Zhang R. (2008). Speciation Characteristics and Potential

Ecological Risk of Heavy Metals in Surface Sediments of Jinzhou Bay. *Marine Environmental Science*, Vol. 27, No. 1, pp. 54 – 58.

FAP 24 (1996). *Final Report*, Main Volume. Water Resource Planning Organisation, Dhaka, Bangladesh.

Ferguson R. I. (1993). Understanding Braiding Processes in Gravel-Bed Rivers: Progress and Unsolved Problems. In Best J. L. and Bristow C. S. (Eds.), *Braided Rivers*, Vol. 75. Geological Society Special Publication, pp. 73 – 87.

Finlayson D. P., Montgomery D. R. and Hallet B. (2002). Spatial Coincidence of Rapid Inferred Erosion with Young Metamorphic Massifs in the Himalayas. *Geology*, Vol. 30, pp. 219 – 222.

Finnegan N. J., Hallet B., Montgomery D. R., Zeitler P. K., Stone J. O., Anders A. M. and Liu Y. (2008). Coupling of Rock Uplift and River Incision in the Namche Barwa – Gyala Peri Massif, Tibet, China. *Geological Society of America Bulletin*, Vol. 120, pp. 142 – 155.

Fontaine T. A., Moore T. D. and Burgoa B. (2000). Distributions of Contaminant Concentration and Particle Size in Fluvial Sediment. *Water Research*, Vol. 34, Issue 13, pp. 3473 – 3477.

Förstner U. (1987). Changes in Metal Mobilities in Aquatic and Terrestrial Cycles. In Patterson J. W. and Pasino R. (Eds.), *Metals speciation, separation and recovery*. Lewis, Chelsea, pp. 3 – 26.

Förstner U. and Muller G. (1973). Heavy Metal Accumulation in River Sediments: A Response to Environmental Pollution. *Geoforum*, Vol. 4, Issue 2. pp. 53 – 61.

Four Rivers Reality (1996). *Mississippi River info*.
Accessed from www.4rivers.com/mississippi/info.html on 07/03/2014.

Freedman J. A. and Stauffer J. R. (2013). Gravel Dredging Alters Diversity and Structure of Riverine Fish Assemblages. *Freshwater Biology*, Vol. 58, No. 2, pp. 261 – 274.

Friend P. F. and Sinha R. (1993). Braiding and Meandering Parameters. In Best J. L., and Bristow C. S. (Eds.), *Braided Rivers*, The Geological Society, London, pp. 105 – 112.

Fu K., Su B., He D., Lu X., Song J. and Huang J. (2012). Pollution Assessment of Heavy

Metals Along the Mekong River and Dam Effects. *Journal of Geographical Sciences*, Vol. 22, Issue 5, pp. 874 – 884.

Gachal G. S., Slater F. M, Nisa Z. and Qadri A . H. (2006). Ecological Effect to the Status of the Indus Dolphin. *Pakistan Journal of Biological Sciences*, Vol. 9, pp. 2117 – 2121.

Gaillardet J., Bernard D., Allbgre C. J., Negrel P. (1997). Chemical and physical denudation in the Amazon River Basin, Chemical Geology, Vol. 142, pp. 141-173.

Galy A. and France-Lanord C. (1999). Weathering Processes in the Ganges–Brahmaputra Basin and the Riverine Alkalinity Budget. *Chemical Geology*, Vol. 159, Issues 1 – 4, pp. 31 – 60.

Galy A. and France-Lanord C. (2001). Higher Erosion Rates in the Himalaya: Geochemical Constraints on Riverine Fluxes. *Geology*, Vol. 29, pp. 23 – 26.

Gao X. and Chen C-TA. (2012). Heavy Metal Pollution Status in Surface Sediments Of the Coastal Bohai Bay. *Water Research*, Vol. 46, Issue 6, pp. 1901 – 1911.

Garbarino J. R., Hayes H., Roth D., Antweider R., Brinton T.I. and Taylor H. (1995). Contaminants in the Mississippi River, *U. S. Geological Survey Circular 1133*, Virginia, U.S.A.

Garzanti E., Andò S., France-Lanord C., Vezzoli G., Galy V. and Najman Y. (2010). Mineralogical and Chemical Variability of Fluvial Sediments 1. Bed Load Sand (Ganga – Brahmaputra, Bangladesh). *Earth and Planetary Sciences Letters*, Vol. 299, Issues 3 – 4, pp. 368 – 381.

Garzanti E., Ando S., France-Lanord C., Censi P., Vignola P., Galy V. and Lupker M. (2011). Mineralogical and Chemical Variability of Fluvial Sediments 2. Suspended-load Silt (Ganga – Brahmaputra, Bangladesh). *Earth and Planetary Sciences Letters*, Vol. 302, pp. 107 – 120.

Gay A., Cerdan O., Delmas M. and Desmet M. (2014). Variability of Suspended Sediment Yields Within the Loire River Basin (France). *Journal of Hydrology*, Vol. 519, pp. 1225 – 1237.

Geddes A. (1960). *The Alluvial Morphology of the Indo-Gangetic Plain: its Mapping and Geographical Significance*. Institute of British Geographers Transactions and Papers 28, pp. 253 – 276.

Gibbs R. J. (1967). The geochemistry of Amazon River system: Part I, The Factors that Control the Salinity and the Composition and Concentration of the Suspended Solids, *Geol. Soc. Amer. Bull*., Vol. 78, No 10, pp. 1203 – 32.

Gilbert G. K. (1917). Hydraulic-Mining Debris in the Sierra Nevada. *Geological Survey* (US), Vol. 105, p. 154.

Gob F., Houbrechts G., Hiver J. M. and Petit F. (2005). River Dredging, Channel Dynamics and Bed Load Transport in an Incised Meandering River (the River Semois, Belgium), *River Research and Applications*. Vol. 21, No. 7, pp. 791 – 804.

González A. E., Rodríguez M. T., Jiménez Sá J. C., Espinosa A. J. F. and Rosa F. J. B. (2000). *Water, Air & Soil Pollution*, Vol. 121, Issues 1 – 4, pp. 11 – 29.

Goodbred Jr S. L. and Kuehl S. A. (1998). Floodplain Processes in the Bengal Basin and the Storage of Ganges–Brahmaputra River Sediment: An Accretion Study Using Cs-137 and Pb-210 geochronology. *Sedimentary Geology*, Vol. 121, No. 3, pp. 239 – 258.

Goodbred Jr S. L. and Kuehl S. A. (1999). Holocene and Modern Sediment Budgets for the Ganges-Brahmaputra River: Evidence for High Stand Dispersal to Floodplain, Shelf and Deep-Sea Depocenters. *Geology*, Vol. 27, pp. 559 – 562.

Goswami D. C. (1985). Brahmaputra River, Assam, India: Physiography, Basin Denudation and Channel Aggradation. *Water Resources Research*, Vol. 21, No. 7, pp. 959 – 978.

Goswami D. C. (1998). Fluvial Regime and Flood Hydrology of the Brahmaputra River, Assam. *Memoir 41*, Geological Society of India, pp. 53 – 75.

Goswami U., Sarma J. N. and Patgiri A. D. (1999). River Channel Changes of the Subansiri in Assam, India. *Geomorphology*, Vol. 30, pp. 227 – 244.

Grabowski R. C., Droppo I. G. and Geraldene W. (2011). Erodibility of Cohesive Sediment: The Importance of Sediment Properties. *Earth Science Reviews*, Vol. 105, pp. 101– 20.

Grimshaw D. L. and Lewin J. (1980). Source Identification for Suspended Sediments. *Journal of Hydrology*, Vol. 47, pp. 151 – 162.

Gupta H. and Gahalaut V. K. (2014). Seismotectonics and Large Earthquake generation in the Himalayan Region. *Gondwana Research*, Vol. 25, Issue 1, pp. 204 – 213.

Gutman G., Janetos A. C., Justice C. O., Moran E. F., Mustard J. F., Rindfuss R. R., Skole D., Turner B. L. II, Cochrane M. A. (Eds.) (2004). *Land Change Science: Observing, Monitoring and Understanding Trajectories of Change on the Earth's Surface.* Remote Sensing and Digital Image Processing Series 6, Kluwer Academic, London.

Harbor D. J., Schumm S. A. and Harvey M. D. (1994). *Tectonic Control of the Indus River*. American Society of Civil Engineers Press, New York, pp. 161 – 175.

Harijan N., Kumarm A., Bhoi S. and Tare V. (2003). Course of River Ganga Over a Century Near Kanpur City Based on Remote Sensing Data. *Journal of the Indian Society of Remote Sensing*, Vol. 31, No. 1, pp. 1 – 2.

Harris N., Bickle M. J., Chapman H., Fairchild I. and Bunbury J. (1998). The Significance of Himalayan Rivers for Silicate Weathering Rates: Evidence from the Bhote Kosi tributary. *Chemical Geology*, Vol. 144, pp. 205 – 220.

Hassan K. I. and Galapatti R. (2014). Erosion Prediction Methods and Design of Equilibrium / Non-Equilibrium Channel Dimensions, In Changkakati P. P. and Dutta P. (Eds.), *Proceedings of the Assam Water Conference 2014*, Water Resources Department, Govt. of Assam, p. 10.

Hawkes J. S. (1997). Heavy Metals. *Journal of Chemical Education*, Vol. 74, No. 11, p. 1374.

Hay W. W. (1998). Detrital Sediment Fluxes from Continents to Oceans. *Chemical Geology*, Vol. 145, pp. 287 – 323.

Heiri O., Lotter A. F. and Lemcke G. (2001). Loss on Ignition as a Method for Estimating Organic and Carbonate Content in Sediments: Reproducibility and Comparability of Results. *Journal of Paleolimnology*, Vol. 25, Issue 1, pp. 101 – 110.

Hietel E., Waldhardt R. and Otte A. (2007). Statistical Modeling of Land-Cover Changes Based on Key Socioeconomic Indicators. *Ecological Economics*, Vol. 62, pp. 496 – 507.

Hjulstrom, F. (1935). Studies of the Morphological Activity of Rivers as Illustrated by the River Fyris. *Bulletin of the Geological Institute*, University of Uppsala, Vol. 25, pp. 221 – 257.

Hosmer D. W. and Lemeshow S. (2000). *Applied Logistic Regression*. John Wiley

and Sons Inc., New York, p. 375.

Hossain M. M. (1992). Total Sediment Load in the Lower Ganges and Jamuna. *Journal of the Institution of Engineers, Bangladesh*, Vol. 20, Issues 1 – 2, pp. 1 – 8.

Howard A. D., Keetch M. E. and Vincent C. L. (1970). Topological and Geometrical Properties of Braided Streams. *Water Resources Research*, Vol. 6, pp. 1674 – 1688.

Hu B., Yang Z., Wang H., Sun X., Bi N. and Li G. (2009). Sedimentation in the Three Gorges Dam and the Future Trend of Changjiang (Yangtze River) Sediment Flux to the Sea. *Hydrology and Earth System Sciences*, Vol. 13, pp. 2253 – 2264.

Hussain M. (1994). *Encyclopedia of India: Assam*. RIMA Publishing House, New Delhi.

Hutton M. and Symon C. (1986). The Quantities of Cadmium, Lead, Mercury and Arsenic Entering the U.K. Environment from Human Activities. *Science of the Total Environment*, Vol. 57, pp. 129 – 150.

ICIMOD (2009). *The Changing Himalayas, Impact of Climate Change on Water Resources and Livelihoods in the Greater Himalayas*: preprint for discussion and comments, International Centre for Integrated Mountain Development, pp. 6 – 7.

Imeson A. C. and Jungerius P. D. (1977). The Widening of Valley Incisions by Soil Fall in a Forested Keuper Area, Luxembourg. *Earth Surface Processes and Landforms*, Vol. 2, pp. 141 – 152.

Imeson A. C., Vis M. and Duysings J. J. H. M. (1984). Surface and Subsurface Sources of Suspended Solids in Forested Drainage Basins in the Keuper Region of Luxembourg. In Burt T.P. and Walling D.E. (Eds.), *Catchment Experiments in Fluvial Geomorphology*. GeoBooks, Norwich, pp. 219 – 234.

Ioannidou E., Flori A., Varouchakis E. A., Georgios G., Anthi Eirini K. V., George P. K. and Nikolaos N. (2015). Determination of Riverbank Erosion Probability Using Locally Weighted Logistic Regression. *Geophysical Research Abstracts*, Vol. 17.

Islam M. R., Begum S. F., Yamaguchi Y. and Ogawa K. (1999). The Ganges and Brahmaputra Rivers in Bangladesh: Basin Denudation and Sedimentation. *Hydrological Processes*, Vol. 13, Issue 17, pp. 2907 – 2923.

Jain C. K. (2004). Metal Fractionation Study on Bed Sediments of River Yamuna, India. *Water Research*, Vol. 38, Issue 3, pp. 569–578.

Jain C. K., Gupta H. and Chakrapani G. J. (2008). Enrichment and Fractionation of Heavy

Metals in Bed Sediments of River Narmada, India. *Environmental Monitoring and Assessment*, Vol. 141, No. 1, pp. 35 – 47.

James A. and Lecce S. A. (2013). Impacts of Land-Use and Land-Cover Change on River Systems. In J. Shroder (ed.), *Treatise on Geomorphology*, Academic Press, pp.768-793.

Jenne F. A. (1968). Controls of Mn, Fe, Co, Ni, Cu and Zn Concentrations in Soils and Water: The Significance of Hydrous Mn and Fe Oxides. Trace inorganics in water, Chapter 21, pp. 337 – 387.

Jiyuan L., Zengxiang Z., Xinliang X., Wenhui K., Wancun Z., Shuwen Z., Rendong L., Changzhen Y., Dongsheng Y., Shixin W. and Nan J. (2010). Spatial Patterns and Driving Forces of Land Use Change in China During the Early 21st Century. *Journal of Geographical Science*, Vol. 20, Issue 4, pp. 483 – 494.

Karbassi A. R. and Amirnezhad R. (2004). Geochemistry of Heavy Metals and Sedimentation Rate in a Bay Adjacent to the Caspian Sea. *International Journal of Environmental Science & Technology*, Vol. 1, No. 3, pp. 191 – 198.

Kemker C. (2014). Sediment Transport and Deposition. *Fundamentals of Environmental Measurements.* Fondriest Environmental Inc. Accessed from http://www.fondriest.com/environmental-measurements/parameters/hydrology/sediment-transport-deposition/ on 01.01.2015.

Kesel R. H. (2003). Human Modifications to the Sediment Regime of the Lower Mississippi River Flood Plain. *Geomorphology*, Vol. 56, Issues 3 – 4, pp. 325 – 334.

Kleinbaum D. G. and Klein M. (2002). *Logistic Regression: A Self Learning Text.* 2nd Edition, Springer-Verlag, New York, p. 513.

Knox J. C. (2001). Agricultural Disturbance in the Driftless Area. *Catena*, Vol. l42, pp. 193 – 224.

Knox J. C. (2006). Floodplain Sedimentation in the Upper Mississippi Valley: Natural versus Human Accelerated. *Geomorphology*, Vol. 79, Issues 3 – 4, pp. 286 – 310.

Kotoky P., Bezbaruah D., Baruah J. and Sarma J. N. (2005). Nature of Bank Erosion Along the Brahmaputra River Channel, Assam, India. *Current Science*, Vol. 88, No. 4, pp. 634 – 640.

Kotoky P., Dutta M. K. and Borah G. C. (2012). Changes in Land Use and Land Cover along the Dhansiri River Channel, Assam – A Remote Sensing and GIS Approach. *J. Geol. Soc. India*, Vol. 79, pp. 61 – 68.

Krishna K. S. (2004). Brahmaputra Flooding: Problems for Administrations and Prospects. In Singh V., Sharma N. and Ojha C. S. P. (Eds.), *The Brahmaputra Basin Water Resources*, Springer Netherlands, p. 315.

Krishnaswami S. and Singh S. K. (2005). Chemical Weathering in the River Basins of the Himalaya, India. *Current Science*, Vol. 89, No. 5, pp. 841 – 849.

Kuehl S. A, Hariu T. M. and Moore W. S. (1989). Shelf Sedimentation off the Ganges-Brahmaputra River System: Evidence for Sediment Bypassing to the Bengal Fan. *Geology*, Vol. 17, pp. 1132 – 1135.

Kumar G. (1997). *Geology of the Arunachal Pradesh*, Geological Society of India, Bangalore.

Kundu A., Matin A. and Mukul M. (2012). Depositional Environment and Provenance of Middle Siwalik Sediments in Tista Valley, Darjiling District, Eastern Himalaya, India. *J. Earth Syst. Sci*., Vol. 121, No. 1, pp. 73 – 89.

Lahiri S. K. and Sinha R. (2012). Tectonic Controls on the Morphodynamics of the Brahmaputra River System in the Upper Assam Valley, India. *Geomorphology*, Vol. 169 – 170, pp. 74 – 85.

Lahiri S. K. and Sinha R. (2014). Morphotectonic Evolution of the Majuli Island in the Brahmaputra Valley of Assam, India Inferred from Geomorphic and Geophysical Analysis. *Geomorphology*, Vol. 227, pp. 101 – 111.

Lane E. W. (1947). Report of the Subcommittee on Sediment Terminology. *Eos Trans*, AGU, Vol. 28, Issue. 6, pp. 936 – 938.

Lane E. W. (1957). *A Study of the Shape of Channels Formed by Natural Streams Flowing in Erodible Material*. Missouri River Division Sediment Series No. 9, U.S. Army Engineering Division Missouri River, Corps of Engineers, Omaha, Nebraska.

Lane E. W. and Borland W. M. (1951). Estimating Bed Load. *Eos Trans*, AGU, Vol. 32, Issue 1, pp. 121 – 123.

Lane S. N., Westaway R. M. and Hicks D. M. (2003). Estimation of Erosion and

Deposition Volumes in a Large, Gravel-Bed, Braided River Using Synoptic Remote Sensing. *Earth Surface Processes and Landforms*, Vol. 28, pp. 249–271.

Larsen I. J. and Montgomery D. R. (2012). Landslide Erosion Coupled to Tectonics and River Incision. *Nature Geoscience*, Vol. 5, pp. 468 – 473.

Latrubesse E. (2008). Patterns of Anabranching Channels: The Ultimate End-Member Adjustment of Mega Rivers. *Geomorphology*, Vol. 101, No. 1, pp. 130–145.

Lawler D. M., Grove J. R., Couperthwaite J. S. and Leeks G. J. L. (1999). Downstream Change in River Bank Erosion Rates in the Swale – Ouse System, Northern England. *Hydrological Processes*, Vol. 13, Issue 7, pp. 977 – 992.

Le T. P. Q., Garnier J., Gilles B., Sylvain T. and Van Minh C. (2007). The Changing Flow Regime and Sediment Load of the Red River, Viet Nam. *Journal of Hydrology*, Vol. 334, pp. 199 – 214.

Lebert M. and Horn R. (1991). A Method to Predict the Mechanical Strength of Agricultural Soils. *Soil and Tillage Research*, Vol. 19, Issues 2 – 3, pp. 275 – 286.

Lee S. (2005). Application of Logistic Regression Model and its Validation for Landslide Susceptibility Mapping Using GIS and Remote Sensing Data. *International Journal of Remote Sensing*, Vol. 26, Issue 7, pp. 1477 – 1491.

Leeder M. R. and Alexander J. (1987). The Origin and Tectonic Significance of Asymmetrical Meander-Belts. *Sedimentology*, Vol. 34, Issue 2, pp. 217–226.

Lenntech Water Treatment and Air Purification (2004). *Water Treatment*, Lenntech, Rotterdamseweg, Netherlands.

Leopold L. B. and Wolman M. G. (1957). River Channel Patterns: Braided, Meandering, and Straight. *U.S.S Geol. Surv. Prof. Pap*., 282-B, pp. 39 – 85.

Lewin J. and Ashworth P. J. (2014). Defining Large River Channel Patterns: Alluvial Exchange and Plurality. *Geomorphology*, Vol. 215, pp. 83 – 98.

Li L., Lu X. and Chen Z. (2007). River Channel Change During the Last 50 Years in the Middle Yangtze River, the Jianli Reach. *Geomorphology*, Vol. 85, Issues 3 – 4, pp. 185 – 196.

Li X., Zhou Y. X., Zhang L. P., and Kuang R. Y. (2014). Shoreline Change of Chongming Dongtan and Response to River Sediment Load: a Remote Sensing Assessment. *Journal of Hydrology*, Vol. 511, pp. 432 – 442.

Liu C., Sui J. and Wan Zhao-Yin. (2008). Sediment Load Reduction in Chinese Rivers. *International Journal of Sediment Research*, Vol. 23, pp. 44 – 55.

Liu J., Wang G., Li H., Gong J. and Han J. (2013). Water and Sediment Evolution in Areas With High and Coarse Sediment Yield of the Loess Plateau. *International Journal of Sediment Research*, Vol. 28, Issue 4, pp. 448 – 457.

Liu J. P., Xue Z., Ross K., Wang H. Z., Yang Z. S., Li A. C. and Gao S. (2009). Fate of Sediments Delivered to the Sea by Asian Large Rivers: Long-Distance Transport and Formation of Remote Alongshore Clinothems. *The Sedimentary Record*, Vol. 7, No. 4, pp. 4 – 9.

Liu Y., Cao Li., Li Z., Wang H., Chu T. and Zhang J. (1984). *Element Geochemistry*, Science Press, Beijing, pp. 80 – 85.

Lohnes R. A. and Handy R. L. (1968). Slope Angles in Friable Loess. *The Journal of Geology*, Vol. 76, No. 3, pp. 247 – 258.

Loizeau J. L., Arbouille D., Santiago S. and Vernet J. P. (1994). Evaluation of a Wide Range Laser Diffraction Grain Size Analyzer for Use With Sediments. *Sedimentology*, Vol. 41, Issue 2, pp. 353 – 361.

Long H. L., Wu X. Q., Wang W. J. and Dong G. H. (2008). Analysis of Urban-Rural Land-Use Change During 1995-2006 and its Policy Dimensional Driving Forces in Chongqing, China. *Sensors*, Vol. 8, pp. 681 – 699.

Lupker M., France-Lanord C., Galy V., Lave´ J. and Kudrass H. (2013). Increasing Chemical Weathering in The Himalayan System Since the Last Glacial Maximum. *Earth and Planetary Science Letters*, Vol. 365, pp. 243 – 252.

Mahajan S. and Panwar P. (2005). Land Use Changes in Ashwani Khad Watershed Using GIS Techniques. *J. Indian Soc. Remote Sens*. Vol. 33, pp. 227 – 232.

Mahanta C. and Saikia L. (2015). The Brahmaputra and Other Rivers of the North-East. In Iyer R. R. (Ed.), *Living Rivers Dying Rivers*, Oxford University Press, New Delhi, p. 155.

Mahanta C. and Subramanian V. (2004). Water Quality, Mineral Transport and Sediment Biogeochemistry. In Singh V., Sharma N. and Ojha C. S. P. (Eds.), *The Brahmaputra Basin Water Resources*, Springer Netherlands, pp. 376 – 400.

Maia P. D., Maurice L., Tessier E., Amouroux D., Cossa D., Pérez M., Moreira-Turcq M.

and Rhéault I. (2009). Mercury Distribution and Exchanges Between Amazon River and Connected Floodplain Lakes. *Science of the Total Environment,* Vol. 407, Issue 23, pp. 6073 – 6084.

Maitra J. (2004): Boundary Dispute Between West Bengal and Jharkhand. *Correspondences and Documents*. Published by CPI(M) District Committee, Malda, pp. 17 – 19.

Martin J. M. and Meybeck M. (1979). Elemental Mass Balance of Material Carried by Major World Rivers. *Marine Chemistry,* Vol. 7, Issue 3, pp. 173 – 206.

Martinez J. M., Guyot J. L., Filizola N. and Sondag F. (2009). Increase in Suspended Sediment Discharge of Amazon River Assessed by Monitoring Network and Satellite Data. *Catena,* Vol. 79, Issue 3, pp. 257 – 264.

Maurice-Bourgoin L, Bonnet M. P., Martinez J. M., Kosuth P., Cochonneau G., Moreira-Turcq P., Guyot J.L., Vauchel P., Filizola N. and Seyler P. (2007). Temporal Dynamics of Water and Sediment Exchanges Between the Curuaí Floodplain and Amazon River Main Stream, Brazil. *Journal of Hydrology,* Vol. 335, pp. 140 – 156.

Maurice-Bourgoin L., Quiroga I., Chincherros J. and Courau P. (2000). Mercury Distribution in Waters and Fishes of the Upper Madeira Rivers and Mercury Exposure in Riparian Amazonian Populations. *Science of the Total Environment,* Vol. 260, Issue 1 – 3, pp. 73 – 86.

McCave I. N., Bryant R. J., Cook H. F. and Coughanowr C. A. (1986). Evaluation of a Laser Diffraction Size Analyzer for Use with Natural Sediments. *J. Sed. Petr*., Vol. 56, pp. 561 – 564.

Meade R. H. (2007). Transcontinental Moving and Storage: the Orinoco and Amazon RiversTransfer the Andes to the Atlantic. In Gupta A. (Ed.), *Large Rivers: Geomorphology and Management,* Wiley, Chichester, pp. 45 – 63.

Mehta A. J. and Partheniades E. (1973). *Depositional Behavior of Cohesive Sediments*. Tech report No. 16, Univ. of Florida, Gainesville, Florida.

Mertes L. A. K., Dunne T. and Martinelli L. A. (1996). Channel-Floodplain Geomorphology along the Solimões–Amazon River, Brazil. *Geological Society of America Bulletin,* Vol. 108, pp. 1089 – 1107.

Miao C. (2010). Recent Changes of Water Discharge and Sediment Load in the Yellow River Basin, China. *Progress in Physical Geography*, Vol. 34, No. 4, pp. 541 – 561.

Miller J. (1997). The Role of Fluvial Geomorphic Processes in the Dispersal of Heavy Metals from Mine Sites. *Journal of Geochemical Exploration*, Vol. 58, Issues 2 – 3, pp. 101 – 118.

Milliman J. D. and Meade R. H. (1983). World-wide Delivery of River Sediment to the Oceans. *The Journal of Geology*, Vol. 91, No. 1, pp. 1 – 21.

Milliman J. D., Rutkowski C. and Meybeck M. (1995). *River Discharge to the Sea: A Global River Index (GLORI).* Netherlands Sea Research Institute (NIOZ). P. 125.

Milliman J. D. and Syvitski P. M. (1992). Geomorphic/ Tectonic Control of Sediment Discharge to the Ocean: The Importance of Small Mountainous Rivers. *The Journal of Geology*, Vol. 100, pp. 525 – 544.

Mitra A., Chowdhury R. and Banerji K. (2012). Concentrations of Some Heavy Metals in Commercially Important Finfish and Shellfish of the River Ganga. *Environmental Monitoring and Assessment*, Vol. 184, Issue 4, pp. 2219 – 2230.

Miyazawa N., Sunada K. and Sokhem P. (2008). Bank Erosion in the Mekong River Basin: Is Bank Erosion in My Town Caused by the Activities of My Neighbors? In Kummu, M., Keskinen, M. & Varis, O. (Eds.), *Modern Myths of the Mekong*, pp. 19 – 26.

Mohindra R., Parkash B. and Prasad J. (1992). Historical Geomorphology and Pedology of the Gandak Megafan, Middle Gangetic plains, India. *Earth Surface Processes and Landforms*, Vol. 17, pp. 643 – 662.

Mondal M. S., Shrama N., Kappas M. and Garg P. K. (2013). Modeling of Spatio-temporal Dynamics of Land Use and Land Cover in a Part of Brahmaputra River Basin Using Geoinformatic Techniques. *Geocarto Int.*, Vol. 28, Issue 7, pp. 632 – 656.

Mookerjea D. (1961). The Kosi - a Challenge in River Control. *Journal of Institution of Engineers*, XLII, 3, p. 125.

Morgan R. P. C. (2005). *Soil Erosion and Conservation*. Blackwell, Oxford. p. 304.

Mosley P. M. (1981). Semi-determinate Hydraulic Geometry of River Channels, South Island, New Zealand. *Earth surface Processes and Landforms*, Vol. 6, pp. 127–

137.

MRC (2010). *State of the Basin Report 2010*. Mekong River Commission, Vientiane, Laos.

Muller G. (1979). Schwermetalle in den Sedimenten des Rheins Veranderungen seit. *Umschau*, Vol. 79, pp. 778 – 783.

Munroe D., Müller D. (2007). Issues in Spatially Explicit Statistical Land-Use/ Cover Change (LUCC) Models: Examples from Western Honduras and the Central Highlands of Vietnam. *Land Use Policy*, Vol. 24, pp. 521– 530.

Nagelkerke N. J. D. (1991). A note on a general definition of the coefficient of Determination. *Biometrika*, Vol. 78, pp. 691 – 692.

Nandi D. R. (2001). *Geodynamics of Northeastern India and the adjoining region*. acb publications, India.

Nanson G. C. and Croke J. C. (1992). A Genetic Classification of Floodplains. *Geomorphology*, Vol. 4, pp. 459 – 486.

Nasermoaddeli M. H. and Pasche E. (2008). Application of Terrestrial 3D Laser Scanner in Quantification of the Riverbank Erosion and Deposition. *Proceedings of River flow 2008*, Turkey, pp. 3 – 5.

NDTV (2016). *Dredging of Brahmaputra Soon to Stop Floods, Erosion*: Sarbananda Sonowal. Accessed from http://www.ndtv.com/india-news/dredging-of-brahmaputra-soon-to-stop-floods-erosion-sarbananda-sonowal-1449306 on 09.11.2016.

NEC (1993). Chapter VIII, Morphological Studies of River Brahmaputra, WAPCOS, pp. VIII – 2.

Negrel P., Allegre C. J., Dupre B. and Lewin E. (1993). Erosion sources determined by inversion of major and trace element ratios and strontium isotopic ratios in river water: The Congo Basin case. *Earth and Planetary Science Letters*, Vol. 120, pp. 59 – 76.

Nikiforova E. M. and Smirnova R. S. (1975). Metal Technophility and Lead Technogenic Anomalies. *Abstract: International Conference on Heavy Metals in the Environment*, Toronto, pp. 94 – 96.

Nishina T., Kien C. N., Noi N. V., Ngoc H. M., Kim C. S., Tanaka S. and Iwasak K.

(2010). Pesticide Residues in Soils, Sediments, and Vegetables in the Red River Delta, Northern Vietnam. *Environmental Monitoring and Assessment*, Vol. 169, Issues 1 – 4, pp. 285–297

Noe G. B. and Hupp C. R. (2009). Retention of Riverine Sediment and Nutrient Loads by Coastal Plain Floodplains. *Ecosystems*, Vol. 12, pp. 728–746.

Norvell W. A. and Lindsay W. L. (1972). Reactions of DTPA Chelates of Iron, Zinc, Copper and Manganese with Soils. *Soil Science Society of America Journal*, Vol. 36, pp. 778 – 783.

Nriagu J. O. (1989). A Global Assessment of Natural Sources of Atmospheric Trace Metals. *Nature*, Vol. 338, pp. 47 – 49.

Nriagu J. O., Pacyna J. (1988). Quantitative Assessment of Worldwide Contamination of Air, Water and Soil by Trace Metals. *Nature*, Vol. 333, pp. 134 – 139.

Nwuche C. O. and Ugoji E. O. (2010). Effect of Co-existing Plant Species on Soil Microbial Activity Under Heavy Metal Stress. *International Journal of Environmental Science and Technology*, Vol. 7, issue 4, pp. 697 – 704.

Nystrand M. I., Österholm P., Nyberg M. E. and Gustafsson J. P. (2012). Metal Speciation in Rivers Affected by Enhanced Soil Erosion and Acidity. *Applied Geochemistry*, Vol. 27, Issue 4, pp. 906 – 916.

Oak R. A. (2014). Permeable Structures with Foundation/ Bed Protection for Anti-erosion Works. In Changkakati P. P. and Dutta P. (Eds.), *Proceedings of Assam Water Conference – 2014*, Water Resources Department, Govt. of Assam, pp. 109 – 116.

Odgaard A. J. (2017). River Management with Submerged Vanes. In Sharma N. (Ed.), *River System Analysis and Management*, Springer Singapore, pp. 251 – 261.

Ohlmacher C. G. and Davis C. J. (2003). Using Multiple Regression and GIS Technology to Predict Landslide Hazard in Northeast Kansas, USA. Engineering Geology, Vol. 69, Issue 3 – 4, pp. 331 – 343.

Ojha C. S. P. and Singh V. P. (2004). Introduction. In Singh V., Sharma N. and Ojha C. S. P. (Eds.), *The Brahmaputra Basin Water Resources*, Springer Netherlands, p. 2.

Ollier C. C. (1969). Weathering. Oliver and Boyd, Edinburg, p. 304.

Osman A. M. and Thorne C. R. (1988). Riverbank Stability Analysis I: Theory. *Journal of Hydraulic Engineering (ASCE)*, Vol. 114, pp. 134 – 150.

Owens P. (2005). Conceptual Models and Budgets for Sediment Management at the River Basin Scale. *Journal of Soils and Sediments*, Vol. 5, Issue 4, pp. 201 – 212.

Ozdemir A. (2011). Landslide Susceptibility Mapping Using Bayesian Approach in the Sultan Mountains (Aks_ehir, Turkey). *Natural Hazards*, Issue 59, pp. 1573 – 1607.

Pahuja S. and Goswami D. (2006). A Fluvial Geomorphology Perspective on the Knowledge Base Brahmaputra. Draft paper No. 3, *Study of Natural Resources, Water and the Environmental nexus for development and growth in Northeast India*, World Bank and Gauhati University.

Pandey M., Tripathi S., Pandey A. K. and Tripathi B. D. (2014). Risk Assessment of Metal Species in Sediments of the River Ganga. *Catena*, Vol. 122, pp. 140 – 149.

Pandey S. K., Singh A. K. and Hasnain S. I. (1999). Weathering and Geochemical Processes Controlling Solute Acquisition in Ganga Headwater – Bhagirathi River, Garhwal Himalaya, India. *Aquatic Geochemistry*, Vol. 5, Issue 4, pp. 357 – 379.

Partheniades E. (2007). *Engineering Properties and Hydraulic Behavior of Cohesive*, CRC, Boca Raton, p. 338.

Peng J., Wang Y. L., Wu J. S., Yue J., Zhang Y. and Li W. F. (2006). Ecological Effects Associated with Land Use Change in China's Southwest Agriculture Landscape. *International Journal of Sustainable Development & World Ecology*, Vol. 13, pp. 315 – 325.

Phillips J. D. (1992). The Source of Alluvium in Large Rivers of the Lower Coastal Plain of North Caroloina. *Catena*, Vol. 19, Issue 1, pp. 59 – 75.

Piper D. Z., Steve Ludington J. S. and Duval H. E. T. (2006). Geochemistry of Bed and Suspended Sediment in the Mississippi River System: Provenance versus Weathering and Winnowing. *Science of the Total Environment*, Vol. 362, pp. 179–204.

Pizzuto J. E. (1984). Bank Erodibility of Shallow Sand-Bed Streams. *Earth Surface Processes and Landforms*, Vol. 9, Issue 2, pp. 113 – 124.

Poddar M. C. (1952). Preliminary Report of the Assam Earthquake, 15th August, 1950 (No. 2). *Bulletins of the Geological Survey of India* (Series B), p. 40.

Pye K. and Blott S. J. (2004). Particle Size Analysis of Sediments, Soils and Related

Particulate Materials for Forensic Purposes Using Laser Granulometry. *Forensic Science International*, Vol. 144, Issue 1, pp. 19 – 27.

Qiao S., Yang Z., Pan Y. and Guo Z. (2007). Metals in Suspended Sediments from the Changjiang (Yangtze River) and Huanghe (Yellow River) to the Sea and Their Comparison. *Estuarine Coastal and Shelf Science*, Vol. 74, Issue 3, pp. 539 – 548.

Quirk J. P. (2001). The Significance of the Threshold and Turbidity Concentrations in Relation to Sodicity and Microstructure. *Australian Journal of Soil Research*, Vol. 39, Issue 6, pp. 1185 – 1217.

Rabitto, I. S., Bastos W.R., Almeida R., Anjos A., De holanda I. B. B., Galvão R. C. F., Filipakneto F., Menezes M. L., Santos C. A. M. and Oliveira Ribeiro C. A. (2011). Mercury and DDT Exposure Risk to Fish-Eating Human Populations in Amazon. *Environment International*, Vol. 37, Issue 1, pp. 56 – 65.

Radoane M., Radoane N., Dumitriu D. and Miclau C. (2008). Downstream Variation in Bed Sediment Size along the East Carpathian Rivers: Evidence of the Role of Sediment Sources. *Earth Surface Processes and Landforms*, Vol. 33, Issue 5, pp. 674 – 694.

Rahman M. M., Hussain M. A., Islam G. M. T., Haque M. A. and Hoque M. M. (2004). Hydro-Morphological Characteristics Around the Meghna Bridge Site in the Meghna River, *Japan Bangladesh Joint Study Project on Floods*; Phase II: Final Report.

Raj P. P. N. and Azeez P. A. (2010). Land Use and Land Cover Changes in a Tropical River Basin: A Case from Bharathapuzha River Basin, Southern India. *Journal of Geographic Information System*, Vol. 2, pp. 185 – 193.

Rapp A. (1960). Recent Development of Mountain Slopes in Kärkevagge and Surroundings, Northern Scandinavia. *Geografiska Annaler*, Vol. 422, pp. 65 – 200.

Raudkivi A. J. (1999). Loose Boundary Hydraulics-Grey zones. In A.W. Jayawardena A. W., Lee J. H. W. and Wang J. W. (Eds.), *River Sedimentation: Theory and Applications*: Proceedings of the Seventh International Symposium on River Sedimentation, Balkema, Rotterdam, Netherlands, p. 5.

Rauret G., Lopez-Sanchez J. F., Sahuquillo A., Rubio R., Davidson C., Ure A. and Quevauvillerc P. (1999). Improvement of the BCR Three Step Sequential

Extraction Procedure Prior to the Certification of New Sediment and Soil Reference Materials. *Journal of Environmental Monitoring*, Issue 1, pp. 57 – 61.

Rengasamy P. and Churchman G. J. (1999). Cation exchange Capacity, Exchangeable Cations and Sodicity. In Peverill K. I., Sparrow L. A. and Reuter D. J. (Eds.), *Soil Analysis: An Interpretation Manual*, CSIRO Publishing, Collingwood.

Richardson W. R. (1997). *Secondary Flow and Channel Change in Braided Rivers*. Unpublished PhD Thesis, School of Geography, University of Nottingham, UK, pp. 281.

Richardson W. R., Thorne C. R. (2001). Multiple Thread Flow and Channel Bifurcation in a Braided River: Brahmaputra–Jamuna River, Bangladesh. *Geomorphology*, Vol. 38, pp. 185 – 196.

Ridgway J. and Shimmield G. (2002). Estuaries as Repositories of Historical Contamination and Their Impact on Shelf Seas. Estuarine, *Coastal and Shelf Science*, Vol. 55, Issue 6, pp. 903 – 928.

Robinson D. A. and Phillips C. P. (2001). Crust Development in Relation to Vegetation and Agricultural Practice on Erosion-Susceptible, Dispersive Clay Soils from Central and Southern Italy. *Soil Tillage Research*, Vol. 60, Issues 1 – 2, pp. 1 – 9.

Robinson W. O. (1927). The Determination of Organic Matter in Soils by means of Hydrogen Peroxide. *Journal of Agricultural Research*, Vol. 34, No. 4, pp. 339 – 356.

Rowell D. L. (1994). Soil Science: Methods and Applications. Longman, p. 350.

Roy N. G. and Sinha R. (2005) Alluvial Geomorphology and Confluence Dynamics in the Gangetic Plains, Farrukhabad – Kannauj Area, Uttar Pradesh, India. *Current Science*, Vol. 88, pp. 2000 – 2006.

RSP (River Survey Project) (1996). *Spatial Representation and Analysis of Hydraulic and Morphological Data.* Report no FAP 24, WARPO, Dhaka, Bangladesh.

Rui Y. K., Qu L. C. and Kong X. B. (2008). Effects of Soil Use Along Yellow River Basin On the Pollution of Soil by Heavy Metals. *Spectroscopy and Spectral Analysis*, Vol. 4, pp. 934 – 936.

Russell R. D. (1937). Mineral Composition of Mississippi River Sands. *Geological Society of America Bulletin*, Vol. 48, No. 9, pp. 1307 – 1348.

Rust B. R. (1978). A Classification of Alluvial Channel Systems. In Miall A. D. (Ed.), *Fluvial Sedimentology*, Canadian Society of Petroleum Geologist, Alberta, pp. 187–198.

Sanford L. P. (2008). Modeling a Dynamically Varying Mixed Sediment Bed with Erosion, Deposition, Bioturbation, Consolidation, and Armoring. *Computers & Geosciences*, Vol. 34, Issue 10, pp. 1263 – 1283.

Santis F. De., Giannossi M. L., Medici L., Summa V. and Tateo F. (2010). Impact of Physico-Chemical Soil Properties on Erosion Features in the Aliano Area (Southern Italy). *Catena,* Vol. 81, Issue 2, pp. 172 – 181.

Santos Bermejo J. C., Beltrán R., Gómez Ariza J. L. (2003). Spatial Variations of Heavy Metals Contamination in Sediments from Odiel River (Southwest Spain). *Environmental International*, Vol. 29, Issue 1, pp. 69 – 77.

Sarin M. M., Borole D. V. and Krishnaswami S. (1979). Geochemistry and Geochronology of Sediments from the Bay of Bengal and the Equatorial Indian Ocean. *Proceedings of the Indian Academy of Sciences*, Vol. 88, pp. 131 – 154.

Sarin M. M., Krishnaswami S., Dilli K., Somayajulu B. L. K. and Moore W. S. (1989). Major Ion Chemistry of the Ganga– Brahmaputra River System: Weathering Processes and Fluxes to The Bay of Bengal. *Geochimca at Cosmochimica Acta*, Vol. 53, Issue 5, pp. 997 – 1009.

Sarkar A., Garg R. D and Sharma N. (2012). RS-GIS Based Assessment of River Dynamics of Brahmaputra River in India. *Journal of Water Resource and Protection*, Vol. 4, No. 2, pp. 63 – 72.

Sarkar M. H. and Thorne C. R. (2006). Morphological Response of the Brahmaputra-Padma-Lower Meghna River System to the Assam Earthquake of 1950. *Braided Rivers*, Special Publication No. 36, International Association of Sedimentologists.

Sarma J. N. (2005). Fluvial Processes and Morphology of the Brahmaputra River in Assam, India. *Geomorphology*, Vol. 70, Issues 3 – 4, pp. 226 – 256.

Sarma J. N. and Phukan M. K. (2004). Origin and Some Geomorphological Changes of Majuli Island of the Brahmaputra River in Assam, India. *Geomorphology*, Vol. 60, pp. 1 – 9.

Schaffernak F. (1922). Neue Grundlagen fur die Berechnung der Geschiebefuhrung in

Flusslaufen, Franz Deuticke (New Bases for Calculating Bed-Load Transportation in River Courses). Leipzig und Wien, p.48.

Schilling K. E., Chan K., Liu H., Zhang Y. (2010). Quantifying the Effect of Land Use Land Cover Change on Increasing Discharge in the Upper Mississippi River. *Hydrology*, Vol. 387, No. 3–4, pp. 343 – 345.

Schulz J. J., Cayuela L., Echeverria C., Salas J. and Benayas J. M. R. (2010). Monitoring Land Cover Change of Dry Land Forest Landscape of Central Chile. *Applied Geography*, Vol. 30, pp. 436 – 447.

Schumm S. A. (1960). The Shape of Alluvial Channels in Relation to Sediment Type. US Geological Survey Professional Paper No. 352-B.

Schumm S. A. (1971). Fluvial Geomorphology: Historical Perspective. In Shen H. W. (Ed.), *River Mechanics*, Collins, Colorado.

Schumm S. A. (1977). *The Fluvial System*. John Wiley & Sons, New York, p. 388

Schumm S. A., Dumont J. F. and Holbrook J. M. (2000). *Active Tectonics and Alluvial Rivers*. Cambridge University Press, Cambridge, p. 276.

Sekely A. C., Mulla D. J. and Bauer D. W. (2002). Streambank Slumping and its Contribution to the Phosphorus and Suspended Sediment Loads of the Blue Earth River, Minnesota. *Journal of Soil and Water Conservation*, Vol. 57, pp. 243 – 250.

Selley R. C. (2000). Weathering and the Sedimentary Cycle. *Applied Sedimentology*. Academic Press, USA, p. 22 – 25.

Seto K. C. and Kaufmann R. K. (2003). Modelling the Drivers of Urban Land Use Change in the Pearl River Delta, China: Integrating Remote Sensing with Socioeconomic Data. *Land Econ.* Vol. 79, pp. 106 – 121.

Sharma N. (2004). Mathematical Modeling and Braid Indicator in Brahmaputra River Basin. *Water Resource*, Vol. 4, pp. 229 – 260.

Sharma N. and Nayak A. (2015). RCC Jack Jetty and Bamboo Submerged Vanes Application for Navigation Fairway in Ganga River of India. Paper 173, *Smart Rivers 2015*, Buenos Aires, Argentina.

Shi C. and Zhang D. D. (2005). A Sediment Budget of the Lower Yellow River, China, Over The Period from 1855 to 1968. *Geografiska Annaler*: Series A, Physical Geography, Vol. 87, Issue 3, pp. 461 – 471.

Simon A. (1989). The Discharge of Sediment in Channelized Alluvial Streams. *Journal of the American Water Resources Association*, Vol. 25, Issue 6, pp. 1177 – 1188.

Simon A. and Darby S. E. (1999). The Nature and Significance of Incised River Channels. In Darby S. E. and Simon A. (Eds.), *Incised river channels*, John Wiley and Sons, Chichester, UK, pp. 3 – 18.

Singh G. (1990). "Soil and Water Conservation in India." In *Proceedings of Symposium on Water Erosion, Settlement and Resource Conservation*, Dehradun, India.

Singh I. B. (1996). Geological Evolution of Ganga Plain- an Overview. *Journal of Palaeontological Society of India*, Vol. 41, pp. 99 – 137.

Singh M, Singh I. B. and Muller G. (2007) Sediment Characteristics and Transportation Dynamics of the Ganga River. *Geomorphology*, Vol. 86, pp. 144 – 175.

Singh S. K., France-Lanord C. (2002) Tracing the Distribution of Erosion in the Brahmaputra Watershed from Isotopic Compositions of Stream Sediments. *Earth and Planetary Science Letters*, Vol. 202, Issues 3 – 4, pp. 645 – 662.

Singh S., Sarin M. M. and France-Lanord C. (2005). Chemical Erosion in the Eastern Himalaya: Major Ion Composition of the Brahmaputra and $^{13}C$ of Dissolved Inorganic Carbon. *Geochimica et Cosmochimica Acta*, Vol. 69, No. 14, pp. 3573 – 3588.

Slaymaker O. (2003). The Sediment Budget as Conceptual Framework and Management Tool. *Hydrobiologia*, Vol. 494, Issues 1 – 3, pp. 71 – 82.

Souza-Filho P. W. M., de Souza E. B., Silva Jr. R. O., Nascimento. Jr. W. R., de Mendonça B. R. V., Guimarães J. T. F., Agnol R. D. and Siqueira J. O. (2016). Four Decades of Land-Cover, Land-Use and Hydroclimatology Changes in the Itacaiúnas River Watershed, Southeastern Amazon. *Journal of Environmental Management*, Vol. 167, pp. 175–184.

Srivastava A. and Singh R. P. (1999). Surface Manifestation Over a Subsurface Ridge. *International Journal of Remote Sensing*, Vol. 20, Issue 18, pp. 3461 – 3466.

Stalenberg B. and Kikumori Y. (2008). Urban Flood Control on the Rivers of Tokyo Metropolitan. In Graaf, R. D. and Hooimeijer, F. (Eds.), *Urban Water in Japan*, Taylor & Francis Group, London, UK, pp. 119 – 141.

Stallard R. F. and Edmond J. M. (1983). Geochemistry of Amazon: The influence of

Geology and Weathering Environment on Dissolved Load. *Journal of Geophysical Research*, Vol. 88, Issue C14, pp. 9671 – 88.

Steiger J., Gurnell A. M., Ergenzinger P. and Snelder D. (2001). Sedimentation in the Riparian Zone of an Incising River. *Earth Surface Processes and Landforms*, Vol. 26, pp. 91–108.

Sternberg H. (1875). Untersuchungen ueber laengen-und querprofil geschiebefuehrende flusse. Zeitschrift fuer das Bauwesen, Vol. 25, pp. 483 – 506. [collected from Radoane et al. (2008)]

Stewart R. J., Hallet B., Zeitler P. K., Malloy M. A., Allen C. M. and Trippett D. (2008). Brahmaputra Sediment Flux Dominated by Highly Localized Rapid Erosion from the Eastern Most Himalaya. *Geology*, Vol. 36, pp. 711 – 714.

Stigliani W. M. (1991). *Chemical Time Bombs: Definition, Concepts and Examples*, IIASA Executive Report 16.

Storti F. and Balsamo F. (2010). Particle Size Distributions by Laser Diffraction: Sensitivity of Granular Matter Strength to Analytical Operating Procedures. *Solid Earth*, Vol. 1, pp. 25 – 48.

Stummeyer J., Marchig V. and Knabe W. (2002). The Composition of Suspended Matter from Ganges-Brahmaputra Sediment Dispersal System During Low Sediment Transport Season. *Chemical Geology*, Vol. 185, pp. 125 – 147.

Subramanian V. and Ramanathan A. L. (1996). Nature of Sediment Load in the Ganges-Brahmaputra River Systems in India. In Milliman J. D. and Haq B. U. (Eds.), *Sea-Level Rise and Coastal Subsidence: Causes, Consequences, and Strategies*, Kluwer Academic Publisher, pp. 151 – 168.

Subramanian V., Richey J. E. and Abbas N. (1985). Geochemistry of River Basins of India, Pt II: Preliminary studies on the particulate C and N in the Ganges-Brahmaputra river system. In Degens E. T., Kempe S. and Herrera R. (Eds.), *Transport of Carbon and Minerals in Major World Rivers*, Mitt. Geol.- Paläont. Inst. Univ. Hamburg, pp. 513 – 518.

Subramanian V., Van Grieken R. and Van't Dack L. (1987). Heavy Metals Distribution in the Sediments of Ganges and Brahmaputra Rivers. *Environmental Geology*, Vol. 9, pp. 93 – 105.

Suif Z., Yoshimura C., Valeriano O. C. S. and Seingheng H. (2013). Spatially Distributed Model for Soil Erosion and Sediment Transport in the Mekong River Basin. *International Water Technology Journal*, Vol. 3, p. 4.

Sumner M. E. (1993). Sodic Soils: New Perspectives. *Australian Journal of Soil Research*, Vol. 31, pp. 683 – 750.

Sun Z., Ma R. and Wand Y. (2009). Using Landsat Data to Determine Land Use Changes in Datong Basin, China. *Environmental Geololgy*. Vol. 57, pp. 1825–1837.

Swamee P. K., Parkash B., Thomas J. V. and Singh S. (2003). Changes in Channel Pattern of River Ganga Between Mustafabad and Rajmahal, Gangetic Plains since 18th Century. *International Journal of Sediment Research*, Vol. 18, pp. 219 – 231.

Swanson K. M., Watson E., Aalto R. E., Lauer J. W., Dietrich W. E., Apte S., Bera M., Marshall A. and Taylor M. (2008). Sediment Load and Floodplain Deposition Rates: Comparison of the Fly and Strickland Rivers, Papua New Guinea. *Journal of Geophysical Research*, Vol. 113, Issue F1, DOI 10.1029/2006JF000623.

Sylla L., Xiong D., Zhang H. Y. and Bangoura S. T. (2012). A GIS Technology and Method to Assess Environmental Problems from Land Use/Cover Changes: Conarkry, Coyah and Dubreka Region Case Study. *The Egyptian Journal of Remote Sensing and Space Sciences*, Vol. 15, pp. 31–38.

Syvitski J. P. M., Vorosmarty C. J., Kettner A. J., and Green P. (2005). Impact of Human on the Flux of Terrestrial Sediment to the Global Ocean. *Science*, Issue 308, pp. 376 –380.

Ta W., Jia X. and Wang H. (2013). Channel Deposition Induced by Bank Erosion in Response to Decreased Flows in the Sand-Banked Reach of the Upstream Yellow River. *Catena*, Vol. 105, pp. 62 – 68.

Takagi T., Oguchi T., Matsumoto J., Grossman M. J. Sarker M. H. and Matin M. A. (2007). Channel Braiding and Stability of the Brahmaputra River, Bangladesh, since 1967: GIS and Remote Sensing Analyses. *Geomorphology*, Vol. 85, pp. 294 – 305.

Takaldany A. E. (2003). Bank Stability Analysis for Predicting Reach Scale Land Loss and Sediment Yield. *Journal of the American Water Resources Association*, Vol. 39, Issue 4, pp. 897 – 909.

Takahasi Y. and Uitto J. I. (2004). Evolution of River Management in Japan: from Focus on Economic Benefits to a Comprehensive View. *Global Environmental Change*, p. 14.

Tandon S. K. and Sinha R. (2007). Geology of Large River Systems. In: Gupta A (Ed.), *Large Rivers*, Wiley, UK.

Tariq J., Ashraf M., Jaffar M. and Afzal M. (1996). Pollution Status of the Indus River, Pakistan, Through Heavy Metal and Macronutrient Contents of Fish, Sediment and Water. *Water Research*, Vol. 30, No. 6, pp. 1337 – 1344.

Tessier A., Campbell P. G. C. and Bisson M. (1979). Sequential Extraction Procedure for the Speciation of Particulate Trace Metals. *Analytical Chemistry*, Vol. 51, Issue 7, pp. 844 – 851.

The Ecologist Asia. (2003). Some Proposed and Existing Dam Projects in Northeast India. *The Ecologist Asia*, Mumbai, India, Vol. 11, No. 1, pp. 48.

Thorne C. R. (1978). *Processes of Bank Erosion in River Channels*, unpublished Ph.D. thesis, University of East Anglia, Norwich, NR 4 7TJ, UK.

Thorne C. R. (1991). Bank Erosion and Meander Migration of the Red and Mississippi Rivers, USA. *Hydrology for the Water Management of Large River Basins* (Proceedings of the Vienna Symposium, August 1991), IAHS Publ. no. 201.

Thorne C. R. and Tovey N. K. (1981). Stability of Composite River Banks. *Earth Surface Processes and Landforms,* Vol. 6, pp. 469 – 484.

Tiwari R. K., Sri Lakshmi S. and Rao K. N. N. (2004). Characterization of Earthquake Dynamics in Northeastern India Regions: A Modern Nonlinear Forecasting Approach. *Pure and Applied Geophysics*, Vol. 161, pp. 865 – 880.

Torfs H. (1995). *Erosion of Mud/ Sand Mixtures*, PhD thesis. Catholieke Universiteit Leuven, Belgium.

Trefry J. H. and Shokes R. F. (1981). History of Heavy Metal Inputs to Mississippi Delta Sediments. In Geyer R. A. (Ed.), *Marine Environmental Pollution*, Elsevier Oceanography Series, Amsterdam-Oxford-New York, pp. 193 – 226.

Tripathy G. R., Singh S. K. and Ramaswamy V. (2014). Major and Trace Element Geochemistry of Bay of Bengal Sediments: Implications to Provenances and Their

Controlling Factors. *Palaeogeography, Palaeoclimatology, Palaeoecology*, Vol. 397, pp. 20 – 30.

Turkian K. K. and Wedephol K. H. (1961). Distribution of the Elements in Some Major Units of the Earth Crust. *Geological Society of America Bulletin*, Vol. 72, No. 2, pp. 175 – 192.

Twidale C. R. (2004). River Patterns and Their Meaning. *Earth-Science Reviews*, Vol. 67, Issues 3 – 4, pp. 159 – 218.

Veldkamp A. and Verburg P. H. (2004). Modelling Land Use Change and Environmental Impact. *Journal of Environmental Management*, Vol. 72, pp. 1 – 3.

Verma S., Mukherjee A., Mahanta C., Choudhury R. and Mitra K. (2016). Influence of geology on groundwater–sediment interactions in arsenic enriched tectono-morphic aquifers of the Himalayan Brahmaputra river basin, *Journal of Hydrology*, Vol. 540, pp. 176–195.

Viers J., Dupre B. and Gaillardet J. (2009). Chemical Composition of Suspended Sediments in World Rivers: New Insights from a New Database. *Science of the Total Environment*, Vol. 407, Issue 2, pp. 853 – 868.

Walker J., Arnborg L. and Peippo J. (1987). Riverbank Erosion in the Colville Delta, Alaska. *Geografiska Annaler*, Vol. 69, No. 1, pp. 61 – 70.

Walling D. E. (1995). Suspended Sediment Transport by Rivers: A Geomorphological and Hydrological Perspective. In: *Proceedings of the International Symposium on Particulate Matter in Rivers and Estuaries* (Reinbek/ Hamberg, March 1994).

Walling D. E. (2006). Human Impact on Land-Ocean Sediment Transfer by the World's Rivers. *Geomorphology*, Vol. 79, No 3 – 4, pp. 192 – 216.

Walling D. E. and Collins A. L. (2008). The Catchment Sediment Budget as a Management Tool. *Environmental Science & Policy*, Vol. 11, pp. 136 – 143.

Walling D. L. (2008). The Changing Sediment Load of the Mekong River. *Ambio*, Vol. 3, Issue 3, p. 150.

Wang C., Dai S. B., Ran L. S., Jiang L. and Li W. T. (2015). Contribution of River Mouth Reach to Sediment Load of the Yangtze River. *Advances in Meteorology*, Article ID 415058, Hindawi Publishing Corporation.

Wang Z. Y., Li Y. and He Y. (2007). Sediment Budget of the Yangtze River. *Water*

*Resources Research*, Vol. 43, Issue 4, p. W04401.

Wanogho S., Gettinby G. and Caddy B. (1987). Particle Size Distribution Analysis of Soils Using Laser Diffraction. *Forensic Science International*, Vol. 33, pp. 117 – 128.

Wasson R. J. (2003). A Sediment Budget for the Ganga-Brahmaputra Catchment. *Current Science*, Vol. 84, No. 8, pp. 1041 – 1047.

Web B. W., Foster I. D. L. and Gurnell A. M. (1995). Hydrology, Water Quality and Sediment Behaviour. In I. D. L. Foster, A. M. Gurnell and B. W. Webb (Eds.), *Sediment and Water Quality in River Catchments*, John Wiley & Sons Ltd., England.

Wedephol K. H. (1971). Environmental Influences on the Chemical Composition of Shales and Clays. *Physics and Chemistry of the Earth*, Vol. 8, pp. 305 – 333.

Weiss E. L. and Frock H. N. (1976). Rapid Analysis of Particle-Size Distributions by Laser Light Scattering. Powder Technology, Vol. 14, Issue 2, pp. 287 – 293.

Wells N. A. and Dorr J. A. (1987) Shifting of Koshi river, Northern India. *Geology*, Vol. 15, pp. 204 – 207.

Weltje G. J. and Prins M. A. (2007). Genetically Meaningful Decomposition of Grain Size Distributions. *Sedimentary Geology*, Vol. 202, pp. 409 – 424.

Wetzel R. G. (2001). *Limnology: Lake and River Ecosystems* (3rd ed.). San Diego, CA, Academic Press.

Wiebe H. (2006). Brahmaputra Flooding and Erosion in Northeast India, Draft paper No. 4. *Study of Natural Resources, Water and the Environmental Nexus for development and growth in Northeast India*, World Bank and Gauhati University.

Wilson C. G., Kuhnle R. A., Bosch D. D., Steiner J. L., Starks P. J., Tomer M. D. and Wilson G. V. (2008). Quantifying Relative Contributions from Sediment Sources in Conservation Effects Assessment Project watersheds, *Journal of Soil and Water Conservation*, Vol. 63, pp. 523 – 531.

Wilson G. V., Fox G. A., Midgley T., Almadhhachi A. and Carson R. (2011). *Bank Erosion on the Upper Mississippi River System*. International Symposium on Erosion and Landscape Evolution (ISELE), Alaska.

Wilson M. J. (1999). The Origin and Formation of Clay Minerals in Soils: Past, Present and Future Perspectives. *Clay Miner*., Vol. 34, pp. 1 – 27.

Winterwerp J. C. and Kesteren W. G. M. (2004). *Introduction to the Physics of Cohesive Sediment in the Marine Environment*. Elsevier, Amsterdam, p. 576.

Wischmeier W. H. and Mannering J. V. (1969). Relation of Soil Properties to its Erodibility. *Soil Science Society of America Proceedings*, Vol. 33, pp. 131 – 137.

Wolman M. G. (1959). Factors Influencing Erosion of a Cohesive River Bank. *American Journal of Science*, Vol. 257, No. 3, pp. 204 – 216.

WRD (2004). *The Task Force for Flood Management/ Erosion Control*. Water Resources Department, Govt. of Assam, pp. 6 – 19.

WRD (2008). *North Eastern Integrated Flood and River Bank Erosion Management Project: Feasibility Study* (PPTA, Phase II). Water Resources Department, Govt. of Assam.

WRD (2016). *Report on First Wave of Flood in June/2015*. Water Resource Department, Govt. of Assam, Assessed from http://assam.gov.in/web/department-of-water-resource/flood-fighting-works on 30.01.2017.

Wu X., Shen Z., Liu R. and Ding X. (2008). Land Use/ Cover Dynamics in Response to Changes in Environmental and Socio-Political Forces in the Upper Reaches of the Yangtze River, China. *Sensors*, Vol. 8, No. 12, pp. 8104 – 8122.

Xiao H. L., Weng Q. H. (2007). The Impact of Land Use and Land Cover Changes on Land Surface Temperature in a Karst Area of China. *Journal of Environmental Management*, Vol. 85, pp. 245 – 257.

Xinhua (2011). *Scientists Pinpoint Sources of Four Major International Rivers*. Xinhua, english.news.cn, http://news.xinhuanet.com/english2010/china/2011-08/22/c_131067137.htm, Assessed on December 12, 2012.

Xu J. (2002). River Sedimentation and Channel Adjustment of the Lower Yellow River as Influenced by Low Discharges and Seasonal Channel Dry-Ups. *Geomorphology*, Vol. 43, Issues 1 – 2, pp. 151 – 164.

Xu K. and Milliman J. D. (2009). Seasonal Variations of Sediment Discharge from the Yangtze River Before and After Impoundment of the Three Gorges Dam. *Geomorphology*, Vol. 104, Issues 3 – 4, pp. 276 – 283.

Xu Y. N., Liang Z. Y., Wang X. D., Li W. W. and Du Y. Q. (2001). Analysis on Bank Failure and River Channel Changes. *Journal of Sediment Research*, No. 4, pp. 41–46.

Xue Z., Liu J. P. and Ge Q. (2011). Changes in Hydrology and Sediment Delivery of the Mekong River in Last 50 Years: Connection to Damming, Monsoon and ENSO. *Earth surface processes and landforms*, Vol. 36, Issue 3, pp. 296 – 308.

Yamini O. A., Kavianpour M. R. and Mousavi S. H. (2017). Experimental Investigation of Parameters Affecting the Stability of Articulated Concrete Block Mattress Under Wave Attack. *Applied Ocean Research*, Vol. 64, pp. 184 – 202.

Yang S. L., Milliman J. D., Li P., and Xu K. (2011). 50,000 Dams Later: Erosion of the Yangtze River and its Delta. *Global and Planetary Change*, Vol. 75, Issues 1 – 2, pp. 14 – 20.

Yang X. and Lu X. X. (2014). Estimate of Cumulative Sediment Trapping by Multiple Reservoirs in Large River Basins: An Example of the Yangtze River basin. *Geomorphology*, Vol. 227, pp. 49 – 59.

Yao Z., Ta W., Jia X. and Xiao J. (2011). Bank Erosion and Accretion along the Ningxia–Inner Mongolia Reaches of the Yellow River from 1958 To 2008. *Geomorphology*, Vol. 127, Issues 1 – 2, pp. 99 – 106.

Yesilnacar E. and Topal T. (2005). Landslide Susceptibility Mapping: A Comparison Of Logistic Regression and Natural Networks Methods in a Medium Scale Study, Hendek Region (Turkey), *Engineering Geology*, Vol. 79, Issues 3 – 4, pp. 251 – 266.

Yi Yuju., Wang Z., Zhang K., Yu G. and Duan X. (2008). Sediment Pollution and its Effect on Fish Through Food Chain in the Yangtze River. *International Journal of Sediment Research*, Vol. 23, Issue 4, pp. 338 – 347.

Zhang Q., Xu C., Becke S. and Jiang T. (2006). Sediment and Runoff Changes in the Yangtze River Basin During Past 50 Years. *Journal of Hydrology*, Vol. 331, Issues 3 – 4, pp. 511 – 523.

Zhang R. J. (1989). *River Dynamics*. Water Power Press, Beijing, China.

Zhang, W. G., Hu Y. M., Hu, J. C., Chang Y., Zhang J. and Liu M. (2008). Impacts of Land Use Change on Mammal Diversity in the Upper Reaches of Minjiang River, China: Implications of Biodiversity Conservation Planning. *Landscape Urban Plan.*, Vol. 85, pp. 195 – 204.

# Appendix I

**Elevation (**from msl**) of Brahmaputra River at a few points**
from the source (Angsi glacier, Latitude: 30º31′27″ N, Longitude: 82º12′34″E) to Bay of Bengal

| Sl. no | Distance from the source (km) | Elevation (m) |
|---|---|---|
| 1 | 0 | 5291.3 |
| 2 | 20 | 4892.0 |
| 3 | 40 | 4809.7 |
| 4 | 80 | 4687.8 |
| 5 | 400 | 4481.1 |
| 6 | 450 | 4437.8 |
| 7 | 585 | 4139.1 |
| 8 | 894 | 3959.3 |
| 9 | 935 | 3921.5 |
| 10 | 1004 | 3845.3 |
| 11 | 1099 | 3764.2 |
| 12 | 1194 | 3595.7 |
| 13 | 1404 | 3203.1 |
| 14 | 1800 | 2310.3 |
| 15 | 1851 | 1264.9 |
| 16 | 2294 | 143.2 |
| 17 | 2750 | 40.5 |
| 18 | 2768 | 39.6 |
| 19 | 3086 | 11.2 |
| 20 | 3453 | 0 |

# Appendix II

**Erosion and deposition (in km$^2$) in different reaches** (1 at the upstream and 16 at the downstream) **of Brahmaputra River in Assam during 1973 – 1994**

| Reach no | North bank | | South bank | | Total | | No change |
|---|---|---|---|---|---|---|---|
| | Erosion | Deposition | Erosion | Deposition | Erosion | Deposition | |
| 1 | 4.9 | 0.2 | 28.7 | 0.1 | 33.6 | 0.3 | 364.0 |
| 2 | 6.4 | 2.9 | 42.1 | 1.1 | 48.5 | 4.0 | 407.3 |
| 3 | 10.7 | 2.7 | 12.3 | 0.5 | 23.0 | 3.1 | 347.4 |
| 4 | 31.3 | 0.2 | 14.2 | 4.2 | 45.5 | 4.5 | 267.2 |
| 5 | 64.4 | 0.7 | 45.2 | 0.0 | 109.6 | 0.7 | 275.5 |
| 6 | 83.1 | 3.5 | 35.7 | 21.9 | 118.8 | 25.4 | 282.7 |
| 7 | 28.7 | 6.3 | 25.6 | 20.5 | 54.3 | 26.8 | 195.9 |
| 8 | 29.8 | 17.4 | 7.3 | 8.7 | 37.2 | 26.2 | 179.6 |
| 9 | 31.4 | 11.6 | 22.0 | 7.2 | 53.4 | 18.9 | 351.7 |
| 10 | 21.5 | 30.1 | 93.7 | 0.5 | 115.2 | 30.6 | 239.7 |
| 11 | 23.3 | 4.9 | 2.2 | 4.2 | 25.5 | 9.1 | 149.7 |
| 12 | 41.2 | 0.5 | 42.6 | 0.0 | 83.8 | 0.5 | 305.6 |
| 13 | 60.7 | 0.6 | 20.1 | 5.1 | 80.8 | 5.8 | 374.8 |
| 14 | 64.3 | 7.6 | 10.5 | 1.3 | 74.7 | 8.8 | 312.3 |
| 15 | 20.8 | 7.0 | 26.0 | 0.6 | 46.8 | 7.6 | 322.0 |
| 16 | 41.0 | 0.0 | 174.3 | 0.0 | 215.3 | 0.0 | 344.2 |
| Total | 563.5 | 96.2 | 602.2 | 75.9 | 1165.7 | 172.0 | 4719.4 |

# Appendix III

**Erosion and deposition (in km$^2$) in different reaches** (1 at the upstream and 16 at the downstream) **of Brahmaputra River in Assam during 1994—2014**

| Reach no | North bank | | South bank | | Total | | No change |
|---|---|---|---|---|---|---|---|
| | Erosion | Deposition | Erosion | Deposition | Erosion | Deposition | |
| 1 | 2.7 | 1.4 | 20.2 | 2.2 | 22.9 | 3.6 | 395.9 |
| 2 | 16.8 | 1.5 | 11.7 | 1.2 | 28.5 | 2.7 | 450.6 |
| 3 | 12.5 | 2.2 | 3.0 | 4.9 | 15.5 | 7.1 | 363.2 |
| 4 | 12.8 | 31.9 | 9.5 | 0.8 | 22.3 | 32.6 | 280.0 |
| 5 | 27.5 | 9.2 | 9.8 | 3.4 | 37.3 | 12.6 | 360.0 |
| 6 | 21.0 | 12.8 | 31.8 | 2.0 | 52.8 | 14.8 | 386.1 |
| 7 | 9.1 | 12.7 | 26.9 | 0.8 | 36.0 | 13.5 | 229.0 |
| 8 | 26.6 | 4.3 | 10.5 | 7.4 | 37.1 | 11.7 | 206.0 |
| 9 | 15.2 | 9.6 | 11.2 | 19.4 | 26.4 | 29.1 | 375.0 |
| 10 | 6.8 | 13.7 | 81.3 | 0.0 | 88.2 | 13.7 | 340.5 |
| 11 | 20.5 | 4.1 | 14.6 | 0.7 | 35.0 | 4.8 | 170.0 |
| 12 | 16.8 | 7.3 | 5.5 | 4.5 | 22.4 | 11.8 | 377.8 |
| 13 | 34.4 | 2.1 | 13.0 | 10.0 | 47.4 | 12.1 | 452.4 |
| 14 | 23.3 | 2.1 | 5.3 | 1.2 | 28.6 | 3.3 | 382.5 |
| 15 | 25.8 | 1.7 | 22.4 | 12.6 | 48.2 | 14.2 | 354.8 |
| 16 | 11.4 | 2.5 | 29.6 | 6.9 | 41.0 | 9.4 | 549.0 |
| Total | 283.3 | 119.0 | 306.2 | 77.9 | 589.5 | 196.9 | 5672.8 |

# Appendix IV

a) **Aggradation and Degradation of Brahmaputra from 1957 to 1977**

| Sl no | Cross sections | Av width of River (m) | Length of reach (m) | Period 1957--1971 | | | Period 1971--1977 | | |
|---|---|---|---|---|---|---|---|---|---|
| | | | | Deposit ($10^6m^3$) | Scour ($10^6m^3$) | Depth of scour per year (cm | Deposit ($10^6m^3$) | Scour ($10^6m^3$) | Depth of scour per year (cm |
| 1 | 2 to 11 | 11464 | 83640 | 956.9 | 104.4 | (-) 6.35 | 214.8 | 881 | 9.92 |
| 2 | 11 to 21 | 12336 | 88230 | 619.7 | 144 | (-) 3.12 | 40.8 | 1077.7 | 15.88 |
| 3 | 21 to 31 | 9616 | 83140 | 181.8 | 948.1 | 6.85 | 458.7 | 648.1 | 3.95 |
| 4 | 31 to 41 | 11220 | 117310 | 546.8 | 515.3 | (-) 0.17 | 317.9 | 1710 | 17.62 |
| 5 | 41 to 51 | 10397 | 109140 | 1126 | 763.7 | (-) 2.28 | 33.9 | 955.9 | 13.54 |
| 6 | 51 to 61 | 13040 | 103020 | 292.8 | 1122 | 4.4 | 512.6 | 885.1 | 4.62 |
| Total | 61 to 2 | 11250 | 584380 | 3724 | 3597.5 | (-) 0.11 | 1579 | 6158 | 10.92 |

(NEC, 1993)

## b) Aggradation and Degradation of Brahmaputra from 1977 to 1989

| Sl no | Cross sections | Av width of River (m) | Length of reach (m) | Period 1977--1981 | | | Period 1981--1989 | | | Period 1957--1989 | | |
|---|---|---|---|---|---|---|---|---|---|---|---|---|
| | | | | Deposit ($10^6m^3$) | Scour ($10^6m^3$) | Depth of scour per year (cm | Deposit ($10^6m^3$) | Scour ($10^6m^3$) | Depth of scour per year (cm) | Deposit ($10^6m^3$) | Scour ($10^6m^3$) | Depth of scour per year (cm) |
| 1 | 2 to 11 | 11464 | 83640 | 331.2 | 279 | (-) 0.69 | 374.7 | 774.7 | 4.63 | 490.7 | 653.9 | 0.53 |
| 2 | 11 to 21 | 12336 | 88230 | 174.9 | 870.3 | 15.9 | 663.3 | 389.4 | (-) 3.15 | 0 | 982.7 | 2.82 |
| 3 | 21 to 31 | 9616 | 83140 | 422 | 447.9 | 0.81 | 315.5 | 198.3 | (-) 1.84 | 89.1 | 953.6 | 3.38 |
| 4 | 31 to 41 | 11220 | 117310 | 271.3 | 559.8 | 5.48 | 513.6 | 956.5 | 4.2 | 23.4 | 2115 | 4.97 |
| 5 | 41 to 51 | 10397 | 109140 | 499.8 | 222 | (-) 6.12 | 970 | 816.3 | (-) 1.69 | 223.5 | 351.6 | 0.35 |
| 6 | 51 to 61 | 13040 | 103020 | 331.7 | 699.4 | 6.84 | 1948 | 172.7 | (-) 16.85 | 798.6 | 592.6 | (-) 0.49 |
| Total | 61 to 2 | 11250 | 584380 | 3724 | 3597 | (-) 0.11 | 4785 | 3308 | (-) 2.5 | 1625 | 5650 | 1.92 |

(NEC, 1993)

# Appendix V

## Shifting of Brahmaputra River (km) from 1911-28

| C/S no | Chainage (km) | Shifting (km) | | | | | | | |
|---|---|---|---|---|---|---|---|---|---|
| | | 1911-28 to 61-70 | | 1961-70 to 71-72 | | 1971-72 to 1983-84 | | 1911-28 to 83-84 | |
| | | L.B. | R.B | L.B. | R.B. | L.B. | R.B. | L.B. | R.B. |
| 2 | 17.34 | 3.00R | 1.30R | 3.85L | 3.50L | 1.25L | 0.50L | 2.10L | 2.70L |
| 3 | 28.05 | 5.00L | 1.00L | 0.20L | 0.50L | 0.50R | 0.20R | 4.70L | 1.30L |
| 4 | 38.25 | 2.75L | 7.01L | 0.25L | 0.05R | 0.75L | 0 | 3.75L | 6.96L |
| 5 | 46.92 | 1.15L | 9.00L | 0 | 0 | 0.75L | 0.35R | 1.90L | 8.65L |
| 6 | 56.61 | 1.00L | 0.20L | 0.05R | 0.25L | 0.20L | 0.60R | 1.15L | 0.15R |
| 7 | 66.3 | 0.60R | 2.00R | 0.20L | 0.10L | 0.15L | 0.50R | 0.25R | 2.40R |
| 8 | 73.44 | 0.15L | 3.50L | 0 | 0.25R | 0 | 3.70R | 0.15L | 0.25R |
| 9 | 82.62 | 0.10L | 0.60R | 0.05R | 0 | 0 | 0.45R | 0.05L | 1.05R |
| 10 | 92.82 | 1.00R | 3.65L | 0.20L | 0 | 0.55L | 1.00R | 0.25R | 2.65L |
| 11 | 100.98 | 0.25L | 3.75R | 0 | 0.20R | 0 | 300R | 0.25R | 6.95R |
| 12 | 109.65 | 0 | 0.60L | 0 | 1.75R | 0 | 1.800R | 0 | 2.95R |
| 13 | 119.85 | 0.20R | 2.30R | 0.30L | 1.45R | 0.25L | 0.80L | 0.35L | 2.95R |
| 14 | 128.01 | 2.00L | 2.00R | 0.60R | 0.60R | 0 | 0.15L | 1.40L | 2.45R |
| 15 | 137.7 | 0.30R | 2.50R | 1.60L | 1.00L | 1.50R | 1.10R | 0.20R | 2.60R |
| 16 | 146.37 | 4.75L | 2.75R | 0.60R | 2.55R | 0 | 0.10L | 4.15L | 5.15L |
| 17 | 156.06 | 4.00L | 0.05R | 0 | 1.25R | 0.30L | 0 | 4.30L | 1.30R |
| 18 | 167.28 | 0.20L | 1.75L | 0.45L | 2.00R | 0.75L | 1.20R | 1.40L | 1.45R |
| 19 | 175.95 | 2.75L | 0.80L | 0.11L | 0 | 0.30L | 0.60R | 3.16L | 0.20L |
| 20 | 182.58 | 1.00L | 0.40R | 0 | 0 | 0.05L | 0.05L | 3.05L | 0.35R |
| 21 | 189.21 | 0 | 3.75L | 0 | 0 | 0 | 1.35R | 0 | 2.40L |
| 22 | 197.37 | 0 | 0 | 0 | 0 | 0 | 0 | 0 | 0 |
| 23 | 206.55 | 0.11L | 1.60R | 0 | 0 | 0 | 1.35R | 0.11L | 0.25L |
| 24 | 213.18 | 0 | 0.10R | 0.10L | 0 | 0 | 0.20R | 0.10L | 0.30R |
| 25 | 218.79 | 0.40L | 1.20L | 0.40L | 0.45L | 0.15R | 4.50R | 0.65L | 2.85R |
| 26 | 224.91 | 1.40L | 4.75L | 0.40R | 0.70L | 0.20L | 0.50L | 1.20L | 5.95L |
| 27 | 234.6 | 0.70L | 4.10L | 0.70R | 0.10R | 1.30R | 2.30R | 1.30R | 1.70L |

| C/S no | Chainage (km) | Shifting (km) | | | | | | | |
|---|---|---|---|---|---|---|---|---|---|
| | | 1911-28 to 61-70 | | 1961-70 to 71-72 | | 1971-72 to 1983-84 | | 1911-28 to 83-84 | |
| | | L.B. | R.B | L.B. | R.B. | L.B. | R.B. | L.B. | R.B. |
| 28 | 241.23 | 1.00L | 3.00R | 0 | 0.70R | 0 | 0.60R | 1.00L | 4.20R |
| 29 | 251.95 | 1.35L | 2.80R | 0.25L | 0.10L | 0.20R | 0.40L | 1.40L | 2.30R |
| 30 | 262.15 | 0 | 3.00L | 0 | 0 | 1.50L | 1.80L | 1.50L | 4.80L |
| 31 | 272.35 | 1.75R | 0.15L | 0.30L | 0.20R | 0.35L | 0.20R | 1.10R | 0.25R |
| 32 | 284.08 | 2.00L | 0.55R | 0 | 0 | 0 | 0.50R | 2.00L | 1.10R |
| 33 | 296.83 | 2.50L | 2.00R | 0 | 0.20L | 0 | 0.10R | 2.50L | 1.90R |
| 34 | 310.1 | 1.00R | 0.75L | 2.00R | 0 | 0 | 0.10R | 3.00R | 0.65L |
| 35 | 325.91 | 0.50R | 0 | 0.20L | 0 | 1.35L | 0 | 1.05L | 0 |
| 36 | 341.21 | 0.40L | 1.50L | 0 | 0.50R | 0 | 1.50R | 0.40L | 0.50R |
| 37 | 352.94 | 3.75L | 3.00L | 0 | 0.75R | 1.25R | 2.75R | 2.50L | 0.50R |
| 38 | 365.18 | 2.00R | 2.00R | 0.25L | 0 | 0.60L | 0 | 1.15R | 2.0R |
| 39 | 371.81 | 0.10R | 4.00R | 0.40L | 2.00L | 0.75L | 0.25R | 1.05L | 2.25R |
| 40 | 383.03 | 4.25L | 0.25R | 0 | 0 | 0 | 1.25L | 4.25L | 1.00L |
| 41 | 389.66 | 1.00L | 1.00R | 0.40L | 0 | 0.50L | 1.50R | 1.90L | 2.50R |
| 42 | 398.33 | 2.50L | 1.50R | 1.25R | 0 | 0.75L | 0 | 2.00L | 1.50R |
| 43 | 412.09 | 3.00L | 0 | 0 | 0.50L | 1.25L | 0.25R | 4.25L | 0.25L |
| 44 | 423.31 | 4.25R | 7.75L | 0 | 6.75R | 0.50L | 0.25R | 3.75R | 0.75R |
| 45 | 439.63 | 3.50R | 2.00R | 1.50L | 0.40R | 1.50R | 3.50R | 3.50R | 5.90R |
| 46 | 453.91 | 2.50R | 5.40R | 0 | 0.20R | 1.75R | 0.15L | 4.25R | 5.45R |
| 47 | 465.13 | 0.75L | 0.35R | 0 | 0.20R | 0 | 0.50R | 0.75L | 1.05R |
| 48 | 474.82 | 1.25L | 1.50L | 0 | 0 | 0.20L | 0.50R | 1.45L | 1.00L |
| 49 | 483.49 | 2.25R | 2.85R | 0 | 0 | 0 | 0.20R | 2.25R | 3.05R |
| 50 | 490.63 | 2.35R | 3.00R | 0.15L | 0 | 2.00L | 0.20R | 0.10R | 3.20R |
| 51 | 498.8 | 0.50L | 4.50R | 0.50L | 1.00L | 0.25R | 0.30R | 0.75L | 3.80R |
| 52 | 505.94 | 1.25L | 2.00R | 0 | 1.25R | 0 | 0.50R | 1.25L | 3.75R |
| 53 | 513.08 | 1.25L | 1.00R | 0 | 0 | 0.30L | 0.20R | 1.55L | 1.20R |
| 54 | 522.77 | 1.20L | 2.50R | 0.20L | 0 | 0.50L | 0 | 1.90L | 2.50R |
| 55 | 531.95 | 2.25L | 0 | 0 | 0 | 0 | 0.60L | 2.25L | 0.60L |

| C/S no | Chainage (km) | Shifting (km) | | | | | | | |
|---|---|---|---|---|---|---|---|---|---|
| | | 1911-28 to 61-70 | | 1961-70 to 71-72 | | 1971-72 to 1983-84 | | 1911-28 to 83-84 | |
| | | L.B. | R.B | L.B. | R.B. | L.B. | R.B. | L.B. | R.B. |
| 56 | 541.13 | 0.40L | 0 | 0 | 0.15R | 0 | 0 | 0.25L | 0.15R |
| 57 | 558.98 | 2.00L | 2.75R | 0.20L | 0.10R | 0.20R | 0.80R | 2.00L | 3.65R |
| 58 | 570.2 | 1.20L | 0.40R | 0 | 0.10R | 0 | 0.25R | 1.20L | 0.25R |
| 59 | 579.38 | 1.75L | 1.55R | 0 | 0 | 0.10R | 0.10R | 1.65L | 1.65R |
| 60 | 589.07 | 3.50L | 0.40R | 0.25L | 0.15L | 0.20R | 0.20R | 3.45L | 0.45R |
| 61 | 601.82 | 1.50L | 3.50R | 0 | 0.25R | 0.50L | 0.10L | 2.00L | 3.65R |
| 62 | 613.04 | 0.75L | 3.00R | 0.10L | 1.35L | 0.10L | 1.25R | 0.95L | 2.90R |

*L: left, R: right, L.B.: left bank, R.B.: right bank*

(NEC,1993)

# Appendix VI

**Elemental composition of sediments and bank materials** (from EDX results)

| **Suspended sediments in monsoon season in location 5** | | |
|---|---|---|
| Element | Weight% | Atomic% |
| O | 24.14 | 44.25 |
| Na | 2.18 | 2.78 |
| Al | 10.33 | 11.23 |
| Si | 15.30 | 15.98 |
| P | 0.44 | 0.42 |
| K | 3.07 | 2.30 |
| Ca | 0.35 | 0.26 |
| Cr | 17.45 | 9.84 |
| Fe | 8.95 | 4.70 |
| Co | 5.08 | 2.53 |
| Ni | 5.93 | 2.96 |
| Cu | 3.29 | 1.52 |
| Zn | 1.55 | 0.69 |
| As | 0.28 | 0.11 |
| Cd | 1.66 | 0.43 |
| Total | 100.00 | 100.00 |

| **Suspended sediments in monsoon season in location 5** | | |
|---|---|---|
| Element | Weight% | Atomic% |
| O | 35.26 | 53.89 |
| Mg | 5.86 | 5.89 |
| Al | 10.22 | 9.26 |
| Si | 19.85 | 17.29 |
| K | 4.04 | 2.53 |
| Ca | 2.78 | 1.70 |
| Fe | 17.41 | 7.62 |
| Ni | 3.42 | 1.42 |
| Zn | 0.99 | 0.37 |
| Pb | 0.17 | 0.02 |
| Total | 100.00 | 100.00 |

| **Suspended sediments in non-monsoon season in location 6** | | |
|---|---|---|
| Element | Weight% | Atomic% |
| N | 1.34 | 3.80 |
| O | 9.15 | 22.72 |
| Mg | 0.62 | 1.01 |
| Al | 2.82 | 4.15 |
| Si | 6.12 | 8.66 |
| S | 0.94 | 1.16 |
| Ca | 7.56 | 7.50 |
| Cr | 33.35 | 25.48 |
| Fe | 14.53 | 10.34 |
| Co | 8.43 | 5.68 |
| Ni | 5.84 | 3.95 |
| Cu | 4.99 | 3.12 |
| Zn | 2.41 | 1.47 |
| As | 1.60 | 0.85 |
| Cd | 0.30 | 0.11 |
| Total | 100.00 | 100.00 |

| **Suspended sediments in non-monsoon season in location 6** | | |
|---|---|---|
| Element | Weight% | Atomic% |
| O | 35.35 | 56.86 |
| Na | 1.18 | 1.32 |
| Mg | 0.19 | 0.21 |
| Al | 8.18 | 7.80 |
| Si | 19.24 | 17.63 |
| P | 1.44 | 1.20 |
| Fe | 12.69 | 5.85 |
| Co | 11.58 | 5.05 |
| Ni | 2.69 | 1.18 |
| Cu | 3.08 | 1.25 |
| Zn | 2.99 | 1.18 |
| As | 1.39 | 0.48 |
| Total | 100.00 | 100.00 |

| **Suspended sediments in monsoon season in location 2** | | |
|---|---|---|
| Element | Weight% | Atomic% |
| O | 39.73 | 56.73 |
| Mg | 7.01 | 6.58 |
| Al | 8.59 | 7.28 |
| Si | 25.33 | 20.61 |
| Ca | 6.33 | 3.61 |
| Fe | 10.85 | 4.44 |
| Zn | 2.16 | 0.76 |
| Total | 100.00 | 100.00 |

| **Suspended sediments in monsoon season in location 2** | | |
|---|---|---|
| Element | Weight% | Atomic% |
| O | 55.09 | 68.84 |
| Mg | 0.07 | 0.06 |
| Al | 0.32 | 0.24 |
| Si | 41.99 | 29.89 |
| K | 0.67 | 0.35 |
| Fe | 1.36 | 0.49 |
| Zn | 0.35 | 0.11 |
| As | 0.15 | 0.04 |
| Total | 100.00 | 100.00 |

| **Bank materials of erosion site *A*** | | |
|---|---|---|
| Element | Weight% | Atomic% |
| O | 42.63 | 60.89 |
| Na | 0.42 | 0.42 |
| Mg | 1.17 | 1.10 |
| Al | 12.60 | 10.67 |
| Si | 23.49 | 19.11 |
| Cl | 0.05 | 0.03 |
| K | 1.55 | 0.91 |
| Ca | 0.93 | 0.53 |
| Fe | 11.11 | 4.55 |
| Ni | 1.85 | 0.72 |
| Cu | 0.80 | 0.29 |
| Zn | 0.95 | 0.33 |
| Sr | 1.11 | 0.29 |
| Hg | 1.34 | 0.15 |
| Total | 100.00 | 100.00 |

| **Bank materials of erosion site *A*** | | |
|---|---|---|
| Element | Weight% | Atomic% |
| O | 42.24 | 61.16 |
| Mg | 4.71 | 4.49 |
| Al | 12.48 | 10.71 |
| Si | 16.51 | 13.62 |
| Cl | 0.29 | 0.19 |
| K | 0.16 | 0.10 |
| Ca | 0.63 | 0.36 |
| Cr | 5.35 | 2.38 |
| Fe | 14.09 | 5.84 |
| Co | 1.03 | 0.41 |
| Ni | 0.80 | 0.32 |
| Zn | 0.12 | 0.04 |
| As | 1.03 | 0.32 |
| Hg | 0.57 | 0.07 |
| Total | 100.00 | 100.00 |

| **Bank materials of erosion site *C*** | | |
|---|---|---|
| Element | Weight% | Atomic% |
| O | 33.19 | 61.20 |
| Al | 3.58 | 3.92 |
| Si | 2.61 | 2.74 |
| Ca | 0.91 | 0.67 |
| Fe | 58.80 | 31.06 |
| Zn | 0.91 | 0.41 |
| Total | 100.00 | 100.00 |

| **Bank materials of non-erosion site *D1*** | | |
|---|---|---|
| Element | Weight% | Atomic% |
| O | 40.26 | 58.14 |
| Na | 1.68 | 1.68 |
| Mg | 0.79 | 0.75 |
| Al | 9.19 | 7.87 |
| Si | 24.64 | 20.27 |
| K | 7.72 | 4.56 |
| Ca | 0.13 | 0.08 |
| Cr | 14.06 | 6.25 |
| Cu | 0.32 | 0.12 |
| Zn | 0.27 | 0.10 |
| Cd | 0.95 | 0.19 |
| Total | 100.00 | 100.00 |

| **Bank materials of non-erosion site *D1*** | | |
|---|---|---|
| Element | Weight% | Atomic% |
| O | 36.67 | 57.94 |
| Mg | 4.07 | 4.23 |
| Al | 6.80 | 6.37 |
| Si | 15.75 | 14.18 |
| P | 0.82 | 0.67 |
| K | 5.54 | 3.58 |
| Fe | 24.36 | 11.03 |
| Co | 2.62 | 1.12 |
| Cu | 0.88 | 0.35 |
| Zn | 0.27 | 0.11 |
| As | 0.56 | 0.19 |
| Cd | 0.29 | 0.06 |
| Pb | 1.36 | 0.17 |
| Total | 100.00 | 100.00 |

| **Bank materials of non-erosion site *D5*** | | |
|---|---|---|
| Element | Weight% | Atomic% |
| O | 26.12 | 49.48 |
| Mg | 1.57 | 1.95 |
| Al | 5.19 | 5.83 |
| Si | 9.70 | 10.47 |
| S | 0.00 | 0.00 |
| Ca | 4.26 | 3.22 |
| Cr | 13.11 | 7.64 |
| Mn | 9.62 | 5.31 |
| Fe | 18.13 | 9.84 |
| Co | 6.31 | 3.25 |
| Ni | 4.72 | 2.44 |
| Cu | 1.15 | 0.55 |
| Pb | 0.12 | 0.02 |
| Total | 100.00 | 100.00 |

| **Erosion site *F*** | | |
|---|---|---|
| Element | Weight% | Atomic% |
| O | 42.46 | 58.98 |
| Na | 0.37 | 0.36 |
| Mg | 0.30 | 0.27 |
| Al | 7.96 | 6.56 |
| Si | 35.69 | 28.24 |
| Cl | 0.66 | 0.41 |
| K | 1.67 | 0.95 |
| Cr | 7.23 | 3.09 |
| Fe | 0.79 | 0.32 |
| Co | 0.66 | 0.25 |
| Cu | 1.11 | 0.39 |
| Cd | 0.76 | 0.15 |
| Hg | 0.35 | 0.04 |
| Total | 100.00 | 100.00 |

| **Erosion site *F*** | | |
|---|---|---|
| Element | Weight% | Atomic% |
| O | 26.24 | 52.32 |
| Mg | 0.03 | 0.04 |
| Al | 3.47 | 4.10 |
| Si | 3.92 | 4.45 |
| Ca | 0.28 | 0.23 |
| Ti | 16.62 | 11.06 |
| Cr | 10.49 | 6.44 |
| Fe | 26.81 | 15.31 |
| Co | 5.63 | 3.05 |
| Ni | 3.00 | 1.63 |
| Cu | 1.51 | 0.76 |
| Zn | 0.68 | 0.33 |
| As | 0.32 | 0.13 |
| Hg | 0.99 | 0.16 |
| Total | 100.00 | 100.00 |

# Appendix VII

**Publications so far** (October, 2017) **from the research work:**

1) '*The Brahmaputra and Other Rivers of the North-East*', in Iyer R. R. (Ed.), 'Living Rivers, Dying Rivers', **Oxford University Press**, New Delhi, 2015. ISBN: 978-0-199-45622-2, pp. 149 – 181.
2) *'Sediment Dynamics in a Large Alluvial River: Characterization of Materials and Processes and Management Challenges',* in Sharma N. (Ed.), 'River System Analysis and Management', **Springer**, 2016. ISBN 978-981-10-1471-0, pp. 47—71.